A STUDY OF PHOTOINDUCED TRANSFORMATIONS OF SUNSCREEN CHEMICAL ABSORBERS

by

Waudo Lyambila

Submitted in fulfilment of the academic requirements for the degree of Doctor of Philosophy in the School of Chemistry, University of KwaZulu-Natal, Durban.

April 2009

Abstract

Solar ultraviolet radiation is known to have deleterious effects on human skin and is a major cause of skin cancer. Therefore, the topical application of sunscreen preparations has gained wide usage for skin protection. These preparations typically contain a variety of chemical absorbers that absorb ultraviolet (UV) radiation and physical blockers that scatter, absorb and reflect UV light. The efficacy of sunscreens can be estimated by the Sun Protection Factor (SPF) which depends on the UV filters present in the formulations. However, although some of these commercial sunscreens have beneficial effects, they can also have undesirable results. It is known that the sunscreens undergo electronic excitation when exposed to UV light which may make them susceptible to photochemical modification. The production of reactive intermediates (e.g. free radicals) and stable photoproducts, either due to photoisomerisation or photofragmentation is a major concern because these species may be toxic and may lead to a reduction in efficacy. Hence a study of the photochemistry of these chemical absorbers found in commercial sunscreens is of great importance.

Photostability and broad-spectrum studies of some Australian commercial sunscreen products were undertaken by means of spectrophotometric and chromatographic methods. The sunscreen products dissolved in methanol solutions were irradiated using simulated solar radiation. High performance liquid chromatography (HPLC) was used to identify and quantify the active chemical ingredients. UV spectrophotometry was used to monitor the spectral absorbance before and after UV exposure of the formulations. Our results show that some of the evaluated photoactive chemical absorbers currently used in sunscreens are unstable upon UV radiation. This was mainly due to either photoisomerisation and/or photofragmentation of some active chemical ingredients.

An examination of the photochemistry of 2-ethylhexyl-*p*-methoxycinnamate (2-EHMC), an ultraviolet B absorber that was found in all the suncare products investigated in this study was undertaken. Irradiation of dilute (~ 10^{-6} M) solutions of EHMC with wavelengths of light greater than 300 nm results in *trans* - *cis*-

photoisomerisation leading to a photostationary equilibrium mixture. However, pure or concentrated solutions of 2-EHMC upon prolonged irradiation showed additional photoproducts. These were isolated by preparative high performance liquid chromatography (HPLC) and characterised by nuclear magnetic resonance (^{1}H NMR) spectroscopy, which was used to identify them as [2 +2] cycloadducts of 2-EHMC. There are 13 possible dimers formed via a [2+2] cycloaddition reaction mechanism across the ethylenic double bond, however only the stable and energetically favoured isomers were isolated.

In addition, *ab initio* molecular orbital calculations have been used to investigate the structures and the transition states of the various dimers resulting from the cycloaddition reactions. Geometry optimizations and energy calculations were performed with the Gaussian 98 program, using the B3LYP density functional and 6-31+G (d) basis set. GaussView was used to visualize the transition state structures. The theoretical calculations predicted the most stable dimer forms. The *trans-trans* configuration at the cyclobutane ring of the 2-EHMC adduct gave relatively more stable photoproducts. The theoretical results have been confirmed by HPLC isolation experiments, which together with the UV spectra of the different products; verify the presence of the different conformers of 2-EHMC.

Preface

The experimental work described in this thesis was carried out in the School of Chemistry, University of KwaZulu-Natal, Westville Campus, Durban from July 2001 to December 2007 under the supervision of Prof. B.S. Martincigh.

These studies represent original work by the author and have not otherwise been submitted in any form for any degree or diploma to any tertiary institution. Where use has been made of the work of others it is duly acknowledged in the text.

DECLARATION 1 – PLAGIARISM

I Waudo Lyambila declare that

1. The research reported in this thesis, except where otherwise indicated, is my original research.

2. This thesis has not been submitted for any degree or examination at any other university.

3. This thesis does not contain other persons' data pictures, graphs or other information, unless specifically acknowledged as being sourced from other persons.

4. This thesis does not contain other persons' writing, unless specifically acknowledged as being sourced from other researchers. Where other written sources have been quoted, then:
    a. Their words have been re-written but the general information attributed to them has been referenced.
    b. Where their exact words have been used, then their writing has been placed in italics and inside quotation marks, and referenced.

5. This thesis does not contain text, graphics or tables copied and pasted from the Internet, unless specifically acknowledged, and the source being detailed in the thesis and in the References sections.

Signed……

DECLARATION 2 - PUBLICATIONS

DETAILS OF CONTRIBUTION TO PUBLICATIONS that form part and/or include research presented in this thesis (include publications in preparation, submitted, *in press* and published and give details of the contributions of each author to the experimental work and writing of each publication)

1. Walyambillah Waudo[1], Bice S. Martincigh[2], Harald Maier[3] and Konrad Brunnhofer[4],

   A study of the photostability and broad-spectrum protection of 25 commercially available Australian sunscreens; in preparation

   [1] Main author, [2] Supervisor, [3, 4] Obtained the UV transmission spectra for all the suncare products and purchased the products.

2. Walyambillah Waudo[1], Bice S. Martincigh[2] and H. Gert Kruger[3]

   A computational study of the photodimerisation of 2-ethylhexyl-*p*-methoxycinnamate; paper in preparation

   [1] Main author, [2] Supervisor, [3] Helped with computational modelling work.

Signed:

Acknowledgements

I would like to express my sincere gratitude to my supervisor, Prof. B.S. Martincigh for guidance and support throughout this project. Her energy and enthusiasm enabled me to receive scholarship funding to advance my academic career. Dr H. G. Kruger deserves a special acknowledgement since he shared with me most of the difficult moments that were related to the computational modelling studies.

My laboratory colleagues, Ali Mohammed Salim, Tavengwa Bunhu, Georges Jasper Mturi, Janine Kasavel, Dr Moses Rotich, Avashnee Sewlall, and Rivash Panday, were always generous with their time, expertise, encouragement, understanding and efforts to create space for research and writing.

I am also grateful to the technical staff, Raj Suchipersadh, Kishore Singh, Logan Murugas, Anita Naidoo and Enoch Mkhize. Kishore Singh, especially for providing help in using new software programmes. You have all been so wonderful; I really couldn't have done it without your help.

I give many thanks to all my friends at the School of Chemistry. The time spent with them has been pleasant memories which I would always like to cherish.

My Kenyan colleagues have just been wonderful. I am proudly grateful to Dr Martin Onani, who supported me with care and love in the most difficult times. You were always a quick phone call away and your emails kept me going. Thanks to Mwalimu Ali, who encouraged me and kept me focused to embark on this work. The wonderful time and comradeship we shared in the lab is fully cherished forever.

Words cannot express my sincere gratitude to my wife, Anne, for her love, dedication, patience and encouragement. I could not have followed this dream without your support and understanding. Our children have been a source of solace and encouragement. Thank you for the sacrifice, for all these belongs to you.

Finally the National Research Foundation for awarding me a bursary and the University of KwaZulu-Natal for graduate assistantship. Jomo Kenyatta University of Agriculture and Technology for granting me study leave.

TABLE OF CONTENTS

List of abbreviations

ACN	Acetonitrile
APCIMS	Atmospheric pressure chemical ionization mass spectrometry
AVO	Avobenzone
BCC	Basal cell carcinoma
Benz-3	Benzophenone-3
BLYP	Becke, Lee, Yang and Parr
$CDCl_3$	Deuterated trichloromethane
^{13}C NMR	Carbon-13 Nuclear Magnetic Resonance Spectroscopy
CPU	Central processing units
COLIPA	European Cosmetic Toiletry and Perfumery Association
DFT	Density functional theory
DNA	Deoxyribonucleic acid
2-EHMC	2-ethylhexyl-*para*-methoxycinnamate
FTIR	Fourier transform infrared
G03	Gaussian 03
G98	Gaussian 98
GC	Gas chromatography
GC-MS	Gas chromatography mass spectrometry
GTO	Gaussian type orbitals
ΔG	Change in Gibbs free energy
H	Hamiltonian operator
HBO lamp	Osram HBO 500W/2 High pressure mercury lamp
^{1}H NMR	Proton Nuclear Magnetic Resonance Spectroscopy
HF	Hartree-Fock
HPLC	High performance liquid chromatography
HS	Homosalate
ΔH	Change in enthalpy
$h\nu$	Electromagnetic radiation
IR	Infrared spectroscopy

IRC	Intrinsic reaction co-ordinates
LCAO	Linear combination of atomic orbitals
MBBT	Methylene bis-benzotriazolyl tetramethyl butylphenol
MBC	Methybenzylidene camphor
MED	Minimal erythemal dose
MeOH	Methanol
MM	Malignant melanoma
MP2	Second order Møller-Plesset
m/z	Mass to charge ratio
NMR	Nuclear magnetic resonance
NMSC	non-melanoma skin cancer
NRF	National Research Foundation
OCTY	Octocrylene
ODS	Octadecyl silane
OT	Octyltriazone
Padimate-O	Octyl dimethyl PABA
PABA	*para*-aminobenzoic acid
PBSA	2-phenylbenzimidazole sulfonic acid
PDA	Photodiode Array
PES	Potential energy surface
PM3	Parametric method number 3
RHF	Restricted Hartree-Fock
RNA	Ribonucleic acid
ROS	Reactive oxygen species
SCC	Squamous cell carcinoma
SED	Standard erythemal dose
SPF	Sun protection factor
STO	Slater type orbitals
SCRF	Onsager self-consistent reaction field
THF	Tetrahydrofuran
TLC	Thin layer chromatography
TS	Transition state
UHF	Unrestricted Hartree-Fock
UVA	Ultraviolet A

UVB	Ultraviolet B
UVC	Ultraviolet C
UVR	Ultraviolet radiation
UV/VIS	Ultraviolet/visible
ψ	Wave function
λ	Wavelength
λ_{max}	Wavelength of maximum absorption
ϕ	Atomic orbitals
^{o}C	Degrees Celsius
ν_{max}	Frequency of maximum absorption
%	Percent

CHAPTER 1

Introduction

This thesis describes an investigation of the broad-spectrum protection and photostability of several Australian sunscreen products. Australian products were chosen in particular because Australia has one of the highest incidences of skin cancer worldwide. The reasons for this escalation are largely unknown although many people believe it can be imputed primarily to a more frequent and prolonged exposure to solar ultraviolet radiation. These topical preparations are of particular interest because they afford the consumer some degree of protection against the harmful effects of solar ultraviolet (UV) radiation. Thus, photochemical reactions involving these preparations are of great concern. In addition, the thesis describes some aspects of the photochemistry of the sunscreen absorber, 2-ethylhexyl-*p*-methoxycinnamate (2-EHMC) which was present in all the products studied.

1.1 Solar UV radiation

Solar UV radiation can be divided in three broad regions, according to its biological effects, namely, the ultraviolet A, B, and C regions [1]. The longest UV wavelengths are found in the ultraviolet A (UVA) region of 320 to 400 nm, which was once thought to be harmless because of its low energy. The intermediate range is ultraviolet B (UVB) from 280 to 320 nm, part of which is absorbed by the stratospheric ozone layer such that it does not reach the earth's surface. The rays in the third region, the ultraviolet C (UVC), are the shortest ranging from 100 to 280 nm. They are the most energetic and hence more deleterious. Luckily, these do not reach the earth's surface because they are absorbed by the ozone layer as well as molecular oxygen and water vapour in the atmosphere. In the absence of the stratospheric ozone layer most of the solar UVC radiation would penetrate to the earth's surface and because of its high energy it would destroy animals and plants in a very short time [2].

In the last few decades it has been noted that the stratospheric ozone layer, that shields us from this harmful UV radiation, is on the decline [2, 3]. The major factor responsible for the destruction of the ozone layer is anthropogenic activities. The emissions of chlorofluorocarbons (CFCs) in the atmosphere are some of the major contributors. These gases, having no natural sources, are non-toxic and inert in the troposphere, but are photolysed in the stratosphere, thereby generating reactive chlorine atoms and radicals that catalytically destroy ozone. Molina and Rowland received a Nobel Prize for chemistry in 1995 for their studies identifying the potential effects of chlorofluorocarbons (CFCs) on stratospheric ozone [4]. Other anthropogenic contributions to ozone depletion may include global changes in land use and the increased emission of nitrogen dioxide as a result of fertilizer applications. The emission of greenhouse gases, such as carbon dioxide and oxides of sulfur, into the atmosphere also have adverse effects on ozone. This has led to a continuous and steady depletion of the ozone protective layer. The depletion of ozone over Antarctica, associated with the polar vortex, creating ‚ozone holes' would also increase the effective environmental UV-dose. These decreasing concentrations of ozone in the stratosphere therefore mean that more UVB radiation can now reach the earth's surface [5, 6]. This then radically influences the effects of UV radiation on the environment. Thus an increase in the UVB that accompanies ozone depletion will increase the amount of biologically active radiation present in ambient sunlight. UVB radiation has long been recognized as the principal cause of erythema and skin cancer [7, 8]. It has been estimated that a 1% decrease in ozone levels is followed by a 1-2% increase in melanoma mortality [9, 10].

In addition, the amount of UV radiation transmitted through the atmosphere depends on other variables besides stratospheric ozone. Apart from the thickness of the ozone layer, the altitude also influences the amount of UV radiation that reaches the earth [11]. The slant angle of the sun is very important. Radiation follows a longer path through the ozone layer (and consequently more UV light is filtered out) at high latitudes and in winter than in low latitudes or in summer. This means that the highest daily values generally occur at the lowest latitudes (tropics) and in summer when the midday sun is closest to overhead. In general, the amount of UV radiation at a particular location on

the earth's surface changes throughout the day and with the season as the sun's position in the sky changes [12, 13].

Because of the biological activity of UVB, such increases are likely to have marked consequences for humans. Some of these consequences could be beneficial, e.g. a greater production of vitamin D in the skin of humans, but is far more likely to be detrimental. During an individual's lifetime, the skin is continuously exposed to a large amount of irradiation from sunlight. The health risks associated with exposure to UV include both acute and chronic effects and will vary according to the nature of exposure. High doses of UV radiation produce sunburn (erythema) in the human body, immune suppression and enhance development of skin cancer [14, 15]. This, of course, varies with occupation, recreational habits, geographical factors and clothing [16] . In addition to the cosmetic ill-effects of chronic exposure to sunlight, skin which has been damaged by sunlight is predisposed to the development of pre-malignant and malignant skin tumours. In addition the risk for skin cancer development is also dependent on an individual's skin characteristics, e.g. skin phototype, genetic predisposition such as the DNA repair disorder *Xeroderma pigmentosum*, and other factors.

1.2 The effects of UV radiation on humans

There are three major human organ systems whose cells and tissues are commonly exposed to solar radiation: the skin, the eye and the immune system. The effects and the associated hazards are discussed in the following sections.

1.2.1 Effects on the skin

The skin is composed of three layers. The outer part is the epidermis, which is usually 75 to 150 μm in thickness, the dermis (middle layer) and subcutaneous tissue (Figure 1). The outermost layer of the epidermis is called the *stratum corneum* and is mainly composed of peeling or dead cells (keratinocytes). This thin layer provides an effective barrier against water loss, trauma and micro-organisms. The dermis contains the

collagen fibres and fibroblasts/fibrocytes that give the skin its elasticity and supportive strength. It also supports the numerous blood vessels, nerves and cells of the immune system. Hair follicles and sweat glands originate in the dermis and open directly onto the skin surface.

Solar UVB radiation is biologically beneficial to humans because it is used for the synthesis of vitamin D from 7-deoxycholesterol which is critically important in the maintenance of healthy bones [17, 18]. It also produces melanin that is responsible for the pigmentation of the skin and is the body's most important protection mechanism against UV radiation. Furthermore, melanin acts as a scavenger for free radicals [19].

The layer of the skin affected by UVB radiation is the epidermis (the *stratum corneum*). The photons of UVB radiation are absorbed in the first layers of skin, composed of dead cells of the *stratum corneum,* and there is no penetration beyond a few millimetres. Hence, the biological effects of UVB radiation are located primarily within the epidermis. However, wavelengths in the UVA region are able to penetrate further and reach the blood system. Therefore the outermost layer of the skin provides considerable

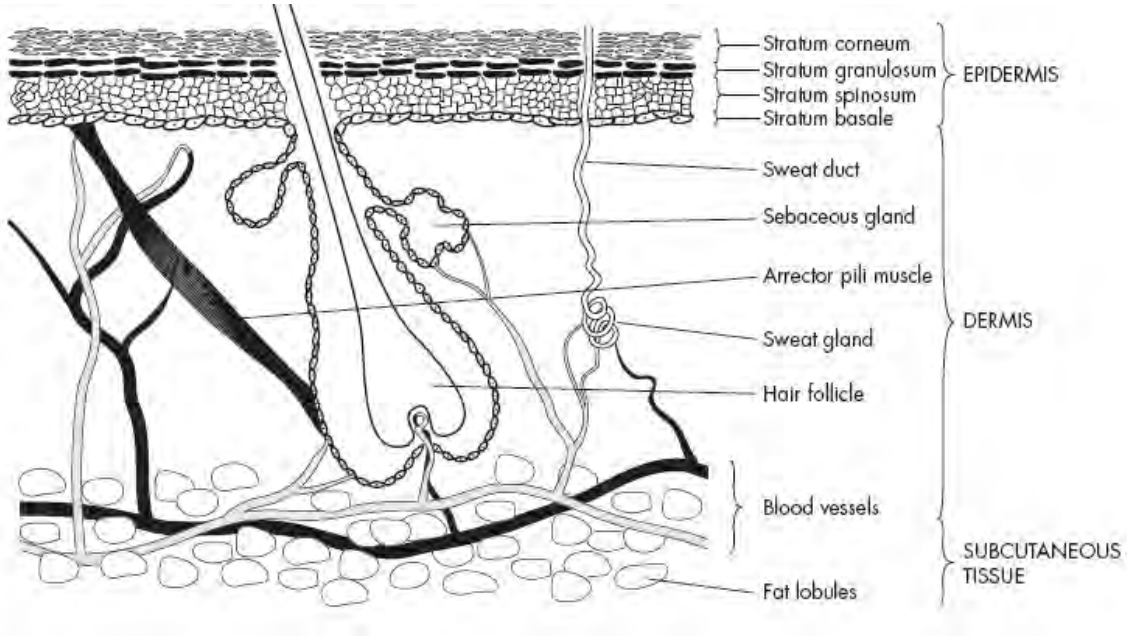

Figure 1 A diagrammatical cross-section through the human skin [20].

protection from sunlight. Although melanin acts as a natural skin sunscreen excessive exposure to UV radiation aggravates the photoprotection mechanism and subsequently leads to increased risk of skin cancer. Symptoms of sunburn include reddening of the skin and, in severe cases, blisters. Whether an individual sunburns or not is dependent on many variables: duration and intensity of exposure, season, latitude, altitude, smoke, clouds and degree of natural protection afforded by the epidermis. The degree of protection is determined by two factors: the thickness of the *stratum corneum* and the quantity of melanin it contains. The severity of the effects of UV radiation on the skin depends on skin pigmentation. People with fair skin are more likely than those with more pigmented skin to experience erythema, oedema and skin discomfort after sunlight exposure and are more likely to develop melanoma than those with darker skin. For example, humans living in equatorial Africa have larger amounts of the dark pigment, melanin, in their skin to protect the skin against UV radiation than humans from the temperate zones [21]. These people are most resistant to sunburn because of the dark pigmentation, but are equally vulnerable after long exposure to UVB. For light–skinned populations the problems due to UVB radiation are enhanced. People with the most sensitive skin can sometimes obtain a moderate to severe sunburn in less than an hour [10]. It has also been demonstrated that small amounts of UVA or solar-simulated UV are capable of producing cutaneous photodamage. Even suberythemal doses of repetitive exposure may lead to photoaging of the skin. Photoaging is the accelerated aging of the skin due to long-term exposure to sunlight, particularly UVA radiation [22]. Symptoms include loss of skin elasticity, wrinkles, altered pigmentation, and a decrease in collagen, a fibrous protein in connective tissue.

Skin cancer is the most common cancer especially among light-skinned people. It is well documented that skin cancer can be caused by overexposure to solar UV light [23]. There are three types of skin cancers that are associated with UV overexposure, namely, basal cell carcinoma (BCC), squamous cell carcinoma (SCC) and cutaneous melanoma (CM). BCC and SCC are generally called non-melanoma skin cancers (NMSC) and, although rarely fatal, they can cause disfiguration. About 75% of basal cell carcinomas and more than one-half of all squamous cell carcinomas occur on the head and neck, which are the sites of highest sun exposure. They also occur on the forearms and hands,

or on any part of the body commonly exposed to the sun. These predominantly arise as a result of direct damage to the DNA by interaction with UVB radiation [24]. The occurrence of non-melanoma skin cancer, for example, is directly correlated with the accumulative doses of UV light over a person's lifetime [25] . Malignant melanoma arising from melanocytes (5 – 10% of epidermal cells) is the least common but most dangerous type of skin cancer with about 25% of diagnosed melanomas resulting in death.[26]. For example, in the United States of America over 60000 new cases of melanoma were diagnosed in 2006 and about 8000 deaths were predicted by the American Cancer Society [27]. A history of exposure to large doses of solar radiation sufficient to cause sunburn in childhood is particularly important in the formation of melanoma which could occur many years later. The incidence of skin cancer increases dramatically with age because older people have had more opportunities to be exposed to UV radiation and their capacity to repair the damage from UV radiation is diminished [28].

Although not incident on the Earth's surface, UV radiation from 245 to 290 nm is efficiently absorbed by DNA and causes damage but penetrates poorly into the skin [29]. However, UVB irradiation to the skin also has direct effects on biomolecules. The four DNA bases (thymine, guanine, cytosine and adenine) have conjugated double bonds and can absorb UV radiation and are promoted to a higher energy level. UVB induces molecular rearrangements of the DNA with characteristic formation of specific photoproducts [30]. These results in a [2 + 2]-cycloaddition between adjacent thymine bases in DNA to form cyclobutane-like *cis, syn*-thymine dimer as the major product (see Figure 2). Other pyrimidine dimers that form upon UV radiation are between thymine and cytosine as well as between cytosine and cytosine, with the latter being the most lethal causing death of cells.

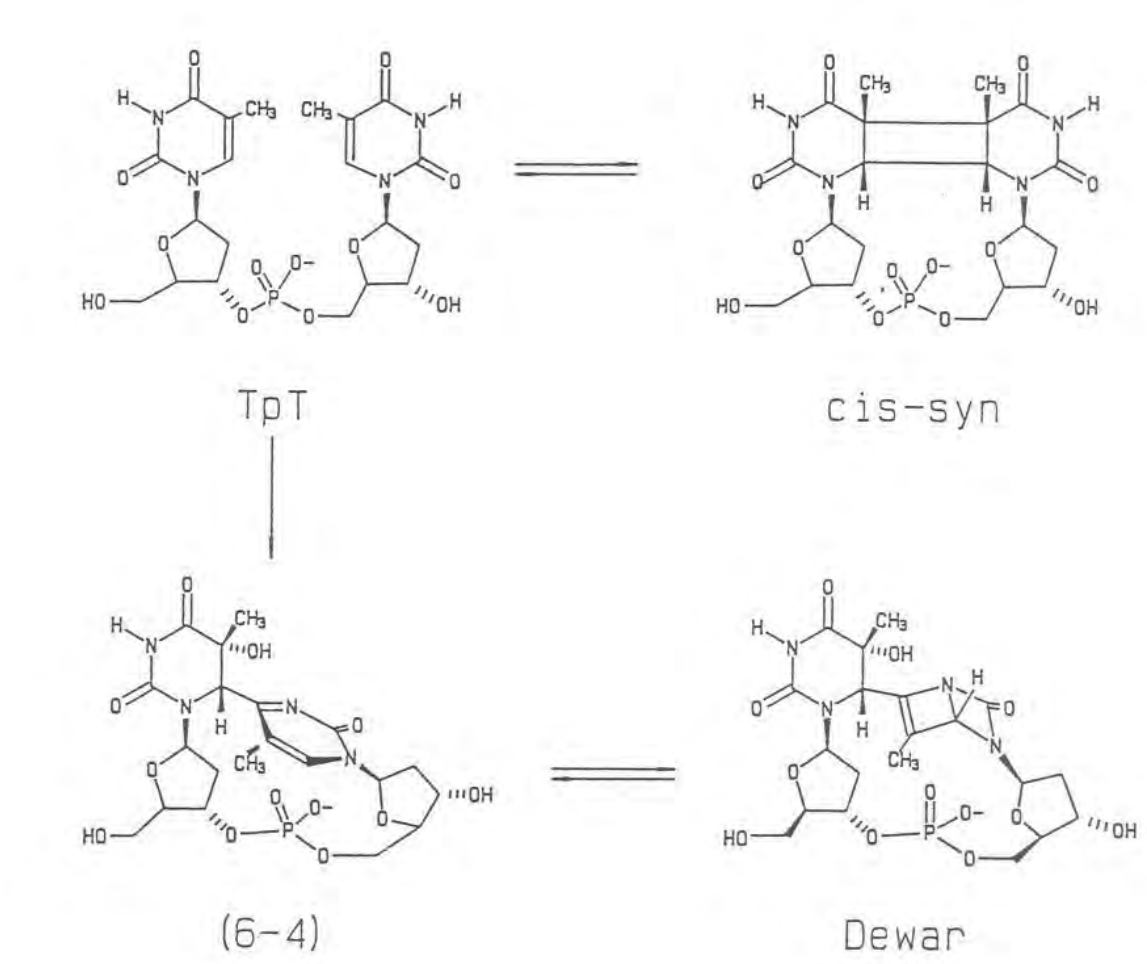

Figure 2 The structures of the cyclobutane dimer (cis-syn) , pyrimidine(6-4) pyrimidone and Dewar pyrimidinone induced in the thymine dinucleotide TpT [31]

The formation of cyclobutane pyrimidine dimers, such as thymine-thymine, and the (6-4) the 6-carbon of the other, is the principal cause of skin cancer as it blocks cell replication and transcription [32]. In the presence of UVA radiation the (6-4) photoproduct may be converted to its Dewar photoisomer, which although quite strained, is stable under physiological conditions [7]. This interaction has recently been demonstrated in human skin *in vivo* [14, 33]. Because the Dewar product is formed from the (6-4) product at wavelengths present in sunlight at sea level, it may hitherto play an unrecognized, and possibly important, role in the mechanism of sunlight-induced skin cancer [7]. Other known effects are the photoisomerisation of *trans-cis* urocanic acid, DNA strand-breaks, DNA-crosslinks, DNA protein crosslinks and the generation of reactive oxygen species (ROS) [34]. In general, the action spectra for the formation of

the photoproducts *in vitro* correlate well with the absorption spectrum of DNA, which has a maximum absorption at about 260 nm. UVR-induced epidermal DNA photoproducts are believed to give rise to mutations, e.g. in the p53 gene, which are thought to be the initial processes in UVR-induced skin cancer. DNA damage leads to a dramatic increase of the p53 protein. The p53 gene is the most frequent target of genetic alteration identified so far in human cancers [35]. The basic function of the p53 protein is to maintain a cell in normal status against various extracellular stresses including UV radiation. Therefore, when the DNA damage is too severe, p53 induces apoptosis of the cell in order to inhibit carcinogenesis.

These DNA photolesions (damage) are repaired by means of the nucleotide excision repair complex and other less important repair mechanisms. Formation of cyclobutane pyrimidine dimers, if not repaired through nucleotide excision repair, lead to signature mutations [36, 37]. The UV signature mutation is associated with dipyrimidine sequences, a C:G to T:A mutation, a mutation of this type is known as a transition, and is defined as a change from one pyrimidine (cytosine or thymine) or purine (guanine or adenine) to the other. The signature mutation caused by ultraviolet light is a CC to TT mutation caused when a CC dimer is mismatched with adenine bases during replication. Because of these mutations the connection between ultraviolet damage to DNA and cancer is quite clear. These CC to TT mutations often show up in the p53 tumour suppressor gene in skin cancers, compromising its watchdog function.

Nucleotide excision repair mechanisms play a central role in preventing carcinogenesis. Patients with *Xeroderma pigmentosum* (XP), a rare genetic condition, are deficient in nucleotide excision repair and are greatly susceptible to the development of skin cancer [38-40]. They have approximately a thousand-fold higher chance of contracting skin cancer than normal subjects [7]. This is because the misrepaired DNA damage results in mutations and it is mutations in genes coding for proteins involved in the regulation of replication bond cell differentiation that lead to skin cancers. Other mutations lead to cell death or benign mutants and tumours. A reduced capacity to excise UVB-induced pyrimidine dimers leaves a patient at an increased risk of developing skin cancer.

Although UVB photons are much more energetic than UVA photons, and are mostly responsible for sunburn, suntanning and photocarcinogenesis, UVA is also suspected of playing a significant role in photoageing. The intensity of UVA that reaches the earth's surface is 10 – 100 fold higher than that of UVB. Some studies have shown that more photons of UVA (approximately 1000 times) are required to produce erythema compared with UVB [41, 42]. Since UVA penetrates the earth's atmosphere more readily than UVB or UVC, there is therefore more UVA than UVB (depending upon the season of the year). The UVB has short wavelength and only penetrates the epidermis while the more intense UVA reaches the dermis, the deeper layers of the skin. Absorption of UVA induces photobiologic effects within the skin that lead to the visible and histological differences of photoaged skin, although mechanisms by which UVA-induced photodamage occur have not been completely determined. The main initial event in the interaction of sunlight with the skin is the generation of excess free radicals, mainly ROS. ROS include free radicals like superoxide anion ($O_2^{\cdot -}$) and the hydroxyl radical ($.OH^{\cdot}$), as well as non-radicals like hydrogen peroxide (H_2O_2) and singlet oxygen ($^1O_2$) [43]. These free radicals are at the beginning of a cascade of molecular biological events with potential damaging and possible beneficial effects. ROS lead to oxidation of DNA, proteins and membrane damage which are considered to be the initial steps with respect to photoageing and UV-induced skin cancer. Consequently, the contribution of UVA to erythema and to possible skin damage can be considerable, in spite of the fact that it is much less damaging per unit photon. To prevent oxidative damage, mammalian cells have developed a complex antioxidant system that includes non-enzymatic antioxidants such as α-tocopherol, ascorbic acid, glutathione and β-carotenoids and enzymatic antioxidants such as superoxide dismutase (SOD), catalase and glutathione peroxidase (GPx).

Some studies have shown that absorption of UVA by *trans*-urocanic acid, a molecule found in large amounts in the epidermis of the skin, forms singlet oxygen. The formation of singlet oxygen causes photodegradation of the skin and results in photoaging of the skin [44] which seems to be a causal factor in some types of cancer.

The work of Setlow *et al*. [45] showed that exposure to UVA radiation could cause melonoma as exhibited in *Xiphophorus,* a special hybrid fish showing the potential role of UVA in the pathogenesis of melanoma. This is also a reason to believe that melanoma could be caused by exposure to wavelengths longer than UVB such as UVA.

1.2.2 Effects on the eyes

The cornea of the eye, which covers the iris and the lens, is the tissue most susceptible to UVB damage. There is little UVB radiation that penetrates past the lens to the vitreous humor or the retina, the tissues behind the lens. The most common eye problem associated with UV exposure is photokeratatis or snow blindness, an inflammation or reddening of the eyeball. Other symptoms include a feeling of severe pain, tearing, avoidance of light, and twitching [10]. These symptoms are prevalent not only among skiers, but also among people who spend time at the beach or other outdoor locations with highly reflective surfaces. Another common ocular disease associated with UVB radiation is cataracts, a degenerative loss in transparency of the lens that frequently results in blindness unless the damaged lens is removed. Cataracts are the leading cause of blindness in humans in the world. More severe, but less widespread, ocular disease is squamous cell carcinoma, which affects the cornea and ocular melanoma, which affects the iris and the related tissues [46].

1.2.3 Effects on the immune system

The human skin contains numerous cells that fight infection that are produced by the immune system. For example, the Langerhans cells have an antigen-presenting function and are an integral part of the immune system. However, Langerhans cells, which migrate through the epidermis, are susceptible to damage. UVB exposure initiates a series of events that modify gene expression profiles and alters the immune system of the skin. As previously mentioned, UVB is responsible for acute skin damage such as sunburn (erythema), photoaging of the skin [47-49] and also induces specific DNA

damages such as cyclobutane dimers and 6-4 photoproducts between neighbouring pyrimidine bases on the same DNA strand which are precursors of skin cancer [50]. The Langerhans' cells limit damage to the immune system by recognizing and destroying malignant cells. However, the incident solar UV radiation interactions can be very detrimental for living tissues since they result in photoallergic and phototoxic responses [51]. This is because of the enhanced UVB radiation that is linked to suppression of these cells. This then reduces resistance to certain tumours and infections. These findings suggest that sun exposure favours the induction of suppressor pathways and hence may limit immune responses against tumour cells. A decrease of local immune system function may contribute to an elevated risk of skin cancer. Some of the examples reported for suppressed immune responses to UVB are herpes, tuberculosis, leprosy, trichinella, candidiasis, leishmaniasis, listeriosis and Lyme disease [10].

1.3 Photoprotection

It has been shown that exposure to UV radiation is significant in the induction of skin cancers. Although melanin acts as a natural skin photoprotectant, excessive exposure to UV radiation aggravates photoprotective mechanisms and subsequently leads to the development of skin cancer [15]. With new emerging evidence of the damaging effects of UVA rays [52, 53] and the depletion of the ozone layer through the use of chlorofluorohydrocarbons, as well as demographic considerations and the popularity of modern leisure outdoor lifestyles, the need for photoprotection and the production of new, safe, and effective sunscreen filters is paramount. The mainstay of photoptotection is broad-spectrum protection and hence the need for developing effective sunscreens to help and allow people to spend longer hours in the sun while reducing the adverse effects. This has led to an upsurge of industrial production of sunscreens.

Sunscreens are topically applied chemical formulations used to protect a user from the deleterious effects of solar UV radiation [54-56]. These topical photoprotectants have been in use for at least eighty years. The first commercial sunscreen appeared in 1928 and contained benzyl salicylate and benzyl cinnamate as the active ingredients [57]. The early chemical sunscreens were less efficient at absorbing radiation than modern

sunscreens and were easily removed by sweat or swimming. However, modern formulations have taken advantage of chemicals which are capable of absorbing larger amounts of energy in the broad spectrum range of both UVA and UVB and, due to their lipid solubility, are retained on the skin and resist removal from the skin.

In addition, the continuing drive to maintain a healthy skin in today's society has also created a huge market for topical photoprotectants. There has been a dramatic growth in the use of sunscreen agents not only in traditional sunscreen products but for a variety of other personal care formulations including facial and body care products. For example, sunscreen agents are included in moisturizers, makeup, lipsticks, shampoos and hair gels in order to prevent the degradation of cosmetic products by sunlight and to provide photoprotection for the consumer. The medical community, through public health campaigns, has been at the forefront of alerting the public of the risks associated with UV radiation.

Sunscreens when properly applied can considerably reduce the risk of squamous cell carcinoma [58, 59]. However in the case of basal cell carcinoma and melanoma, studies tend to be controversial as less evidence is adduced to the reduction of their occurrences with the use of sunscreens. There have even been cases where there is an increased risk for users [59]. A recent study revealed the protection against UV-induced immunosuppression by commercial sunscreens [60].

There are two measures of a sunscreen's effectiveness: The Sun Protection Factor (SPF) and its substantivity, i.e. the ability for the sunscreen product to remain adsorbed on the skin despite washing, swimming or perspiration. The (SPF) is defined as the ratio of the minimal dose of UVB expressed as Joules per cm^2 required to produce minimal erythema on protected skin to that required to produce the same minimal erythema on unprotected skin usually assessed about 24 hours after irradiation [61]. This can be expressed mathematically as follows:

$$\text{SPF} = \frac{\text{Minimal Erythymal Dose in sunscreen-protected skin}}{\text{Minimal Erythymal Dose in non-sunscreen-protected skin}}$$

The sun protection factors are determined by measuring protection only against UVB radiation. This is done by irradiating the backs of a panel of subjects with skin types I, II, and III according to Fitzpatrick skin classification model [62] and estimating the minimal erythemal dose by producing sunburn. SPF determinations are done *in vivo* according to the European Cosmetic Toiletry and Perfume Association (COLIPA) standards where the erythemal dose in the skin is measured [63]. The determination of SPF with UVA is not yet possible on human skin. Evaluation of UVA protection remains a problem because of the very large doses required to induce UVA erythema. Hence, UVA protection is not considered in SPF testing. However, *in vivo* methods such as immediate pigment darkening (IPD), persistent pigment darkening (PPD) and protection factor in UVA are presently being used for evaluating the efficacy of sunscreens against UVA. The calculation of the SPF also allows for comparison of efficacies between sunscreens as a measure of effectiveness.

Substantivity is the sunscreen's ability of maintaining its features on the skin under stressful conditions including continued and repetitive water exposure or sweating [64]. Otherwise any induced decomposition may reduce its screening effects and generate toxic degradation products [65]. There are presently several approaches for improving the substantivity of sunscreen formulations, such as natural and synthetic complex polymer preparation [66], proper solvent selection [67] and encapsulation processes [68, 69].

Although the sunscreen is primarily used as a strategy against sunburn, paradoxically it has also been associated with an increased risk for the development of skin cancer. There have been reports of increased numbers of skin cancers, which have been associated with the indiscriminate increase in the usage of sunscreens [70-73]. Skin cancer has become prevalent especially in modern times and maybe the increase can be related to the wider use of skin creams either for protective purposes or merely for beauty. The adoption of sunscreen usage, may have inadvertently fuelled an increase in cutaneous malignant melanoma (CMM) incidence [70, 74]. This is because the use of photoprotectants invites prolonged sun exposure and in the end this is followed by increased UV radiation reaching the skin [75].

Secondly, another possibility for this sunburn might not be due to a failure of a sunscreen *per se*, but rather due to the failure to use the sunscreen appropriately. Although it is recommended that an application thickness of 2 mg cm^{-2} would suffice the reality might be different. This is because people tend to apply far less sunscreen than is usually recommended. A number of studies have shown that consumers apply approximately one quarter to a half of the amounts used to measure SPF [76, 77]. Consequently, the SPF achieved will be considerably less than that expected and in many cases it will be half of that indicated by the product label. Therefore the protection against solar-induced erythema under real conditions is dependent upon the amount of sunscreen applied. When too little is applied it is believed that a lower sun protection will result than that indicated on the label [78].

Thirdly, studies have shown that the skin creams, which contain sunscreen chemical absorbers, could photolyse due to absorption of UV radiation to produce photoproducts that are carcinogenic or mutagenic [79].

Therefore the effectiveness of sunscreens depends on their ability to absorb or reflect sunlight, their formulation and their ability to withstand contact with water (through swimming) or perspiration.

1.4 Sunscreen formulations and their photochemistries

Sunscreens are designed to give a consumer the best possible protection. Therefore, in pursuit of this, each sunproduct formulator aims to give the consumer some special unique quality that is both aesthetically pleasing and at the same time inexpensive. As a result, the number and the ratio of ingredients of each product vary from one brand to the next, affecting the performance accordingly. Hence, the protective function of sunscreens is determined by the composition of their active ingredients. The present-day active ingredients incorporated into the formulations of sunscreens are classified into two broad categories, namely: as physical blockers or chemical absorbers. Table 1 shows a typical formulation found in a sunscreen.

Table 1 The approximate concentrations of some ingredients found in sunscreen formulations [61].

Ingredient	Content /% m/m
Cetyl alcohol	2
Waxes	1 – 5
UV-absorbers (actives)	1 – 25
Stearic Acid	1-5
Glycerin	≤ 5
Stearyl dimethicone	10
Triethanolamine	≤ 1.5
Preservatives	≤ 1
Deionised water	55-80

1.4.1 Physical blockers

Physical blockers are mostly inorganic compounds which reduce the amount of light penetrating the skin by creating a physical barrier that reflects, scatters or absorb the UV light reaching the skin surface. The most commonly used physical blockers include substances such as titanium dioxide (TiO_2), zinc oxide (ZnO) and iron oxide (Fe_2O_3). However, these substances are pigments which tend to whiten the skin when applied and are visible and therefore not aesthetically appealing. However, there are now newer micronized (10 – 100 nm) reflecting powders providing broad-spectrum protection against UV radiation through a combination of scattering and absorption [80]. Since micronized physical sunscreens reflect at wavelengths shorter than the visible spectrum they are invisible and thus more cosmetically acceptable. Micronized titanium dioxide is also chemically stable and does not cause photoallergic or contact dermatitis [81, 82]. Although it is effective in blocking shorter UV wavelengths, it has been reported that titanium dioxide can produce a number of functional changes in the cell membrane via photolysis [83, 84]. However, there are concerns that TiO_2 when irradiated with sunlight is photocatalytically active and can penetrate the skin to cause single and double–strand breaks in the DNA. Therefore the damage to the skin and subsequent damage to the

DNA is a matter of greater concern [85]. Therefore, to reduce the possibility of such activity on living tissues TiO_2 is often coated when used in cosmetic preparations. Microfine zinc oxide is transparent on the skin and does not produce the opaque "pasty" colour of zinc oxide as with the larger particle sizes [86].

1.4.2 Chemical absorbers

Chemical absorbers are usually organic compounds having a single or multiple aromatic structures often with attached hydrophobic groups (e.g. carbonyl moieties) to improve their absorbing properties. They are mostly aromatic acids or their esters or salts with the exception of the benzophenones. In fact, the esters are generally either *ortho*- or *para*- disubstituted aromatic compounds. This allows for electron delocalization, thereby allowing the compound to absorb the appropriate wavelength before it reaches the skin.

To be able to appreciate the functionality of sunscreen filters, it is important to have a brief understanding of their photochemistry. They can be considered to be photon-absorbing agents. They absorb radiation in the UV region and should undergo rapid vibrational relaxation back to the ground state or relax by photoemission. Once in the ground state, these molecules absorb another photon thereby repeating the process. In this way, the skin is shielded from damage by UV radiation. Therefore, any molecule which dissipates absorbed energy via harmless pathways can serve as a sunscreen absorber thereby eliminating any possible route to DNA damage. However, this is not always the case as the molecule may dissipate this energy as long-wave radiation and return to its original ground state or photoisomerisation, photodegradation and photosensitization can occur. This may lead to non-UV absorbing photoproducts.

The mechanism of absorption of light by chemical sunscreens and the possible routes for the dissipation of energy is illustrated in Figure 3 and will be discussed briefly. Firstly a molecule in the ground state absorbs a photon of energy and this causes it to be promoted to an excited electronic state. This is the first excited singlet state in which the electron spin orientation is maintained. The molecule in the singlet state can return to

the ground state by dissipating its energy through several pathways. It does this by either emitting its energy thermally as heat through a series of vibrational relaxation transitions (non- radiative decay) or as a photon of energy of longer wavelength by a process known as fluorescence (radiative decay). Although these are the preferred pathways for a sunscreen, as the harmful radiation is dissipated in a harmless way, this is not always the case. The molecule in the excited singlet state may also react with another molecule to form photoproducts or may transfer its energy by intersystem crossing to the triplet state. The triplet excited state can decay to the ground state via non-radiative (emission of heat) or radiative de-excitation (emission of a photon). The latter process is called phosphorescence as it occurs between two states of different spin.

Since the triplet excited state is long-lived ($\sim 10^{-4}$ s) it can readily undergo photochemical or energy transfer reactions. Among the photochemical reactions are processes like photofragmentation, photoisomerisation, cycloaddition and photoaddition/substitution reactions. These processes may alter or destroy the UV radiation absorption capacity of a sunscreen and are therefore undesirable. A molecule in a triplet state is also capable of transferring its energy to a nearby molecule. The triplet excited state (D*) acts as an energy donor to molecule (A) which is an acceptor. This phenomenon known as photosensitisation is illustrated in reaction (1.1).

$$D^* + A \rightarrow D + A^* \qquad [1.1]$$

The donor is referred to as a photosensitiser and this process may only happen if the energy of D* is greater than that of A*. Although this may be a desirable pathway for energy dissipation, photosensitization can lead to the formation of undesirable and often toxic products.

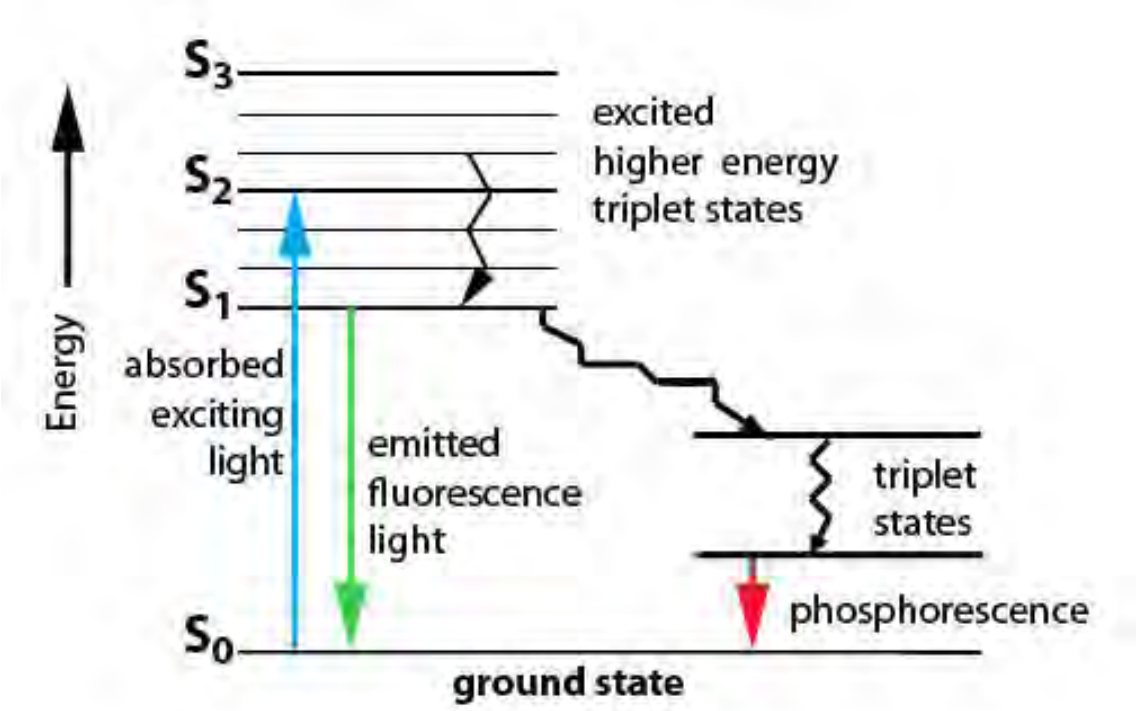

Figure 3 A Jablonski diagram showing the deactivation pathways of an excited molecule [87].

Ideally the energy acquired through absorption of solar radiation by active ingredients should be dissipated by radiative decay (fluorescence and phosphorescence), self-quenching or internal conversion and vibrational relaxation. However, photochemical reactions that give rise to many products, some with unexpected bond rearrangements frequently occur. Because chemical sunscreens are applied topically to the skin in relatively high concentrations (up to 25%), contact sensitisation of the skin can occur. Similarly, because these chemicals absorb radiation, they have the potential to cause photosensitisation of the skin.

The modern UV filters are currently classified into seven broad categories as shown in Figure 4 [61]. They are subdivided into different groups based on their ability to absorb either UVA or UVB radiation as follows: UVA (benzophenones, anthranilates and dibenzoylmethanes) or UVB (*p*-aminobenzoic acid derivatives, salicylates, cinnamates and camphor derivatives) and a few miscellaneous chemicals. Another attractive aspect of chemical sunscreens is that they are colourless as they do not absorb visible light and are therefore cosmetically acceptable to most people.

Cinnamates

These are basically UVB absorbers. 2-Ethylhexyl-*p*-methoxycinnamate (2-EHMC) is the most commonly used UVB chemical absorber in sunscreen products and is commercially available in its *trans* form. When *trans*-2-EHMC is irradiated by UV light it has been shown to isomerise to the *cis*-form [88, 89]. Although both the *trans*- and *cis*-isomers are good UV absorbers they have different absorption efficacies. This isomerisation results in UV absorbance changes during use thereby losing some of its absorbing ability. There also exists a photostationary state between the *trans*- and *cis*-isomers during continuous irradiation. In addition, it has also been shown that irradiation of pure or neat EHMC causes it to not only to isomerise but also to dimerise with itself through a [2 + 2]-cycloaddition reaction forming 13 possible isomers [90]. The dimerisation of 2-EHMC reduces further its absorption power. This definitely requires some elucidation and it is this aspect that has been investigated in this work.

There is also speculation that 2-EHMC can photobind to constituents of DNA [91]. The production of these photoproducts [lesions] could alter the biological function of DNA and cause adverse, mutagenic and carcinogenic effects [45, 92]. 2-EHMC has been shown to be mutagenic in the *Ames Salmonella typhimurium* test [93] and an initiator of tumours in hairless mice [94], although the relevance of these latter findings to human use is unknown. The work of Butt and Christensen [95] has also shown the toxic potential of 2-EHMC to mouse cells after UV radiation. This toxicity was attributed to the existence of photoproducts after 2-EHMC had been exposed to UV radiation. Although the probability of adduct formation between 2-EHMC and constituents of DNA could be low there can be a cumulative effect.

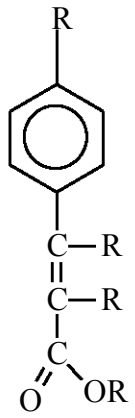

Cinnamate derivatives

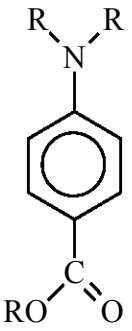

p-aminobenzoic acid derivatives

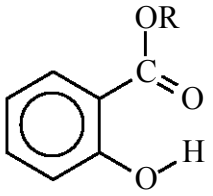

Salicylate derivatives

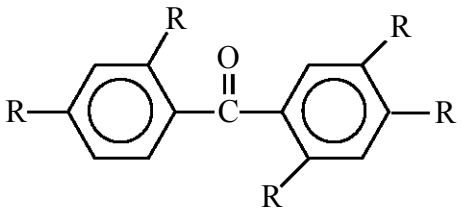

Benzophenone derivatives

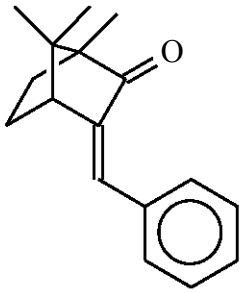

Camphor derivatives

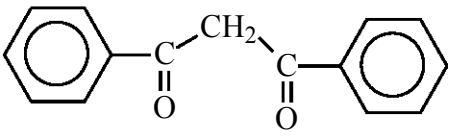

Dibenzoylmethane derivatives

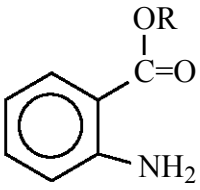

Anthranilate derivatives

Figure 4 The seven major groups of chemical absorbers currently used in the preparation of sunscreen formulations.

Para-aminobenzoic acid

This is a UVB absorber which was initially one of the most widely used products. This was an effective agent although harmful side effects have been detected. It has been shown to photofragment and also acts as a triplet state sensitizer converting the harmless triplet oxygen $^3O_2$ into the more phototoxic singlet oxygen $^1O_2$ [96]. *Para*-aminobenzoic acid (PABA), has been shown to be absorbed by human cells [97] and photosensitise the dimerisation of thymine in DNA [97-99]. The photoproducts, which besides thymine dimers can include dimers formed between thymine and other nucleic acid bases, affect the normal genetic functioning. These photoproducts in the DNA are known to be toxic. Oxidized bases in DNA are potentially mutagenic and are also implicated in the process of carcinogenesis [98]. Therefore PABA is no longer used and it has been replaced as an active ingredient in sunscreens by its esters such as octyl dimethyl PABA (padimate-O). ODPABA has been relatively photostable although the work of Roscher *et al*. [100] showed that it can photodegrade. It has been shown by the work of Knowland *et al*. [101, 102] that can generate free radicals which are known to break DNA strands and inflict other damage most notably at guanine-cytosine (GC) base pairs [103].

Camphor derivatives

These benzylidene camphor derivatives are used as UVB absorbers and are often combined with other sunscreening agents. A detailed study of some benzylidene camphor derivatives has been published [104, 105]. Deflandre *et al.* [106] showed that methylbenzylidene camphor (MBC) can photoisomerise initially but reaches a photostable equilibrium between its isomers (i.e. *trans/cis*). Tarras-Wahlberg *et al*. [79] have observed that MBC in a thin film of an appropriate emulsion underwent an initial loss in absorbance due to a *trans-cis* photoisomerisation before attaining a photostationary state under continuous illumination. It has also been reported to have an estrogenic activity [107].

Salicylates

These are used alongside other UVB absorbers to enhance UVB absorption since on their own relatively high concentrations are required as they are very weak UV

absorbers. The salicylates have a low molar absorption coefficient. These were found to be fairly photostable [108].

2-*Phenylbenzimidazole sulfonic acid*

This is a UVB absorber with an absorption spectrum between 290 and 320 nm and a maximum absorption at approximately 302 nm. This is used in conjunction with other UVB absorbers. The work of Serpone *et al.* [109] using solvents of different polarities has shown that PBSA can photodegrade. It appears that the degree of photodegradation is dependent on the nature of the solvent or emulsion. Sewlall, however, found PBSA to be photostable but showed it can actually cause DNA cleavage [110]. This is supported by the studies of Stevenson and Davies [111] who showed that although PBSA does not bind to the calf thymus DNA it still causes DNA cleavage.

Dibenzyolmethane derivatives

These are mostly UVA absorbers. The most frequently used UVA absorber is 4-*tert*-butyl-4′-methoxydibenzoylmethane (avobenzone or Parsol 1789) which efficiently absorbs in the UVA region with a maximum absorption ranging from 350 nm to 360 nm depending on the solvent used. Avobenzone exists in two tautomeric forms: the enol-form and the keto-form. The eno-form is predominant in solution and this is the form that is found in sunscreen formulations and is responsible for absorption in the UVA region as shown in the work of Andrae *et al*. [112]. It has been shown that dibenzoylmethanes lose much of their UVA absorption capacity after UV radiation through tautomerization, fragmentation and formation of new products with distinctly altered UV absorption characteristics [79, 113]. Avobenzone has been shown to photofragment/photodegrade upon exposure to UV radiation [113, 114] and thus it does not only photodegrade but also produces carbon-centred free radicals. The formation of free radicals and other short-lived reactive intermediates associated with irradiated sunscreen active ingredients has been shown to be toxic [34, 115]. The interaction between photoproducts and the thymine and thymidine bases does occur, increasing the rate of formation of potentially carcinogenic DNA photoproducts (e.g. the cyclobutane type pyrimidine dimers) [116]. Tarras-Wahlberg *et al.* [79] have also shown the loss of

absorption of avobenzone in solution, further reducing its efficacy. In general the photostability of avobenzone is largely influenced by solvent effects [117].

Modern sunscreen formulations use avobenzone in combination with 2-EHMC to offer broad-spectrum protection. However, investigations have shown that avobenzone seems to enhance the photodegradation of EHMC in a formulation where the two are in combination [118, 119]. Panday has shown that avobenzone photosensitizes the photoisomerisation of 2-EHMC [119]. However, Chatelain *et al*. [120] have been able to photostabilise these avobenzone/2-EHMC combinations by the addition of bis-ethylhexyloxyphenol methoxyphenyl triazine (Tinosorb).

Benzophenones

Some of the frequently used benzophenone absorbers are benzophenone-1, benzophenone-3, benzophenone-4 and benzophenone-8. Benzophenone-3 is the most commonly used benzophenone found in sunscreens and absorbs most efficiently in the UVB region and the UVA (320 – 400 nm) range with absorption peaks at 295 and 325 nm. The work of Serpone *et al*. [109] has shown benzophenone-3 to be unstable when irradiated in either a non-polar or a polar solvent at wavelengths greater than 290 nm. It has been shown to act as a photosensitiser in the generation of singlet oxygen [96]. There is now evidence that benzophenone-3 can be absorbed systemically following topical application to the skin [121]. The work of Sewlall [110] has shown that benzophenone-1 and benzophenone-8 cause DNA strand breaks. Schallreuter *et al.* [122] have reported that the oxidation of benzophenone-3 after topical skin application causes it to photofragment into benzophenone-3 semiquinone which is a highly potent electrophile. This reacts with anti-oxidant systems resulting in their inactivation which is harmful to the homeostatis of the epidermis.

Anthranilates

The most common among these are methyl anthranilate and homomethyl-N-acetyl anthranilate. They also tend to have low molar absorption coefficients and hence are weak absorbers on their own. Consequently, they are used in combination with other

active ingredients to enhance the sun protection factor. They have also been found to photosensitise the formation of singlet oxygen in a range of solvent systems [123].

A cursory look at some studies, however, has indicated that sunscreen active ingredients may undergo photofragmentation or photoisomerisation; transfer the energy acquired by absorption to other molecules or when applied to the skin react directly with biomolecules. Photofragmentation of sunscreen active ingredients is undesirable because it causes the absorbing molecule to dissociate into reactive fragments or intermediates (e.g. free radicals). In addition, this would reduce the efficacy of the sunscreen.

It is therefore apparent that understanding the photochemistry of sunscreens is of prime importance. This is particularly important since some side effects such as photoallergic contact dermatitis that have been observed in a few people when sunscreens were used [51, 124]. There is a wide variety of commercial formulations that are being marketed delivering protection against both parts of sunlight radiation (UVA 320-400 nm and UVB 280-320 nm). Therefore these UV filters have maximum allowed concentrations that have been set by various regulatory authorities in Australia, Europe, Japan and the USA. The concentrations of the UV filters in the sunscreen formulations must be monitored to assure the labelled SPF in the commercial preparations without exceeding the authorized levels. The sun protection factor (SPF) is measure of how one would burn while wearing a photoprotectant and when without it. This experimentally derived number is intended to provide the consumer with information concerning sunscreen products, giving an approximation of its protective effect on the skin against UVB. Therefore, a SPF 15 means that a sunbather protected by one of these formulations could remain in the sun 15 times as long as before obtaining a burn.

Therefore, in order to ensure adequate photoprotection during usage, the photochemical behaviour of sunscreen agents needs to be determined under conditions that parallel those encountered in the finished suncare preparations. Consequently, rapid, precise and accurate methods for checking the purity and spectroscopic characteristics of these products are necessary. Regular analyses are also required in the development of new

UV filters to check for their stability. Any photoproducts can also be monitored as part of quality control to see if they have any potential for toxic or allergic effects.

1.5 Photostability studies of some commercial sunscreens

Amongst all the properties studied during the formulation of new sunscreen preparations, the one major concern that draws special attention is the possible changes in screening efficiency under light irradiation. To be effective the filter should be stable photochemically in sunlight. Thus, a good UV absorber must dissipate the absorbed energy in a manner safe to the consumer. This means that the dissipation of excitation energy should proceed at a faster rate than side reactions. The ideal sunscreen is one where no photochemical or photosensitizing transformation of its components occurs with the formulation or on the skin. A high screening efficiency can only be guaranteed if a UV filter is of high photostability. Hence the photostability is of primary importance for the effectiveness of sunscreen products, since the decomposition of the UV filters under sunlight exposure reduces their expected screening capacity. If a sunscreen undergoes photodegradation it loses absorbance and its protective properties are reduced below those expected from the level of the active ingredients it contains [79, 125]. Therefore, any change in ultraviolet absorption might have undesirable consequences in terms of photoprotection or photoxicity, since it is due to a photochemical modification of the screening agent involved. The possible formation of photoproducts, their chemical reactions and their accumulation on/in human skin may have deleterious effects. This form of photoproducts can be irreversible. In this case, it leads to unknown photoproducts whose accumulation on the skin may cause damage. On the other hand the reaction can be reversible, leading to a photostationary equilibrium which depends entirely on the chemical structure of the screening agent, the nature of the cosmetic vehicle and the wavelength distribution of the light employed. In this case, a rapid change in the absorption of the composition is observed, followed by stabilization when equilibrium is reached.

There is no standard method to measure photostability and hence both *in vivo* and *in vitro* methods are used. The photostability and the photodegradation of sunscreen agents

have been studied by many workers by monitoring the absorption spectra over time, e.g. the shift in the UV maxima [126] or the irreversible disappearance of the chromophore [106]. Maier *et al*. [127] using a spectroscopic approach, which was based on spectral transmission measurements of thin films of sunscreens smeared on the quartz slides, observed that commercial sunscreens were photounstable when exposed to solar-simulated UV radiation. In a similar study, they found that commercial photoprotective lipsticks lost protection especially in the UVA region while displaying high photostability in the UVB region [128].

Sayre and Dowdy [118] showed that not only did avobenzone contained in sunscreen products photodegrade upon exposure to solar-simulated radiation, but that UVB absorbers, such as 2-EHMC, also photodegraded when in the presence of avobenzone hence also losing its photoprotective capacity. Panday [119] has shown that avobenzone photosensitizes the photoisomerisation of *trans*-EHMC.

Tarras-Wahlberg *et al.* [79] showed that the absorbance of sunscreens changed after irradiation with both UVB and UVA radiation. They used gas chromatography-mass spectrophotometry to isolate and identify the resulting photoproducts. The mass-spectral analysis showed, for example, that 2-EHMC photoisomerised from the *trans*- to the *cis*-isomer and that this decreased the absorbance.

A detailed study of the *trans-cis* isomerisation of some benzylidene camphor derivatives has been published [104, 105]. Deflandre *et al.* [106] performed studies which showed that methylbenzylidene can photoisomerise initially but reaches a photostationary state between its *trans*- and *cis*-isomers when exposed to UV radiation. A similar study with cinnamic acid derivatives has been reported [129]. Similarly, several works have been devoted to the study of *p*-aminobenzoic acid decomposition [130]. It is known that aqueous solutions of *p*-aminobenzoic acid form several reactive intermediates during UV irradiation. These reactive species are capable of reacting with oxygen to produce singlet oxygen which is toxic [131]. It has been shown that dibenzoylmethanes lose much of their UVA absorbance after UV radiation through tautomerisation,

fragmentation and formation of new products with distinctly altered UV absorption characteristics [79, 113].

The efficacy of sunscreen products can also be dependant on the solvent in which they are dissolved [132]. It has been observed for various sunscreen absorbers studied in different solvents, that their wavelength of maximum absorbance (λ_{max}) and their molar absorption coefficients change [133]. The λ_{max} undergoes a red or bathochromic shift in moving from non-polar to polar solvents. The work of Serpone *et al*. [109] demonstrated that the spectral behaviour of the sunscreen products was solvent dependent. However, they further suggested that the photochemical changes that take place when a chemical filter is exposed to UVB/UVA sunlight need to be determined under conditions that parallel those encountered in actual usage of the sunscreen products.

Campos *et al*. [134] have also carried out an assessment of the photostability of commercial products of different filter combinations and found that the photostability and hence the efficacy was dependent on the nature of the UV filter combinations, as the products showed different UVA/UVB ratios with irradiation time.

The lack of photostability of UV filters is now recognized as a common problem for sunscreen products, which become degraded by UV radiation thus losing their photoprotective characteristics [79, 127], and even becoming photooxidizing agents [96, 122]. Photodegradation can take place in several steps, which include one or more of the active ingredients. The absorbed radiation can excite the absorbing molecules and raise them to a higher energy level, which can be very reactive. If the molecule cannot be relaxed, bond cleavage and free radicals formation can occur. These free radicals can attack a variety of molecules and even form more free radicals. The products of photodegradation have the potential to be mutagenic or toxic.

Many groups have studied the photostability of single UV filters or combinations of them [104, 135]. Only a few studies have evaluated UV filter stability in ready-to–use cosmetic formulations [125]. Most of the studies have been carried out in dilute

solutions which may not be suitable as this is less representative of what could happen under actual conditions of use. Since the UV filters are normally never used alone and are always combined with other UV filters and other numerous excipients, the actual concentrations in sunscreen formulations is likely to be different from those used in most photochemical investigations. Hence, it is important to determine the photostability of the commercially available formulations.

1.6 The aims of this study

The purpose of this study was to assess the photostability and broad-spectrum protection of some commercially available Australian sunscreen products before and after exposure to solar-simulated radiation. Unlike other studies that have mainly concentrated on pure filters we investigated off-the-shelf ready to use formulations. Samples were irradiated with solar-simulated radiation and their photochemical changes were monitored by both spectroscopic and chromatographic methods.

The efficacy of the sunscreens can be estimated by the Sun Protection Factor (SPF), which depends on the UV filter content of the formulation. These substances (i.e. filters) need to be in sunscreens in order to obtain the expected protection during the shelf-life of the products. It is known that the chemical sunscreens undergo electronic excitation when exposed to UV light which may make them susceptible to decomposition [136]. Therefore it is of interest to know if any degradation occurs after application of the sunscreen product to the skin during a period of sun exposure. UV spectral transmission measurements were carried out by the use of ultraviolet (UV/vis) spectrophotometry. High performance liquid chromatography (HPLC) was used to separate, identify and quantify the chemical absorbers present in the commercial sunscreens before and after irradiation. The identity of any photoproducts formed in the suncare products was confirmed by high performance liquid chromatography-mass spectrometry.

This study also involved the identification and the quantification of the chemical absorbers present in the suncare products by using HPLC. This was done in order to check whether the concentrations of the individual chemical UV filters in sunscreen

products complied with the recommended amounts stipulated by the European Cosmetic Toiletry and Perfumery Association (COLIPA). Since there is no universally accepted methodology used to separate and quantify a mixture of filters, an in-house technique was developed and validated for the analysis of the commercial sunscreen products. The method was based on the extraction of these compounds from their initial matrix followed by HPLC analysis. This method offers good reproducibility and low detection limits that render it suitable for the routine screening of these compounds in commercial sunscreen products. This methodology is discussed in Chapter 2 of the thesis.

Since UVA plays an important role in the induction of skin cancer, chronic photoageing and photoimmune suppression it is imperative to evaluate the degree of broad-spectrum protection afforded by sunscreens. The *in vitro* critical wavelength and UVA/UVB ratio methods have been used in this study to evaluate the broad-spectrum protection of the commercial sunscreen products. The photostability and broad-spectrum assessment of the commercial products is described in Chapter 3.

Another aim of this study was to investigate some aspects of the photochemistry of 2-ethylhexyl-*p*-methoxycinnamate which was present in all the sunscreen products studied. In particular, the photoisomerisation and the photodimerisation reactions of 2-EHMC, both of which reduce its absorption efficiency, were studied. Solutions of 2-EHMC were irradiated and the photoproducts were analysed by HPLC. These were collected as fractions and were identified by HPLC-MS, NMR and FTIR. In order to further understand the mechanisms for their formation some theoretical studies using computational methods were carried out to determine the lowest energy geometrical structures of the photoproducts of 2-EHMC and hence their relative stabilities. These methods were used to elucidate the mechanism of the photodimerisation reaction. This aspect of the research is described in Chapters 4 and 6.

REFERENCES

1. Pathak, M.A., *Sunscreens Principles of Photoprotection*, in *Sunscreens; development, evaluation and regulatory aspects*, N.J. Lowe, N.A. Shaath and M.A. Pathak, Editors. 1997, Marcel Dekker: New York. pp. 229-248.
2. De Gruijl, F.R., *Health effects from stratospheric ozone depletion and interactions with climate change.* Photochemical and Photobiological Sciences, 2003, **2** 16-28.
3. Slaper, H., Velders, G.J.M., Daniel, J.S., De Gruijl, F.R., van der Leun, J.C, *Estimates of ozone depletion and skin cancer incidence to examine the Vienna Convention achievements.* Nature, 1996, **384** 256–258.
4. Molina, M.J., Rowland, F.S., *Stratospheric Sink for Chlorofluoromethanes - Chlorine Atomic-Catalysed Destruction of Ozone.* Nature, 1974, **249**(5460) 810-812.
5. Diffey, B.L., *Solar ultraviolet radiation effects on biological systems.* Physics in Medicine and Biology, 1991. **36,** 299 –328.
6. Russell; J.R., *Ozone depletion and cancer risk* Lancet 1987, **ii** 443-6.
7. Taylor, J.S., *DNA, Sunlight, and Skin cancer.* Symposium on Molecular Architecture, 1990, **67**(10) 835-841.
8. Green, H.A., Drake, L., *Aging, Sun Damage, and Sunscreens.* Clinics in Plastic Surgery, 1993, **20**(1), 1-8.
9. Diffey, B., *Climate change, ozone depletion and the impact on ultraviolet exposure of human skin.* Physics in Medicine and Biology, 2004. **49**(1), 1-11.
10. Longstreth, J., De Gruijl, F.R., Kripke, M.L., Abseck, S., Arnold, F., Slaper, H.I., Velders, G., Takizawa, Y., van der Leun, J.C., *Health risks.* Journal of Photochemistry and Photobiology B-Biology, 1998, **46**(1-3), 20-39.
11. Rigel, D.S., Rigel, E.G., Rigel A.C, *Effects of altitude and latitude on ambient UVB radition.* Journal of American Academy Dermatology, 1999, **40** 114-16.
12. Fredrick, J.E., Snell, H.E., Haywood, E.K., *Solar ultraviolet radiation at the earth's surface.* Photochemistry and. Photobiology, 1989, **50** 443-450.
13. Madronich, S., McKenzie, R. L., Bjorn, L.O., Caldwell, M.M., *Changes in biologically active ultraviolet radiation reaching the Earth's surface.* Journal of Photochemistry and Photobiology B: Biology 1998. **46** 5-19.
14. Matsumura, Y., Ananthaswamy, H.N., *Toxic effects of ultraviolet radiation on the skin.* Toxicology and Applied Pharmacology, 2004, **195**(3) 298-308.

15. Urbach, F., *Ultraviolet radiation and skin cancer of humans.* Journal of Photochemistry and Photobiology B-Biology, 1997, **40**(1) 3-7.
16. Gies, H.P., Wright, J., *Measured solar ultraviolet radiation exposures of outdoor workers in Queensland in the building and construction industry.* Photochemistry and Photobiology, 2003, **78** 342-348.
17. Garland, C.F., Garland, F.C., *Do sunlight and vitamin D reduce the likehood of colon cancer?* International Journal of Epidemiology, 1980, **9** 227-231.
18. Holick, M.F., *Vitamin D deficiency.* New England Journal of Medicine, 2007, **357** 266-281.
19. Dixon, K.M., Mason, R.S., *Vitamin D.* The International Journal of Biochemistry and Cell Biology, 2009, **41** 982-985.
20. SKINstructure, *A diagrammatical cross-section through human skin.* www.pharpress.com/shop/samples/T&Tch1 (accessed, 13th June, 2007).
21. Gies, P.H., Roy, C.R., Toomey, S., McLennan, A., *Protection against solar ultraviolet radiation.* Mutation Research, 1998 **422**(1) 15-22.
22. Armstrong, B.K., Kricker, A., *The epidemiology of UV induced skin cancer.* Journal of Photochemistry and Photobiology B: Biology, 2001. **63**(1-3) 8-18.
23. Madronich, S., De Gruijl, F.R., *Skin-Cancer and UV-Radiation.* Nature, 1993,**366,**23.
24. Haywood, R., Wardman, P., Sanders, R., Linge, C., *Sunscreens inadequately protect against ultraviolet-A-induced free radicals in skin: Implications for skin aging and melanoma?* Journal of Investigative Dermatology, 2003. **121**(4) 862-868.
25. Bataille, V., *Genetic epidemiology of melanoma.* European Journal of Cancer, 2003. **39**(10) 1341-1347.
26. Young, A.R., Potten, C.S., Nikaido, O., Parsons, P.G., Boenders, J.G., Ramsden, J.M., Chadwick, C.A., *Human Melanocytes and Keratinocytes Exposed to UVB or UVA In Vivo Show Comparable Levels of Thymine Dimers.* The Journal of Investigative Dermatology, 1998, **111** 936–940.
27. Lund, L.P., Timmins, G.S., *Melanoma, long wavelength ultraviolet and sunscreens: Controversies and potential solutions.* Pharmacolgy and Therapeutics, 200, **114** 198.-207.
28. Gilchrest, B.A., Eller, M.S., Geller, A.C., Yaar, M., *The pathogenesis of melanoma induced by ultraviolet radiation.* New England Journal of Medicine, 199, **340** 1341–8.

29. Bruls, W.A., Slaper, H., van der Leun, J.C., Berrens, L., *Transmission of human epidermis and stratum corneum as a function of thickness in the ultraviolet and visible wavelengths.* Photochemistry and Photobiology, 1984, **40** 485-494.

30. Young, A.R., *Chromophores in human skin.* Physics in Medicine and Biology, 1997, **42**(5) 789-802.

31. Taylor, C.R., Cohrs, M.P., *DNA, light and Dewar pyrimidinones: the structure and biological significance of TpT3.* Journal of American Chemical Society, 1987, **109** 2834-2835.

32. Franklin, W.A., Haseltine, W.A., *The role of the (6-4) photoproduct in ultraviolet light-induced transition mutations in E. coli.* Mutation Research, 1986, **165** 1-7.

33. Jean, S., De Meo, M., Sabatier, A.S., Laget, M., Hubaud, J.C., Verrando, P., Dumenil, G., *Evaluation of sunscreen protection in human melanocytes exposed to UVA or UVB irradiation using the alkaline comet assay.* Photochemistry and Photobiology, 2001, **74**(3) 417-423.

34. Sarasin, A., *The molecular pathways of ultraviolet-induced carcinogenesis.* Mutation Research-Fundemental and Molecular Mechanisms of Mutagenesis, 1999, **428** 5-10.

35. Nishigori, C., *Cellular aspects of photocarcinogenesis.* Photochemical and Photobiological Sciences, 2006, **5** 208-214.

36. Goodsell, D.S., *The molecular perspective: Ultraviolet light and pyrimidine dimers.* Stem Cells, 2001. **19**(4) 348-349.

37. Sinha, R.P., Hader, D.P., *UV-induced DNA damage and repair: a review.* Photochemical and Photobiological Sciences, 2002, **1**(4) 225-236.

38. Papadopoulos, A.J., Schwartz, R.A., Sarasin, A., Lambert, W.C., *The xeroderma pigmentosum variant in a Greek patient.* International Journal of Dermatology, 200, **40**(7) 442-445.

39. Sollitto, R.B., Kraemer, K.H., DiGiovanna, J.J., *Normal vitamin D levels can be maintained despite rigorous photoprotection: Six years' experience with xeroderma pigmentosum.* Journal of the American Academy of Dermatology, 1997, **37**(6) 942-947.

40. Kraemer, K.H., Levy, D.D., Parris, C.N., Gozukara, E.M., Moriwaki, S., Adelberg, S., Seidman, M.M., *Xeroderma pigmentosum and related disorders: examining the linkage between defective DNA repair and cancer.* Journal of Investigative Dermatology, 1994, **103** 96-101.

41. Willis, I., Cylus, L, *UVA erythema in skin: is it a sunburn?* The Journal of Investigative Dermatology, 1977, **68(3)** 128-9.

42. Hawk, J.L.M., Black, A.K., Jaenicke, K.F., Barr, R.M.; Soter, N.A.; Mallett, A I.; Gilchrest, B.A.; Hensby, C.N.; Parrish, J.A.; Greaves, M W., *Increased concentrations of arachidonic acid, prostaglandins E2, D2, and 6-oxo-F1α, and histamine in human skin following UVA irradiation* Journal of Investigative Dermatology, 1983 **80(5)** 496-9.

43. Sarna, T., Sealy, R.C., *Free radicals from Eumelanins; quantum yields and wavelength dependence.* Archives of Biochemistry and Biophysics, 1984, **232** 574-578.

44. Hanson, K.M., Simon, J.D., *Epidermal trans-uronic acid and the UVA - induced photoaging of the skin.* Proceedings of the National Academy of Sciences of the United States of America, 1998, **95** 10576-10578.

45. Setlow, R.B., Wookhead, A.D., Grist, E., *Animal model for UV-radiation induced melanoma: platyfish-swordtail hybrid.* Proceedings of the National Academy of Sciences of the United States of America, 1989, **86**(22) 8922-8926.

46. Longstreth, J.D., De Gruijl, F.R., Kripke, M.L., Takizawa, Y., van der Leun, J.C., *Effects of increased solar ultraviolet radiation on human health.* Ambio, 1995. **24** 153–165.

47. Gilchrest, B.A., *A review of skin ageing and its medical therapy.* British Journal of Dermatology, 1996. **135**(6) 867-875.

48. Bissett, D.L., Hannon, D.P., Orr, T.V., *An Animal-Model of Solar-Aged Skin - Histological, Physical, and Visible Changes in Uv-Irradiated Hairless Mouse Skin.* Photochemistry and Photobiology, 1987. **46**(3) 367-.369

49. Bissett, D.L., Hillebrand, G.G., Hannon, D.P., *The Hairless Mouse as a Model of Skin Photoaging - Its Use to Evaluate Photoprotective Materials.* Photodermatology, 1989, **6**(5) 228-233.

50. Degruijl, F.R., Forbes, P.D., *UV-Induced Skin-Cancer in a Hairless Mouse Model.* Bioessays, 1995, **17**(7) 651-660.

51. Schmidt, T., Ring, J., Abeck, D., *Photoallergic contact dermatitis due to combined UVB (4-methylbenzylidene camphor and octyl methoxycinnamate) and UVA (benzophenone-3 and butyl methoxydibenzoylmethane) absorber sensitization.* Dermatology, 1998. **196**(3) 354-357.

52. Garland, C.F., Garland, F.C., Gorham, E.D., *Epidemiologic evidence for different roles of ultraviolet A and B radiation in melanoma mortality rates.* Annals of Epidemiology, 2003. **13**(6) 395-404.

53. Wang, S.Q., Setlow, R; Berwick, M., Polsky, D., Marghoob, A.A., Kopf, A.W., Bart, R.S., *Ultraviolet A and melanoma: A review.* Journal of the American Academy of Dermatology, 2001, **44**(5) 837-846.

54. Thompson, S.C., Jolley, D., Marks, R., *Reduction of Solar Keratoses by Regular Sunscreen Use.* New England Journal of Medicine, 1993. **329**(16) 1147-1151.

55. Gasparro, F.P., Mitchnick, M., Nash, J.F., *A review of sunscreen safety and efficacy.* Photochemistry and Photobiology, 1998. **68**(3) 243-256.

56. Elmets, C.A., Anderson, C.Y., *Sunscreens and photocarcinogenesis: An objective assessment.* Photochemistry and Photobiology, 1996, **63**(4) 435-440.

57. Woodruff, J., *Creactive Developments (cosmetics).* Chemistry in Britain, 2002, **1** 5-10.

58. Naylor, M.F., Boyd, A., Smith, D.W., Cameron, G.S., Hubbard, D., Neldner, K.H., *High Sun Protection Factor Sunscreens in the Suppression of Actinic Neoplasia.* Archives of Dermatology, 1995, **131**(2) 170-175.

59. Green, A., Williams, G., Neale, R., Hart, V., Leslie, D., Parsons, P., Marks, G.C., Gaffney, P., Battistutta, D., Frost, C., Lang, C., Russell, A., *Daily sunscreen application and betacarotene supplementation in prevention of basal-cell and squamous-cell carcinomas of the skin: a randomised controlled trial.* Lancet, 1999, **354**(9180) 723-729.

60. Roberts, L.K., Beasely, D.G., Learn, D.B., Giddens, L.D., Beard, J., Stanfield, J.W., *Ultraviolet spectral energy differences affect the ability of sunscreen lotions to prevent ultraviolet-radiation-induced immunosuppression.* Photochemistry and Photobiology, 1996, **63**(6) 874-884.

61. Lowe, N.J., Shaath, N.A., *Sunscreens: Development, Evaluation and Regulatory Aspects*, ed. N.A. Shaath. 1990, New York: Marcel Dekker, Inc. USA. pp 222-232.

62. Fitzpatrick, T.B., *The validity and practicality of sun-reactive skin types I through VI.* Archives of Dermatology, 1988, **124**(6) 869-871.

63. COLIPA, *European Cosmetic, Toiletry and Perfumery Association.* COLIPA SPF Test Method, Brussels, 1994. **94/289**.

64. Hayden, C.G., Roberts, M.S., Benson, H.A.E., *Systemic absorption of sunscreen after topical application,* Lancet 1997. **350** 863–864.

65. Hayden, C.G., Cross, S.E., Anderson, C., Saunders, N.A., Roberts, M.S., *Sunscreen penetration of human skin and related keratinocyte toxicity after topical application.* Skin Pharmacology and Physiology, 2005, **18**(4) 170-174.

66. Coelho, G.L.N., Dornelas, C.B., Soares, K.C.C., dos Santos, E.P., VergnaninI, A.L., dos Santos. T.C., Rodrigues, C.R., Castro, H.C., Dias, L.R.S., Cabral, L.M., *Preparation and Evaluation of Inclusion Complexes of Commercial Sunscreens in Cyclodextrins and Montmorillonites: Performance and Substantivity Studies.* Drug Development and Industrial Pharmacy, 2008, **34** 536–546.

67. Pathak, M.A., *Sunscreens - Topical and Systemic Approaches for Protection of Human-Skin against Harmful Effects of Solar-Radiation.* Journal of the American Academy of Dermatology, 1982, **7**(3) 285-312.

68. Scalia, S., Tursilli, R., Bianchi, A., Lo Nostro, P., Bocci, E., Ridi, F., Baglioni, P., *Incorporation of the sunscreen agent, octyl methoxycinnamate in a cellulosic fabric grafted with - cyclodextrin.* International Journal of Pharmaceutics, 2006, **308** 155–159.

69. Perugini, P., Simeoni, S., Scalia, S., Genta, I., Modena, T., Conti, B., Pavanetto, F., *Effect of nanoparticle encapsulation on the photostability of the sunscreen agent, 2-ethylhexyl-p-methoxycinnamate.* International Journal of Pharmaceutics, 2002, **246**(1-2) 37-45.

70. Garland, C.F., Garland, F.C., Gorham, E.D., *Effect of Sunscreens on UV Radiation-Induced Enhancement of Melanoma Growth in Mice.* Journal of the National Cancer Institute, 1994, **86**(10) 798-799.

71. Garland, C.F., Garland, F.C., Gorham, E.D., *Could Sunscreens Increase Melanoma Risk.* American Journal of Public Health, 1992, **82**(4) 614-615.

72. Garland, C.F., Garland F.C., *Rising trends in melanoma. An hypothesis concerning sunscreen effectiveness.* Annals of epidemiology, 1993, **4** 451.

73. Wright, M.W., Wright, S.T., Wagner, R.F., *Mechanisms of sunscreen failure.* Journal of the American Academy of Dermatology, 2001, **44**(5) 781-784.

74. Westerdahl, J., Ingvar, C., Masback, A., Olsson, H., *Sunscreen use and malignant melanoma.* International Journal of Cancer, 2000, **87**(1) 145-150.

75. Autier, P., Dore, J.F., Negrier, S., Lienard, D., Panizzon, R., Lejeune, F.J., Guggisberg, D., Eggermont, A.M.M., *Sunscreen use and duration of sun exposure: a double-blind, randomized trial.* Journal of the National Cancer Institute, 1999, **91**(15) 1304-1309.

76. Azurdia, R.M., Pagliaro, J.A., Diffey, B.L., Rhodes, L.E., *Sunscreen application by photosensitive patients is inadequate for protection.* British Journal of Dermatology, 1999, **140**(2) 255-258.

77. Tarroux, R., Fassalit, M., Hemmerle, J., Ginestar, J., *Influence of applied quantity, water immersion and air drying on covering and microstructure of physical sunscreens films.* International Journal of Cosmetic Science, 2000. **22** 447-458.

78. Bimczoka, R., Gers-Barlag, H., Mundt, C., Klette, E., Bielfeldt, S., Rudolph, T, *Influence of applied quantity of sunscreen products on the sun protection factor* Skin Pharmacology and Physiology, 2007. **20**(1) 57-64.

79. Tarras-Wahlberg, N., Stenhagen, G., Larko, O., Rosen, A., Wennberg, A. M., Wennerstrom, O., *Changes in ultraviolet absorption of sunscreens after ultraviolet irradiation.* Journal of Investigative Dermatology, 1999, **113**(4) 547-553.

80. DeBuys, H.V., Levy, S.B., Murray, J.C., Madey, D.L., Pinnell, S.R., *Modern approaches to photoprotection.* Dermatologic Clinics, 2000. **18**(4) 577-90.

81. Schulz, J., Hohenberg, H., Pflucker, F., Gartner, E., Will, T., Pfeiffer, S., Wepf, R., Wendel, V., Gers-Barlag, H., Wittern, K. P., *Distribution of sunscreens on skin.* Advanced Drug Delivery Reviews, 2002. **54** 157-163.

82. Maier, T., Korting, H. C., *Sunscreens - Which and what for?* Skin Pharmacology and Physiology, 2005. **18**(6) 253-262.

83. Kubota, Y., Shuin, T., Kawasaki, C., Hosaka, M., Kitamura, H., Cai, R., Sakai, H., Hashimoto, K., Fujishima, A., *Photokilling of T-24 Human Bladder-Cancer Cells with Titanium-Dioxide.* British Journal of Cancer, 1994, **70**(6) 1107-1111.

84. Wamer, W.G., Yin, J.J., Wei, R.R., *Oxidative damage to nucleic acids photosensitized by titanium dioxide.* Free Radical Biology and Medicine, 1997. **23**(6) 851-858.

85. Dunford, R., Salinaro, A., Cai, L.Z., Serpone, N., Horikoshi, S., Hidaka, H., Knowland, J., *Chemical oxidation and DNA damage catalysed by inorganic sunscreen ingredients.* Febs Letters, 1997, **418**(1-2) 87-90.

86. Mitchnick, M.A., Fairhurst, D., Pinnell, S.R., *Microfine zinc oxide (Z-Cote) as a photostable UVA/UVB sunblock agent.* Journal of the American Academy of Dermatology, 1999, **40**(1) 85-90.

87. http//www/UVic/ail/techniques/epi-fluorescence.html. *jablonski diagram*. [cited 2nd March 2010].

88. Broadbent, J.K., *Photochemical studies of sunscreen constituents*, M.Sc. Dissertation, University of Natal, Durban, South Africa, 1994.

89. Kowlaser, K., *Photoproduct formation in the irradiated sunscreen absorber 2-ethylhexyl-p-methoxycinnamate*, M.Sc. Dissertation, University of Natal, Durban, South Africa, 1998.

90. Broadbent, J.K., Martincigh, B.S., Raynor, M.W., Salter, L.F., Moulder, R., Sjoberg, P., Markides, K.E., *Capillary supercritical fluid chromatography combined with atmospheric pressure chemical ionisation mass spectrometry for the investigation of photoproduct formation in the sunscreen absorber 2-ethylhexyl-p-methoxycinnamate.* Journal of Chromatography A, 1996. **732**(1) 101-110.

91. Martincigh, B.S., Kowlaser, K., Raynor, M.W., *Photoproducts of 2-ethylhexyl-para-methoxycinnamate.* Photochemistry and Photobiology, 1999, **69** 64S-64S.

92. Seidlova-Wuttke, D., Jarry, H., Christoffel, J., Rimoldi, G., Wuttke, W., *Comparison of effects of estradiol (E2) with those of octylmethoxycinnamate (OMC) and 4-methylbenzylidene camphor (4MBC) - 2 filters of UV light - on several uterine, vaginal and bone parameters.* Toxicology and Applied Pharmacology, 2006. **210**(3) 246-254.

93. Bonin, A.M., Arlauskas, A.P., Angus, D.S., Baker, R.S.U., Gallagher, C.H., Grenoak, G., Lanebrown, M.M., Meher-Homji, K.M., Reeve, V., *UV-absorbing and other sun-protecting substances: genotoxicity of 2-ethylhexyl p-methoxycinnamate.* Mutation Research, 1982. **105** 303 -308.

94. Lanebrown, M.M., Gallagher, C.H., Greenoak, G. E., Reeve, V.E., Baker, R.S., Bonin, A., *Sunscreens and UV Carcinogenesis.* Medical Journal of Australia, 1980 **2**(8) 463-463.

95. Butt, S.T., Christensen, T, *Toxicity and phototoxicity of chemical sun filters.* Radiation Protection Dosimetry, 2000. **91** 283-286.

96. Allen, J.M., Gossett, C.J., Allen, S.K., *Photochemical formation of singlet molecular oxygen in illuminated aqueous solutions of several commercially available sunscreen active ingredients.* Chemical Research in Toxicology, 1996, **9**(3) 605-609.

97. Sutherland, B.M., *Para-Aminobenzoic Acid Sunlamp Sensitization of Pyrimidine Dimer Formation and Transformation in Human-Cells.* Photochemistry and Photobiology, 1982, **36**(1) 95-97.

98. Aliwell, S.R., Martincigh, B.S., Salter, L.F., *Photoproducts Formed by near-UV Irradiation of Thymine in the Presence of P-Aminobenzoic Acid.* Journal of Photochemistry and Photobiology A:Chemistry, 1994. **83**(3). 223-228.

99. Fisher, G.J., Johns, H.E., *Ultraviolet photochemistry of thymine in aqueous solution.* Photochemistry and Photobiology, 1970. **11** 429-444.

100. Roscher, R.M., Lindemann, M.K.O., Kong, S.B., Cho, C.G., Jiang, P., *Photodecomposition of several compounds commonly used as sunscreens.* Journal of Photochemistry and Photobiology A-Chemistry, 1994. **80** 417-421.

101. Knowland, J., McKenzie, E.A., McHugh, P.J., Cridland, N.A., *Sunlight-Induced Mutagenicity of a Common Sunscreen Ingredient.* Febs Letters, 1993. **324**(3) 309-313.

102. Gulston, M., Knowland, J., *Illumination of human keratinocytes in the presence of the sunscreen ingredient Padimate-O and through an SPF-15 sunscreen reduces direct photodamage to DNA but increases strand breaks.* Mutation Research-Genetic Toxicology and Environmental Mutagenesis, 1999, **444**(1) 49-60.

103. McHugh, P.J., Knowland, J., *Characterization of DNA damage inflicted by free radicals from a mutagenic sunscreen ingredient and its location using an in vitro genetic reversion assay.* Photochemistry and Photobiology, 1997, **66**(2) 276-281.

104. Beck, I., Deflandre, A., Lang, G., Arnaud, R., Lemaire, J., *Study of the Photochemical Behavior of Sunscreens - Benzylidene Camphor and Derivatives.* International Journal of Cosmetic Science, 1981, **3** 139-152.

105. Beck, I., Deflandre, A., Lang, G., Arnaud, R., Lemaire, J., *Study of the Photochemical Behavior of Sunscreens Benzylidene Camphor and Derivatives .2. Photosensitized Isomerization by Aromatic Ketones and Deactivation of the 8-Methoxypsoralen Triplet-State.* Journal of Photochemistry, 1985. **30**(2) 215-227.

106. Deflandre, A., Lang, G., *Photostability Assessment of Sunscreens - Benzylidene Camphor and Dibenzoylmethane Derivatives.* International Journal of Cosmetic Science, 1988. **10**(2) 53-62.

107. Schlumpf, M., Cotton, B., Conscience, M., Haller, V., Steinnmann, B., Lichtensteiger, W., *In Vitro and in vivo estrogenicity of UV screens.* Environmental Health Perspectives, 2001. **109** 239-44.

108. Roelandts, R., Vanhee, J., Bonamie, A., Kerkhofs, L., Degreef, H., *A Survey of Ultraviolet Absorbers in Commercially Available Sun Products.* International Journal of Dermatology, 1983. **22**(4) 247-255.

109. Serpone, N., Salinaro, A., Emeline, A.V., Horikoshi, S., Hidaka, H., Zhao, J.C., *An in vitro systematic spectroscopic examination of the photostabilities of a random set of commercial sunscreen lotions and their chemical UVB/UVA active agents.* Photochemical and Photobiological Sciences, 2002. **1**(12) 970-981.

110. Sewlall, A., *DNA cleavage photoinduced by benzophenone-based sunscreens*, M.Sc. Dissertation, University of Natal, Durban, South Africa, 2003

111. Stevenson, C., Davies, R.J.H., *Photosensitization of guanine-specific DNA damage by 2-phenylbenzimidazole and the sunscreen agent 2-phenylbenzimidazole-5-sulfonic acid.* Chemical Research in Toxicology, 1999, **12** 38-45.

112. Andrae, I., Bringhen, A., Boehm, F., Gonzenbach, H., Hill, T., Mulroy, L., Truscott, T.G., *A UVA filter (4-tert-butyl-4-methoxydibenzoylmethane): photoprotection reflects photophysical properties.* Journal of Photochemistry Photobiology B, 1997, **37** 147-150.

113. Schwack, W., Rudolph, T., *Photochemistry of Dibenzoyl Methane UVA Filters .1.* Journal of Photochemistry and Photobiology B-Biology, 1995, **28**(3) 229-234.

114. Mturi, G.J., *An investigation of the photostabilization of sunscreen absorbers by plant polyphenols*, M.Sc. Dissertation, University of KwaZulu-Natal, Durban, South Africa, 2005.

115. Godar, D.E., *UVA1 radiation triggers two different final apoptotic pathways.* Journal of Investigative Dermatology, 1999, **112**(1) 3-12.

116. Damiani, E., Greci, L., Parsons, R., Knowland, J., *Nitroxide radicals protect DNA from damage when illuminated in vitro in the presence of dibenzoylmethane and a common sunscreen ingredient.* Free Radical Biology and Medicine, 1999, **26**(7-8) 809-816.

117. Lowe, N.J., Shaath, N.A., *Sunscreens: Development, Evaluation and Regulatory Aspects*. 1990, New York: Marcel Dekker, Inc. USA. pp 211-233.

118. Sayre, R.M., Dowdy, J.C., *Photostability testing of avobenzone.* Allured's Cosmetics & Toiletries, 1999. **114**(5) 85-91.

119. Panday, R., *A Photochemical investigation of two sunscreen absorbers in a polar and a non-polar medium*, M.Sc. Dissertation, University of Natal, Durban, South Africa, 2002

120. Chatelain, E., Gabard, B., *Photostabilization of butyl methoxydibenzoylmethane (Avobenzone) and ethylhexyl methoxycinnamate by bis-ethylhexyloxyphenol methoxyphenyl triazine (Tinosorb S), a new UV broadband filter.* Photochemistry and Photobiology, 2001. **74**(3) 401-406.

121. Gonzalez, H., Farbrot, A., Larko, O., Wennberg, A.M., *Percutaneous absorption of the sunscreen benzophenone-3 after repeated whole-body applications, with and without ultraviolet irradiation.* The British Journal of Dermatology 2006. **154**(2) 337-40.

122. Schallreuter, K.U., Wood, J.M., Farwell, D.W., Moore, J., Edwards, H.G.M., *Oxybenzone oxidation following solar irradiation of skin: Photoprotection versus antioxidant inactivation.* Journal of Investigative Dermatology, 1996, **106**(3) 583-586.

123. Gaspar, L.R., Campos, P., *Evaluation of the photostability of different UV filter combinations in a sunscreen.* International Journal of Pharmaceutics, 2006. **307**(2) 123-128.

124. Schauder, S., Ippen, H., *Contact and photocontact sensitivity to sunscreens - Review of a 15-year experience and of the literature.* Contact Dermatitis, 1997. **37**(5) 221-232.

125. Gonzalez, H.; Tarras-Wahlberg, N.; Strömdahl, B.; Juzeniene, A.; Moan, J., Larkö, O., Wennberg, A *Photostability of commercial sunscreens upon sun exposure and irradiation by ultraviolet lamps.* British Journal of Dermatology, 2007. **7** 1-9.

126. Flindt - Hansen, H., .Nielsen, C.J., Thune, P., *Measurements of the photodegradation of some PABA and some PABA derivatives.* Photodermatology, 1988. **5** 257-261.

127. Maier, H., Schauberger, G., Brunnhofer, K., Honigsmann, H., *Change of ultraviolet absorbance of sunscreens by exposure to solar-simulated radiation.* Journal of Investigative Dermatology, 2001, **117**(2) 256-262.

128. Maier, H., Schauberger, G., Martincigh, B.S., Brunnhofer, K., Honigsmann, H., *Ultraviolet protective performance of photoprotective lipsticks: change of spectral*

transmittance because of ultraviolet exposure. Photodermatology Photoimmunology and Photomedicine, 2005, **21**(2) 84-92.

129. Morliere, P., Avice, O., Melo, T.S. E., Dubertret, L., Giraud, M., Santus, R., *A Study of the Photochemical Properties of Some Cinnamate Sunscreens by Steady-State and Laser Flash-Photolysis.* Photochemistry and Photobiology, 1982. **36**(4) 395-399.
130. Gasparro, F.P., *UV-induced photoproducts of para-aminobenzoic acid.* Photodermatology, 1985, **2** 151-157.
131. Allen, S.K., Allen, J.M., Lingg, B., *Drugs: Photochemistry and Photostability*. Photostabilities of several chemical compounds used as active ingredients in sunscreens, ed. A. Albini and E. Fasani. 1998, Cambridge: Royal Society of Chemistry. pp. 171-176.
132. Agrapidispaloympis, L.E., Nash, R.A., Shaath, N.A., *The Effect of Solvents on the Ultraviolet Absorbency of Sunscreens.* Journal of the Society of Cosmetic Chemists, 1987, **38**(4) 209-221.
133. Shaath, N.A., Agrapidispaloympis, L.E., Nash, R.A., *The Effect of Solvents on Sunscreen Agents.* Journal of the Society of Cosmetic Chemists, 1986. **37**(4) 290-292.
134. Gaspar, L.R., Maia Campos, P.M.B.G, *Photostability and efficacy studies of topical formulations containing UV-filters combination and vitamins A, C and E.* International Journal of Pharmaceutics., 2007, **343** 181–189.
135. Schrader, A., Jakupovic, J., Baltes, W., *Photochemical studies on trans-3-methylbutyl 4-methoxycinnamate.* Journal of the Society of Cosmetic Chemists, 1994, **45** 43-52.
136. Shaath, N.A., *On the Theory of Ultraviolet-Absorption by Sunscreen Chemicals.* Journal of the Society of Cosmetic Chemists, 1987. **38**(3) 193-207.

CHAPTER 2

High performance liquid chromatographic methodology for the analysis of commercial sunscreens

2.1 Introduction

There are several analytical techniques that can be utilised in the analysis of sunscreens as has been discussed in the extensive review by Salvador *et al.* [1]. Sunscreen formulations are complex since they contain both active and inactive ingredients of varied nature. Sunscreens contain a wide variety of chemical absorbers which absorb radiation to greater or lesser extent over certain regions of the UV spectrum, thereby offering some protection to human skin from the harmful effects of UV radiation [2, 3]. Depending upon the range in which they absorb, these chemical absorbers can be classified as either UVA or UVB absorbers or both [4]. There are very few single chemical actives that are capable of absorbing the full range of the UV spectrum needed to provide proper broad-spectrum protection. Therefore the use of sunscreens incorporating both UVA and UVB chemical absorbers has become of increasing importance because of the need for broadband protection [5, 6]. For this reason the sunscreen formulation contains various UV filters at different concentrations whose maximum limit is regulated by various authorities in Europe, USA, Japan and Australia. Most of these UV filters have a very distinct UV absorption spectrum, which can be a useful identification tool, to distinguish amongst them. UV/vis spectroscopy has been used mostly to quantitate mixtures of up to two active ingredients [7, 8]. However, UV spectroscopic methods alone are insufficient for identification and quantitation. Hence, both chromatographic and spectroscopic techniques were used in this study to quantify the active ingredients.

Chromatographic techniques have been the most widely used methods for both quantitative and qualitative analysis of active ingredients in sunscreens [9-13]. High performance liquid chromatography (HPLC) is a versatile technique that has enabled the simultaneous determination of several active ingredients in sunscreen products [12, 14, 15]. Chisvert *et al.* [12] have reported the possibility of simultaneous analysis of eighteen active chemical ingredients in both model formulations and commercial sunscreens. Another advantageous aspect of HPLC analysis is that it allows for the determination of very polar, high molecular mass and/or thermolabile analytes. This is achievable by merely altering the chromatographic conditions, e.g. the composition of mobile phase or stationary phase or both. In particular, C8 or C18 reversed-phase columns have been used for separation and quantitation [1, 16, 17]. Separations carried out on normal phase columns like silica gel are much less often used [11]. HPLC also has an additional advantage in that it is applicable to all sunscreens without the need for any derivatisation of the compounds as in the case of gas chromatography [18]. Although gas chromatography is widely used because of its good separation power, sometimes the inactive ingredients present in cosmetics give peaks that mask or overlap those of the sunscreen agents [19]. This, of course, would be an undesirable scenario. In general, the sole requirement of a sample for HPLC analysis is that it is soluble in a solvent which will not damage the column or interfere with the detector response. Since HPLC is a non-destructive method, the resolved components of a mixture may be collected, thus allowing HPLC to be used as a preparative technique.

One of the aims of this study was to develop a rapid and efficient HPLC method for the simultaneous determination of the active chemical ingredients found in commercial sunscreens. The chromatographic technique devised was used to confirm the identity and quantitate the active chemical ingredients in the sun care products. This is important since the efficacy of sunscreens is dependent on the UV-filter content of the formulation. It is known that the active ingredients can cause photocontact dermatitis and allergic reactions [20, 21]. Therefore, the maximum content of each UV-filter in a sunscreen is usually legislated and it becomes necessary to monitor their concentrations to ensure their compliance with regulations.

2.2 Experimental

2.2.1 Materials

Twenty five different commercially available sunscreen products were purchased from the Australian market. Eleven sunscreens contained only organic chemical filters while fourteen had a combination of inorganic and organic chemical filters. Table 2 lists the products with details of the active ingredients contained therein and the corresponding SPF value. The samples were stored at room temperature and in the dark and opened only immediately before analysis.

Table 2 The Australian sunscreens assessed, the active chemical ingredients listed on the product packaging and their corresponding SPF values.

Sample Code	SPF	Active Ingredients*	**Protection range**	
			UVB	**UVA**
AU 1	30+	EHMC, AVO, MBC	✔	✔
AU 2	15+	EHMC, AVO, Benz-3	✔	✔
AU 3	30	EHMC, PBSA, TiO_2	✔	✔
AU 4	30+	EHMC, OCT, ZnO	✔	✔
AU 5	30+	EHMC, MBC, ZnO	✔	✔
AU 6	30+	EHMC, MBC, ZnO	✔	✔
AU 7	30+	EHMC, AVO, MBC, OT	✔	✔
AU 8	30+	EHMC, MBC, ZnO	✔	✔
AU 9	15	EHMC, Benz-3, TiO_2	✔	✔
AU 10	30+	EHMC, AVO, MBC	✔	✔
AU 11	15	EHMC, AVO	✔	✔
AU 12	30+	EHMC, MBC, ZnO	✔	✔
AU 13	30+	EHMC, Benz-3, TiO_2	✔	✔
AU 14	30+	EHMC, MBC, ZnO	✔	✔
AU 15	30+	EHMC, AVO, OT	✔	✔
AU 16	30+	EHMC, MBC, ZnO	✔	✔
AU 17	30+	EHMC, MBC, ZnO	✔	✔
AU 18	30+	EHMC, AVO, MBC	✔	✔
AU 19	30+	EHMC, MBC, ZnO	✔	✔
AU 20	30+	EHMC, Benz-3, HS, ODM-PABA	✔	✔
AU 21	30+	EHMC, OCT, ZnO	✔	✔
AU 22	30+	EHMC, OCT, ZnO	✔	✔
AU 23	15+	EHMC, Benz-3	✔	✔
AU 24	30+	EHMC, AVO, Benz-3, TiO_2	✔	✔
AU 25	30+	EHMC, AVO	✔	✔

*EHMC - 2-ethylhexyl-*p*-methoxycinnamate; AVO - avobenzone; MBC - 4-methylbenzylidene camphor; HS - homosalate; Benz-3 - benzophenone-3; PBSA - 2-phenylbenzimidazole sulfonic acid; OCT - octocrylene; OT - octyltriazone; ODM-PABA - octyl dimethyl *para*-aminobenzoic acid (padimate-O); TiO_2 - titanium dioxide; ZnO - zinc oxide.

All reagents and solvents were of analytical or HPLC grade. Methanol and acetonitrile were purchased from BDH HiperSolv Chemicals Ltd. The samples of pure UV filters were obtained from different sources. Benzophenone-3, avobenzone, 2-ethylhexyl-*p*-methoxycinnamate, octocrylene and octyltriazone were obtained from BASF and 4-methylbenzylidene camphor and 2-phenylbenzimidazole sulfonic acid were obtained from Merck. Deionised water was obtained from a Milli-Q^{50} water purification system (Millipore, Bedford, MA, USA) and was used in all procedures.

2.2.2 Chromatographic conditions

The HPLC chromatographic system comprised a Waters 600 multisolvent delivery system connected to a Waters 996 photodiode array (PDA) detector and a Perkin-Elmer 2000 series autosampler. The system was connected to a De'Mark Pentium II personal computer and controlled by using Waters Millennium Version 4.00 software.

A reversed-phase Nucleosil C100 C18 column of 250 mm length, 4.6 mm internal diameter and 5 µm particle size was used. A disposable Waters Guard-Pak µ-Bondapak C18 pre-column insert was used to protect the analytical column. The detection wavelength used was 310 nm for most of the active ingredients except for avobenzone which was determined at 360 nm as it does not absorb at 310 nm.

The mobile phase of methanol-water (85:15% v/v) was prepared by using Millipore Water from a Milli-Q^{50} water purifying unit. The solvent was normally prepared by measuring out separately the appropriate volumes of methanol and water in a measuring cylinder before mixing. This was to avoid inconsistencies in the eluent composition that result from the contraction of methanol-water mixtures [22]. The solvent was filtered through a Millipore 0.45 µm filter before subsequently feeding it into the reservoir. This was then degassed with helium at the rate of 30 mL min^{-1}. The flow rate of the eluent was 1 mL min^{-1}.

The samples were filtered by passing them through 0.45 µm Millex syringe filters to ensure that no particulate matter was introduced into the HPLC column. An injection volume of either 10 µL or 20 µL of the sample was used. All experiments were performed using isocratic conditions and also at room temperature.

2.2.3 Sample preparation

A mass of 0.5 g of the sunscreen product was transferred into a 50-mL volumetric flask. A 20 mL aliquot of HPLC-grade methanol was added to dissolve the active ingredients. This was then placed in an ultrasonic bath for 30 minutes to aid the dissolution of the active ingredients in the sunscreen. The samples were then diluted to the mark with methanol.

In order to test the reliability of the proposed methodology for the extraction of the UV filters from the sunscreens, a recovery analysis was carried out by using the standard addition method. Therefore several samples were spiked with a known amount of analyte and were subjected to the same extraction procedure as the samples. In short, a known amount of a pure active ingredient was spiked into one of the commercial sunscreen products. A mass of 0.5 g of the sunscreen plus a known amount of the active chemical ingredient was transferred to a 50-mL volumetric flask and dissolved in methanol. This was placed in an ultrasonic bath for 30 minutes. The solution was filtered through a Millipore 0.45 µm syringe filter. The prepared solution was then injected into the HPLC. Three replicate samples were prepared and triplicate injections of each sample were performed. The sample injections were interspersed with blank injections, so as to eliminate the effects of any carry-over from the previous injections. The HPLC analysis for these samples was carried out with the same operating conditions as for the standards.

2.2.4 Sample quantitation

The quantitative determination of the UV filters was performed by using external standards. Standard stock solutions of the UV-filters were prepared by accurately weighing appropriate masses of the pure active chemical ingredients. The weighed ingredients were then transferred to 100-mL volumetric flasks and diluted to volume with HPLC-grade methanol to make 1 x 10^{-3} M stock solutions. The stock solutions were stored in the dark by wrapping them with aluminium foil to prevent exposure to any stray light. A working set of standard solutions in the concentration range of 1 x 10^{-3} M to 1 x 10^{-6} M was prepared from each stock solution by serial dilution. These were used to establish the linear range and calculate the limits of detection and quantitation. The lower concentration was the minimum detectable concentration limit under our experimental conditions.

2.3 Results and Discussion

2.3.1 Chromatography

The chromatographic method developed was used to confirm the identity of the active ingredients in suncare products. It was successfully utilized in the separation of most of the components in the samples. An isocratic mobile phase consisting of methanol/water was used to accomplish the separation of the active ingredients from each other. However, the separation and identification of avobenzone proved problematic especially when found in combination with 2-EHMC. The baseline separation gave difficulties due to the tailing peak which could cause avobenzone to elute in the same time window as 2-EHMC. This was overcome by monitoring avobenzone at a wavelength of 360 nm which is its wavelength of maximum absorption since 2-EHMC does not absorb in this region.

2.3.2 Selectivity

A typical HPLC chromatogram of sunscreen sample is shown in Figure 5. Good resolution between the examined chromatographic peaks was observed. Table 3 shows the retention times observed at the optimum detection wavelength for the sunscreen agents investigated in this study.

All retention times were reproducible under the experimental conditions used, the average standard deviation being less than 2%. In the actual sample analysis, unknown peaks were identified from the retention times, which were checked and confirmed with the standards, if necessary. The ingredients in the suncare products were eluted as fairly symmetrical peaks and were well resolved from one another (see Figure 5). The method was successfully applied to quantify the active ingredients.

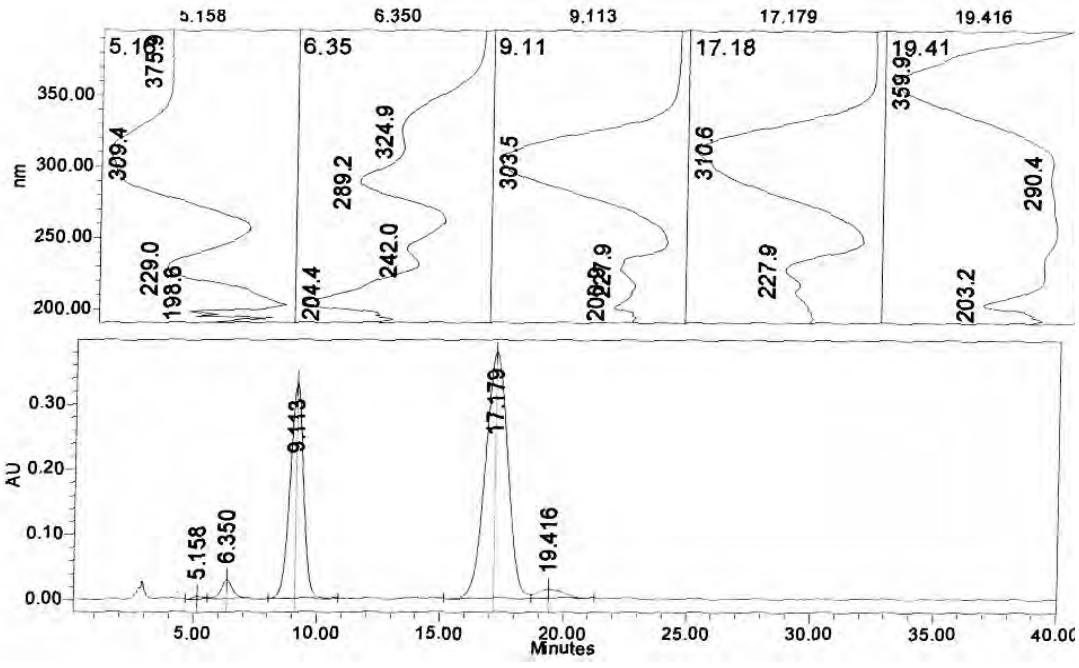

Figure 5 A typical chromatogram of a sample of a commercial sunscreen. Separation was carried out on a Nucleosil C100 C18 column using 85% (v/v) MeOH/H_2O) as the mobile phase at a flow rate of 1 mL min^{-1}., injection volume – 10 µL. The detection wavelength was set at 310 nm. The order of elution was Benz-3 at 6.3 min, MBC at 9.1 min, EHMC at 17.18 min and AVO at 19.42 min.

Table 3 The parameters of the HPLC analysis of commercial sunscreens.

Active chemical ingredients	Wavelength/nm		Retention time/min				
	Detection	Maximum absorption	1	2	3	Mean	STD
EHMC	310	310	19.2	19.57	19.46	19.41	0.16
AVO	360	358	21.47	21.88	21.67	21.67	0.17
MBC	310	303	9.36	9.46	9.41	9.41	0.04
Benz-3	310	285, 325	6.3	6.18	6.53	6.45	0.11
ODM-PABA	310	303	18.36	18.56	18.48	18.47	0.08
PBSA	310	243, 304	2.1	1.93	2.5	2.03	0.07
OCT	310	305	11.86	11.56	11.48	11.48	0.16
OT	310	311	18.61	18.72	18.84	18.72	0.12
HS	310	308	20.67	20.58	20.52	20.59	0.08

* Chromatographic conditions: eluent 85% v/v MeOH/H_2O, flow rate: 1 mL min^{-1}, column: Nucleosil C100 C18.

2.3.3 Calibration curves of UV filters

The calibration graphs were constructed by plotting the peak areas versus the concentrations of the standards injected on the HPLC column. The calibration curves were constructed with at least five different concentrations. The linearity was evaluated by least squares linear regression with triplicate determinations at each concentration level. The UV absorbance for all the individual analytes was measured at the detection wavelength as indicated in Table 3. The data listed in Appendix C (Tables C1 to C9) were used to construct the calibration curves shown in Appendix D (Figures D1 to D18).

Regression analysis revealed that the calibration curves of all the chemical agents considered were linear in the investigated concentration range with correlation coefficients greater than 0.992. Their slopes were used in the quantitation of the

sunscreen agents contained in the commercial sunscreens. The analytical parameters of representative calibration curves are summarised in Table 4.

Table 4 Data obtained by the analytical validation of the active chemical ingredients.

Active ingredient	Parameters					
	Linearity range/ 10^{-5} M	Slope (b)/10^{11}	Standard error of slope/10^{6}	R^2/	LOD/ µM	LOQ/ µM
EHMC	2.0-64	2.7	5.0	0.992	0.61	1.83
Benz-3	6.9-44	1.17	0.86	0.998	0.22	0.73
AVO	0.5-32	3.71	2.61	0.996	0.21	0.69
MBC	1.5-140	5.02	0.77	0.997	0.46	1.52
PBSA	7.7-100	1.26	0.11	0.999	0.22	0.73
OCT	1.0-30	0.16	0.90	0.997	0.17	0.56
OT	0.2-14	1.41	0.82	0.999	0.17	0.56
HS	0.3-20	0.11	0.076	0.993	0.22	0.73
ODM-PABA	0.3-86	1.02	27.52	0.992	0.27	0.89

On different days, quality control solutions containing individual sunscreen agents were used to check the calibration method. The calibration curve could be used on subsequent days when the coefficient of variability (CV) of the quality control samples was less than 2%, failing which a new calibration curve would be established.

2.3.4 Precision and accuracy

Precision is defined as the intra-day and inter-day variability. The repeatability (intra-day variability) was established by the relative standard deviation (RSD) calculated from three injections of low and high concentrations. This was achieved by evaluating the samples at the same concentration and on the same day. Three sample solutions were prepared and assayed.

The intermediate precision (inter-day variability) was evaluated with the relative standard deviation obtained from data of three calibration curves performed on three different days. Three different concentrations (low, middle and high) of the standards were prepared. The chromatographic precision was evaluated by the repeated analyses in triplicate of the same sample. The overall RSD values for the intra-day and inter-day precision were better than 3.8%. The method provided good reproducibility and sensitivity for the quantification of the active ingredients in the sunscreen products.

The reliability of the HPLC method and therefore its applicability was calculated by the recovery yield between the value found with a calibration curve and the true value incorporated in the sunscreen preparations. This was achieved by performing recovery experiments. The experiments were carried out by spiking with different amounts of authentic standards containing a known content of the active ingredients. The samples were treated according to the sample preparation procedure described in Section 2.2.3. The mean recovery of the filters from the spiked samples was calculated and the results are shown in Table 5. The recovery of the method ranged from 94.6 to 103% for all the products and showed good correlation over a relatively wide concentration range. It can be attested that excellent recoveries and precision were observed.

Table 5 Recovery studies of the active chemical agents in sunscreens**.**

Active ingredient	mass added/g	mass found/g	% Recovery
2-EHMC	0.0283	0.0278	98.2
Benz-3	0.011	0.0108	97.3
AVO	0.0163	0.0154	94.6
MBC	0.101	0.096	96.5
PBSA	0.015	0.0154	102.6
OCT	0.116	0.118	101.3
OT	0.113	0.109	96.4
HS	0.124	0.121	98.3
ODM-PABA	0.015	0.0146	97.3

2.3.5 Limits of detection and quantitation

The limit of detection (LOD) is defined as the lowest amount of analyte which can be detected at known confidence interval. This is normally the concentration that leads to a signal three times larger than the noise [(S/N) = 3]. It is also defined as the analyte concentration that gives a signal equal to $y_b + 3.3S_b$, where y_b is the signal of a blank and S_b is its standard deviation. In the unweighted least-squares method it is quite suitable in practice to use $S_{y/x}$ instead of S_b and the value of the calculated slope instead of y_b [23]. It can also be stated as follows:

$$\text{LOD is } [X - X_b] = 3S_b,$$

where X is the signal from the sample, X_b is the signal from the analytical blank and S_b is the standard deviation (SD) of the reading for the analytical blank.

The limit of quantitation (LOQ) is the lowest amount of an analyte which can be quantitated and similarly to LOD is defined as $[X - X_b] = 10S_b$. This simply means that the quantitation limit is a concentration giving a signal that is ten times the magnitude of noise level. Thus

$$LOD = \frac{3.3Sy/x}{b} \qquad \text{and} \qquad LOQ = \frac{10Sy/x}{b}$$

where *b* is the slope of the regression line.

The LOD and LOQ values were determined based on the standard deviation amongst responses and the slope of the regression equation of a curve constructed at the lower concentration levels (1-10 µg mL^{-1}). Based on the above equations, the calculated LOD and LOQ values are shown in Table 6.

The parameters of the individual calibration curves together with the calculated detection limits (three times the signal to noise ratio) are given in Table 6. It is evident

that the proposed procedure offers the required sensitivity for the determination of the studied compounds at the low and ultra-low concentration levels.

2.3.6 Determination of UV filters in suncare products

The samples were prepared as described in Section 2.2.3. The separation and quantitation of the active chemical ingredients was carried out under isocratic elution. A volume of 10 µl of the filtered solution of each sample was injected into the HPLC instrument and each sample was determined in triplicate. The peaks in the chromatograms were identified by comparing their retention times and the UV spectra with those of the standards. The retention times of the peaks and the shape of UV spectra (λ_{max}) do create a reliable tool to positively identify similar compounds. This allowed the confirmation of the active ingredients as given on the product packaging for all the commercial products investigated The quantification of the active ingredients was carried out by use of external standard calibration curves as described in Section 2.3.3. Table 6 shows results of the quantitation analysis of the products investigated in this study. The amounts of the active ingredients determined in the commercial samples were within the permissible levels of the European Cosmetic Toiletry and Perfumery Association (COLIPA).

Table 6 Calculated % of the active ingredients present in the commercial sunscreens

Product	Concentration/ % m/m								
	2-EHMC	MBC	AVO	Benz-3	PBSA	OCT	OT	HS	ODM-PABA
AU1	7.7±0.83	2.50±0.06	1.91±0.3						
AU2	7.66±0.84		1.0±0.3	2.34±0.3					
AU3	6.91±0.83				1.95±0.4				
AU4	6.64±0.83					1.91±0.3			
AU5	7.87±0.83	2.43±0.06							
AU6	7.00±0.83	2.46±0.06							
AU7	6.89±0.82	3.48±0.06	1.1±0.3				2.4±0.07		
AU8	6.84±0.83	0.97±0.06							
AU9	8.84±0.83			2.35±0.3					
AU10	7.48±0.83	3.17±0.06	1.90±0.3						
AU11	7.33±0.83		1.93±0.3						
AU12	6.91±0.83	0.97±0.06							
AU13	7.49±0.83			2.58±0.3					
AU14	7.48±0.82	2.45±0.06							
AU15	8.8±0.83		1.8±0.3				4.94±0.07		
AU16	6.86±0.83	0.98±0.06							
AU17	7.02±0.83	0.98±0.06							
AU18	7.36±0.83	2.56±0.06	1.9±0.3						
AU19	6.91±0.83	0.98±0.06							
AU20	5.92±0.83			4.1±0.3				2.47±0.2	4.71±0.1
AU21	9.23±0.83					3.76±0.3			
AU22	8.64±0.83					3.72±0.3			
AU23	6.82±0.83			3.4±0.3					
AU24	7.18±0.83		1.4±0.3	2.7±0.02					
AU25	8.39± 0.83		1.7±0.01						
COLIPA [24]	**10**	**4**	**5**	**10**	**5**	**10**	**5**	**10**	**10**

*Each value is the mean ± 95% confidence interval of nine determinations. The confidence interval was calculated according to the method detailed in Appendix I. The raw data can be found in Appendix H.

2.4 Conclusion

A chromatographic method has been developed to separate and quantify the active ingredients in commercial sunscreens. The method was evaluated for its validity by using a statistical approach and all the parameters (i.e. accuracy, precision, linearity) were validated. The peak areas of the active ingredients had a linear response over a wide concentration range. The method was successfully applied for the qualitative and quantitative analysis of the active chemical ingredients in the commercial suncare products. The results indicated that the HPLC technique could be readily utilised as an analytical method for the quantification of the active chemical ingredients. This has also shown the utility of HPLC with a PDA detector to accomplish the analysis in a short time of less than 20 minutes and the ability to avail UV spectral information of the active ingredients present concurrently.

REFERENCES

1. Salvador, A., Chisvert, A., *Sunscreen analysis - A critical survey on UV filters determination.* Analytica Chimica Acta, 2005, **537,** (1-2), 1-14.
2. Gasparro, F.P., Mitchnick, M., Nash, J.F., *A review of sunscreen safety and efficacy.* Photochemistry and Photobiology, 1998, **68,** (3), 243-256.
3. De Gruijl, F.R., *Skin cancer and solar UV radiation.* European Journal of Cancer, 1999, **35,** (14), 2003-2009.
4. Lowe, N.J., Shaath, N.A., *Sunscreens: Development, Evaluation and Regulatory Aspects*, ed. N.A. Shaath. 1990, New York: Marcel Dekker, Inc. USA. pp 222-232.
5. Gasparro, F.P., *Sunscreens, skin photobiology, and skin cancer: The need for UVA protection and evaluation of efficacy.* Environmental Health Perspectives, 2000, **108**, 71-78.
6. DeBuys, H.V., Levy, S.B., Murray, J.C., Madey, D.L., Pinnell, S.R., *Modern approaches to photoprotection.* Dermatologic Clinics, 2000, **18,** (4), 577-590.
7. Azevedo, J.S., Viana, N.S., Soares, C.D.V., *UVA/UVB sunscreen determination by second-order derivative ultraviolet spectrophotometry.* Farmaco, 1999, **54,** (9), 573-578.
8. Chisvert, A., Salvador, A., Pascual-Marti, M.C., *Simultaneous determination of oxybenzone and 2-ethylhexyl 4-methoxycinnamate in sunscreen formulations by flow injection-isodifferential derivative ultraviolet spectrometry.* Analytica Chimica Acta, 2001, **428,** (2), 183-190.
9. Vanquerp, V., Rodriguez, C., Coiffard, C., Coiffard, L.J.M., De Roeck-Holtzhauer, Y., *High-performance liquid chromatographic method for the comparison of the photostability of five sunscreen agents.* Journal of Chromatography A, 1999, **832,** (1-2), 273-277.
10. Potard, G., Laugel, C., Baillet, A., Schaefer, H., Marty, J.P., *Quantitative HPLC analysis of sunscreens and caffeine during in vitro percutaneous penetration studies.* International Journal of Pharmaceutics, 1999, **189,** (2), 249-260.
11. Simeoni, S., Tursilli, R., Bianchi, A., Scalia, S., *Assay of common sunscreen agents in suncare products by high-performance liquid chromatography on a cyanopropyl-*

bonded silica column. Journal of Pharmaceutical and Biomedical Analysis, 2005, **38,** (2), 250-255.

12. Chisvert, A., Pascual-Marti, M.C., Salvador, A., *Determination of UV-filters in sunscreens by HPLC.* Fresenius Journal of Analytical Chemistry, 2001, **369,** (7-8), 638-641.
13. Ikeda, K., Suzuki, S., Watanabe, Y., *Determination of Sunscreen Agents in Cosmetic Products by Reversed-Phase High-Performance Liquid-Chromatography.* Journal of Chromatography, 1989, **482,** (1), 240-245.
14. Schakel, D.J., Kalsbeek, D., Boer, K., *Determination of sixteen UV filters in suncare formulations by high-performance liquid chromatography.* Journal of Chromatography A, 2004, **1049,** (1-2), 127-130.
15. Meijer, J., Loden, M., *Stability Analysis of 3 UV-Filters Using Hplc.* Journal of Liquid Chromatography, 1995, **18,** (9), 1821-1832.
16. Chisvert, A., Pascual-Marti, M.C., Salvador, A., *Determination of the UV filters worldwide authorised in sunscreens by high-performance liquid chromatography - Use of cyclodextrins as mobile phase modifier.* Journal of Chromatography A, 2001, **921,** (2), 207-215.
17. Salvador, A., Chisvert, A., *An environmentally friendly ("green") reversed-phase liquid chromatography method for UV filters determination in cosmetics.* Analytica Chimica Acta, 2005, **537,** (1-2), 15-24.
18. Granger, K.L., Brown, P.R., *The chemistry and HPLC analysis of chemical sunscreen filters in sunscreens and cosmetics.* Journal of Liquid Chromatography and Related Technologies, 2001, **24,** (19), 2895-2924.
19. Paulus, G.L., *Gas-Liquid Chromatographic Characterization of Sunscreens in Suntan Preparations.* Journal of the Association of Official Analytical Chemists, 1972, **55,** (1), 47-54.
20. Schmidt, T., Ring, J., Abeck, D., *Photoallergic contact dermatitis due to combined UVB (4-methylbenzylidene camphor and octyl methoxycinnamate) and UVA (benzophenone-3 and butyl methoxydibenzoylmethane) absorber sensitization.* Dermatology, 1998, **196,** (3), 354-357.
21. Schauder, S., Ippen, H., *Photoallergic and Allergic Contact-Dermatitis from Dibenzoylmethanes and Other Sunscreens.* Hautarzt, 1988, **39,** (7), 435-440.

22. Christie, W.W., *HPLC and Lipids: A practical guide*. 1987: Pergamon Press, Oxford. pp.35-41.
23. Thomsen, V., Schatzlein, D., Mercuro, D., *Limits of detection in spectroscopy.* Spectroscopy, 2003, **18,** (12), 112-114.
24. COLIPA, *European Cosmetic, Toiletry and Perfumery Association.* COLIPA SPF Test Method, Brussels, 1994, **94/289**.

CHAPTER 3

A study of the photostability and broad-spectrum protection of 25 commercially available Australian sunscreens

Walyambillah Waudo[1], Bice S. Martincigh[1], Harald Maier[2] and Konrad Brunnhofer[3]

[1]School of Chemistry, University of KwaZulu-Natal, Westville Campus, Private Bag X54001, Durban, 4000, Republic of South Africa, [2]Division of Special and Environmental Dermatology, Medical University of Vienna, Vienna, Austria and [3]Austrian Consumers' Association, Vienna, Austria

Abstract

Photostability studies on some commercial Australian sunscreen products were undertaken by means of spectrophotometric and chromatographic methods. High performance liquid chromatography was used to identify and quantify the active ingredients. UV spectrophotometry was used to monitor the spectral absorbance before and after UV irradiation of the preparations. The photoinstability and broad-spectrum protection of the suncare products was also evaluated by means of *in vitro* methods, namely, the Boots star rating system based on the UVA/UVB ratio, the spectral photoinstability and the critical wavelength. Our results show that some of the photoactive chemical absorbers commonly being used in sunscreens are unstable upon UV radiation. It was noted that upon absorption of UV radiation some of the products showed formation of additional photoproducts as revealed by high performance liquid chromatography. This was mainly due to either photodegradation and/or photoisomerisation of the chemical absorbers, 2-ethylhexyl-*p*-methoxycinnamate, 4-methylbenzylidene camphor and avobenzone. Also there were decreases in the

absorption of UVA/B sunlight which implies a reduction in the expected photoprotection against deleterious solar radiation. The loss is more noticeable in the UVA region where all of the products containing avobenzone in their formulations, except for one, become photounstable. All the suncare products showed good photostability in the UVB range. This further showed that a mere complex filter combination did not prevent the photoinactivation of the suncare products. In total eight of the twenty five assayed suncare products were found to be photounstable. Yet it was these products which initially showed good broad-spectrum protection because they contained the long wavelength UVA absorber, avobenzone, in their formulation. The photostable products did not afford protection at wavelengths greater than 340 nm.

1. Introduction

Solar radiation is essential to all living organisms on earth as it is a source of energy. However, excessive radiation is also known to have deleterious effects on human skin. An overexposure to the ultraviolet (UV) radiation part of the solar spectrum is a major causal factor in the development of skin cancer, sunburn, photoageing and suppression of the immune system [1, 2].

The growing awareness of the dangers associated with overexposure to UV radiation has necessitated measures for photoprotection. Among some of the agents advocated for use are sunscreens. Sunscreens are designed to give a consumer the best possible protection against harmful UV radiation [3, 4]. Therefore, an effective sunscreen agent not only has to be a substance with a large absorption coefficient in the UV region or an effective scattering agent (e.g. TiO_2) but must also be able to harmlessly dissipate the absorbed energy. Sunscreens are topically applied to specifically either prevent or reduce UV-induced cellular damage [4]. In addition, the sunscreen should remain on the skin surface without penetrating into the systemic circulation [5, 6]. If the UV absorbers permeate into the systemic circulation, photoprotection is lost and the skin is susceptible to damage from the sun and toxic effects if absorbed. It is also necessary to ensure that the screening agent does not interact with any neighbouring molecules either by direct

combination or by initiating a photochemical reaction through energy transfer. Therefore special attention needs to be paid to the photophysical and photochemical behaviour of sunscreen agents.

Sunscreen products contain chemical absorbers, which are mainly organic compounds possessing single or multiple aromatic structures sometimes conjugated with carbon-carbon double bonds and/or carbonyl moieties, and also physical blockers which are inorganic oxides, e.g. titanium dioxide (TiO_2) and zinc oxide (ZnO). These active agents act by either absorbing, reflecting or scattering the UV radiation thus preventing it from impinging on the skin. They are normally incorporated in an oil-in-water emulsion although sometimes water-in-oil emulsion systems are also used. The sunscreen products are highly lipophilic and are easily accumulated on the human skin.

The performance of a sunscreen product is measured in terms of the Sun Protection Factor (SPF). The SPF is defined as the ratio of the amount of energy required to produce a minimal erythema on sunscreen-protected skin to the amount of energy required to produce the same level of erythema on unprotected skin. SPF determinations are done *in vivo* according to the European Cosmetic Toiletry and Perfumery Association (COLIPA) standards where only the erythemal dose of UVB is considered. This experimentally derived number is intended to provide the consumer with an approximation of the protective efficacy of the product on the skin against UVB radiation. For example, a SPF of 15 means that a sunbather protected by one of these formulations can remain in the sun 15 times longer than without sunscreen before obtaining a burn. The measure of SPF is solely based on UVB dosage and presently there is no standardized method of measuring the efficacy of UVA blocking sunscreens.

Although UVA radiation is not particularly erythemogenic it is important in many photosensitivity reactions and perhaps in long-term effects [7]. It is known to play an important role in the induction of skin cancer [8, 9] and so modern sunscreens are expected to offer broad-spectrum protection. Since no single active ingredient is capable of providing a broad-spectrum absorption or a high enough SPF value, multiple individual sunscreen chemical actives are used in combinations of varying

concentrations. For example, 2-ethylhexyl-*p*-methoxycinnamate (2-EHMC), benzophenone-3, 4-methylbenzylidene camphor (MBC) and 4-*tert*-butylmethoxydibenzoylmethane (avobenzone) are among the UV filters that are usually combined in sunscreen formulations because their UV absorption spectra have overlapping bands and the mixture allows a good photoprotection in the whole range of UVB and UVA radiation. The combinations work synergistically or otherwise to offer better protection and tend to be more economical than one sunscreen filter [10]. The inorganic agents increase the optical pathway of the photons in the topically applied absorbing formulation. In this way more photons are absorbed hence increasing the SPF value.

The safety and the efficacy of the UV filters are regulated and approved by national and international health authorities. Sunscreen products are normally sold as cosmetic products except in the USA where they are considered as drugs and thus regulated by the USA Food and Drug Administration. The efficacy of a sunscreen is partly dependent on the concentrations of the active UV filters present therein and on the proper product application as it has to be applied both evenly and in sufficient amounts to achieve adequate protection. Therefore, these UV filters have maximum allowed concentrations that have been set by various national regulatory authorities in Australia, Europe, Japan and the USA. These chemicals are added to the consumer sunscreen product in amounts of up to 10% [11]. This aspect is particularly important as some studies have shown that side effects, such as photoallergic contact dermatitis, are experienced in a few people when higher concentrations of the sunscreens are applied [12, 13]. However, sunscreen efficacy and safety studies have generated controversy concerning the use of sunscreens. Several studies have indicated that the use of sunscreens has inadvertently increased the high incidence of skin cancer. This could be due to four factors. Firstly, it has been shown that people tend to apply less of the suncare product than the normally recommended 2 mg cm^{-2}, which is the amount used to determine the SPF value [14, 15]. Secondly, the use of sunscreens tends to encourage people to stay longer in the sun than they would normally do if they were not wearing a sunscreen, thereby risking greater skin damage [16]. Thirdly, since the SPF value is a measure solely based on UVB radiation there is an inadvertent exposure to UVA radiation, which tends to cause

indirect damage to DNA and hence increases the risk of the development of skin cancer [17]. Fourthly, some studies have shown that some sunscreens may tend to break down upon UV irradiation and thereby providing less protection and also possibly form toxic degradation products which are in contact with the skin.

The lack of photostability of UV filters is now recognized as a common problem for sunscreen products, which become experience reduced efficiency by UV radiation thus losing their photoprotective characteristics [18, 19], and even becoming photooxidizing agents [20, 21]. The photoinstability of some chemical filters can be enhanced when two or more organic sunscreen agents are combined in a formulation [22]. The absorbed radiation excites the absorbing molecules and raises them to a higher energy level, which can be more reactive. An enhanced reactivity of the electronically excited molecules can have very adverse effects upon biological systems. If the molecule does not undergo relaxation via harmless pathways, bond cleavage and free radicals will occur. These free radicals can attack one or more molecules and even form more free radicals.

Photodegradation can take place in several steps which include one or more of the active ingredients. If a sunscreen undergoes photodegradation or photodecay it loses absorption efficiency and its protective properties are reduced below those expected from the level of the active ingredients it contains. The possible formation of photoproducts, their chemical reactions and their accumulation on/in human skin may have deleterious effects. The loss of efficiency in absorption and the formation of photodegradation products may induce photoallergy, phototoxic reactions and skin irritation [23, 24]. A high screening efficiency can only be guaranteed if a UV filter is of high photostability [25, 26]. There is no standard method to measure photostability and both *in vivo* and *in vitro* methods are used [18, 27]. The photostability and the photodegradation of sunscreen agents have been studied by many workers by monitoring the spectral changes over time, e.g. the shift in the UV maxima [28] or the irreversible disappearance of the chromophore [29]. Maier *et al*. [18] have shown that suncare products lose their protection upon exposure to solar UV radiation. The work of Tarras-Wahlberg *et al.* [19] also indicates the changes in absorbance of sunscreens that

were measured before and after irradiation with both UVA and UVB radiation. They used gas chromatography-mass spectrometry to isolate and identify the resulting photoproducts. Therefore, the photochemical instability of suncare products containing various UV filters represents a major challenge to the industry as the nature of the photoproducts formed could be toxic. These toxic products may directly or indirectly induce oxidative damage on tissue constituents in human skin, just as UVA radiation does. Therefore in order to ensure adequate photoprotection during usage the photochemical behaviour of sunscreen agents needs to be determined under conditions that parallel those encountered in the finished suncare preparations.

Many groups have studied the photostability of single UV filters or combinations of them [30, 31]. Only a few studies have analyzed UV filter stability in ready-to–use cosmetic formulations [32]. Most of the studies are often carried out in dilute solutions which may not be suitable as this is less representative of what could happen under actual conditions of use. Since the UV filters are normally never used in isolation as they are always combined with other UV filters and other numerous excipients, the actual concentrations in sunscreen formulations could be different from those used in most photochemical investigations.

In this study, the photostability and broad-spectrum protection of twenty five (25) different commercially available products that were purchased from the Australian market has been investigated. Unlike other studies that have mainly concentrated on pure UV filters we investigated off-the-shelf ready-to-use formulations. We have used both spectroscopic and chromatographic techniques to study the photophysical or photochemical changes that are likely to take place when commercial sunscreens are exposed to UV radiation. The analyses were performed before and after UV exposure. The advantage for such a double-barreled approach is that one is able to monitor the changes in absorbance and also at the same time monitor the structural changes in the UV filters and determine any photoproducts formed. The photoproducts can also be monitored as part of quality control in order to determine if they have any potential toxic or allergic effects.

2. Experimental

2.1 Materials

Twenty five different commercially available sunscreen products were purchased from the Australian market. Eleven sunscreens contained only organic chemical filters while fourteen had a combination of inorganic and organic chemical filters. Table 7 lists the products with details of the active ingredients contained therein and the corresponding SPF value.

Table 7 The Australian sunscreens assessed, the active chemical ingredients contained therein and their corresponding SPF numbers.

Sample Code	SPF	Active Ingredients*	Protection range	
			UVB	UVA
AU 1	30+	2-EHMC, AVO, MBC	✔	✔
AU 2	15+	2-EHMC, AVO, Benz-3	✔	✔
AU 3	30	2-EHMC, PBSA, TiO_2	✔	✔
AU 4	30+	2-EHMC, OCT, ZnO	✔	✔
AU 5	30+	2-EHMC, MBC, ZnO	✔	✔
AU 6	30+	2-EHMC, MBC, ZnO	✔	✔
AU 7	30+	2-EHMC, AVO, MBC, OT	✔	✔
AU 8	30+	2-EHMC, MBC, ZnO	✔	✔
AU 9	15	2-EHMC, Benz-3, TiO_2	✔	✔
AU 10	30+	2-EHMC, AVO, MBC	✔	✔
AU 11	15	2-EHMC, AVO	✔	✔
AU 12	30+	2-EHMC, MBC, ZnO	✔	✔
AU 13	30+	2-EHMC, Benz-3, TiO_2	✔	✔
AU 14	30+	2-EHMC, MBC, ZnO	✔	✔
AU 15	30+	2-EHMC, AVO, OT	✔	✔
AU 16	30+	2-EHMC, MBC, ZnO	✔	✔
AU 17	30+	2-EHMC, MBC, ZnO	✔	✔
AU 18	30+	2-EHMC, AVO, MBC	✔	✔
AU 19	30+	2-EHMC, MBC, ZnO	✔	✔
AU 20	30+	2-EHMC, Benz-3, HS, ODM-PABA	✔	✔
AU 21	30+	2-EHMC, OCT, ZnO	✔	✔
AU 22	30+	2-EHMC, OCT, ZnO	✔	✔
AU 23	15+	2-EHMC, Benz-3	✔	✔
AU 24	30+	2-EHMC, AVO, Benz-3, TiO_2	✔	✔
AU 25	30+	2-EHMC, AVO	✔	✔

*2-EHMC - 2-ethylhexyl-*p*-methoxycinnamate; AVO - avobenzone; MBC - 4-methylbenzylidene camphor; HS - homosalate; Benz-3 - benzophenone-3; PBSA - 2-phenylbenzimidazole sulfonic acid; OCT - octocrylene; OT - octyltriazone; ODM-PABA - octyl dimethyl *para*-aminobenzoic acid (padimate-O); TiO_2 - titanium dioxide; ZnO - zinc oxide.

The samples were stored at room temperature and in the dark and opened only immediately before analysis.

All reagents and solvents were of analytical or HPLC grade. Methanol and acetonitrile were purchased from BDH HiperSolv Chemicals Ltd. The samples of pure UV sunscreen filters were obtained from different sources. Benzophenone-3, avobenzone, 2-ethylhexyl-*p*-methoxycinnamate, octocrylene and octyltriazone were from BASF and 4-methylbenzylidene camphor and 2-phenylbenzimidazole sulfonic acid were from Merck. Deionised water was obtained from a Milli-Q^{50} water purification system (Millipore, Bedford, MA, USA) and was used in all procedures.

2.2 UV irradiation

Sunscreen products were smeared onto quartz glass slides covering an average surface area of 10 cm^2. The slides were weighed before application of the sunscreen product. Each product was applied onto the quartz slides by circular movements of a gloved finger according to the method described by Maier *et al*. [33]. The quartz slides were re-weighed to check the exact mass of sunscreen product applied. In each case an area density of 1.0 ± 0.1 mg cm^{-2} was applied. It is important to note that the efficacy of a sunscreen is highly dependent upon its correct application. The amount used in this study was more realistic amount since it has been demonstrated [34, 35] that, in actual use, people apply between 0.50 and 1.00 mg cm^{-2}. This amount is significantly lower than the COLIPA and FDA [18] recommended application density of 2 mg cm^{-2} at which the SPF of sunscreens is measured [36, 37].

After application of the sunscreen product, the quartz slides were dried for 30 minutes at a constant temperature of 26 ºC and a relative humidity of 50% to allow for moisture equilibration. They were then irradiated with a solar simulator (COLIPA Dermasun Dr Hönle 400F/5, Dr Hönle Lichttechnik GmbH, Planegg, Germany) using a radiometrically-defined homogenous field of irradiance (determined by a Solar Light SL 5D spectroradiometer, Solar Light, Philadelphia, PA, USA), with increasing UV doses

of solar- simulated radiation. The samples were taken for transmission measurements after each dose of radiation. Two independent replicate samples of each product were prepared and analysed in this manner.

In addition, for those samples that were determined to be photounstable, a weighed sample of the suncare product was placed on a Petri-dish and exposed to solar radiation for a period of six hours. This was then dissolved in appropriate amounts of methanol and the photoproducts formed were determined chromatographically.

2.3 UV spectroscopy

Solutions of pure chemical filters for UV absorption analysis were accurately prepared. A 50 mg sample of the pure sunscreen active ingredient was weighed accurately into a 100-mL volumetric flask and diluted to the mark with methanol. The resulting stock solution was serially diluted to make solutions of appropriate concentrations, such that their absorbance readings at the wavelength of maximum absorbance fell below 2. This is because at higher concentrations there are deviations from linearity according to Beer's law. All the absorption spectra were acquired with a Perkin Elmer Lambda 35 double-beam UV/Visible spectrophotometer at a constant spectral bandwidth of 1.0 nm using a matched pair of 1 x 1 cm quartz cells. Pure HPLC methanol was used as a reference. The UV response for each chemical constituent was measured at its wavelength of maximum absorbance. The UV spectra were used as an identification and purity check of the compounds separated by high performance liquid chromatography.

For each of the 25 commercial sunscreen products the spectral transmittance, T_λ, for both the UVB (280-320 nm) and the UVA ranges (320-400 nm), was measured before and after irradiation with 2, 5, 10 and 20 MED of solar-simulated radiation by means of a Varian Cary 3E UV/Visible spectrophotometer connected to a Labsphere DRA-CA-30 integrating sphere.

2.3.1 Data Analysis

The determination of the degree of broad-spectrum protection and the photoinstability of the 25 sunscreen products was based on three different *in vitro* approaches: the Boots' star rating based on spectrophotometric analysis [38], the critical wavelength method [39] and the method proposed by Maier *et al*. [18].

The transmittance spectrum of a sunscreen product in either the UVA or UVB region was averaged in order to produce one value which describes the amount of UVA or UVB blocking. The average transmittance in each region is given by

$$T(UVA)_{av} = \frac{\sum_{320}^{400} T_\lambda \Delta\lambda}{\sum_{320}^{400} \Delta\lambda} \quad \text{and} \quad T(UVB)_{av} = \frac{\sum_{280}^{320} T_\lambda \Delta\lambda}{\sum_{280}^{320} \Delta\lambda} \qquad [2.1]$$

where T_λ is the transmittance at a particular wavelength and $\Delta\lambda$ is the measured wavelength interval. The percent transmittance blocking for the UVA or UVB region is given as 100% - $T(UVA)_{av}$ or 100% - $T(UVB)_{av}$ respectively, where $T(UVA)_{av}$ or $T(UVB)_{av}$ is expressed as a percentage.

The spectral transmittance values, T, were converted to spectral absorbance (A) values by means of the following formula

$$A = 2 - \log (\%T) \qquad [2.2]$$

The „UVA ratio' (R) was then calculated, which is the ratio of the total absorption in the UVA to that in the UVB region.

$$R, \frac{\alpha UVA}{\alpha UVB} = \frac{\sum_{320}^{400} A_\lambda \Delta\lambda}{\sum_{280}^{320} A_\lambda \Delta\lambda} \qquad [2.3]$$

where αUVA and αUVB are the total absorption in the UVA and UVB regions respectively. The Boots star rating is based on the requirement that a good sunscreen should have a UVA ratio of greater than 0.6 [38].

The critical wavelength (λ_c) describes a method for classifying the broad-spectrum protection properties of sunscreens throughout the whole of the UV (290 - 400 nm) region. This is also determined spectrophotometrically from the UV-spectra, where the spectral transmittance, T, is measured and then converted to spectral absorbance by means of Equation 2.2. To calculate the critical wavelength, the area under the absorbance curve (AUC) is set at 100%. The critical wavelength, λ_c, is the wavelength at which 90% of the area under the curve is reached starting from 290 nm. This is essentially the wavelength below which 90% of the sunscreen's UV absorbance occurs. The following formula (Equation 2.4) according to the work of Diffey [39] is applied:

$$\int_{290}^{\lambda_c} A(\lambda)\delta\lambda = 0.9 \int_{290}^{400} A(\lambda)\delta\lambda \qquad [2.4]$$

where A(λ) is the absorbance of the sunscreen product at wavelength λ, λ_c is the critical wavelength and δλ is the wavelength interval used in the integral summation. A five-point scale is used to classify suncare products according to the method reported by Diffey [40].

The data obtained from UV-spectrophotometry were also analyzed according to the method proposed by Maier *et al.* [18] in order to determine the photostability or photoinstability of the sunscreen products. The change in the spectral transmittance after a defined exposure (MED dose), D, at a given wavelength, λ, $\Delta T_{\lambda,D}$, was calculated from the difference between the spectral transmittance before UV exposure, $T_{\lambda,0}$, and the spectral transmittance $T_{\lambda,D}$ for a defined UV dose D, at that wavelength:

$$\Delta T_{\lambda,D} = T_{\lambda,0} - T_{\lambda,D} \qquad [2.5]$$

The quantity $\Delta T_{\lambda,D}$, is referred to as the spectral photoinactivation.

The mean difference of the transmittance, $\Delta T_{\lambda,D}$, was calculated for both the UVB (280 – 320 nm) and UVA (320 - 400 nm) ranges for all the illumination doses applied. The criterion for photoinactivation was based on the assumption of the minimum erthyma dose of 10 MED which is received on average by the human skin every day. A sunscreen product was labelled photounstable if the mean photoinactivation was greater than 5% and photostable if the value was less than or equal to 5%.

2.4 High performance liquid chromatography

The chromatographic system comprised a Waters 600 multisolvent delivery system connected to Waters 996 photodiode array (PDA) detector and a Perkin-Elmer 2000 series autosampler. The system was connected to a De'Mark Pentium II personal computer and controlled by using Waters Millennium Version 4.00 software.

Separations were performed on a reversed-phase Nucleosil C100 C18 column of 250 mm length, 4.6 mm internal diameter and 5 μm particle size fitted with a disposable Waters Guard-Pak μ-Bondapak C18 pre-column insert to protect the analytical column. A solvent composition of 85:15% (v/v) methanol-water was used for the isocratic elution of the samples of suncare products obtained before and after irradiation. The solvent was filtered through a Millipore 0.45 μm filter and was continuously degassed with helium before and during use. The flow rate of the eluent was 1 mL min^{-1}. The wavelength of detection was set at 310 nm as compromise absorption wavelength that allows for satisfactory responses for most analytes, apart from avobenzone that was monitored at 360 nm.

Sample solutions were prepared by weighing 50 mg of a suncare product and dissolving it in 20 mL of methanol into a 50-mL beaker followed by placement in an ultrasonic bath for 30 minutes. The mixture was transferred into a 50-mL volumetric flask and diluted to the mark with methanol. The samples were filtered by passing them through 0.45 μm Millex syringe filters to ensure that no particulate matter was introduced into the HPLC column. An injection volume of either 10 μL or 20 μL of the sample was used. All experiments were performed at room temperature.

Calibration curves obtained by using an external standard method were constructed for the quantification of the active ingredients in the suncare products. These were linear in the assayed range of concentrations. The degree of photodegradation was evaluated by comparing the peak areas of the sunscreen products of the irradiated samples with those obtained by analysing an equivalent amount of the unirradiated samples.

2.5 High performance liquid chromatography – mass spectroscopy studies

An Agilent HPLC 1100 series HPLC/MS instrument (Agilent Technologies, San Jose, CA) comprising a quatenary solvent delivery system, an on-line degasser, an autosampler, a column thermostat and interfaced to an Agilent LC/MSD Trap 1100 series was used. The column was an Agilent Zorbax Eclipse XDB-C18 reversed-phase column (5 μm, 50 x 4.6 mm). The sample injection volume was 5 μL and the eluent flow rate was 1mL min^{-1}. Liquid chromatography – mass spectroscopy analyses were performed in the isocratic mode (85:15% v/v MeOH/H_2O). Mass spectra were recorded between 100 and 1000 m/z in the atmospheric pressure chemical ionization positive mode. The heated capillary temperature was set at 155 ^oC and the APCI vaporizer temperature at 300 ^oC. The capillary voltage was 3500 V and the spray voltage 5 kV.

3 Results and Discussion

3.1 Characterisation of samples

Twenty five different samples of commercial sunscreens were purchased from the Australian market. The aim of this investigation was to examine the photostability of the organic filters in these commercial sunscreens and then determine, if any, the chemical structures of the photodegradation or photo-products. Photostability is an essential factor for a commercial sunscreen to effectively provide protection against the harmful effects of both UVA and UVB solar radiation. The decomposition of the UV filters under sunlight exposure reduces their expected screening capacity. All the suncare

products investigated in this study contained the UV filters as listed on the container labels. Most of the products consisted of at least two chemical absorbers covering both the UVA and UVB regions. Only three of the products had four active chemical ingredients present. The most common UV absorber was 2-EHMC which was found in all the products. MBC was the second most frequently used absorber occurring in twelve products while AVO, which is a UVA absorber, was found in ten products. Other filters were also found in various permutations with 2-EHMC as shown in Table 8 which lists the different UV-filter combinations contained in the suncare products investigated. A total of twelve different filter combinations were identified and are presented in order of increasing complexity. All the sunscreen products containing the various filter combinations were analysed for their photostability and for the concentrations of the UV filters by means of spectroscopic and chromatographic techniques respectively.

Table 8 Details of the active chemical ingredients in the suncare products investigated in this study.

Brand code of suncare product	**Active chemical ingredients**
AU (11, 25)	2-EHMC, AVO
AU 23	2-EHMC, Benz-3
AU (1, 10, 18)	2-EHMC, MBC, AVO
AU 2	2-EHMC, Benz-3, AVO
AU (5, 6, 8, 12, 14, 16, 17, 19)	2-EHMC, MBC, ZnO
AU 3	2-EHMC, PBSA, TiO_2
AU (4, 21, 22)	2-EHMC, OCT, ZnO
AU (9, 13)	2-EHMC, Benz-3, TiO_2
AU 15	2-EHMC, AVO, OT
AU 24	2-EHMC, AVO, Benz-3, TiO_2
AU 7	2-EHMC, AVO, MBC, OT
AU 20	2-EHMC, Benz-3, HS, ODM-PABA

*2-EHMC - 2-ethylhexyl-*p*-methoxycinnamate; AVO - avobenzone; MBC - 4-methylbenzylidene camphor; HS - homosalate; Benz-3- benzophenone-3; PBSA – 2-phenylbenzimidazole sulfonic acid; OCT - octocrylene; OT - octyltriazone; ODM-PABA - octyl dimethyl *para*-aminobenzoic acid (padimate-O)

The concentrations of the active chemical ingredients in the various products were determined by using external standard calibration curves. Table 9 shows the mean percentage concentrations (% m/m) determined for the different active ingredients in the commercial sunscreens. The concentrations were found to be within the recommended levels of the European Cosmetic Toiletry and Perfumery Association (COLIPA).

3.2 Spectroscopic analysis of pure chemical absorbers

The UV absorption spectra of all the pure chemical actives contained in the commercial sunscreens were obtained and are displayed in Figure 6. It can be seen that there is an overlap of the spectra. Most of these UV filters absorb maximally in the UVB region. AVO is the most commonly used UVA filter. Although benzophenone-3 can be considered as a UVA filter it, however, only covers the shorter UVAII (320-340 nm) wavelength range with maximum absorption at 285 nm in methanol. It is this overlapping absorption that becomes useful when the filters are combined together as they have an additive effect in absorbance hence improving the overall SPF value of the suncare formulation. For example, the combination of a UVB filter (2-EHMC) and UVA filter (AVO) results in a wider spectral coverage than would be achieved by the individual active agents. The wavelengths of maximum absorption for each of the sunscreen filters are listed in Table 10.

Table 9 Concentrations of the active chemical ingredients present in the commercial sunscreens investigated **[41]**

Product	Concentration/ % m/m								
	2-EHMC	MBC	AVO	Benz-3	PBSA	OCT	OT	HS	ODM-PABA
AU1	7.7±0.83	2.50±0.06	1.91±0.3						
AU2	7.66±0.84		1.0±0.3	2.34±0.3					
AU3	6.91±0.83				1.95±0.4				
AU4	6.64±0.83					1.91±0.3			
AU5	7.87±0.83	2.43±0.06							
AU6	7.00±0.83	2.46±0.06							
AU7	6.89±0.82	3.48±0.06	1.1±0.3				2.4±0.07		
AU8	6.84±0.83	0.97±0.06							
AU9	8.84±0.83			2.35±0.3					
AU10	7.48±0.83	3.17±0.06	1.90±0.3						
AU11	7.33±0.83		1.93±0.3						
AU12	6.91±0.83	0.97±0.06							
AU13	7.49±0.83			2.58±0.3					
AU14	7.48±0.82	2.45±0.06							
AU15	8.8±0.83		1.8±0.3				4.94±0.07		
AU16	6.86±0.83	0.98±0.06							
AU17	7.02±0.83	0.98±0.06							
AU18	7.36±0.83	2.56±0.06	1.9±0.3						
AU19	6.91±0.83	0.98±0.06							
AU20	5.92±0.83			4.1±0.3				2.47±0.2	4.71±0.1
AU21	9.23±0.83					3.76±0.3			
AU22	8.64±0.83					3.72±0.3			
AU23	6.82±0.83			3.4±0.3					
AU24	7.18±0.83		1.4±0.3	2.7±0.02					
AU25	8.39±0.83		1.7±0.01						
COLIPA	**10**	**4**	**5**	**10**	**5**	**10**	**5**	**10**	**10**

*Each value is the mean ± 95% confidence interval of nine determinations. The confidence interval was calculated according to the method detailed in Appendix H. The raw data can be found in Appendix K.

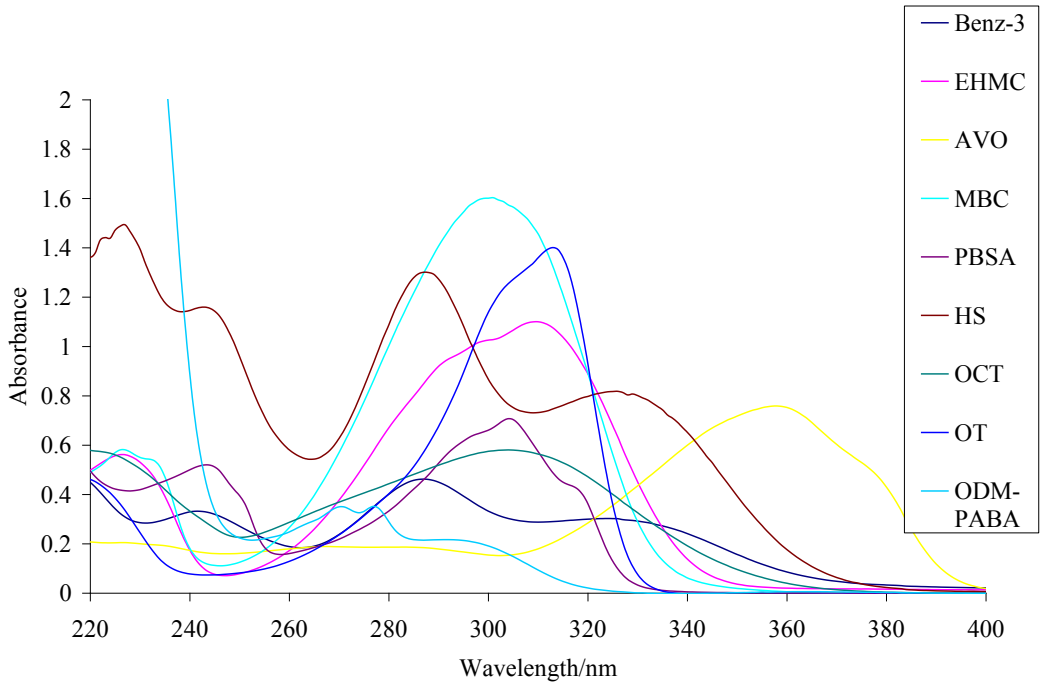

Figure 6 The UV absorption spectra of the pure sunscreen agents dissolved in methanol. Absorption spectra were recorded in a 1-cm pathlength quartz cuvette against methanol in the reference cell.

Table 10 The wavelengths of maximum absorption of the sunscreen active ingredients.

Active chemical ingredients	Wavelength of maximum absorption/nm
2-EHMC	310
AVO	358
MBC	303
Benz-3	242, 285, 325
ODM-PABA	303
PBSA	243, 304
OCT	305
OT	311
HS	306

3.3 Investigation of the change in UV absorbance of sunscreen products upon irradiation

The photostability of the active ingredients in suncare products was investigated both spectroscopically and chromatographically. Since a number of the samples had similar filter

combinations (as shown in Table 2) only the results of a representative sample will be discussed. The loss of absorbance and hence the efficacy of the suncare product can occur because of possible modification occurring to the chemical actives during UV irradiation [42].

Eight samples contained 2-EHMC, MBC and ZnO as the main active chemical components, i.e. samples AU 5, 6, 8, 12, 14, 16, 17 and 19. Figure 7 shows the UV transmission spectra for sample AU 5 obtained before and after exposure to increasing doses of solar-simulated UV radiation. It was observed that there was a negligible change in absorbance in the UVB region during the time of UV exposure. However, in the UVA region the sample showed transmission due to the fact that there was no active chemical agent present to absorb in this region since 2-EHMC and MBC are both UVB absorbers. A close observation of the shapes of the spectra shows an initial steady increase in transmission from about 340 nm then attaining a plateau between 350 nm to 370 nm before another gradual increase. The partial absorption in this region can be attributed to the presence of the inorganic filter, namely ZnO. The overall shapes of the spectra remained virtually the same during the entire exposure to increasing UV radiation. This product was assessed to be photostable and later also assessed to be so by the quantitative methods applied to the UV – spectral data.

The samples were also assessed for their photostability by HPLC. This technique is useful since it is possible to carry out a quantitative and qualitative analysis of the sunscreen ingredients present before and after irradiation. An analysis of irradiated sunscreen samples by HPLC was used to provide some information on the type of photoproducts formed in photounstable formulations upon exposure to UV radiation. The chromatograms for both the unirradiated and the irradiated samples were recorded. HPLC quantitation of suncare products was carried out before and after irradiation. The peak areas were used to determine the degree of photodegradation.

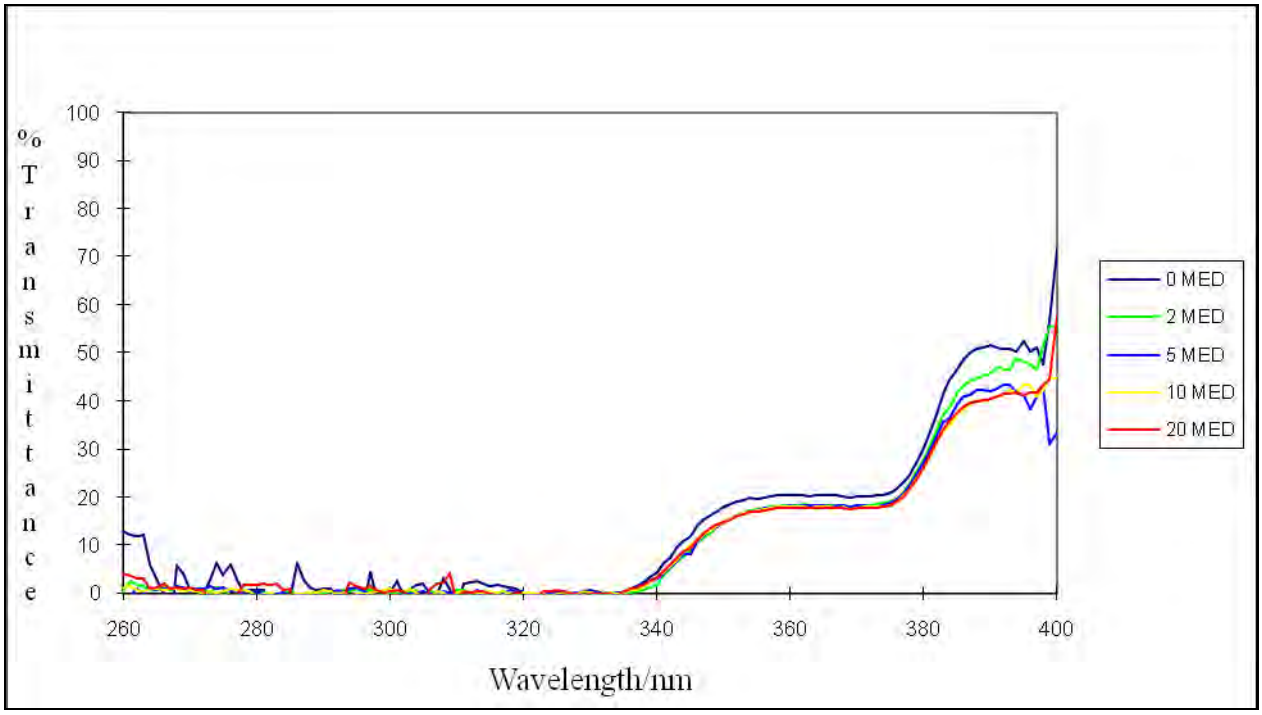

Figure 7 UV transmission spectra of AU 5 with increasing doses of UV radiation.

Figure 8 is a HPLC chromatogram of unirradiated AU 5 showing the two peaks due to 2-EHMC at 19.453 min and MBC at 9.719 min.

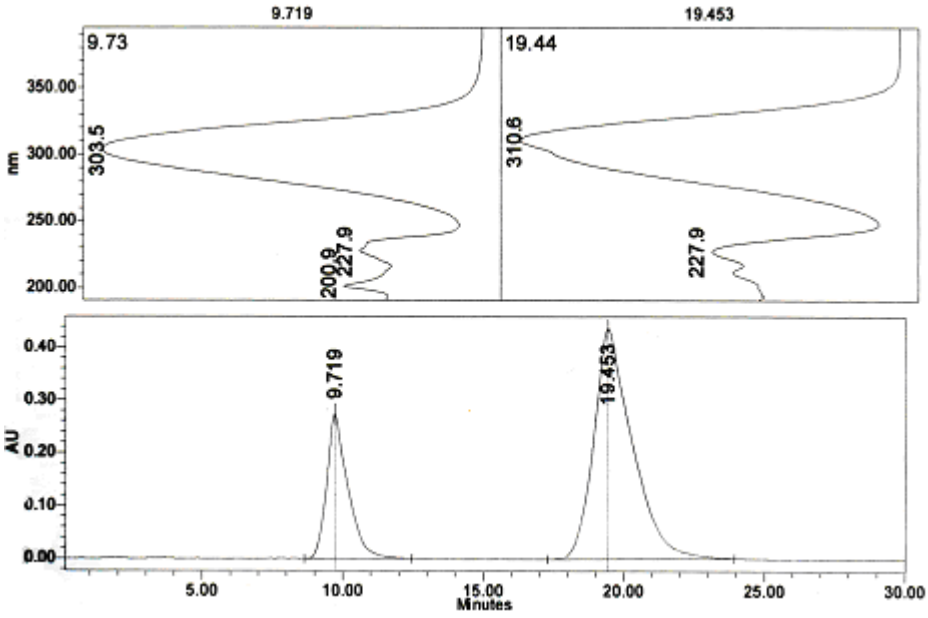

Figure 8 The HPLC chromatogram of unirradiated AU 5 separated on a Nucleosil C100 C_{18} column, eluent 85% MeOH/H_2O, flow rate 1 mL min^{-1} , injection volume – 10 µL and detection wavelength of 310 nm. The order of elution is MBC and 2-EHMC.

Upon irradiation the sample showed the emergence of two new peaks associated with the *cis*-forms of *trans*-2-EHMC at 15.224 min and *trans*-MBC at 10.867 min (Figure 9). It is known that *trans*-2-EHMC photoisomerises to its *cis*-form upon exposure to UV radiation [43]. The *trans*-MBC can also photoisomerise in more or less the same way as *trans*-2-EHMC [19].

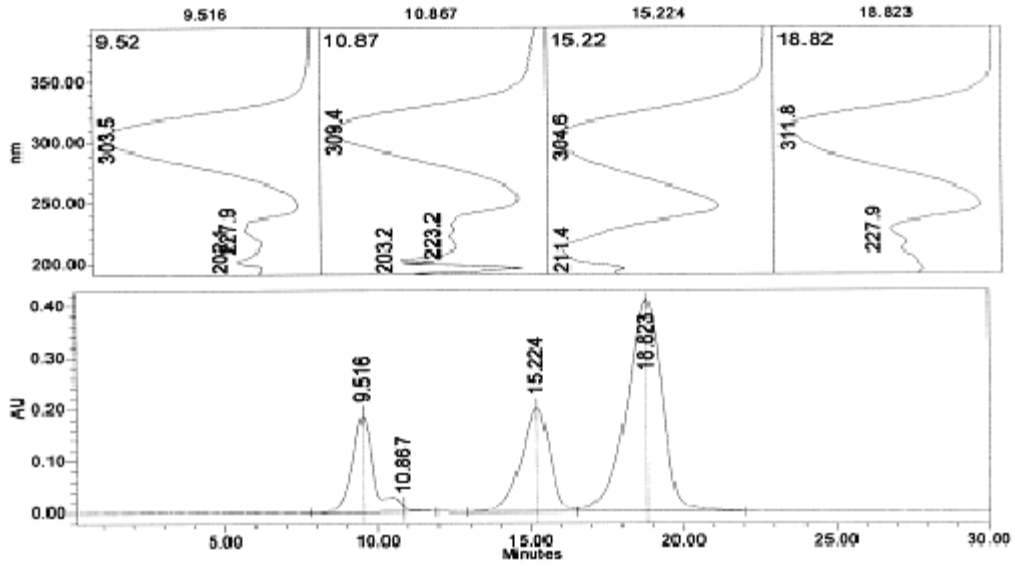

Figure 9 HPLC chromatogram of irradiated AU 5 separated on a Nucleosil C100 C_{18} column, eluent 85% MeOH/H_2O, flow rate 1 mL min^{-1} , injection volume – 10 µL and detection wavelength of 310 nm. The order of elution is *trans*-MBC, *cis*-MBC, *cis*-2-EHMC and *trans*-2-EHMC.

It has been shown that benzylidene camphor filters can undergo E/Z isomerisation in irradiated solutions but no degradation was observed [31]. However, Bonda [44] argues that not all molecules that isomerise are destructive to the molecule. There might be cases where isomerisation is reversible or where it has little effect on the spectral attenuation. This energy dissipation can actually contribute to photostability [45]. Samples AU 6, 8, 12, 14, 16, 17 and 19 which contained the same three active ingredients behaved similarly.

The irradiated sample was also analysed by high performance liquid chromatography-mass spectroscopy to ascertain the formation of the photoproducts. Figure 10 shows the HPLC chromatogram obtained and has four peaks labelled M_1, M_2, E_1 and E_2 which correspond to the *trans*-MBC, *cis*-MBC, *cis*-2-EHMC and *trans*-2-EHMC respectively. Figure 11 is the total ion chromatogram obtained and the peaks labelled M_1, M_2, E_1 and E_2 correspond to the peaks shown in the HPLC chromatogram. The significance of this result was the confirmation

that indeed *trans*-MBC and *trans*-2-EHMC had photodegraded to their *cis*-forms upon UV irradiation as seen by the value of the molecular masses.

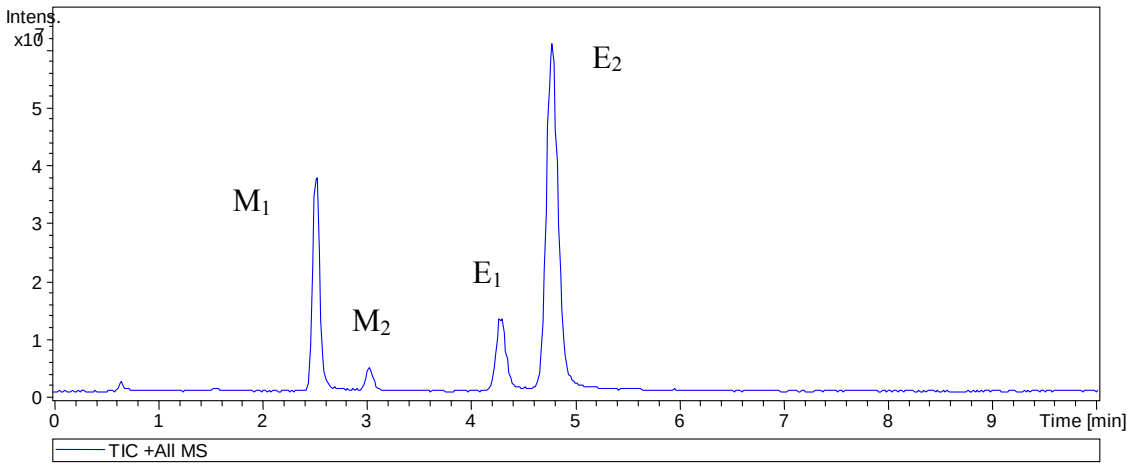

Figure 10 HPLC chromatogram of irradiated AU 5 analysed on the Agilent Zorbax Eclipse XDB-C18 column by isocratic elution at a flow rate of 1 mL min^{-1}, injection volume – 5 µL with the Agilent 1100 Series HPLC with UV detection at 310 nm. The order of elution was *trans*-MBC, *cis*-MBC, *cis*-2-EHMC and *trans*-2-EHMC.

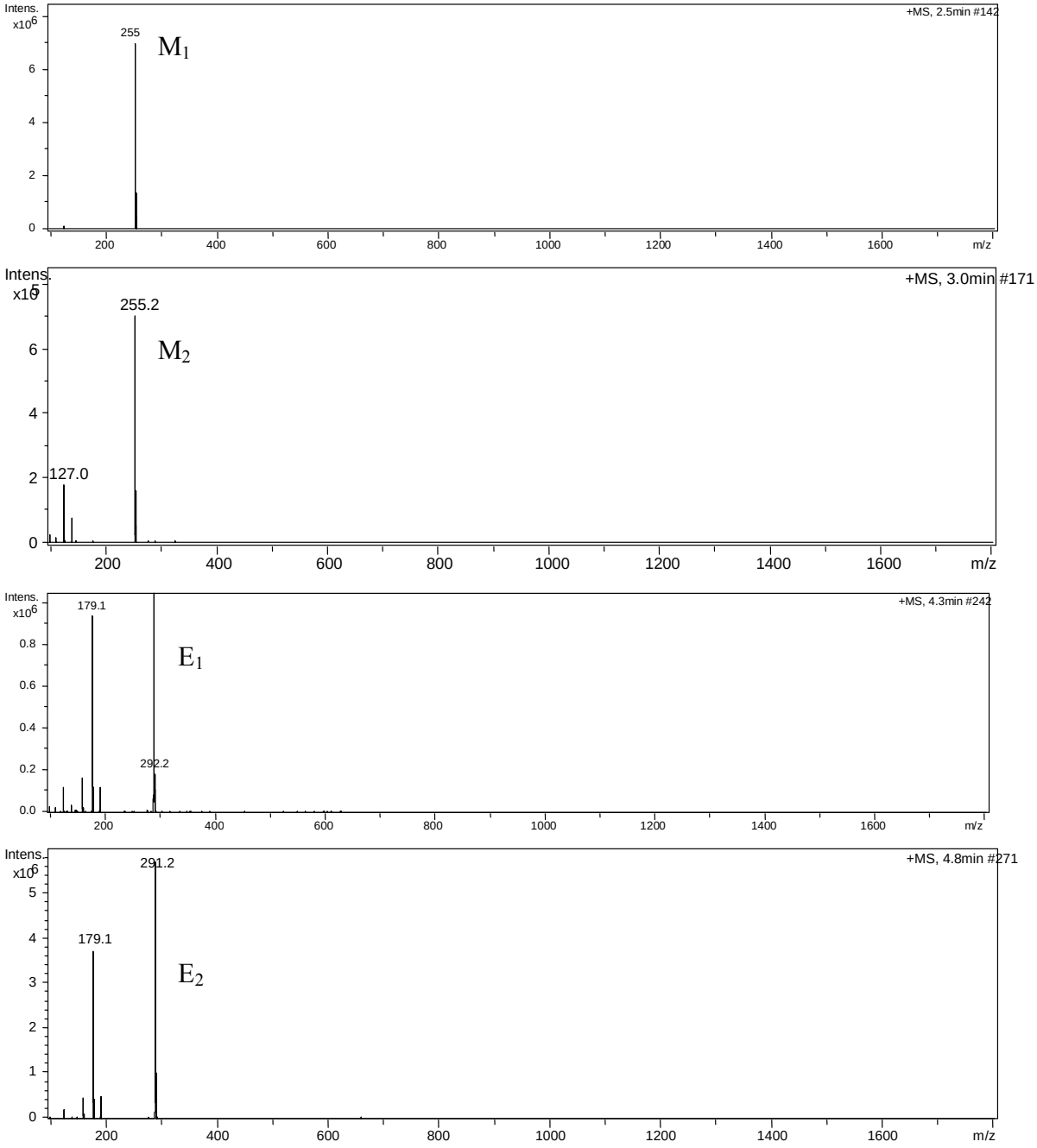

Figure 11 Mass spectra of the peaks labeled M1, M2, E1 and E2 in Figure 10.

Sample AU 3 was the only one that contained 2-EHMC, PBSA and TiO_2 as the active ingredients. The preparation displayed good photostability in the UVB region but was completely transparent in the UVA region (Figure 7). This is consistent with the non-absorbance in the UVA region of the two chemical actives (i.e. 2-EHMC and PBSA) present. The low transmission in the UVAII (320-340 nm) range could be due to the presence of TiO_2,

which is a physical blocker for UVA radiation [46]. The shapes of the transmission spectra remained essentially the same throughout the irradiation period. This product was therefore classified as photostable.

Sample AU 3 was also subjected to HPLC studies. Figure 12 shows the HPLC chromatogram obtained before irradiation. The unirradiated sample shows the presence of the two ingredients, namely, 2-EHMC at 19.79 min and PBSA at 1.99 min. Upon irradiation the sample shows the presence of a new peak at 16.267 min as shown in Figure 13. This was associated with the photoisomerisation of *trans*-2-EHMC to the *cis*-form [47, 48]. PBSA is not altered by UV exposure which was also observed in the study by Sewlall [49]. However, Serpone *et al.* [50] seem to suggest otherwise as they have shown that PBSA photodegrades upon irradiation with UV light. However, this product was assessed to be stable.

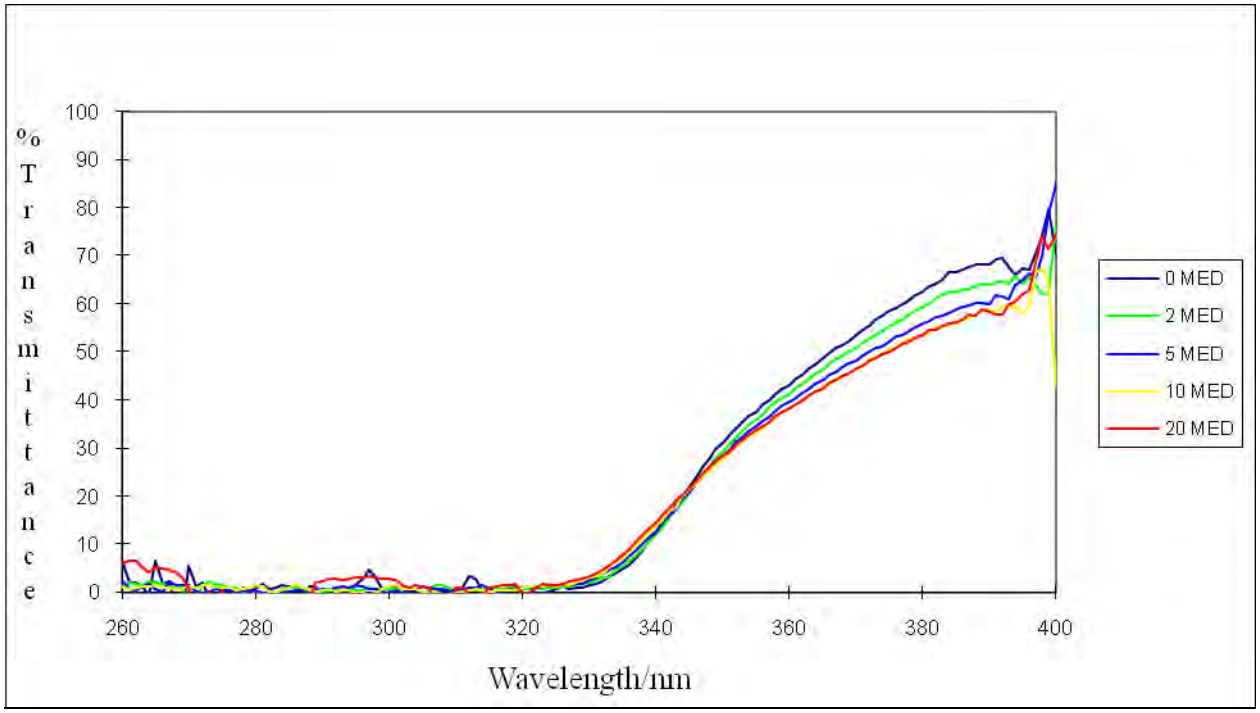

Figure 12 UV transmission spectra of AU 3 with increasing UV doses of radiation**.**

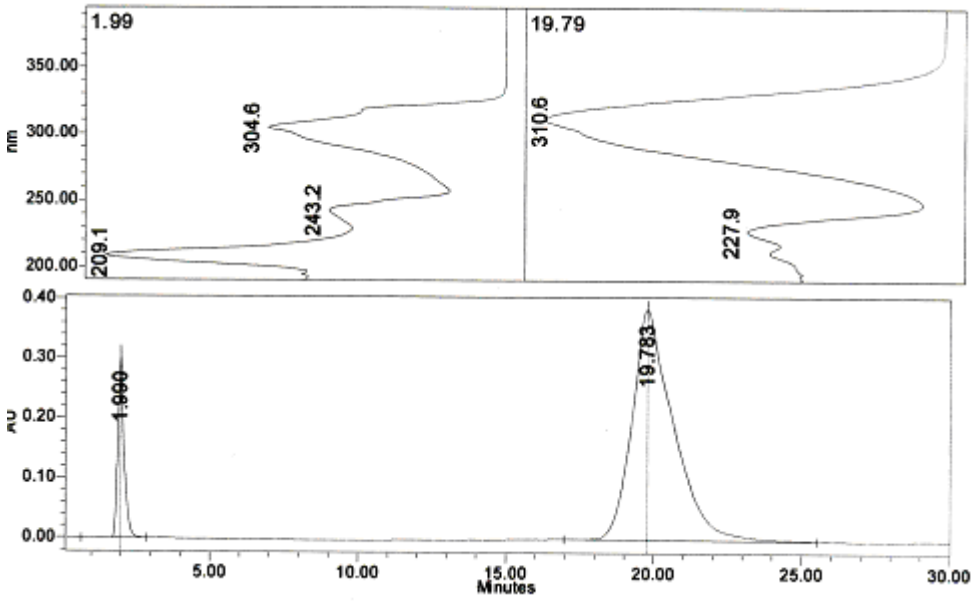

Figure 13 HPLC chromatogram of unirradiated AU 3 separated on a Nucleosil C100 C_{18} column, eluent 85% MeOH/H_2O, flow rate 1 mL min^{-1} , injection volume – 10 µL and detection wavelength of 310 nm. The order of elution is PBSA and *trans*-2-EHMC.

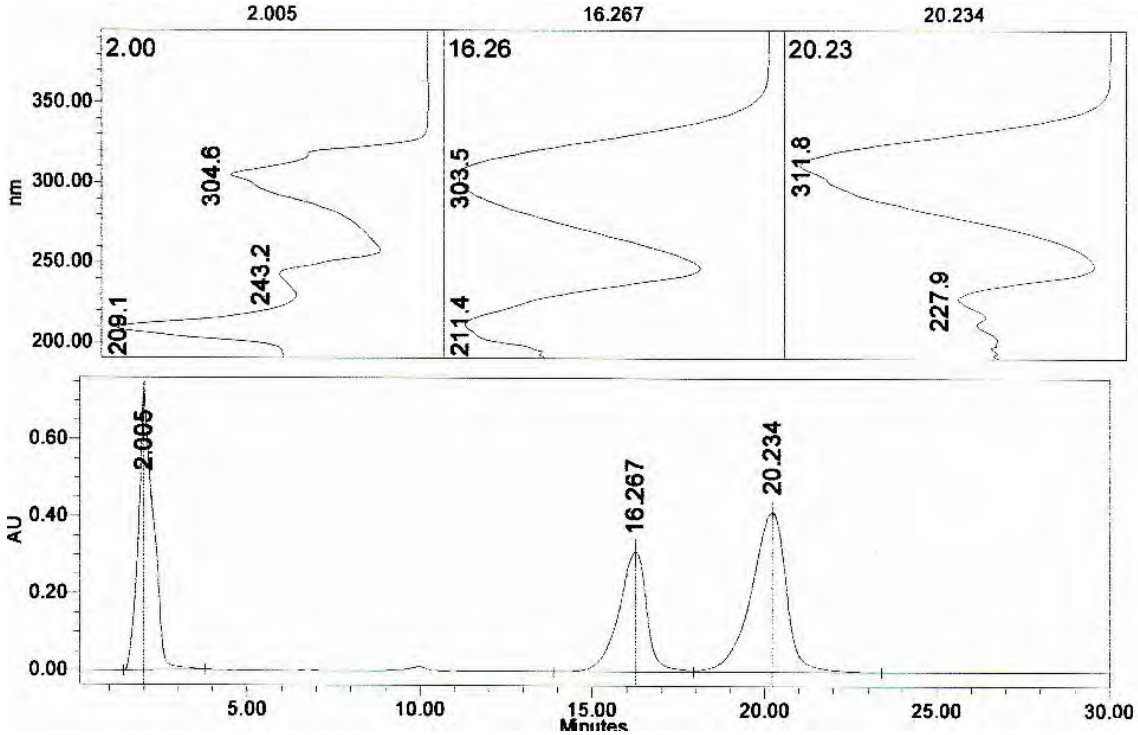

Figure 14 HPLC chromatogram of irradiated AU 3 separated on a Nucleosil C100 C_{18} column, eluent 85% MeOH/H_2O, flow rate 1 mL min^{-1} , injection volume – 10 µL and detection wavelength of 310 nm. The order of elution is PBSA, *cis*-2-EHMC and *trans*-2-EHMC.

Samples AU 4, 21 and 22 contained 2-EHMC, OCT and ZnO as the active chemical agents. These chemical filters are essentially UVB absorbers. Figure 15 shows the UV transmission spectra of AU 4 with increasing dose levels of UV radiation. There was no transmittance exhibited in the UVB region. However, there was essentially complete transmission in the UVA region and therefore this product offered no protection in the UVA region. The presence of octocrylene in the product is normally used to photostabilize 2-EHMC [51]. This product was considered to be photostable.

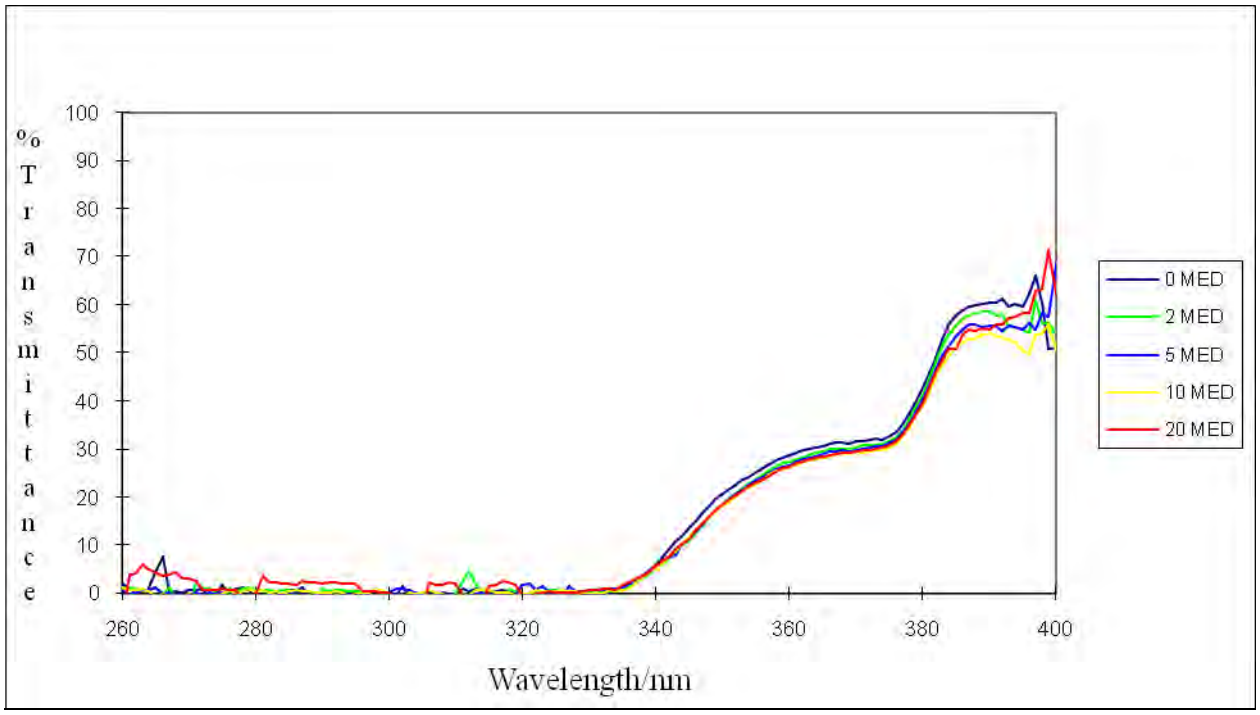

Figure 15 UV transmission spectra of AU 4 with increasing doses of UV radiation.

The HPLC chromatogram (Figure 16) shows two peaks due to octocrylene at 11.552 min and 2-EHMC at 19.216 min. Upon irradiation a new peak was observed at 15.724 min due to the isomerisation of *trans*-2-EHMC to its *cis*-form as shown in Figure 17. In comparison octocrylene, a cyanoacrylate derivative similar to the cinnamates, showed no photodegradation. The photostability could be in part attributed to the lack of geometrical isomers in this trisubstituted double bond system [52].

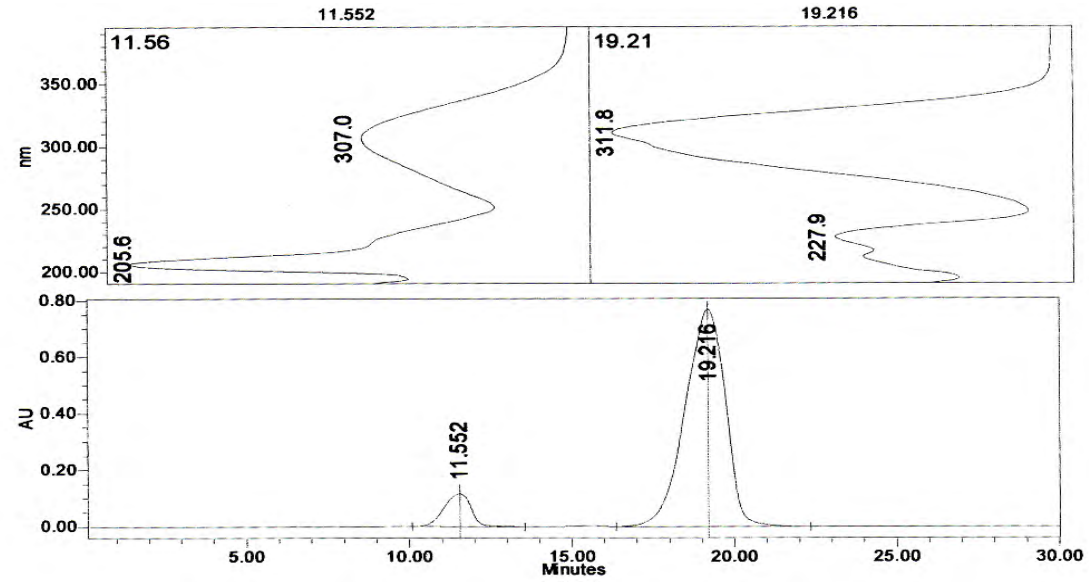

Figure 16 HPLC chromatogram of unirradiated AU 4 separated on a Nucleosil C100 C_{18} column, eluent 85% MeOH/H_2O, injection volume – 10 µL, flow rate 1 mL min^{-1} and detection wavelength of 310 nm. The order of elution is octocrylene and *trans*-2-EHMC.

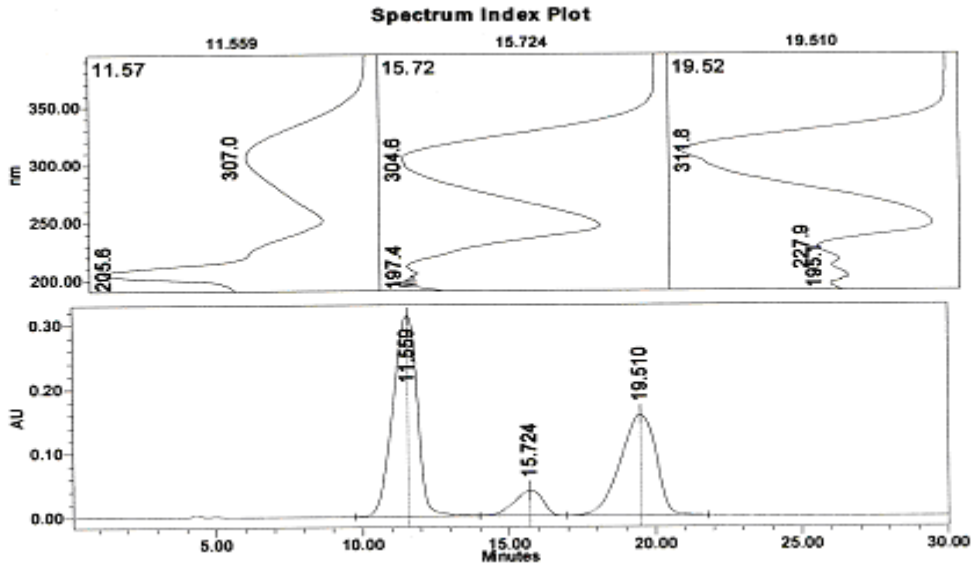

Figure 17 HPLC chromatogram of irradiated AU 4 separated on a Nucleosil C100 C_{18} column, eluent 85% MeOH/H_2O, flow rate 1 mL min^{-1} , injection volume – 10 µL and detection wavelength of 310 nm. The order of elution is octocrylene, *cis*-2-EHMC and *trans*-2-EHMC.

Samples AU 9 and 13 contained 2-EHMC, Benz-3 and TiO_2 in their formulations. Figure 18 shows the transmission spectra of AU 9. Although Benz-3 is used as a UVA absorber, it

absorbs most efficiently in the UVB region and the shorter UVAII (320-340 nm) range with two absorption peaks at 285 and 325 nm [53] and also as seen in Figure 1 and Table 4. From the spectra, it is evident that this product is photostable even though it covers a very small spectral range. However, this product was observed to be transparent in the longer wavelength UVA region (340-400 nm). The shapes of the transmission spectra remained essentially the same throughout the irradiation period. The presence of TiO_2 in the sample is responsible for the low transmission observed at the shorter UVA region for this formulation. When this sample was compared with sample AU 23 (Figure 15) which had the same active chemical agents but did not have any TiO_2 a greater transmission was observed in the UVA region for AU9. This can be explained by the fact that AU 23 contained more Benz-3 which absorbs in the UVAII range.

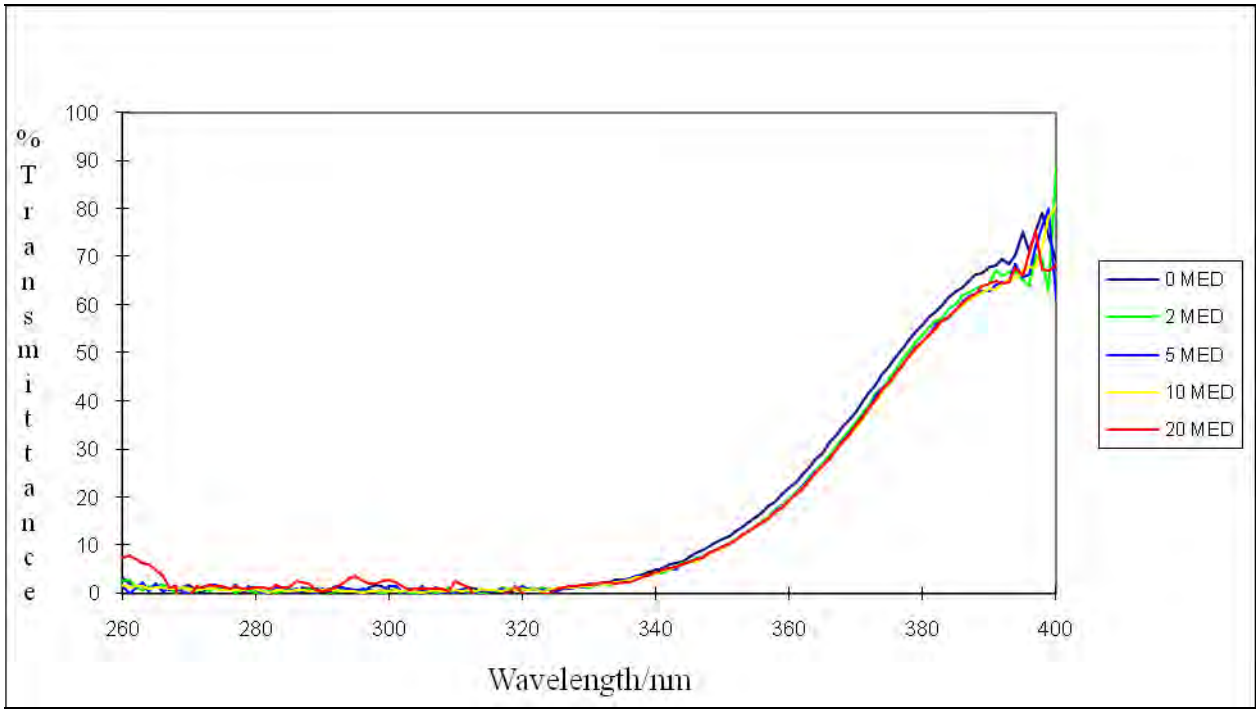

Figure 18 UV transmission spectra of AU 9 with increasing doses of UV radiation.

The HPLC chromatogram (Figure 20) shows the presence of two compounds: Benz-3 at 6.56 min and 2-EHMC at 19.644 min. Benz-3 offers protection essentially in the UVB region although it also provides some protection in the shorter UVA range. Upon irradiaton of the sample a new peak appeared at 15.91 min which is associated with photoisomerisation of *trans*-2-EHMC to its *cis*-form (Figure 20). The *cis*-form has a lower molar absorption

coefficient (1.84 x 10^4 dm^3 mol^{-1} cm^{-1}) than the *trans*-2-EHMC (2.45 x 10^4 dm^3 mol^{-1} cm^{-1}) and hence is a less efficient absorber [54].

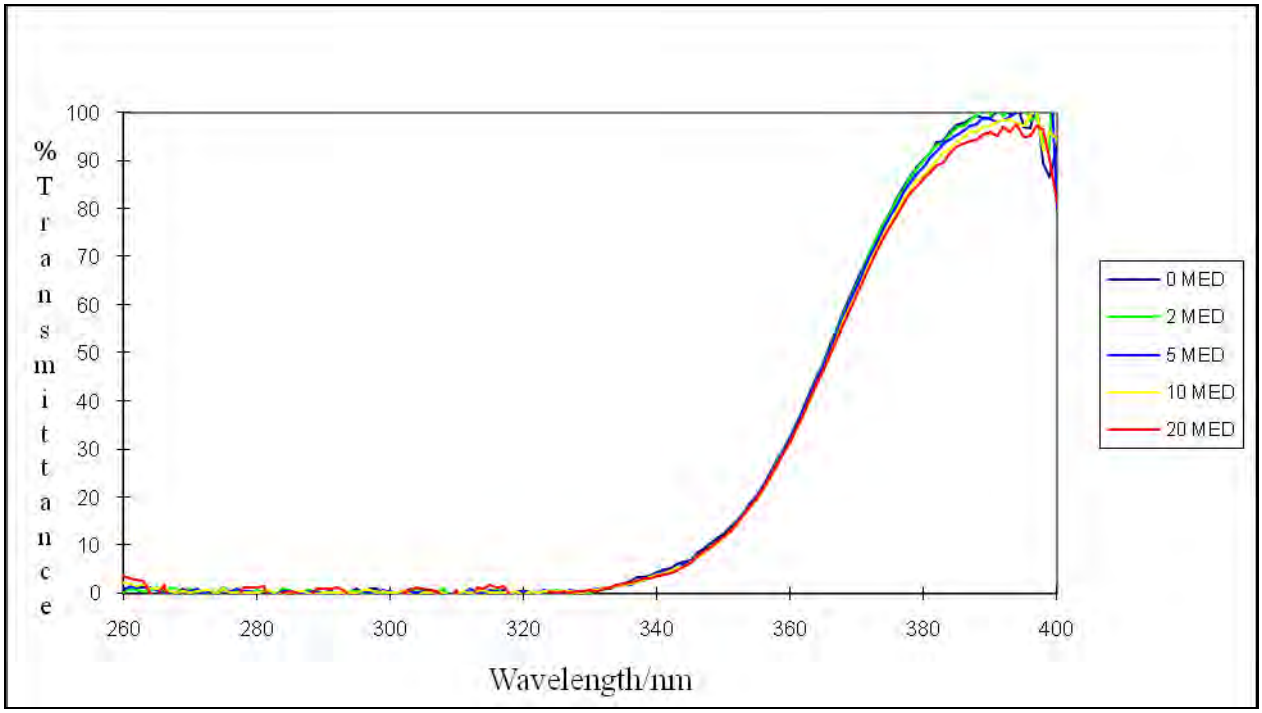

Figure 19 UV transmission spectra of AU 23 with increasing doses of UV radiation.

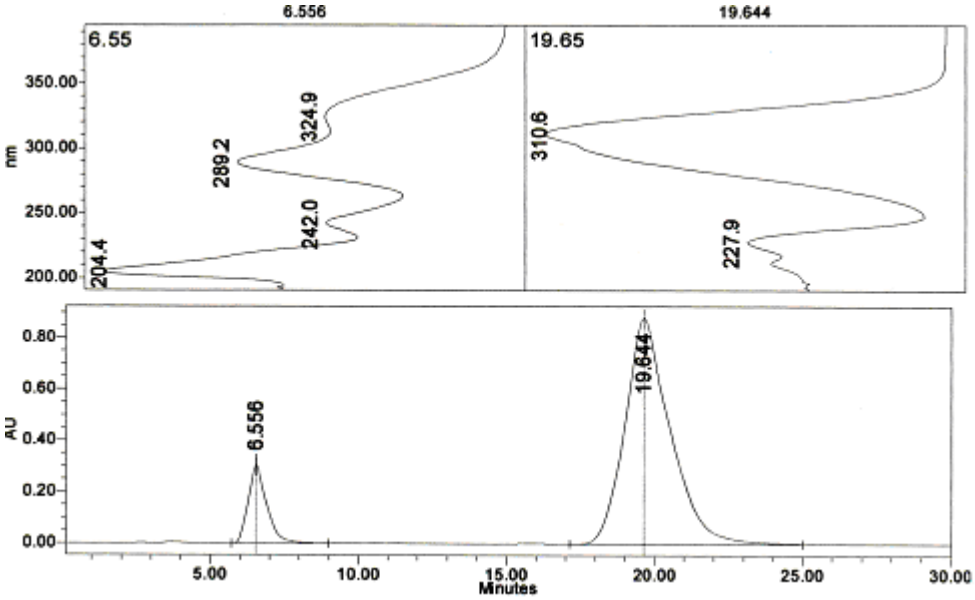

Figure 20 HPLC chromatogram of unirradiated AU 9 separated on a Nucleosil C100 C_{18} column, eluent 85% MeOH/H_2O, flow rate 1 mL min^{-1} , injection volume – 10 µL and detection wavelength of 310 nm. The order of elution is Benz-3 and *trans*-2-EHMC.

Benz-3 is normally considered a safe and photostable UV filter. However, some studies show that in the presence of Benz-3, 2-EHMC tends to photodegrade much faster as Benz-3 seems to have a photosensitizing effect [50]. The work of Schallreuter *et al.* [21] shows that Benz-3 can be oxidized to yield a photoproduct known as oxybenzone semiquinone. This is a highly potent electrophile as it reacts with antioxidant systems resulting in their inactivation. This would be harmful to the homeostatis of the epidermis [21]. This photoproduct was not observed in this work.

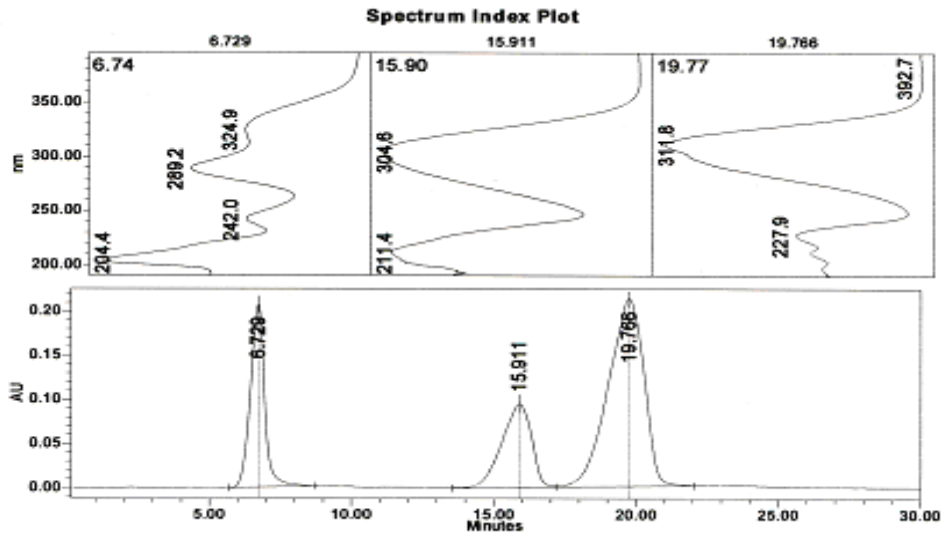

Figure 21 HPLC chromatogram of irradiated AU 9 separated on a Nucleosil C100 C_{18} column, eluent 85% MeOH/H_2O, flow rate 1 mL min^{-1} , injection volume – 10 µL and detection wavelength of 310 nm. The order of elution is Benz-3, *cis*-2-EHMC and *trans*-2-EHMC.

Samples AU 11 and 25 contained 2-EHMC and AVO as the active chemical agents. AVO is the most commonly used UVA filter. Figure 22 shows the UV transmission spectra of sample AU 11. This is a broad spectrum sunscreen. It displayed photostability in the UVB region but it lost absorbance in the UVA region upon exposure to increasing doses of UV radiation. There is a very marked increase in the loss of absorbance especially at 20 MED. The loss of absorbance in the UVA region can be attributed to the photodegradation of AVO, following a keto-enol isomerisation as has been shown in other investigations [55-57]. The filter combination of AVO and 2-EHMC is known to be photounstable as the two absorbers tend to

photodegrade into other products [58]. The presence of AVO tends to enhance the photodegradation of 2-EHMC when the two are formulated in combination. The work of Panday [59] showed that AVO photosensitises the photoisomerisation of 2-EHMC which accounts for some photodegradation in the UVB region. The destabilisation of 2-EHMC in the presence of AVO is also probably caused by a photochemical reaction of the two compounds, which occurs in a similar way as in the case of the photocyclodimerization of 2-EHMC with itself [30, 43]. When AVO undergoes photoreactions it may react with 2-EHMC to form cycloaddition products and perhaps other photoproducts which may contribute to the overall decrease in absorbance [22, 60]. The loss in the absorbance makes this product photounstable in the UVA region.

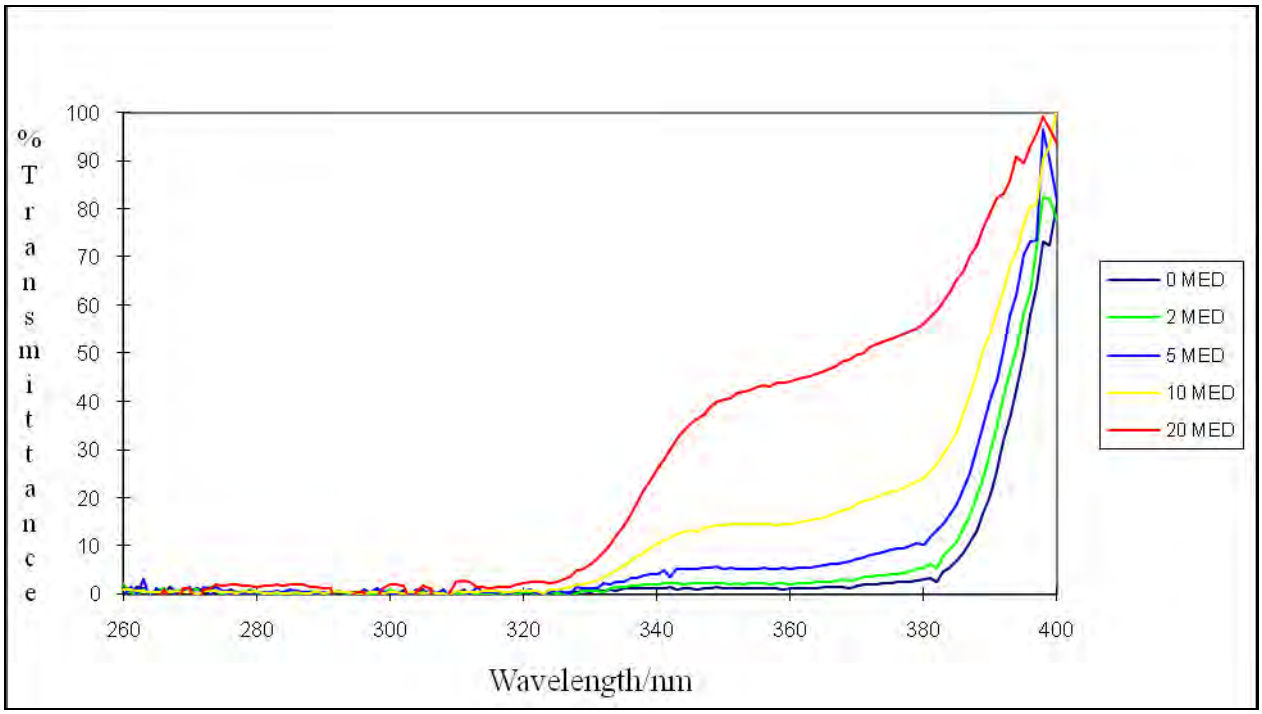

Figure 22 UV transmission spectra of AU 11 with increasing doses of UV radiation.

Figure 23 shows the 2-EHMC peak monitored at 310 nm and Figure 24 shows that of AVO monitored at 358 nm before irradiation. Upon irradiation there was a second peak associated with 2-EHMC appearing at 16.58 min which could be assigned to the *cis*-isomer. However, after irradiation the presence of the AVO peak was undetectable. This showed that AVO had photodegraded.

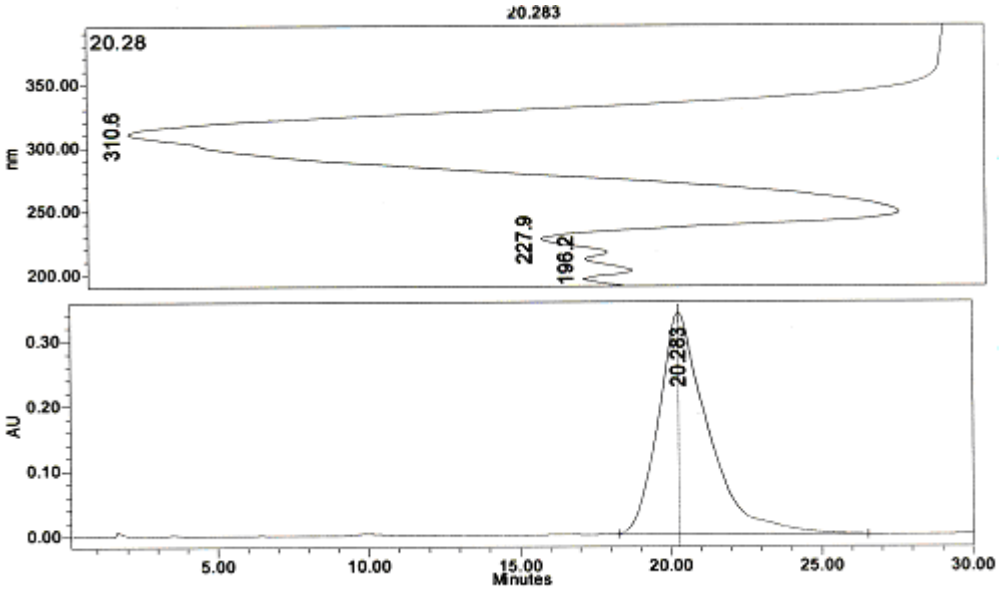

Figure 23 HPLC chromatogram of AU 11 separated on Nucleosil C100 C_{18} column, eluent 85% MeOH/H_2O, flow rate 1 mL min^{-1} , injection volume – 10 µL and detection wavelength of 310 nm. This shows the peak due to *trans*-2-EHMC.

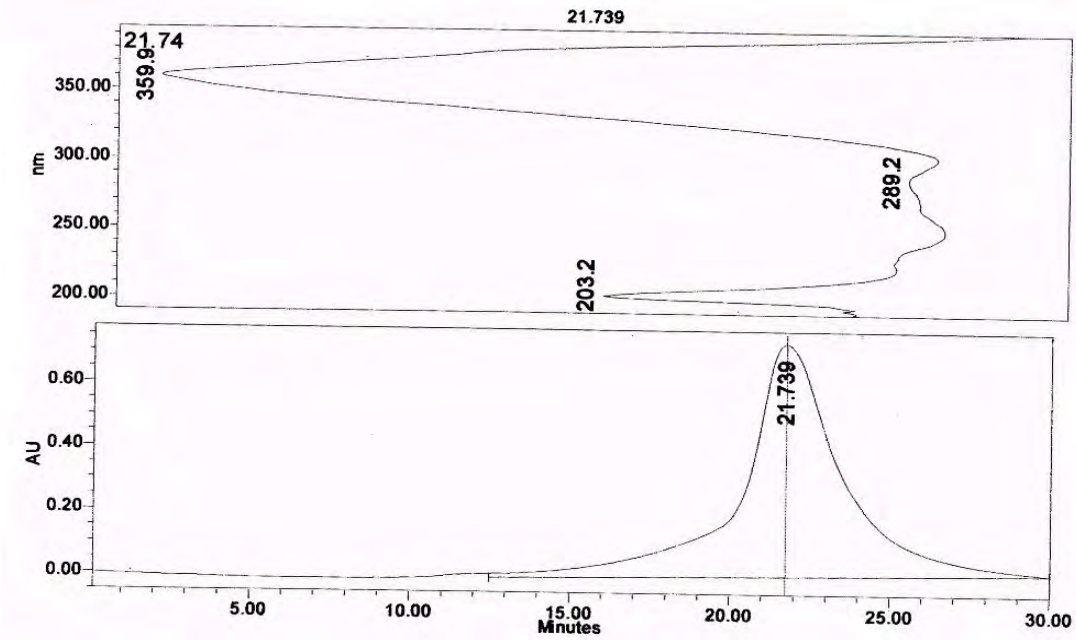

Figure 24 HPLC chromatogram of AU 11 separated on Nucleosil C100 C_{18} column, eluent 85% MeOH/H_2O, flow rate 1 mL min^{-1} , injection volume – 10 µL and detection wavelength at 358 nm showing the peak due to AVO.

Sample AU 15 consisted of 2-EHMC, AVO and OT as the active ingredients. Figure 25 shows the transmission spectra of AU 15 obtained upon exposure to varying levels of UV

radiation. At 0 MED the product offered broad-spectrum protection covering effectively both the UVA and UVB regions. This is a broad-spectrum sunscreen which displays good absorption in the UVB region but gradually loses its absorption capacity in the UVA region upon increasing doses of UV radiation. The shapes of the transmission spectra were significantly changed with increasing UV exposure. The loss of protection in the UVA region can be attributed to the photodegradation of AVO as observed for sample AU 11. However, the inclusion of OT does not decrease the transmission of UV radiation in the UVA region. This is evident in this product as the photoloss is in fact enhanced. Hence this product was classified as photounstable.

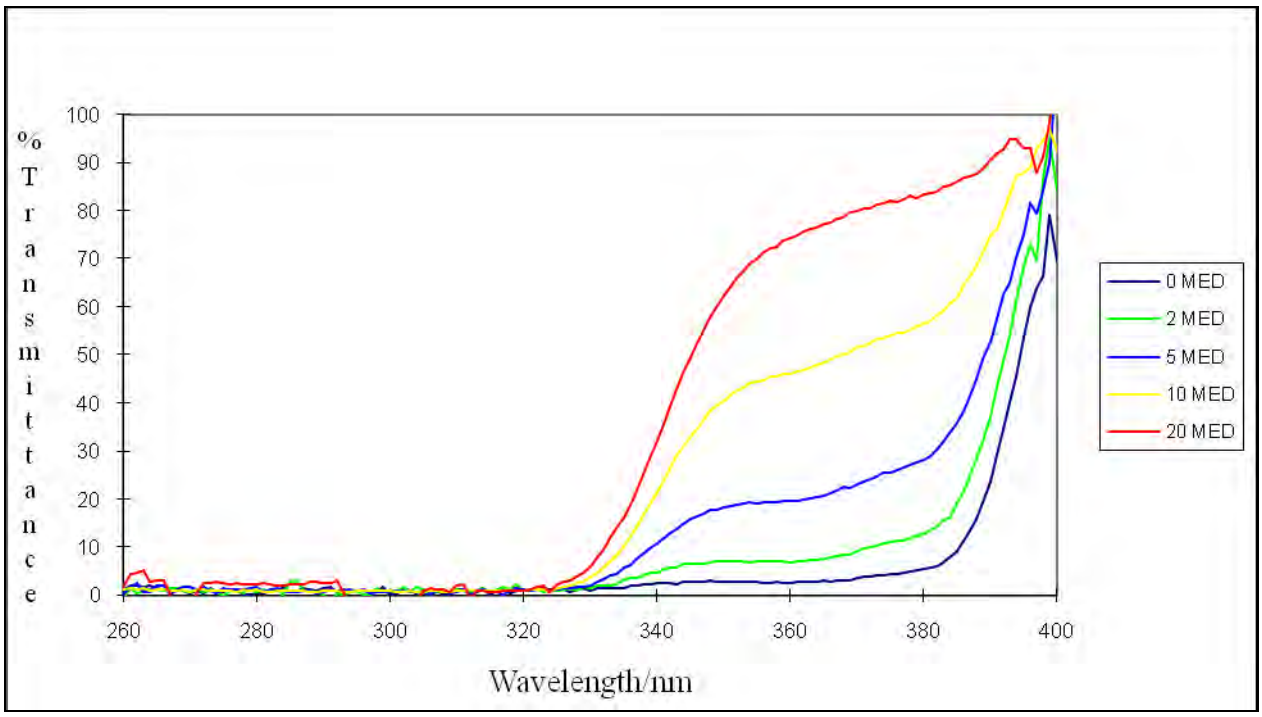

Figure 25 UV transmission spectra of AU 15 with increasing levels of UV radiation

The HPLC chromatogram of unirradiated AU 15 is as shown in Figure 26 whereas Figure 27 shows the HPLC chromatogram of AVO detected at 360 nm. Figure 28 shows the chromatogram obtained after irradiation of the sample. A new peak emerged at 15.47 min associated with the *cis*-form of *trans*–2-EHMC. The peak due to AVO at 22.54 min has reduced significantly in magnitude confirming that indeed the loss of absorbance in the UVA region is due to the photodegradation of AVO. Figure 24 shows the reduced peak of AVO when it was monitored at 360 nm. OT is meant to stabilize AVO and is normally considered photostable upon exposure to UV light [45, 61]. It is believed that AVO is able to transfer the

absorbed UV energy to OT instead of undergoing alternative reactions which result in loss of its absorption efficiency [44]. This does not appear to be the case here.

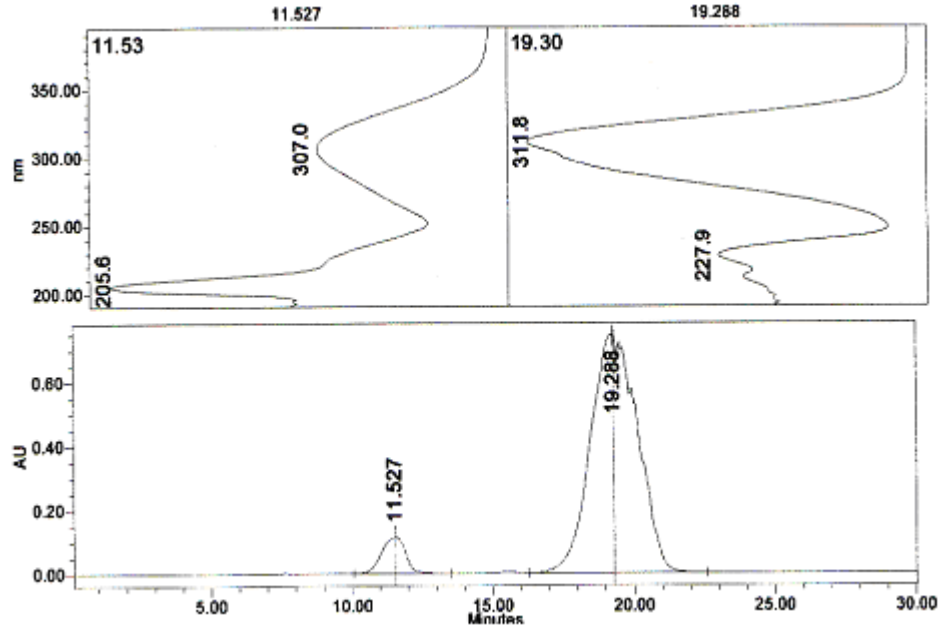

Figure 26 HPLC chromatogram of unirradiated AU 15 separated on a Nucleosil C100 C_{18} column, eluent 85% MeOH/H_2O, flow rate 1 mL min^{-1} , injection volume – 10 µL and detection wavelength of 310 nm. The order of elution is OT and *trans*-2-EHMC.

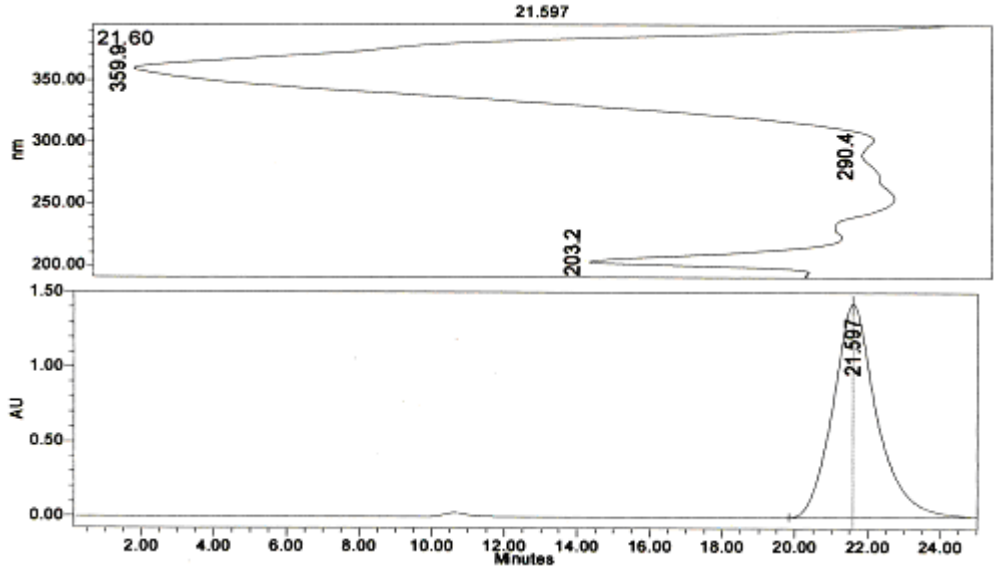

Figure 27 HPLC chromatogram of AU 15 separated on Nucleosil C100 C_{18} column, eluent 85% MeOH/H_2O, flow rate 1 mL min^{-1} , injection volume – 10 µL and detection wavelength at 360 nm showing the peak due to AVO.

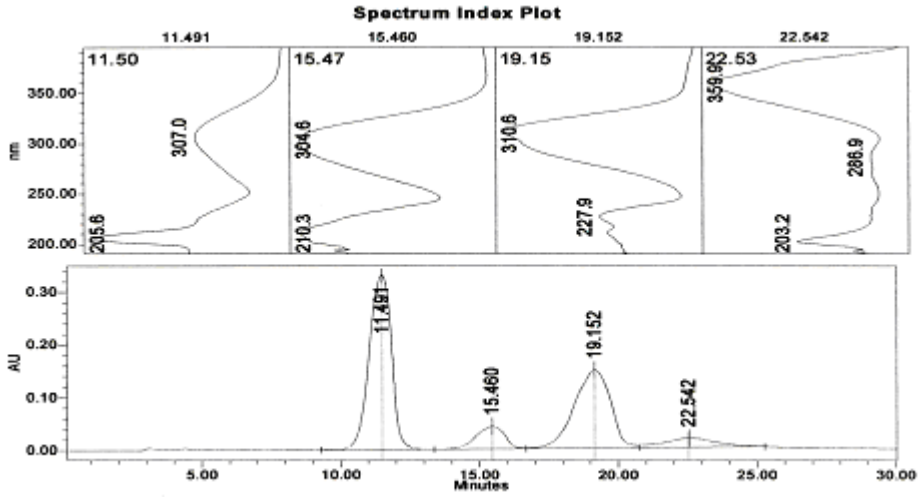

Figure 28 HPLC chromatogram of irradiated AU 15 separated on a Nucleosil C100 C_{18} column, eluent 85% MeOH/H_2O, flow rate 1 mL min^{-1} , injection volume – 10 µL and detection wavelength of 310 nm. The order of elution is OT, *cis*-2-EHMC, *trans*-2-EHMC and AVO**.**

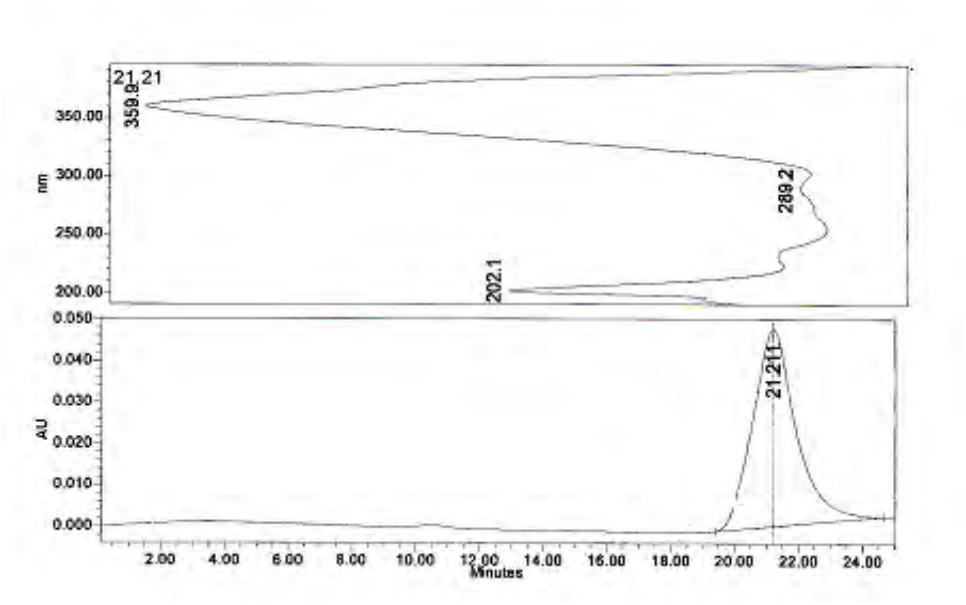

Figure 29 HPLC chromatogram of irradiated AU 15 separated on Nucleosil C100 C_{18} column, eluent 85% MeOH/H_2O, flow rate 1 mL min^{-1} , injection volume – 10 µL and detection wavelength at 360 nm showing the peak due to AVO

Samples AU 1, AU 10 and AU 18 contained 2-EHMC, AVO and MBC as the active agents. Figure 30 shows the UV transmission spectra for AU 1. The formulation showed good photostability in the UVB region. It is also evident that at 0 MED there is good broad-spectral coverage which is in keeping with the expected broad-spectrum filter combination. However,

in this formulation there was an initial gradual increase in transmission with increasing doses of radiation.

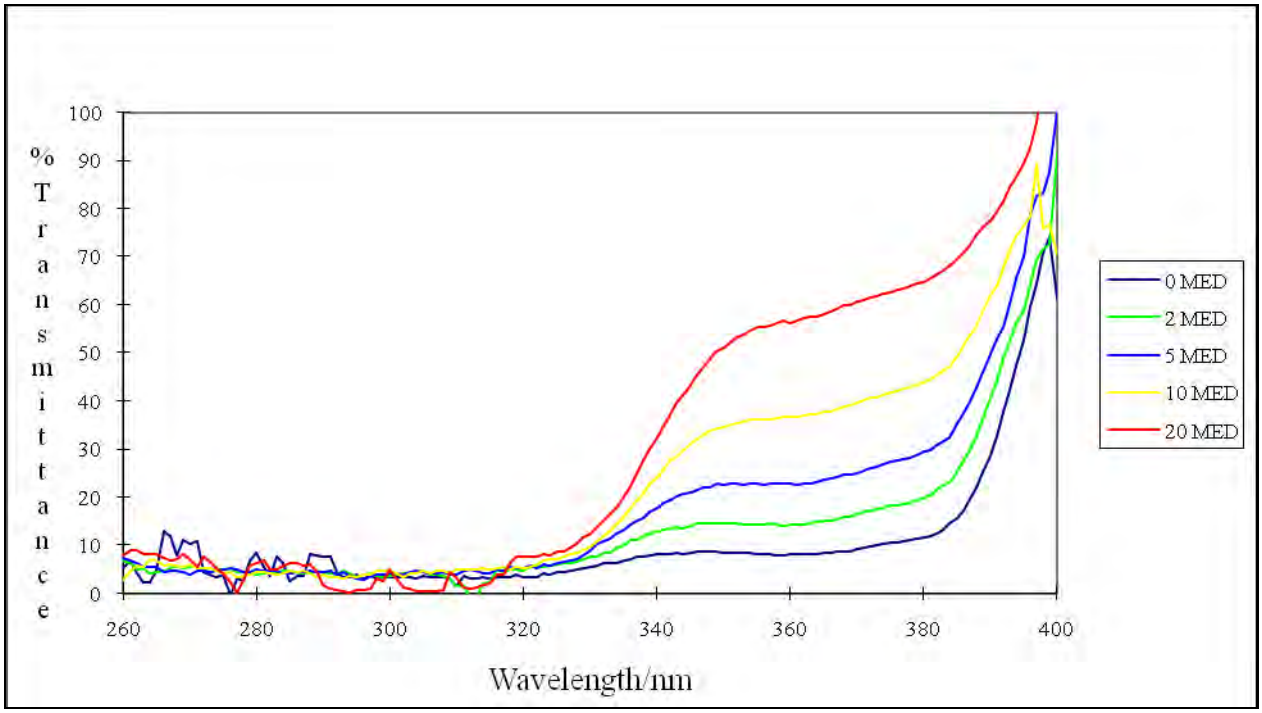

Figure 30 UV transmission spectra of AU 1 with increasing doses of UV irradiation.

There was then a marked increase in transmittance as the sample was exposed to 20 MED. This change in the UVA region can be attributed to the loss of absorbance of AVO which is known to photodegrade upon UV exposure [55]. The presence of MBC is thought to exert a photostablizing effect on avobenzone. Berset *et al.* [62] have reported that even low concentrations of MBC (0.5-3%) in a formulation are sufficient to preserve 80-90% of the avobenzone from photodegradation. However, here despite the presence of MBC, this product was assessed as photounstable in the UVA region as there is a steady increase in photoinstability with increase in irradiation dosage. From our results there was no indication that MBC reduces the photodegradation of AVO.

The chromatograms for the unirradiated sample are shown in Figures 31 and 32. The unirradiated sample shows the presence of the three ingredients 2-EHMC, AVO and MBC. The peak due to AVO was clearly observed at wavelength 360 nm as seen in Figure 32.

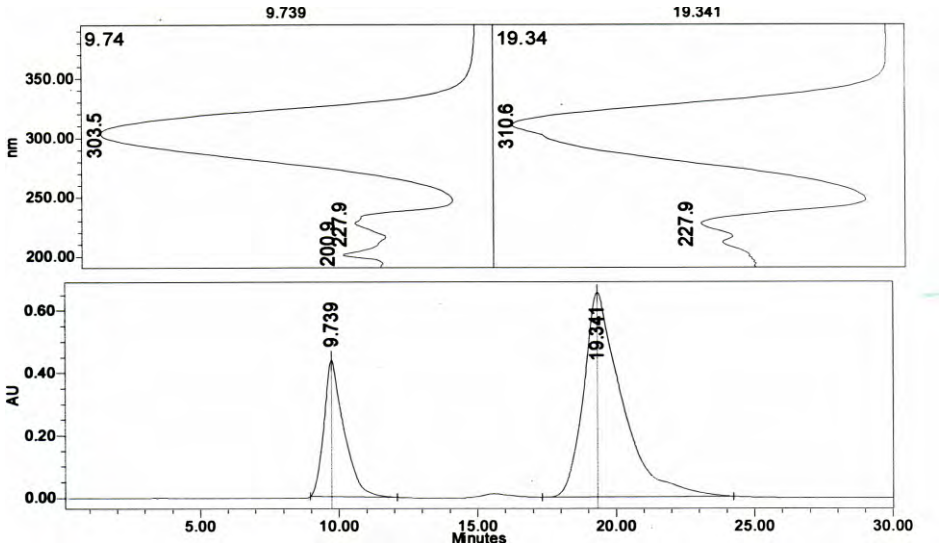

Figure 31 HPLC chromatogram of unirradiated AU 1 separated on a Nucleosil C100 C_{18} column, eluent 85% MeOH/H_2O, flow rate 1 mL min^{-1} , injection volume – 10 µL and detection wavelength of 310 nm. The order of elution is MBC and *trans*-2-EHMC.

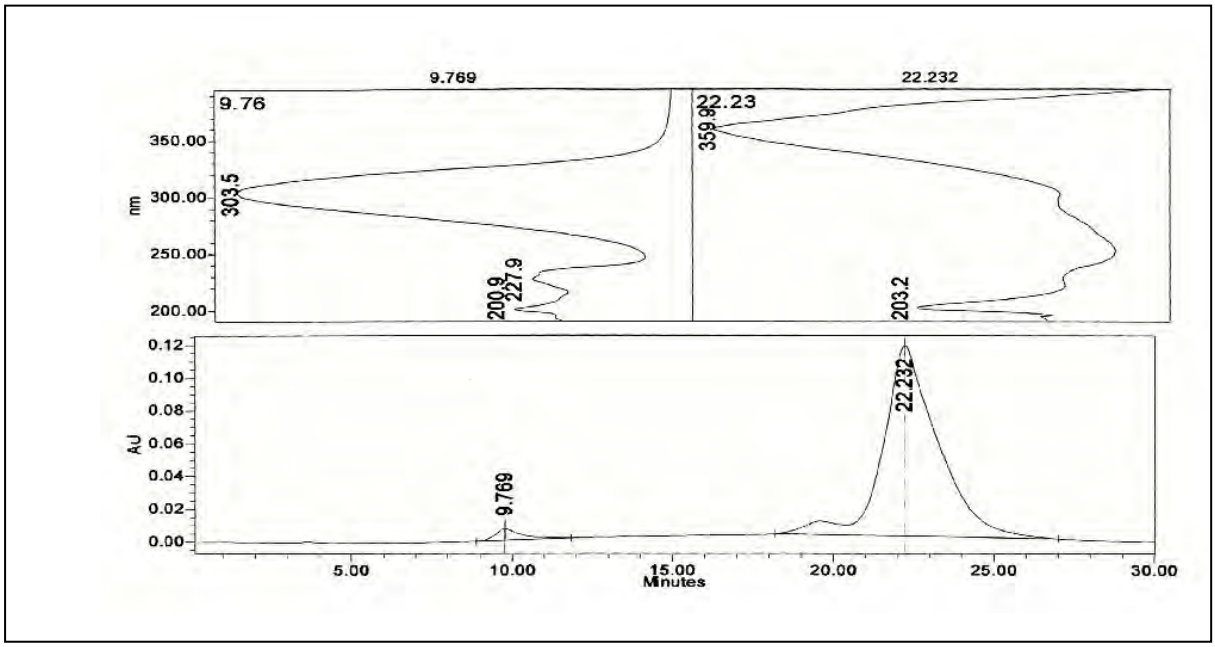

Figure 32 HPLC chromatogram of unirradiated AU 1 separated on a Nucleosil C100 C_{18} column, eluent 85% MeOH/H_2O flow rate 1 mL min^{-1} , injection volume – 10 µL and detection wavelength of 360 nm. The order of elution is MBC, *trans*-2-EHMC (at 19.5 min) and AVO.

Upon irradiation the sample showed the presence of new peaks as shown in Figure 33. This would be associated with the photodegradation of the *trans*-2-EHMC to the *cis*-form [19, 47] and likewise *trans*-MBC to its *cis*-form [19]. The presence of AVO, which is a UVA absorber, can be shown effectively when the chromatograms were monitored at 360 nm which is the wavelength that it absorbs maximally. Upon irradiation we note the presence of AVO was not detected indicating that photodegradation has taken place.

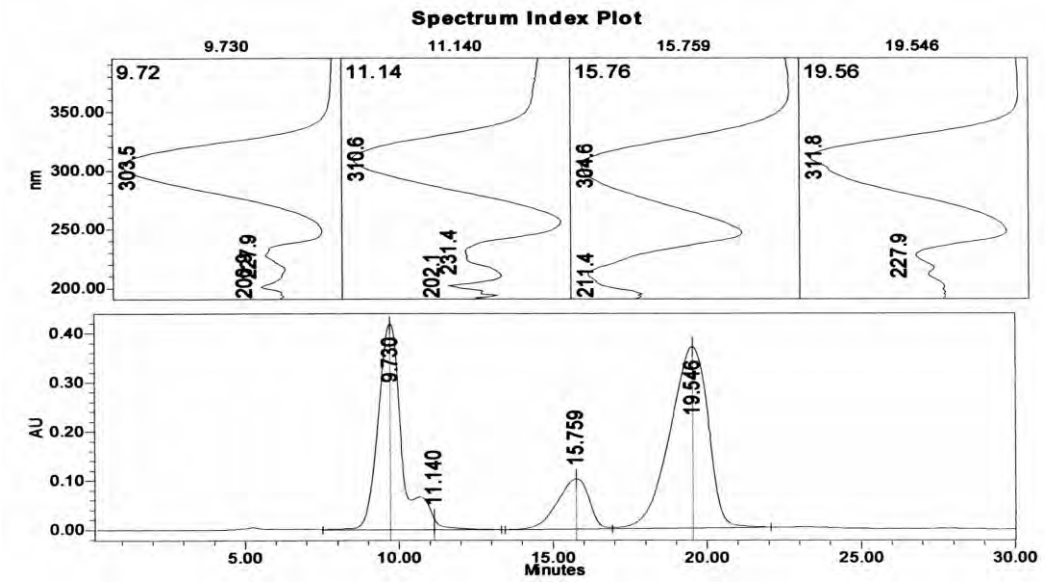

Figure 33 HPLC chromatogram of irradiated AU 1 separated on a Nucleosil C100 C_{18} column, eluent 85% MeOH/H_2O flow rate 1 mL min^{-1} , injection volume – 10 µL and detection wavelength of 310 nm. The order of elution is *trans*-MBC, *cis*-MBC, *cis*-2-EHMC and *trans*-2-EHMC.

The irradiated sample was also analysed by high performance liquid chromatography-mass spectrometry to ascertain the formation of photoproducts. Figure 34 shows the HPLC chromatogram obtained and has five peaks labelled A, M_1, M_2, E_1 and E_2 which correspond to AVO, *trans*-MBC, *cis*-MBC, *cis*-2-EHMC and *trans*-2-EHMC respectively. Figure 35 is the total ion chromatogram obtained and peaks labelled A, M_1, M_2, E_1 and E_2 correspond to the peaks shown in the HPLC chromatogram. The significance of this result was the confirmation that indeed *trans*-MBC and *trans*-2-EHMC had photodegraded to their *cis*-forms upon UV irradiation as seen by the data for the molecular masses. The intensity of the absorption peak of the AVO was also significantly reduced. However, no AVO photoproducts were detected.

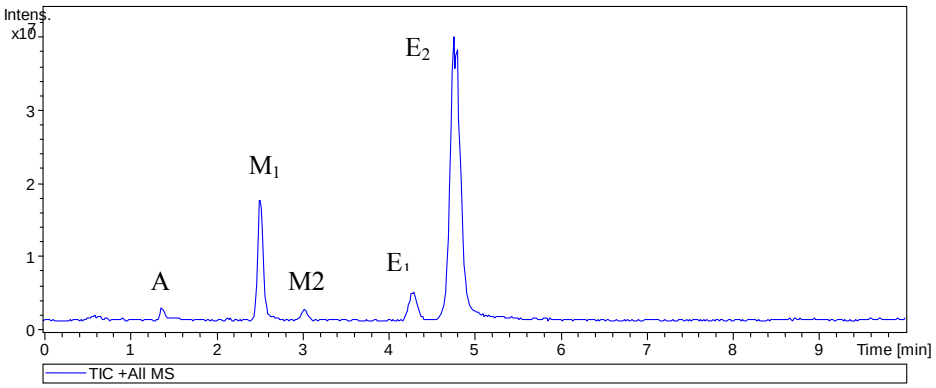

Figure 34 HPLC chromatogram of irradiated AU 1 analysed on the Agilent Zorbax Eclipse XDB-C18 column by isocratic elution at a flow rate 1 mL min^{-1} and injection volume – 5 µL with the Agilent 1100 Series HPLC with UV detection at 310 nm. The order of elution, AVO, *trans*-MBC, *cis*-MBC, *cis*-2-EHMC and *trans*-2-EHMC.

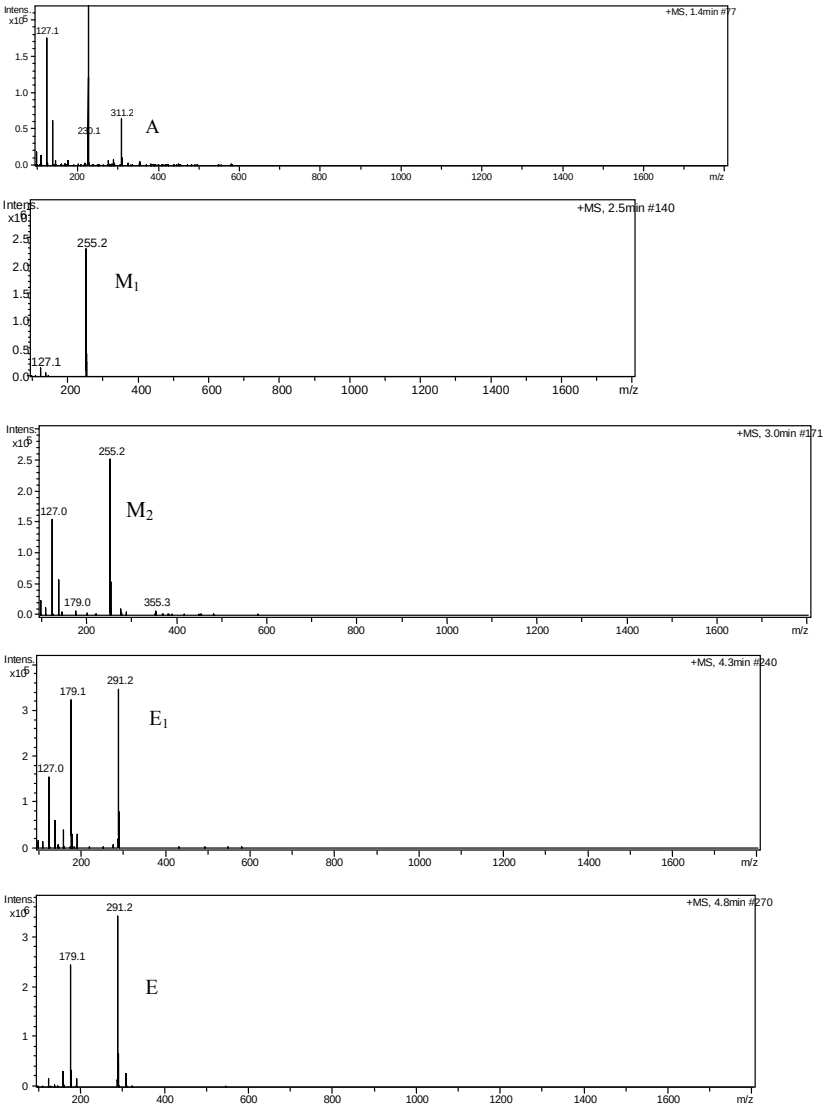

Figure 35 Mass spectra of the peaks labelled A, M1, M2, E1 and E2 in Figure 34.

Samples AU 2 and AU 24 consisted of 2-EHMC, AVO and Benz-3 as the active agents. In addition, sample AU 24 contained TiO_2 as an inorganic physical blocker. The transmission spectra of AU 2 are shown in Figure 36. This product was photostable in the UVB region. However, in the UVA region the product gradually loses its absorption efficiency with increasing doses of simulated solar radiation. This is due to the transformation of AVO as it is known to photodegrade upon exposure to UV radiation [29, 55]. The presence of Benz-3 in the sample which absorbs well through the UVAII (320-340 nm) region seems to enhance the formulation performance in the UVAII region as there is reduced transmittance when compared with sample AU 1. It significantly augments UVB protection when it is employed in a given formulation because of an additive effect. However, there was still a marked increase in transmission in the longer wavelength range hence the product was considered photounstable in the UVA region.

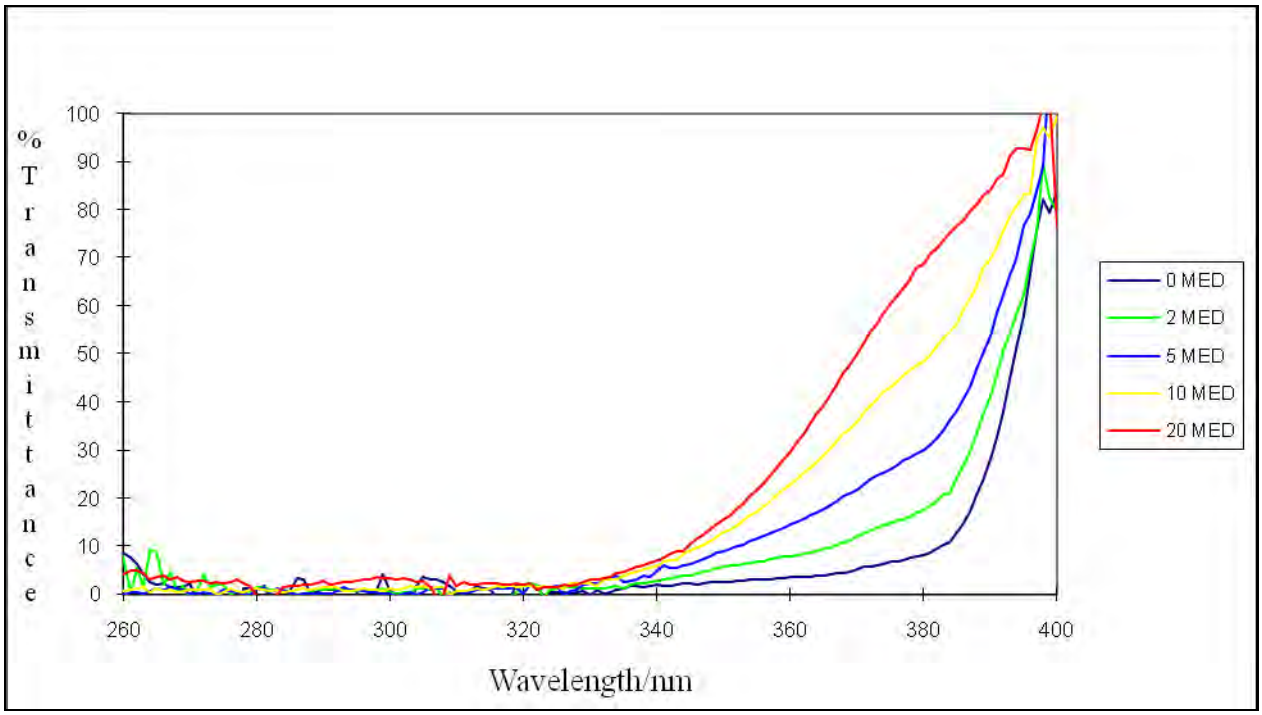

Figure 36 UV transmission spectra of AU 2 with increasing doses of radiation.

Figure 37 is the HPLC chromatogram showing only the presence of 2-EHMC and Benz-3 prior to irradiation. AVO was detectable at a wavelength of 360 nm as seen in Figure 38.

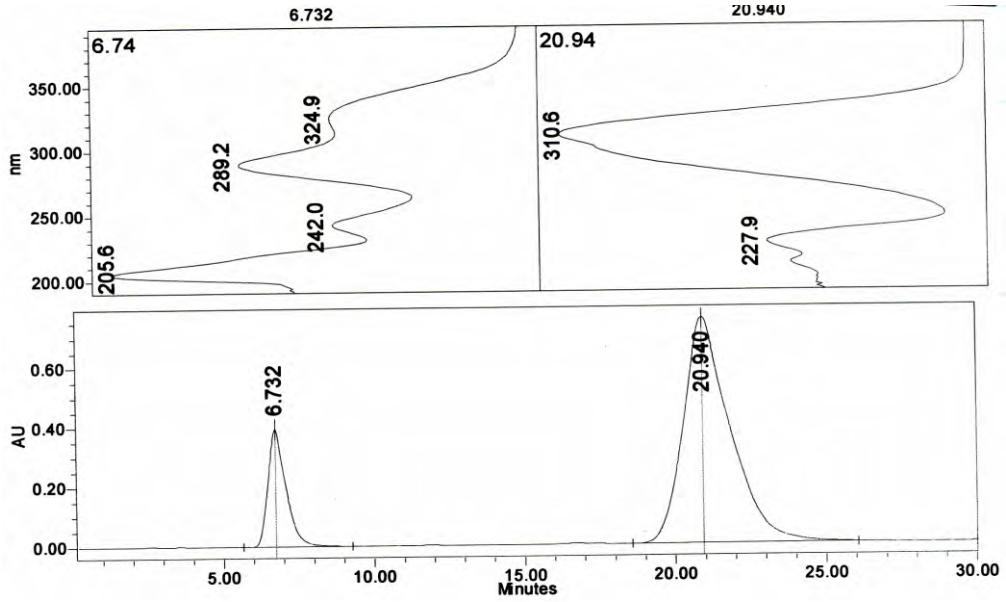

Figure 37 HPLC chromatogram of unirradiated AU 2 separated on a Nucleosil C100 C_{18} column, eluent 85% MeOH/H_2O, flow rate 1 mL min^{-1} , injection volume – 10 µL and detection wavelength of 310 nm. The order of elution is Benz-3 and *trans*-2-EHMC.

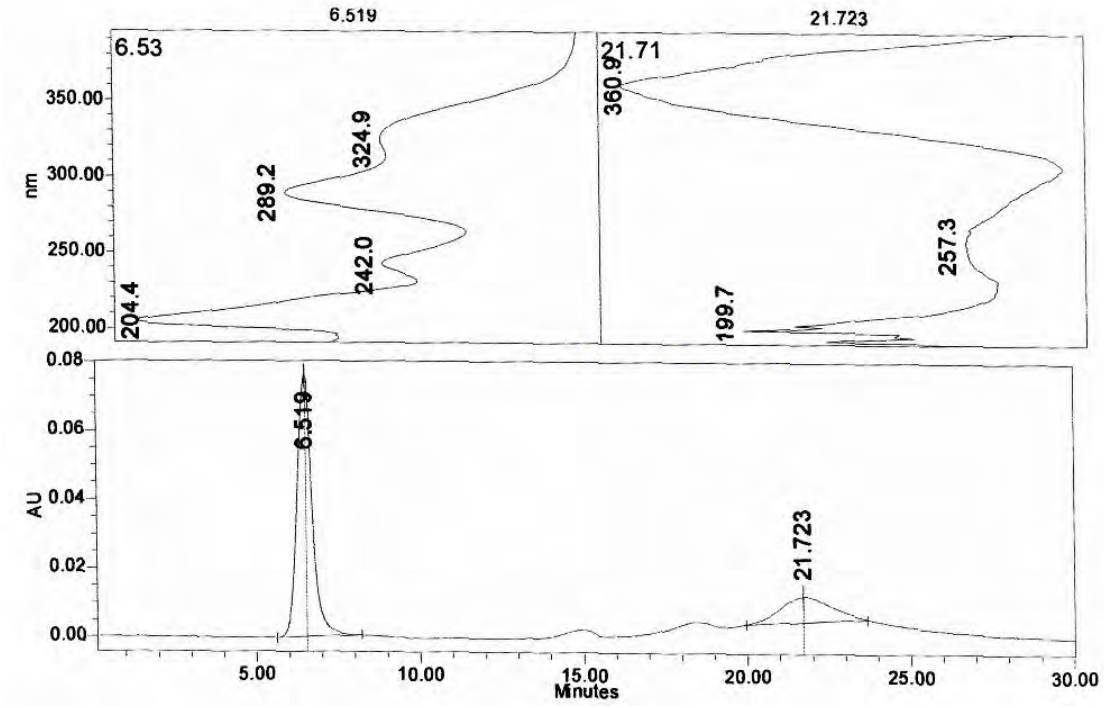

Figure 38 HPLC chromatogram of unirradiated AU 2 separated on a Nucleosil C100 C_{18} column, eluent 85% MeOH/H_2O, flow rate 1 mL min^{-1} , injection volume – 10 µL and detection wavelength of 360 nm. The order of elution is Benz-3 and AVO.

Upon exposure to solar simulated UV radiation a new peak appeared at 15.840 min associated with the photoisomerisation of *trans*-2-EHMC to the *cis*-isomer (Figure 39). The peak due to AVO was no longer detectable at 360 nm implying a complete photodegradation.

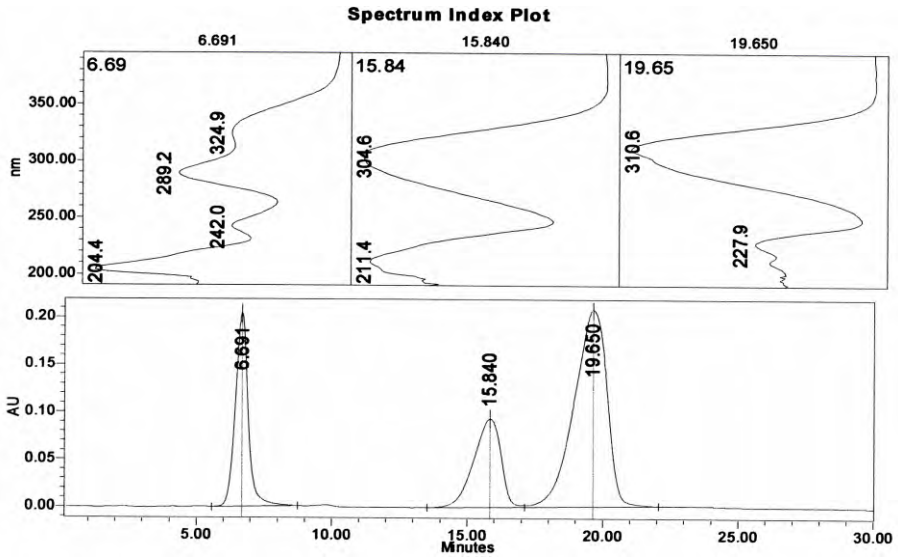

Figure 39 HPLC chromatogram of irradiated AU 2 separated on a Nucleosil C100 C_{18} column, eluent 85% MeOH/H_2O, flow rate 1 mL min^{-1} , injection volume – 10 µL and detection wavelength of 310 nm. The order of elution is Benz-3, *cis*-2-EHMC and *trans*-2-EHMC. AVO was not detectable even at 360 nm.

When AVO is combined with 2-EHMC a bimolecular reaction pathway leads to the rapid photodegradation of both the dibenzoylmethane derivative and 2-EHMC [52]. Although AVO is a significant addition to sunscreen products to achieve broad-spectrum UV protection, its potential to degrade other ingredients in formulations where it is used raises some concerns. AVO on its own is also known to photodegrade and the photodegradation products are potentially toxic.

Sample AU 7 was one of the formulations that had a combination of four filters. It consisted of 2-EHMC, AVO, MBC and OT as the active filters. Figure 40 shows the UV transmission spectra of AU 7. This formulation displayed high photostability in the UVB region but gradually loses absorbance during UV exposure with increasing doses of simulated solar radiation. This formulation displayed a rather unexpected trend since it was assumed to display a high photostability in both the UVA and UVB regions. The presence of the four filters, although thought to have a synergistic effect on the overall performance, is not evident in this product. The presence of MBC and OT in the formulation has been shown to stabilize

the photodegradation of AVO [45]. However, this product was assessed as photounstable because of the loss of its absorptivity at higher doses of radiation.

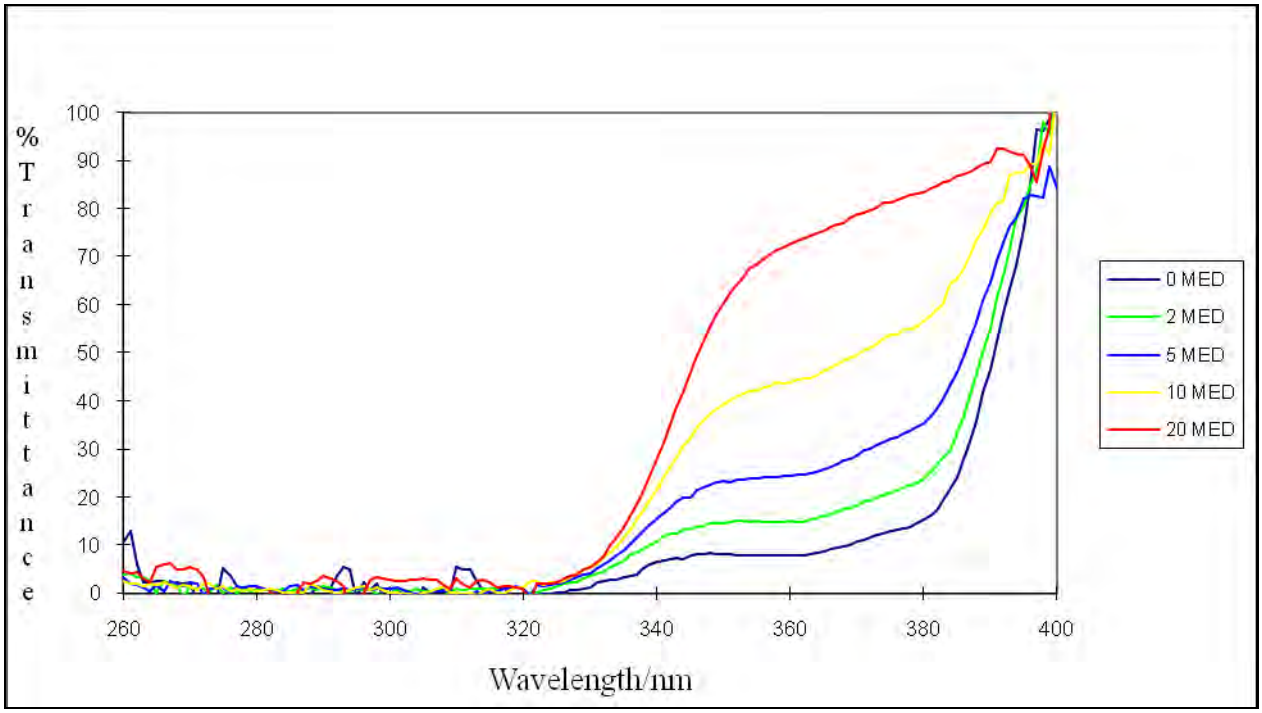

Figure 40 UV transmission spectra of AU 7 with increasing doses of radiation.

Sample AU 20 was the other formulation that had a combination of four filters. These were 2-EHMC, Benz-3, HS and Padimate-O. Figure 41 shows the transmission spectra of the sample. This formulation showed good photostability in the UVB region. Benz-3 is considered a UVA/UVB filter, for it shows maximum absorbance in the UVAII region at 325 nm. At wavelengths greater than 325 nm the product is transparent in the UVAI region as none of the filters used absorb in this region. This was evident from the minimal change in its filtering capacity in the UVA region as seen from the shapes of UV transmission spectra. Hence the product was declared as photostable both in the UVA and UVB regions even though it did not offer broad spectrum protection.

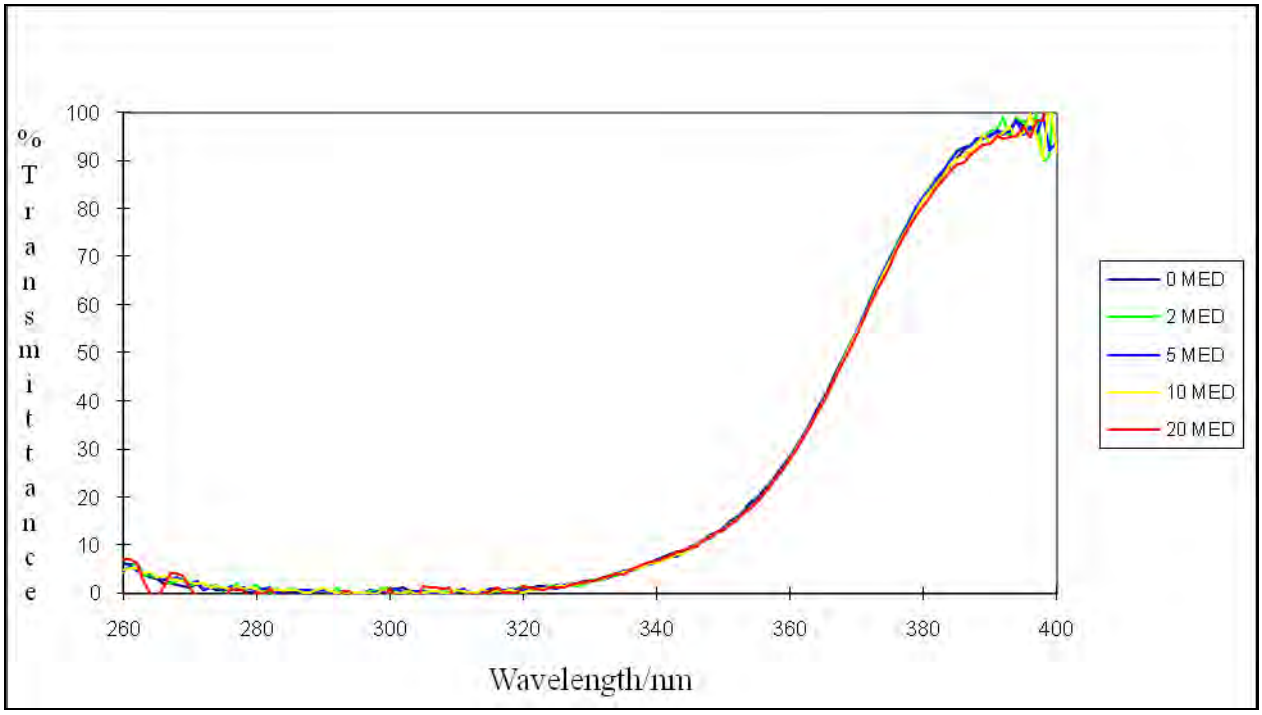

Figure 41 UV transmission spectra of AU 20 with increasing radiation doses.

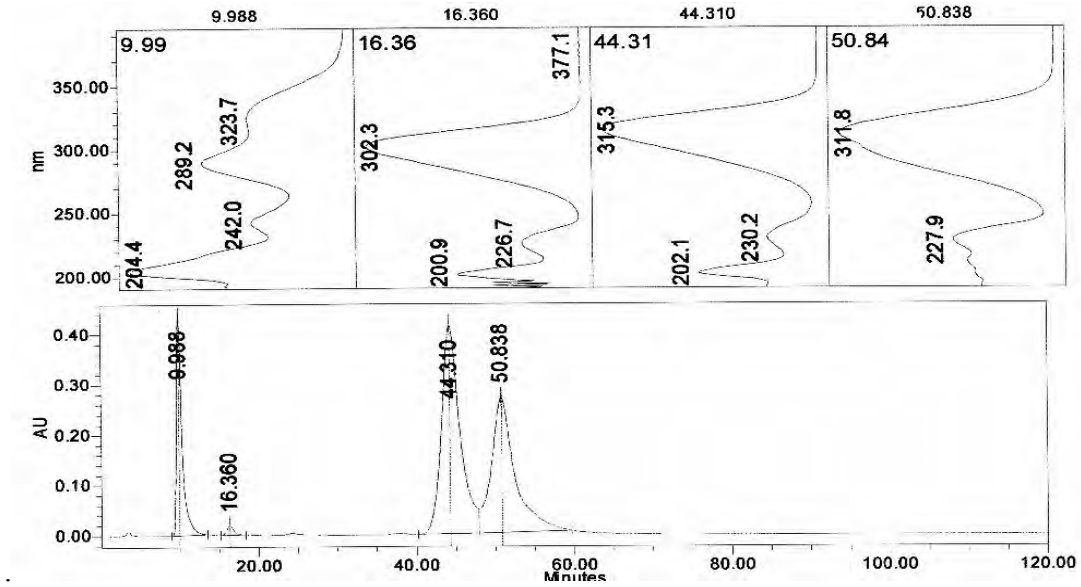

Figure 42 HPLC chromatogram of unirradiated AU 20 separated on a Nucleosil C100 C18 column, eluent 75% MeOH/H_2O, flow rate 1 mL min^{-1} , injection volume – 10 µL and detection wavelength of 310 nm. The order of elution is Benz-3, HS, ODM-PABA and *trans*-2-EHMC.

Figure 42 shows the HPLC chromatogram of AU 20. This formulation presented challenges to separate the active ingredients with the eluent composition that had been used for the other

samples. The presence of homosalate is known to present difficulties in the separation. However, by changing the eluent composition to 75% (v/v) methanol-water, some separation as shown in Figure 43 was possible. Upon irradiation the formulation showed another peak at 15.820 min which is associated with photoismerisation of 2-EHMC (see Figure 38). The other chemical ingredients remain unchanged. This formulation was assessed to be photounstable from the transmission spectra.

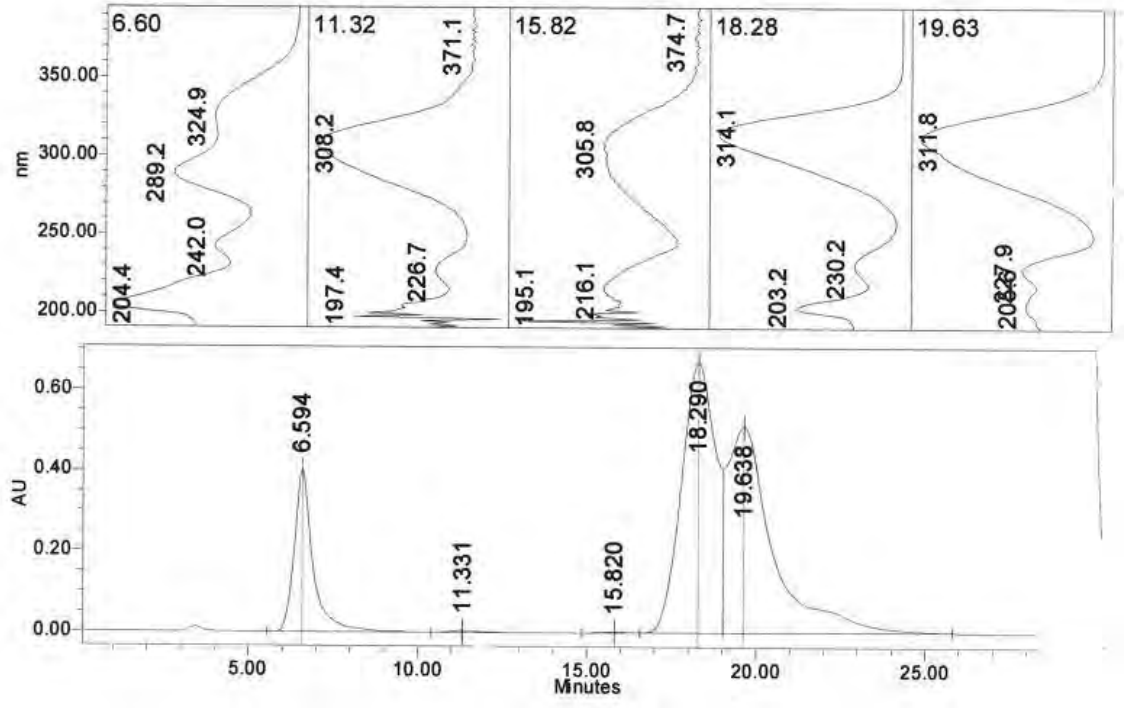

Figure 43 HPLC chromatogram of unirradiated AU 20 separated on a Nucleosil C100 C_{18} column, eluent 75% MeOH/H_2O, flow rate 1 mL min^{-1} , injection volume – 10 µL and detection wavelength of 310 nm. The order of elution is Benz-3, HS, ODM-PABA and *trans*-2-EHMC.

3.4 *In vitro* assessment of the photostability of sunscreen products

The mean spectral photoinstabilities of different sunscreen products were calculated according to the method described by Maier *et al.* [18] and the results are presented in Table 11. A mean photoinstability of ≥ 5% for an irradiation of 10 MED in the UVA (ΔT_A) or in the UVB (ΔT_B) range was set as the threshold value. This UV exposure corresponds closely to the expected amount of radiation the human skin is exposed to daily [62].

Of the twenty five sunscreen formulations analyzed, eight, namely, AU 1, 2, 7, 10, 11, 15, 18 and 25, showed photoinstabilities that were significantly higher than the threshold value of 5% in the UVA region after exposure to 10 MED radiation. None of the products showed photoinstability in the UVB region. Most of the photounstable products showed a steep increase in the UV transmission in the range between 330 and 350 nm.

On analyzing the photounstable products it was found that six out of the twelve different filter combinations contained AVO and five of these combinations were photounstable as shown in Table 11. HPLC quantitation was carried out on the photounstable products to determine the degree of photodegradation by using the peak areas. The percentage loss (% m/m) of the active ingredients in the different suncare products are listed in Table 11. This is in agreement with other studies, which relates this phenomenon to the photodegradation of AVO present [18, 33, 34] and hence makes the complete sunscreen product photounstable. It must also be pointed out that all the products that were photounstable also contained 2-EHMC. A combination of 2-EHMC and AVO has been shown to be unstable by other workers [58] in particular because AVO photosensitises the photodegradation of 2-EHMC. However, in this work the photostability in the UVB region was not affected.

There was only one product (AU 24) which although it contained AVO, 2-EHMC and Benz-3 as did AU 2 did not show photoinstability. This can possibly be attributed to the low concentration of AVO present. In addition, the inclusion of TiO_2 as a UVA physical blocker in AU 24 could enhance the overall performance of the formulation. This TiO_2 may have served to block UV radiation from reaching the AVO and hence reducing AVO photodegradation. Although the photostability behaviour of AVO has been suggested to be sensitive to experimental conditions and is highly dependent on the chemical environment [63], this was not observable in this study. For example, it is known that AVO is photostable in polar protic solvents and photounstable in non-polar and aprotic solvents [59, 64, 65]. Nevertheless, AVO is still being used worldwide for broad-spectrum protection. This is because it offers a unique absorption spectrum as well as a very high molar absorption coefficient [63].

Table 11 Photoinactivation in the UVA (320-380 nm) range, (ΔT_A %) and the UVB (280 - 320 nm) range, (ΔT_B %) for different radiation doses in MED.

	%Transmittance		Photoinactivation after UV exposure							
MED	0		2		5		10*		20	
Product	T_A	T_B	ΔT_A	ΔT_B	ΔT_A	ΔT_B	ΔT_A	ΔT_B	ΔT_A	ΔT_B
AU1	8.19	4.11	-5.47	0.41	-11.79	-0.25	**-21.42**	-0.28	-35.13	1.01
AU2	3.55	0.58	-4.00	0.30	-9.41	-0.05	**-16.65**	-0.54	-23.62	-1.38
AU3	31.56	0.54	1.41	0.07	2.55	0.01	3.28	0.10	3.06	0.22
AU4	20.18	0.23	1.01	-0.56	1.18	0.33	1.74	0.17	1.54	0.33
AU5	14.71	0.11	1.94	0.18	1.98	0.09	2.17	0.09	2.20	0.16
AU6	26.99	-0.32	1.93	0.22	2.17	-0.52	2.86	-0.36	2.50	1.06
AU7	13.04	1.92	-6.07	0.15	-13.98	0.27	**-26.47**	0.15	-42.09	0.11
AU8	11.29	-0.05	1.12	0.33	1.35	-0.39	1.49	-0.13	1.20	1.28
AU9	30.93	3.40	1.76	0.36	1.51	0.16	2.19	0.30	1.83	0.66
AU10	6.58	2.93	-1.08	0.22	-4.89	-0.33	**-10.71**	-0.50	-22.57	0.27
AU11	2.87	0.28	-2.06	0.01	-6.24	-0.28	**-15.04**	-0.48	-36.19	-0.23
AU12	9.83	0.07	0.21	0.03	0.02	-0.04	0.04	0.06	-0.02	-0.16
AU13	20.02	1.48	0.23	-0.06	0.39	0.00	0.50	-0.01	0.74	1.00
AU14	20.60	0.03	1.31	-0.08	1.66	-0.05	2.21	-0.01	2.11	-0.14
AU15	2.97	0.90	-3.83	-0.06	-13.09	0.04	**-30.99**	0.00	-49.07	0.31
AU16	10.41	0.00	0.34	-0.15	0.26	-0.09	0.61	-0.06	0.55	0.28
AU17	11.31	-0.31	0.28	-0.54	0.55	-0.34	0.68	-0.40	0.72	-0.41
AU18	14.49	6.35	-4.05	-0.67	-9.63	-0.99	**-18.12**	-1.66	-30.24	-2.33
AU19	7.97	0.35	-0.35	0.27	-0.97	0.31	-1.12	0.37	-1.22	0.66
AU20	29.47	0.12	0.12	-0.33	0.21	-0.31	0.43	-0.25	0.54	0.65
AU21	7.75	0.03	0.07	-0.07	0.27	0.02	0.40	0.01	0.33	0.08
AU22	8.30	0.20	0.09	0.14	-0.50	0.18	-0.19	0.21	-0.09	0.32
AU23	31.87	0.12	0.29	-0.12	0.53	-0.04	1.18	-0.03	1.47	0.40
AU24	0.64	0.00	-0.23	0.00	-0.60	0.00	-1.46	-0.02	-3.87	-1.09
AU25	4.27	-0.05	-2.70	-0.91	-10.00	-0.21	**-28.62**	-0.33	-64.41	-0.73

* A photoinstability of ≥5% for an exposure of 10 MED was used to distinguish between photounstable and photostable products.

Table 12 The photounstable products investigated in this study and the percentage (% m/m) loss of active ingredients in the suncare products.

Product	% m/m loss of active ingredients				
	2-EHMC	AVO	MBC	Benz-3	OT
AU 1	19.17	undetectable	2.2	-	-
AU 2	26.90	86.47	-	0	-
AU 7	18.71	85.65	3.0	-	-
AU 10	29.87	undetectable	2.28	-	0
AU 11	33.45	undetectable	-	-	-
AU 15	30.63	91.20	-	-	0
AU 18	19.7	undetectable	1.7	-	-
AU 25	27.85	undetectable	-	-	-

3.5 *In vitro* assessment of the broad-spectrum UV protection of sunscreen products

The importance for sunscreens to offer broad-spectrum UV protection has gained prominence in the formulation of modern sunscreens. This is because of the realisation of the important role UVA has in the induction of skin cancer [66]. However, at the moment there is no universally accepted methodology that is being used in the assessment of the UVA protection. The commonly used *in vivo* methods are the immediate pigment darkening (IPD), persistent pigment darkening (PPD) and the protection factor in the UVA (PFA) [67, 68]. The present SPF values are merely based on the determination *in vivo* on human subjects using an erythemal end-point due to exposure to UVB radiation [40]. In this study the critical wavelength method and the UVA/UVB ratio have been used to assess the broad-spectrum protection of the suncare products.

3.5.1 The critical wavelength method

This is an *in vitro* method proposed by Diffey [39] to assess broad-spectrum UV protection of a sunscreen formulation. The area under the curve in the absorption spectrum was calculated for the UVA (320-400 nm) and UVB (290-320) regions after irradiation. The critical wavelength was calculated as explained in Section 2.3.1. Table 13 shows the calculated critical wavelengths for different MEDs. For the photounstable compounds the critical wavelengths tend to decrease with increasing doses of radiation. This is in agreement with the

increase in photoinstability in the UVA region as has been discussed for these formulations. The spectroscopic data were analyzed for broad-spectrum classification by taking a minimum critical wavelength of 370 nm as proposed by Diffey [39]. From this it appears that seven products (AU 3, 4, 6, 9, 13, 14, 20 and 23) did not meet this criterion. Although some of these products did contain an inorganic filter (either TiO_2 or ZnO), it would appear that it does not seem to change the status much. There have been some studies that suggest that the presence of TiO_2 can actually accelerate the photodegradation of AVO [27, 52] and this could be seen as loss in absorbance in the UVA region with increasing doses of UV radiation.

Table 13 Calculated critical wavelengths at different MEDs.

	Critical wavelength/(nm) at different MED				
Product	0	2	5	10	20
AU1	378	377	374	370	351
AU2	377	374	378	361	356
AU3	360	357	359	359	363
AU4	369	369	372	368	369
AU5	374	374	374	373	377
AU6	369	369	367	369	370
AU7	373	369	364	354	341
AU8	375	377	373	375	376
AU9	358	358	357	358	358
AU10	379	377	375	374	369
AU11	376	375	371	368	362
AU12	373	373	373	372	373
AU13	365	364	364	365	367
AU14	370	367	369	368	369
AU15	376	373	368	353	341
AU16	372	374	374	371	373
AU17	376	371	372	373	375
AU18	377	377	374	372	366
AU19	373	376	382	374	376
AU20	355	352	351	351	356
AU21	372	370	371	370	370
AU22	370	369	369	369	370
AU23	351	349	349	349	351
AU24	380	380	378	376	375
AU25	374	373	370	357	332

Although these formulations do not meet the broad-spectrum requirement they are all photostable. At 10 MED the critical wavelength (λ_c) has only decreased by 1 to 2 nm (except

in the case of AU 20). However, for the photounstable products identified λ_c is lowered by 5 to 23 nm.

According to the Boots star rating system, a minimum value of the critical wavelength of 325 nm was set for a product to claim broad-spectrum protection (see Table 14). Therefore, considering this value the formulations investigated in this study would meet the criterion even though some did not contain any UVA absorbers. The proposed value of 370 nm by Diffey is a better alternative as it eliminates all formulations that did not incorporate a UVA filter in their system. This would remove any confusion that may be encountered by the consumer and therefore the consumer will be well informed on the level of UV-protection when choosing a sunscreen.

Table 14 The critical wavelength ranges and the broad-spectrum-rating (the number of stars).

Broad-spectrum classifications of sunscreens	
Critical wavelength (λ_c)/nm	Broad-spectrum rating/no. of stars
$\lambda_c < 325$	0
$325 \leq \lambda_c < 335$	1
$335 \leq \lambda_c < 350$	2
$350 \leq \lambda_c < 370$	3
$370 \leq \lambda_c$	4

3.5.2 UVA/UVB ratio method

This method was only applied to the eight photounstable products that had been determined by the mean spectral values according to the method proposed by Maier *et al.* [18]. The area under the curve in the absorption spectrum was calculated for the UVA (320 – 400 nm) and UVB (290 - 320 nm) regions before and after irradiation. The ratio of the mean UVA to the mean UVB absorbance was calculated as described in the method of Diffey [40]. This ratio is a measure of the UVA absorbing performance in relation to that in the UVB region. The changes of the UVA/UVB ratio under different amounts of irradiation are shown in Table 15

and are graphically displayed in Figure 44. It can be observed for the photounstable formulations, that the UVA/UVB ratio decreases slightly in the initial stages of irradiation. This means that there is simultaneous degradation of both UVA and UVB absorbers. This was verified by HPLC analysis which did show photodegradation of the active ingredients (mostly 2-EHMC and AVO) in the suncare products. However, with increasing dosage the UVA/UVB ratio drops significantly and then levels off implying a faster degradation taking place in the UVA region.

Table 15 Changes of UVA/UVB ratio for the photounstable products.

Product		Mean Absorbance (A) at different MEDs				
		0	2	5	10	20
AU 1	UVA	0.978	0.785	0.649	0.520	0.378
	UVB	1.461	1.439	1.370	1.359	1.848
	UVA/UVB ratio	**0.667**	**0.546**	**0.474**	**0.383**	**0.205**
AU 2	UVA	1.364	1.088	0.915	0.779	0.692
	UVB	1.850	2.114	2.303	1.938	1.602
	UVA/UVB ratio	**0.737**	**0.515**	**0.397**	**0.402**	**0.432**
AU 7	UVA	0.831	0.696	0.560	0.439	0.339
	UVB	1.696	1.793	1.873	1.852	1.596
	UVA/UVB ratio	**0.490**	**0.388**	**0.299**	**0.237**	**0.212**
AU 10	UVA	1.055	1.001	0.856	0.715	0.537
	UVB	1.549	1.569	1.492	1.463	1.398
	UVA/UVB ratio	**0.681**	**0.638**	**0.574**	**0.489**	**0.384**
AU 11	UVA	1.439	1.217	0.988	0.733	0.444
	UVB	2.567	2.497	2.351	2.104	1.744
	UVA/UVB ratio	**0.561**	**0.487**	**0.420**	**0.348**	**0.255**
AU 15	UVA	1.378	1.101	0.817	0.571	0.4111
	UVB	2.137	2.090	2.128	2.049	1.914
	UVA/UVB ratio	**0.645**	**0.527**	**0.384**	**0.279**	**0.215**
AU 18	UVA	0.749	0.660	0.566	0.456	0.343
	UVB	1.197	1.157	1.133	1.093	1.078
	UVA/UVB ratio	**0.626**	**0.570**	**0.499**	**0.417**	**0.318**
AU 25	UVA	1.281	1.111	0.844	0.543	0.288
	UVB	1.928	1.613	2.241	2.327	1.727
	UVA/UVB ratio	**0.664**	**0.689**	**0.377**	**0.233**	**0.167**

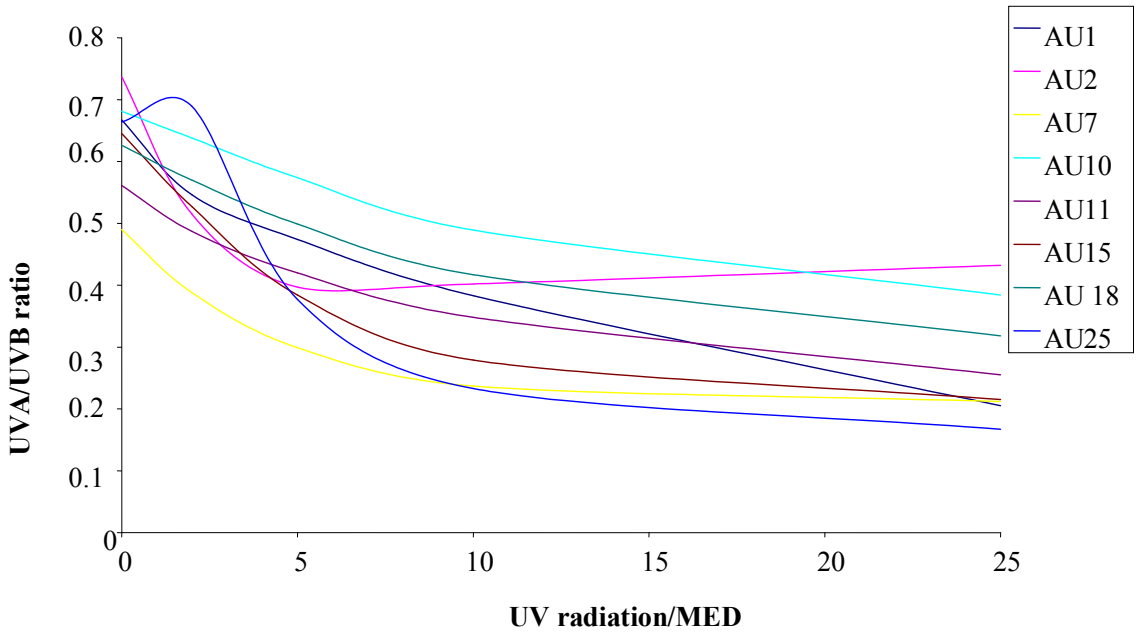

Figure 44 The changes of UVA/UVB ratio for the photounstable formulations.

A comparison of AU 10 which consisted of 2-EHMC, AVO and MBC and AU 11 that had 2-EHMC and AVO alone, shows that although these products had similar UVA/UVB ratios at the beginning there was a remarkable difference upon exposure to varying doses of irradiation. The degradation of AU 11 was much faster than that noted for AU 10. This can be explained by the fact that in the presence of AVO the degradation of 2-EHMC is enhanced, although the photosensitising effect of AVO on 2-EHMC was not evident at this point since there was no change in the photostability of the product in the UVB region. However, the HPLC results showed the photoisomerisation of 2-EHMC. In the case of AU 10 the additional presence of MBC is thought to have a stabilising effect hence lessening the degree of photodegradation. This is in accordance with other studies that show that MBC is normally incorporated in the formulations to stabilise AVO [62, 69]. However, this aspect was difficult to see from the transmission spectra recorded here as there was a steady increase in photoinstability in the UVA region with increasing doses of irradiation. The HPLC results show that MBC photoisomerises.

The UVA/UVB absorption ratio is an indicator of the performance of suncare products. The larger the value of the ratio the better the broad-spectrum protection. In general, it would appear that the addition of another filter to the AVO/2-EHMC filter combination restores some UV-absorbance of the product. The change in the value of UVA/UVB ratio was highest in AU 25 which contained only EHMC and AVO. When compared with other samples like AU 1 and AU 18 which contained MBC in addition the reduction in the UVA/UVB ratio is much less. This is represented graphically in Figure 39. Although the UVA/UVB ratio drops significantly in the first 10 MED it seems to stay at the same level up to 25 MED. The UVA/UVB absorption ratio had a good correlation to HPLC analysis especially with compounds that had 2-EHMC/AVO filter combination, where the degree of photodegradation in the UVA region was high. These data show that the stabilization of UV filters can be achieved with an adequate formulation. This would be the case as the UVA/UVB ratio is higher for products that have an additional filter as seen for AU1, 2, 7, 10, 15 and 18.

It is common to use the Boots star rating system based on the UVA/UVB ratio according to Table 16 for broad-spectrum classification [71]. The values indicate the product loses its broad-spectrum coverage as can be seen from the decreasing UVA/UVB ratios for the suncare products shown in Table 16.

Table 16 The Boots star rating system

UVA/UVB ratio	**Stars**	**Category**
0.0 to 0.2	no rating	
0.21 to 0.4	one star	minimum
0.41 to 0.6	two stars	moderate
0.61 to 0.8	three stars	good
0.81 to 0.9	four stars	superior
> 0.91	five stars	ultra

Table 17 is a summary of the photostability status for various combinations of filters in the suncare products and the degree of broad-spectrum protection afforded.

Table 17 Comparison of the photostability and broad-spectrum protection results obtained with different methods.

	Transmission spectra				HPLC	Maier	λ_c (0 MED)	λ_c (10 MED)
Product	320 nm	340 nm	380 nm	S	S	S	B-S	B-S
AU 1	✓	✓	✓	X	X	X	✓	✓
AU 2	✓	X	X	X	X	X	✓	X
AU 3	✓	X	X	✓	X	✓	X	X
AU 4	✓	✓	X	✓	X	✓	X	X
AU 5	✓	✓	X	✓	X	✓	✓	✓
AU 6	✓	✓	X	✓	X	✓	X	X
AU 7	✓	X	X	X	X	X	✓	X
AU 8	✓	X	X	✓	X	✓	✓	✓
AU 9	✓	X	X	✓	X	✓	X	X
AU 10	✓	✓	✓	X	X	X	✓	✓
AU 11	✓	✓	✓	X	X	X	✓	X
AU 12	✓	✓	X	✓	X	✓	✓	✓
AU 13	✓	X	X	✓	X	✓	X	X
AU 14	✓	X	X	✓	X	✓	✓	X
AU 15	✓	✓	✓	X	X	X	✓	X
AU 16	✓	✓	X	✓	X	✓	✓	✓
AU 17	✓	✓	X	✓	X	✓	✓	✓
AU 18	✓	✓	✓	X	X	X	✓	✓
AU 19	✓	✓	X	✓	X	✓	✓	✓
AU 20	✓	X	X	✓	X	✓	X	X
AU 21	✓	✓	X	✓	X	✓	✓	✓
AU 22	✓	✓	X	✓	X	✓	X	X
AU 23	✓	✓	X	✓	X	✓	X	X
AU 24	✓	✓	✓	✓	X	✓	✓	✓
AU 25	✓	✓	✓	X	X	X	✓	X

*S – photostable; B–S – broad-spectrum, λ_c – critical wavelength

From the data presented the following conclusions can be drawn:

- Visual inspection of the transmission curves and their classification as unstable concurs with the photoinactivation method of Maier. This gives credence to the 5% limit set as a criterion for photoinstability.
- On the other hand, HPLC analyses showed that in all the products there was modification of the active ingredients. This is due to the fact that all products contained 2-EHMC and in each case it photoisomerised. This also occurred in all the 12 products that contained MBC which also isomerised. Nine products contained AVO and all photodegraded except for AU 24.

- Visual inspection of the transmission curves for broad-spectrum protection did not concur well with the critical wavelength. Only eight products containing AVO (not AU 2) showed low transmission in the UVAI region. However, the critical wavelength classified products not containing any absorber that absorb in this region (i.e. were transparent) as broad-spectrum (e.g. AU 5, 6, 8, 12, 14, 16, 17, 19). In total the λ_c classified seventeen products as broad-spectrum protectants.
- Of the eight photounstable products, three products still met the 370 nm λ_c criterion after 10 MED of irradiation.
- After 10 MED of irradiation, 14 products did not meet the 370 nm λ_c criterion. These are the 8 products that originally did not meet the criterion, 5 of the photounstable products and AU 20.

This study indicated that the photostability of the sunscreens cannot be wholly determined by one technique. Although the spectral information shows that the product does not absorb and it is photostable according to Maier's method, the HPLC showed the product to be photounstable. This was due to photoisomerisation of 2-EHMC, MBC and the photodegradation of AVO.

4 Conclusion

The photostabilitity and the ultraviolet broad-spectrum protection of different commercial sunscreens were investigated. The results demonstrate that the sunscreen products were photostable in the UVB region but those that contained AVO tended to lose their absorptivity with increasing doses of UV radiation in the UVA region. Photostability assessment of the sunscreens by HPLC showed that the photoinstability was mainly as a result of the photoisomerisation of the two chemical absorbers 2-EHMC and MBC and the photodegradation of AVO. The loss is more noticeable in the UVA region due to the photodegradation of AVO. This decrease in absorbance of the sunscreen agrees with previously published reports and has been attributed to either phototautomeristion or photodegradation [55, 57]. The loss of absorption, for example, in sunscreen lotions shown by the cinnamate [43, 72] derivatives when UV-irradiated is associated with the photoisomerisation process while for the dibenzoylmethane derivatives they undergo phototautomerisation [29]. The *trans*-form of 2-EHMC photoisomerises across the ethylenic

double bond to yield the *cis*-form and possibly some photodimers [43]. Since the *cis*-isomer absorbs UV radiation less efficiently than *trans*-2-EHMC, the photoinduced isomerisation of the sunscreen agent decreases its UV-protective capacity [19, 62]. This photoisomerisation can be rapid and reversible leading to a mixture of the *cis* and *trans*- isomers but it did not affect the UVB photostability. However, the impact of AVO photosensitising the photodegradation of 2-EHMC was not evident from the UV transmission spectra as there was no change in photostability of the product in the UVB region. In this situation the isomerisation rate and the photostationary isomer ratio will depend on the compound, the spectrum of the light source and the matrix (solvent, co-solutes). Therefore the final performance of a sunscreen preparation has a lot to do with the filter mixture and the emulsion type. Non-absorbing degradation products can also cause an additional decrease in absorbance. Dibenzoylmethane derivatives display loss of absorbance during keto/enol tautomerization, fragmentation and formation of new products with distinctly altered UV absorption characteristics [19, 55]. The keto-form absorbs at shorter wavelengths (i.e. 260 nm), with the spectrum showing only weak absorptions in the UVB and UVA regions. Similar studies by Maier *et al.* [18] and Serpone *et al.* [50] have shown comparable results. The addition of octocrylene to formulations containing dibenzoylmethane sunscreens, such as AVO, is thought to improve the overall photostability of the sunscreen formulation. This is because octocrylene acts as a quencher of the excited state of avobenzone and hence photostabilises avobenzone by removing its excitation energy and dissipating it through a non-destructive pathway [73]. However, in this work the presence of octocrylene did not stop the photodegradation of AVO. It is well known that the photochemical reaction of dibenzoylmethane derivatives depends highly on the formula in which they are incorporated and therefore the use of another formula could lead to different results. AVO is known to be relatively photostable in polar aprotic solvents like methanol yet relatively photolabile in nonpolar and polar aprotic solvents like cyclohexane [59] and DMSO resulting in a number of photoproducts.

The photodegaradation of sunscreens can produce some unknown photoproducts with unknown toxicological properties whose effect on human skin could be significant [74, 75]. In principle, sunscreens are designed for external application to the outermost layers of the skin. However, sunscreens may penetrate the skin and also cause dermatological side-effects, e.g. dermatitis or allergies [24]. This photodecomposition of the UV filters results in the formation of free radicals and other reactive toxic intermediates which may directly or

indirectly initiate skin damage. For example, 2-EHMC and MBC have recently been shown to penetrate through human skin *in vitro* and *in vivo* resulting in nanomolar concentrations [5, 76-78]. Hence, the function of many other organs may be affected by these two sunscreens, either directly by the effects through estrogen receptors or indirectly by toxic effects or effects in the thyroid gland [79]. The photoproducts produced could have a deleterious effect on human skin, which still remains to be determined. The fact that there is possible percutaneous absorption by the human body after topical sunscreen application may lead to their bioaccumulation in the fatty tissues [6, 80]. Each chemical product is distributed differently in human skin, some are accumulated in the *stratum corneum* and others penetrate the skin.

A broad-spectrum sunscreen provides protection in the whole of the UVB/UVA range. This protection should include both UVAI and UVAII. Although most of the suncare products indicated on their labels that they were broad-spectrum sunscreens the results showed that most of them were only protective in the shorter UVA range. The rapid loss in absorption in the UVA region is an unwelcome scenario in that one is exposed to more UVA radiation. This is because the UVA-absorbing capacity is reduced and hence the product does not offer the kind of protection which one would expect. Since the sun protection factor is a measure of the protection against erythema, mainly caused by UVB, it therefore means that the SPF of this compound does not change. As a result, when this substance is used, much higher levels of UVA penetrate basal cell layers of the epidermis than one would expect from the initial absorbance spectrum. Therefore the decrease of the UVA absorptive capacity results in an increase of the direct UVA-induced skin damage. It is known that UVA generates more oxidative stress and, at levels found in sunlight, it is ten times more efficient than UVB at causing lipid peroxidation leading to plasma membrane damage [81, 82]. Therefore, individuals relying on sunscreens as their sole form of photoprotection against UV radiation are subjected to a greater cumulative sun exposure than anticipated by the consumer.

The data would seem to support the findings reported for South African commercial sunscreens by Bunhu [83]. These data demonstrate that formulations which contain combinations of octocrylene, octyl salicylate, 2-EHMC, Benz-3 and AVO are not photostable during UV exposure. The presence of a second or third filter does not eliminate either photoisomerisation or photodegradation. This is because photodegradation of most of these compounds occurs simultaneously in a sample, and this might have an additive or possibly

even a synergistic effect compounding the photodegradation process. This loss in absorbance would imply that there is inadequate UV protection during long hours to UV exposure. In addition, solar radiation may lead to the formation of certain by-products with more harmful effects than the parent compounds [84].

All sunscreens are aromatic compounds with attached carbonyl groups which can undergo efficient intersystem crossing in the excited state to form triplets. The triplets have enough energy to act as sensitizers towards normal air, if present, and to produce singlet oxygen. The production of singlet oxygen can lead to an attack of the sunscreen agent or any other compound present in the sunscreen mixture that is susceptible to oxidation by singlet oxygen. Therefore when the sunscreen is applied to the skin, the secondary photoreactions induced by the sunscreen agents can be complex.

The performance of a photoactive compound or a combination of photoactive compounds in a sunscreen is difficult to predict based on the levels of photoactive compounds in the formulation. The stability results of some of the commercial UV filters reported here do indicate that perfect photostabilty is still not easily achievable especially when a formulation includes one or more photoactive compounds that suffer from relatively rapid photodegradation such as 2-EHMC or AVO. Neither the combination of various organic filters nor the addition of inorganic filters seems to guarantee photostability. Each sunscreen formulation has a particular photochemical behaviour with relation to filter mixture and emulsion type. The mixing of two or more sunscreen active agents leads to a photochemistry different from the photochemistry of each component alone and the reaction of combined sunscreens is strongly concentration and medium dependent. The stability of each product is dependent on the solvent environment. In the finished sunscreen formulation the choice of ingredients and particularly the choice of filter combination can lead to interactions which can give less favourable or often significantly more favourable results. As many studies show, UV filters undergo various transformations upon exposure to UV radiation. It is therefore important that combining UV absorbers should give an absorption spectrum of the end-product with the desired absorption at the highest efficacy and at minimal concentrations and costs. The appearance on the market of other UVA sunscreens such as Tinosorb M and S which are photostable should be encouraged in modern day suncare formulations.

The photostability analysis of commercial sunscreens both spectrophotometrically and chromatographically has shown that some of the evaluated suncare products are photounstable. The loss is mainly attributed to either photoisomerisation or photodegradation of 2-EHMC, AVO and MBC. The combination of 2-EHMC and AVO was unstable regardless of which other active chemical ingredients were included in the sunscreen. This study has shown the advantage of using both techniques for one can easily identify formation of photoproducts.

REFERENCES

1. Matsumura, Y., Ananthaswamy, H.N., *Toxic effects of ultraviolet radiation on the skin.* Toxicology and Applied Pharmacology, 2004, **195,** (3), 298-308.
2. Urbach, F., *Ultraviolet radiation and skin cancer of humans.* Journal of Photochemistry and Photobiology B-Biology, 1997, **40,** (1), 3-7.
3. Wulf, H.C., Poulsen, T., Brodthagen, H., Houjensen, K., *Sunscreens for Delay of Ultraviolet Induction of Skin Tumors.* Journal of the American Academy of Dermatology, 1982, **7,** (2), 194-202.
4. Thompson, S.C., Jolley, D., Marks, R., *Reduction of Solar Keratoses by Regular Sunscreen Use.* New England Journal of Medicine, 1993, **329,** (16), 1147-1151.
5. Sarveiya, V., Risk, S., Benson, H.A., *Skin penetration and systemic absorption of sunscreens after topical application.* Journal of the American Academy of Dermatology, 2004, **50,**(3), 275-285.
6. Jiang, R., Roberts, M.S; Collins, D.M; Benson, H.A.E., *Absorption of sunscreens across human skin: an evaluation of commercial products for children and adults.* British Journal of Clinical Pharmacology, 1999, **48,** (4), 635-637.
7. Lim, H.W., Naylor, M., Honigsmann, H., Gilchrest, B.A., Cooper, K., Morison, W., DeLeo, V.A., Scherschun, L., *American Academy of Dermatology Consensus Conference on UVA protection of sunscreens: Summary and recommendations.* Journal of the American Academy of Dermatology, 2001, **44,**(3), 505-508.
8. Wang, S.Q., Setlow, R., Berwick, M., Polsky, D., Marghoob, A.A., Kopf, A.W., Bart, R.S., *Ultraviolet A and melanoma: A review.* Journal of the American Academy of Dermatology, 2001, **44,**(5), 837-846.
9. Moan, J., Dahlback, A., Setlow, R.B., *Epidemiological support for an hypothesis for melanoma induction indicating a role for UVA radiation.* Photochemistry and Photobiology, 1999, **70,** (2), 243-247.
10. Ladermann, H., *Synergy effects between organic and inorganic filters in sunscreen.* Journal of Biomedical Optics, 2005, **10**, 1408.
11. Schreurs, R., Lanser, P., Seinen, W., Van Der Burq, B., *Estrogenic activity of filters determined by an in vitro reporter gene assay and an in vivo transgenic zebrafish assay.* Archive Toxicology, 2002, **76,** (5–6), 257–261.

12. Schmidt, T., Ring, J., Abeck, D., *Photoallergic contact dermatitis due to combined UVB (4-methylbenzylidene camphor and octyl methoxycinnamate) and UVA (benzophenone-3 and butyl methoxydibenzoylmethane) absorber sensitization.* Dermatology, 1998, **196,** (3), 354-357.
13. English, J.S.C., White, I.R., Cronin, E., *Sensitivity to Sunscreens.* Contact Dermatitis, 1987, **17,** (3), 159-162.
14. Wulf, H.C., Stender, I.M., Lockandersen, J., *Sunscreens used at the beach do not protect against erythema: a new definition of SPF is proposed.* Photodermatology Photoimmunology and Photomedicine, 1997, **13,** (4), 129-132.
15. Bech-Thomsen, *Sunbathers' application of sunscreen is probably inadequate to obtain the sun protection factor assigned to the preparation.* Photodermatology Photoimmunology and Photomedicine, 1992, **9**, 242-244.
16. Autier, P., Dore, J.F., Negrier, S., Lienard, D., Panizzon, R., Lejeune, F.J., Guggisberg, D., Eggermont, A.M.M., *Sunscreen use and duration of sun exposure: a double-blind, randomized trial.* Journal of the National Cancer Institute, 1999, **91,** (15), 1304-1309.
17. Azizi, E., Iscovich, J., Pavlotsky, F., Shafir, R., Luria, I., Federenko, L., Fuchs, Z., Milman, V., Gur, E., Farbstein, H., Tal, O., *Use of sunscreen is linked with elevated naevi counts in Israeli school children and adolescents.* Melanoma Research, 2000, **10,** (5), 491-498.
18. Maier, H., Schauberger, G., Brunnhofer, K., Honigsmann, H., *Change of ultraviolet absorbance of sunscreens by exposure to solar-simulated radiation.* Journal of Investigative Dermatology, 2001, **117,** (2), 256-262.
19. Tarras-Wahlberg, N., Stenhagen, G., Larko, O., Rosen, A., Wennberg, A.M., Wennerstrom, O., *Changes in ultraviolet absorption of sunscreens after ultraviolet irradiation.* Journal of Investigative Dermatology, 1999, **113,** (4), 547-553.
20. Allen, J.M., Gossett, C.J., Allen, S.K., *Photochemical formation of singlet molecular oxygen in illuminated aqueous solutions of several commercially available sunscreen active ingredients.* Chemical Research in Toxicology, 1996, **9,** (3), 605-609.
21. Schallreuter, K.U., Wood, J.M., Farwell, D.W., Moore, J., Edwards, H.G.M., *Oxybenzone oxidation following solar irradiation of skin: Photoprotection versus antioxidant inactivation.* Journal of Investigative Dermatology, 1996, **106,** (3), 583-586.
22. Dondi, D., Albini, A., Serpone, N., *Interactions between different solar UVB/UVA filters contained in commercial sunceams and consequence loss of UV protection.* Photochemical and Photobiological Sciences, 2006, **5**, 835-843.

23. Roscher, R.M., Lindemann, M.K.O., Kong, S.B., Cho, C.G., Jiang, P., *Photodecomposition of several compounds commonly used as sunscreens.* Journal of Photochemistry and Photobiology A-Chemistry, 1994, **80**, 417-421.
24. Schauder, S., Ippen, H., *Contact and photocontact sensitivity to sunscreens - Review of a 15-year experience and of the literature.* Contact Dermatitis, 1997, **37,** (5), 221-232.
25. Gasparro, F.P., Mitchnick, M., Nash, J.F., *A review of sunscreen safety and efficacy.* Photochemistry and Photobiology, 1998, **68,** (3), 243-256.
26. Stenberg C; Larko, O., *Sunscreen application and its importance for the sun protection factor.* Archives of Dermatology, 1985, **121,**(11), 1400-1402.
27. Stokes, R.P., Diffey,B.L., *In vitro assay of high-SPF sunscreens.* Journal of the Society of Cosmetic Chemists, 1997, **48,** (6), 289-295.
28. Flindt-Hansen, H., Nielsen, C.J., Thune, P., *Measurements of the photodegradation of some PABA and some PABA derivatives.* Photodermatology, 1988, **5**, 257-261.
29. Deflandre, A., Lang, G., *Photostability Assessment of Sunscreens - Benzylidene Camphor and Dibenzoylmethane Derivatives.* International Journal of Cosmetic Science, 1988, **10,** (2), 53-62.
30. Schrader, A., Jakupovic, J., Baltes, W., *Photochemical studies on trans-3-methylbutyl 4-methoxycinnamate.* Journal of the Society of Cosmetic Chemists, 1994, **45**, 43-52.
31. Beck, I., Deflandre, A., Lang, G., Arnaud, R., Lemaire, J., *Study of the Photochemical Behavior of Sunscreens - Benzylidene Camphor and Derivatives.* International Journal of Cosmetic Science, 1981, **3,** (3), 139-152.
32. Gonzalez, H., Tarras-Wahlberg, N.; Strömdahl, B., Juzeniene, A., Moan, J., Larkö, O., Rosén, A., Wennberg, A.M., *Photostability of commercial sunscreens upon sun exposure and irradiation by ultraviolet lamps.* British Journal of Dermatology, 2007, **7**, 1-9.
33. Maier, H., Schauberger, G., Martincigh, B.S., Brunnhofer, K., Honigsmann, H., *Ultraviolet protective performance of photoprotective lipsticks: change of spectral transmittance because of ultraviolet exposure.* Photodermatology Photoimmunology & Photomedicine, 2005, **21,** (2), 84-92.
34. Maier, H., Schauberger, G., Brunnhofer, K., Honigsmann, H., *Assessment of thickness of photoprotective lipsticks and frequency of reapplication: results from a laboratory test and a field experiment.* British Journal of Dermatology, 2003, **148,** (4), 763-769.
35. Azurdia, R.M., Pagliaro, J.A., Diffey, B.L., Rhodes, L.E., *Sunscreen application by photosensitive patients is inadequate for protection.* British Journal of Dermatology, 1999, **140,** (2), 255-258.

36. Castanedo-Cazares, J.P., Lepe, V., Gordillo-Moscoso, A., Moncada, B., *Ultraviolet radiation doses of Mexican schoolchildren.* Salud Publica De Mexico, 2003, **45,** (6), 439-444.
37. Taylor, S.R.D., *"SunSmart Plus": the more informed use of sunscreens.* Medical Journal of Australia, 2004, **180,** (1), 36-37.
38. Springsteen, A., Yurek, R., Frazier, M., Carr, K.F., *In vitro measurement of sun protection factor of sunscreens by diffuse transmittance.* Analytica Chimica Acta, 1999, **380,** (2-3), 155-164.
39. Diffey, B.L., Tanner, P.R., Matts, P.J., Nash, J.F., *In vitro assessment of the broad-spectrum ultraviolet protection of sunscreen products.* Journal of the American Academy of Dermatology, 2000, **43,** (6), 1024-1035.
40. Diffey, B.L., *A method for broad spectrum classification of sunscreens.* International Journal of Cosmetic Science, 1994, **16**, 47-52.
41. COLIPA, *European Cosmetic, Toiletry and Perfumery Association.* COLIPA SPF Test Method, Brussels, 1994, **94/289**.
42. Diffey, B., Stokes, R.P., Forestier, S., Mazilier, C., Rougier, A, *Suncare product photostability: a key parameter for more realistic in vitro efficacy evaluation.* European Journal of Dermatology, 1997, **7**, 226-228.
43. Broadbent, J.K., Martincigh, B.S., Raynor, M.W., Salter, L.F., Moulder, R., Sjoberg, P., Markides, K.E., *Capillary supercritical fluid chromatography combined with atmospheric pressure chemical ionisation mass spectrometry for the investigation of photoproduct formation in the sunscreen absorber 2-ethylhexyl-p-methoxycinnamate.* Journal of Chromatography A, 1996, **732,** (1), 101-110.
44. Bonda, C., Marinelli, P., *The photochemistry of sunscreen photostability.* Agro Food Industry Hi-Tech, 2000, **11,** (1), 29-31.
45. Bonda, C., *The photostability of sunscreen actives: A review.* Cosmetic Science and Technology Series, 2005, **28**, 321-349.
46. Mitchnick, M.A., Fairhurst, D., Pinnell, S.R., *Microfine zinc oxide (Z-Cote) as a photostable UVA/UVB sunblock agent.* Journal of the American Academy of Dermatology, 1999, **40,** (1), 85-90.
47. Broadbent, J.K., *Photochemical studies of sunscreen constituents;* M.Sc. Dissertation, University of Natal, Durban, South Africa, 1994.
48. Pattanaargson, S., Munhapol, T., Hirunsupachot, N., Luangthongaram, P., *Photoisomerization of octyl methoxycinnamate.* Journal of Photochemistry and Photobiology A:Chemistry, 2004, **161,**(2-3), 269-274.

49. Sewlall, A., *DNA cleavage photoinduced by benzophenone-based sunscreens;* M.Sc. Dissertation, University of Natal, Durban, South Africa, 2003.

50. Serpone, N., Salinaro, A., Emeline, A.V., Horikoshi, S., Hidaka, H., Zhao, J.C., *An in vitro systematic spectroscopic examination of the photostabilities of a random set of commercial sunscreen lotions and their chemical UVB/UVA active agents.* Photochemical and Photobiological Sciences, 2002, **1,** (12), 970-981.

51. Gaspar, L.R., Campos, P., *Evaluation of the photostability of different UV filter combinations in a sunscreen.* International Journal of Pharmaceutics, 2006, **307,** (2), 123-128.

52. Damiani, E., Baschong, W., Greci, L., *UV-Filter combinations under UV-A exposure: Concomitant quantification of over-all spectral stability and molecular integrity.* Journal of Photochemistry and Photobiology B: Biology, 2007, **87**, 95–104.

53. DeBuys, H.V., Levy, S.B., Murray, J.C., Madey, D.L., Pinnell, S.R., *Modern approaches to photoprotection.* Dermatologic Clinics, 2000, **18,** (4), 577-590.

54. Martincigh, B.S., Kowlaser, K., Raynor, M.W., *Photoproducts of 2-ethylhexyl-para-methoxycinnamate.* Photochemistry and Photobiology, 1999, **69**, 64S-64S.

55. Schwack, W., Rudolph, T., *Photochemistry of Dibenzoyl Methane UVA Filters.* Journal of Photochemistry and Photobiology B-Biology, 1995, **28,**(3), 229-234.

56. Cantrell, A., McGarvey, D.J., *Photochemical studies of 4-tert-butyl-4'-methoxydibenzoylmethane (BM-DBM).* Journal of Photochemistry and Photobiology B-Biology, 2001, **64,**(2-3), 117-122.

57. Andrae, I., Bringhen, A., Boehm, F., Gonzenbach, H., Hill, T., Mulroy, L., Truscott, T.G., *A UVA filter (4-tert-butyl-4-methoxydibenzoylmethane): photoprotection reflects photophysical properties.* Journal of Photochemistry Photobiology B-Biology, 1997, **37**, 147-150.

58. Sayre, R.M., Dowdy, J.C., Gerwig, A.J., Shields, W.J., Lloyd, R.V., *Unexpected photolysis of the sunscreen octinoxate in the presence of the sunscreen avobenzone.* Photochemistry and Photobiology, 2005, **81,** (2), 452-456.

59. Panday, R., *A Photochemical investigation of two sunscreen absorbers in a polar and a non-polar medium;* M.Sc. Dissertation, University of Natal, Durban,South Africa, 2002.

60. Johncock, W., *Sunscreen interactions in formulations.* Allured's Cosmetics and Toiletries. , 1999, **114,** (9), 75-82.

61. Damiani, E., Rosati, L., Castagna, R., Carloni, P., Greci, L., *Changes in the ultraviolet absorbance and hence the protective efficacy against lipid peroxidation of organic sunscreens after UVA irradiation.* Journal of Photochemistry and Photobiology B: Biology, 2006, **82**, 204-213.

62. Berset, G., Gonzenbach, H., Christ, R., Martin, R., Deflandre, A., Mascotto, R.E., Jolley, J.D.R., Lowell, W., Pelzer, R., Stiehm, T. , *Proposed protocol for determination of photostability. Part I: cosmetic filters.* International Journal of Cosmetic Science, 1996, **18**, 167-177.

63. Huong, S.P., Rocher, E., Fourneron, J.D., Charles, L., Monnier, V., Bund, H., Andrieu, V., *Photoreactivity of the sunscreen butylmethoxydibenzoylmethane (DBM) under various experimental conditions.* Journal of Photochemistry and Photobiology A: Chemistry, 2008, **196,** 106–112.

64. Bonda, C., Marinelli, P., Trivedi, J., Hopper, S., Wentworth, G., *Avobenzone photostability in simple polar and non-polar solvent systems.* Journal of Cosmetic Science, 1998, **49,** (3), 210-212.

65. Mturi, G.J., Martincigh, B.S., *Photostability of the sunscreening agent 4-tert-butyl-4-methoxydibenzoylmethane (avobenzone) in solvents of different polarity and proticity.* Journal of Photochemistry and Photobiology, A: Chemistry, 2008, 200, 410-420.

66. Seite, S., Moyal, D., Richard, S., de Rigal, J., Leveque, J.L., Hourseau, C., Fourtanier, A., *Mexoryl (R) SX: A broad absorption UVA filter protects human skin from the effects of repeated suberythemal doses of UVA.* Journal of Photochemistry and Photobiology, B-Biology, 1998, **44,** (1), 69-76.

67. Kullavanijaya, P., Lim, H.W., *Photoprotection.* Journal of the American Academy of Dermatology, 2005, **52,**(6), 937-958.

68. Cole, C., Vanfossen, R., *Measurement of Sunscreen UVA Protection - an Unsensitized Human-Model.* Journal of the American Academy of Dermatology, 1992, **26,**(2), 178-184.

69. Osterwalder, U., Mongiat, S., Herzog, B., *In vitro and in vivo assessment of UVA protection of sunscreens with traditional actives ZNO and avobenzone and new UV absorbers MBBT and BEMT.* Journal of the American Academy of Dermatology, 2004, **50,** (3),135-136.

70. Wunsch, T., Westenfelder, H., *New aspects in sunscreens.* Nov; Paris, Step Publishing Ltd., 1998, **17-18**, 56 - 60.

71. Gonzalez, H., Farbrot, A., Larko, O., Wennberg, A.M., *Percutaneous absorption of the sunscreen benzophenone-3 after repeated whole-body applications, with and without ultraviolet irradiation,* The British Journal of Dermatology 2006, **154,** (2), 337-340.

72. Morliere, P., Avice, O., Melo, T. S. E., Dubertret, L., Giraud, M., Santus, R., *A Study of the Photochemical Properties of Some Cinnamate Sunscreens by Steady-State and Laser Flash-Photolysis,* Photochemistry and Photobiology, 1982, **36,** (4), 395-399.

73. Chatelain, E, Gabard, B., *Photostabilization of butyl methoxydibenzoylmethane (Avobenzone) and ethylhexyl methoxycinnamate by bis-ethylhexyloxyphenol methoxyphenyl triazine (Tinosorb S), a new UV broadband filter.* Photochemistry and Photobiology, 2001, **74,** (3), 401-406.

74. Nohynek, G.J., Schaefer, H., *Benefit and risk of organic ultraviolet filters.* Regulatory Toxicology and Pharmacology, 2001, **33,**(3), 285-299.

75. Cambon, M., Isaachar, N., Castelli, D., Robert, C, *An in vivo method to assess the photostability of UV filters in a sunscreen.* Journal of Cosmetic Science. 2001, **52**, 1-11.

76. Chatelain, E., Gabard, B., Surber, C., *Skin penetration and sun protection factor of five UV filters: Effect of the vehicle.* Skin Pharmacology and Applied Skin Physiology, 2003, **16,**(1), 28-35.

77. Janjua, N.R., Mogensen, B., Andersson, A.M., Petersen, J.H., Henriksen, M., Skakkebaek, N. E., Wulf, H.C., *Systemic absorption of the sunscreens benzophenone-3, octyl-methoxycinnamate, and 3-(4-methyl-benzylidene) camphor after whole-body topical application and reproductive hormone levels in humans.* Journal of Investigative Dermatology, 2004, **123,**(1), 57-61.

78. Potard, G., Laugel, C., Baillet, A., Schaefer, H., Marty, J.P., *Quantitative HPLC analysis of sunscreens and caffeine during in vitro percutaneous penetration studies.* International Journal of Pharmaceutics, 1999, **189,** (2), 249-260.

79. Seidlova-Wuttke, D., Jarry, H., Christoffel, J., Rimoldi, G., Wuttke, W., *Comparison of effects of estradiol (E2) with those of octylmethoxycinnamate (OMC) and 4-methylbenzylidene camphor (4MBC) - 2 filters of UV light - on several uterine, vaginal and bone parameters.* Toxicology and Applied Pharmacology, 2006, **210,** (3), 246-254.

80. Potard, G., Laugel, C., Schaefer, H., Marty, J.P., *The stripping technique: In vitro absorption and penetration of five UV filters on excised fresh human skin.* Skin Pharmacology and Applied Skin Physiology, 2000, **13,** (6), 336-344.

81. Dubertret, L., Serraftircazes, D., Jeanmougin, M., Morliere, P., Averbeck, D., Young, A.R., *Phototoxic Properties of Perfumes Containing Bergamot Oil on Human Skin - Photoprotective Effect of UVA and UVB Sunscreens.* Journal of Photochemistry and Photobiology B-Biology, 1990, **7,** (2-4), 251-259.

82. Gaboriau, F., Morliere, P., Marquis, I., Moysan, A., Geze, M., Dubertret, L, *Membrane damage induced in cultured human skin fibroblasts by UVA irradiation.* Photochemical and Photobiological Sciences, 1993, **58**, 515-520.

83. Bunhu, T., *An assessment of the photostability of South Afican commercial sunscreens;* M.Sc Dissertation, University of KwaZulu-Natal, Durban, 2006.

84. Giokas, D.L., Salvador, A., Chisvert, A., *UV filters: From sunscreens to human body and the environment.* Trends in Analytical Chemistry, 2007, **26,** (5), 360-374.

CHAPTER 4

Photochemical studies of 2-ethylhexyl-*p*-methoxycinnamate

4.1 Introduction

The photochemical behaviour of 2-ethylhexyl-*p*-methoxycinnamate (*trans*-2-EHMC; Figure 45) is of primary importance since it is presently among the most widely used UVB absorbers in sunscreen formulations [1, 2]. A purified sample of 2-EHMC (also known as octyl methoxycinnamate) is a pale yellow oil immiscible with water and soluble in organic oils and solvents such as methanol or ethanol. It absorbs in the UV region between 290 and 320 nm with a maximum absorption at approximately 310 nm. Its molar absorption coefficient (ε) is 2.5 x 10^4 dm^3 mol^{-1} cm^{-1} in methanolic solutions [3]. It is this high molar absorption coefficient in the UVB spectral region that makes it an important UVB sunscreen filter. It is used as an active chemical ingredient in sun care products at an average concentration of 2 - 5% with a maximum limit of 10% [4].

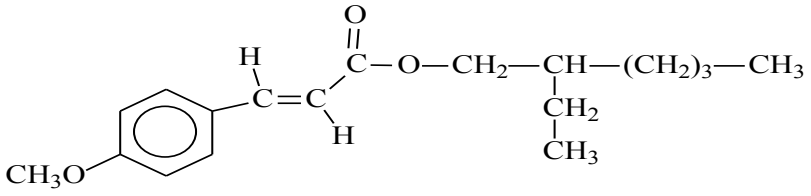

Figure 45 Chemical structure of *trans*-2-EHMC.

The presence of the methoxy group attached to the aromatic ring assists in electron delocalization across the molecule necessary for the UV absorption of wavelengths centered at 310 nm (see Figure 46). The 2-ethylhexyl chain decreases its water solubility thus making it suitable for waterproof/water resistant sunscreen formulations.

The photostability of a sunscreen agent is an essential requirement for an effective and safe UV filter, since degradation during sunlight exposure will not only decrease the initial photoprotective capacity but can also generate harmful photolytic products [5, 6]. Therefore, in order to ensure adequate photoprotection during usage, the compound not only should have a high absorbance but must also be able to harmlessly dissipate the absorbed energy. Otherwise this would expose consumers to these potentially toxic photodegradation products. Hence the photochemical behaviour of the sunscreen agents needs to be determined. Another important requirement is that sunscreens should remain on the skin surface and should not penetrate into the systematic circulation despite perspiration and bathing [7, 8].

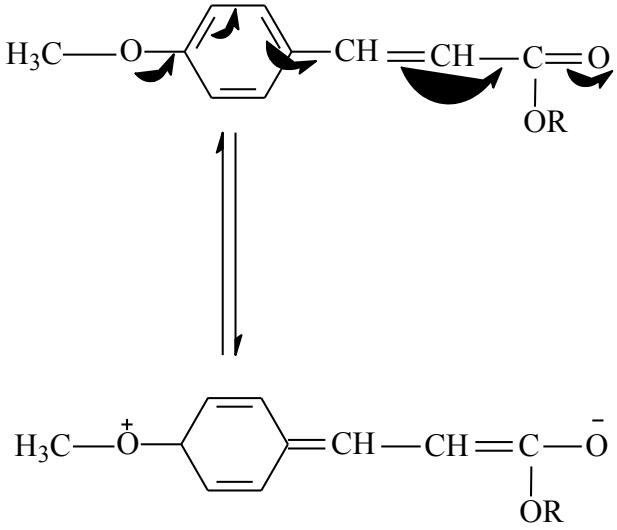

Figure 46 Electron delocalization in 2-EHMC.

Although 2-EHMC is an efficient UVB absorber, recent studies have shown that it undergoes marked photochemical changes upon exposure to sunlight. Morliere *et al*. [9], by means of steady state and laser photolysis, showed a decrease in absorbance of 2-EHMC which was solely attributed to photoisomerisation. The *trans*- and *cis*-isomers of 2-EHMC were the only species present and no other photodegradative products were identified (Figure 47). The results showed a fast loss in absorbance during the first five minutes and a decrease in the *trans*- and an increase in the *cis*-isomer. The rapid loss in absorbance was attributed to isomerisation rather than degradation since the *cis*-isomer is a less efficient UVB absorber [10]. Deflandre and Lang [11] incorporated 2-EHMC into an emulsion and then spread the emulsion in a very thin film between two finely roughened quartz plates. They irradiated the sample with a xenon solar simulator and measured the absorbance before and after

irradiation. It was found that 2-EHMC degraded by 4.5% after one hour in sunlight reaching a photostationary equilibrium shortly after exposure began. This was then followed by photodegradation. The loss in absorbance results in a decrease in the protective capacity. A study by Serpone *et al*. [12] has reported on the photostability of 2-EHMC in different organic solvents showing a rapid and significant photodegradation. The degree of photodegradation was found to be dependent on the solvent vehicle and its polarity that is used in the formulation. Tarres-Wahlberg *et al.* [13] investigated the photostability of 2-EHMC by applying a thin film of the sunscreen between two quartz slides and then irradiating it. They monitored the changes in the UV absorbance during and after irradiation, after which GC-MS was used to isolate and identify the resulting photoproducts. The GC revealed the formation of a photoproduct whose mass spectrum was similar to that of the original substance; hence it was assigned as the *cis*-isomer. Similar studies carried out by Pattanaargson *et al.* [14] show that 2-EHMC rapidly undergoes geometrical *trans-cis* isomerisation under the influence of natural sunlight. The establishment of a photostationary equilibrium between the two isomers (*trans* and *cis*) is also dependent on the polarity of the solvents.

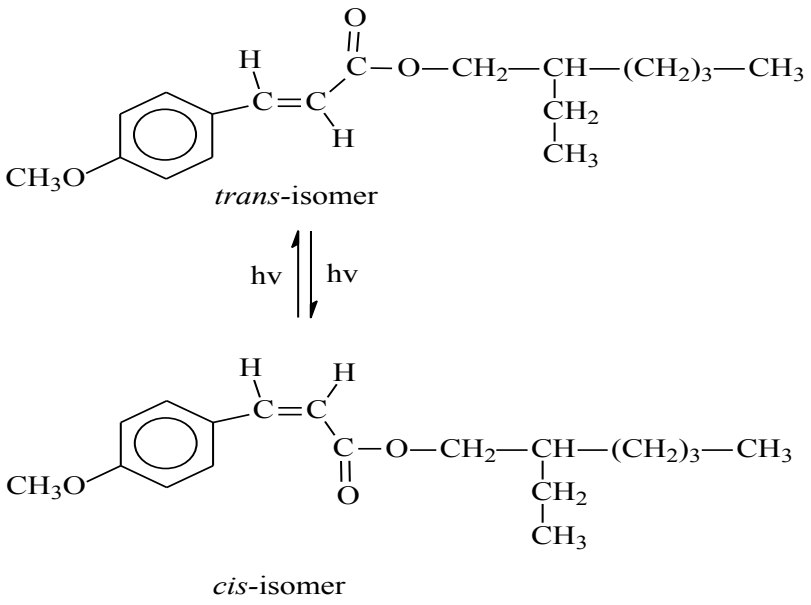

Figure 47 The photoisomerisation of 2-EHMC.

The UV spectrum of 2-EHMC shows a bathochromic shift of the wavelength of maximum absorption (λ_{max}) in the UVB region (290-320 nm) from a non-polar solvent to a polar one [15, 16]. The equilibrium was found to shift more to the *trans*-form of 2-EHMC when less

polar solvent was used. In a more recent study of Huong *et al.* [17] they show that the isomerisation process is rapid and that the distribution of the two isomers depends more on their chemical environment than on the actual irradiation power.

The investigations of Broadbent *et al*. [1], making use of capillary supercritical fluid chromatography combined with atmospheric pressure chemical ionisation mass spectrometry (SCF-APCIMS), showed that commercially available *trans*-2-EHMC isomerises to the *cis*-form upon irradiation with wavelengths of light greater than 300 nm thereby losing some of its absorbing ability [1, 18]. There also exists a photostationary state between the *trans*- and *cis*-isomers during continuous irradiation. Before the equilibrium state is reached, degradation is very fast. It has also been shown that irradiation of pure or even solutions of as low as 0.1 M 2-EHMC [19] does not only cause it to isomerise but also to dimerise with itself through a [2 + 2]-cycloaddition reaction as shown in Figure 48. There is a possible formation of about 15 isomers resulting from the cycloaddition as shown in Figure 49 [20]. The dimerisation of 2-EHMC further reduces its absorption power. In addition, the extent of photodimerisation of 2-EHMC has been shown to be dependent on concentration and the polarity of the solvent used.

Similar [2 + 2]-cycloaddition photodimerisation reactions of related cinnamic acid derivatives have been studied [21, 22]. It is well established that cinnamic acid derivatives undergo photodimerisation through cyclobutane formation at the C-C double bond part of the cinnamic moieties on photoirradiation at wavelengths greater than 300 nm. The photoreactivity and the structure of the photoproducts are determined predominantly by the spatial orientation of the two relevant chromophores. It exhibits a topochemical reaction [23]. Some of these cinnamic acids dimerise upon irradiation with UV light in the solid state while in dilute solution only *trans-cis* isomerisation occurs but no dimerisation is observed. In addition to the reversible photoisomerisation which causes a reduction in UV absorption of cinnamates, irreversible reactions of *p*-methoxycinnamates occur in some solvents at the high concentrations used in skin care products and these are accompanied by a further reduction of UVB absorbance [24]. Photodimerisation across the propenylic double bonds to give trullic acid-type products through a [2 + 2] cycloaddition process has been proposed as the likely mechanism [24].

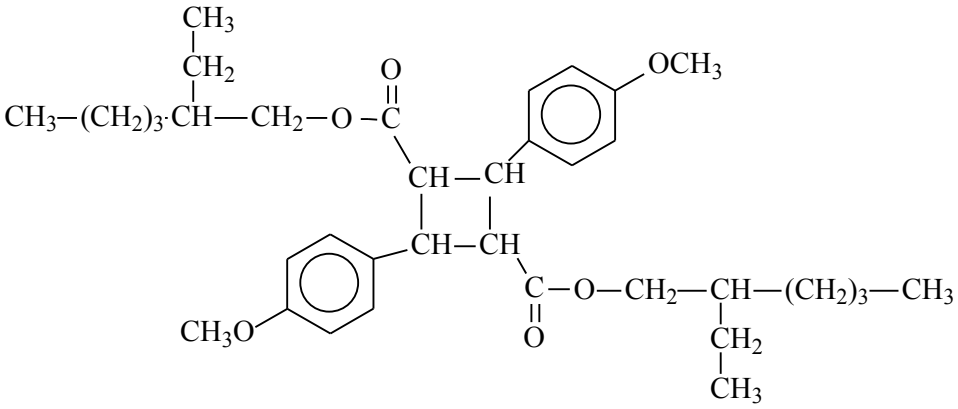

Figure 48 The chemical structure of the 2-EHMC dimer.

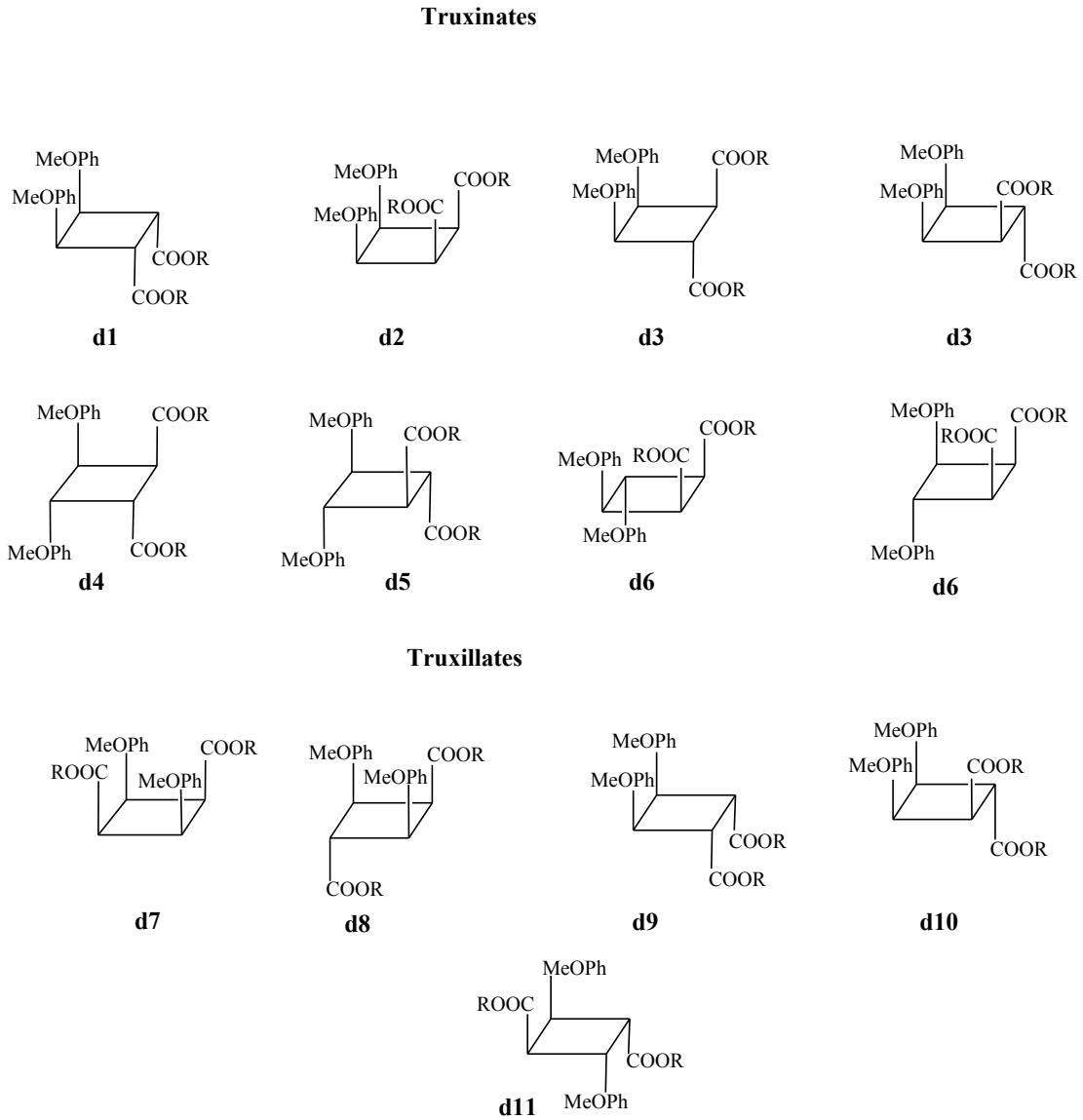

Figure 49 Possible structures of the 2-EHMC dimer adapted from Robinet *et al.* [20].

There are several studies that show the potential toxicity of 2-EHMC. The mutagenicity of 2-EHMC was demonstrated in the *Ames Salmonella Typhimurium* test and as an initiator of tumours in mice [25, 26]. Mohammed *et al.* [27] showed that irradiation of *trans*-p-[α-^{14}C]-methoxycinnamic acid (p-MCA) and calf thymus DNA with UV light resulted in the incorporation of the radiolabel into DNA. The levels of incorporation were greater for single stranded (denatured) DNA as opposed to native DNA. The label was covalently bound to DNA and the incorporation involved photocycloaddition of the ethylenic bond on *p*-MCA and the 5, 6-double bond of the pymiridine bases in DNA. Since 2-EHMC is similar in structure to methoxycinnamic acid, differing only in that it possesses an ethylhexyl alkyl side chain, it is possible then that it would bind to the constituents of DNA in a similar manner [28]. The production of these photoproducts [lesions] could alter the biological function of DNA of serving as a template for the replication as well as transcription into ribonucleic acid (RNA) for protein synthesis. Therefore these lesions can cause lethal, mutagenic and carcinogenic effects [29, 30]. Since 2-EHMC dimers form readily in concentrated solutions, there is a possibility that in a similar fashion, photoproducts could form between the 2-EHMC molecule and constituents of DNA like thymine or thymidine. The results obtained by Ingouville [19] showed no adduct formation between 2-EHMC and thymine. However, the work of Kowlaser [28, 31] showed the formation of a photoproduct between *trans*-2-EHMC and thymidine-5-monophosphate indicating that 2-EHMC has a potential to form mutagenic photoproducts in DNA should it penetrate into the nucleus of the cell.

Another potential source of toxicity is the ability of some chemical absorbers to photosensitise the formation of pyrimidine dimers which are known to be precursors to skin cancer. A study by Aliwell *et al.*[32] has shown that PABA photosensitised the formation of thymine dimer in pUC19 plasmid DNA and this was also observed in the study by Sutherland [33]. Bolton *et al.* [35] showed that PBSA photosensitises thymine dimer formation when irradiated with UV light of wavelengths greater than 300 nm. These dimers are known to form from the triplet state of the pyrimidine base. However, the lowest triplet excited state for thymine, the DNA base with lowest triplet energy, has been determined to be 315 kJ mol^{-1} [36]. The lowest triplet energy of 2-EHMC is 239 kJ mol^{-1} [37]. Since triplet-triplet energy transfer occurs for donors whose triplet energies are above, equal to, or 8 to 12 kJ lower than the acceptor, it is unlikely that 2-EHMC can photosensitize formation of thymine triplets and hence the formation of pyrimidine dimers [32, 33].

Studies by Butt and Christensen [38] have shown the toxic potential of 2-EHMC to mouse cells after UV irradiation. This toxicity was attributed to the existence of photoproducts after 2-EHMC had been exposed to UV radiation. Although the probability of adduct formation between 2-EHMC and constituents of DNA could be low there can be a cumulative effect. Recently some studies have shown that 2-EHMC could have estrogenic properties, thus acting as an endocrine active chemical [39, 40]. Allen *et al.* [41] have also reported the ability of 2-EHMC in aqueous solutions to photosensitise the formation of singlet oxygen. Since singlet oxygen is a highly reactive oxidant it is likely it will enhance photodegradation with consequent diminution of UVB absorbance. Therefore the toxic potential of the UV-induced degradation products is of great significance. This will definitely require elucidation, as a change in the UV absorption of the compound is harmful in terms of photoprotection and phototoxicity.

All of the commercial sunscreens investigated in this study contained *trans*-2-ethylhexyl-*p*-methoxycinnamate as a major active chemical component. It was also of major interest since previous workers [1, 19, 31] in our laboratory have shown that formation of photoproducts resulting from UV irradiation of 2-EHMC also occurs. The present study focuses on the UV spectral changes that 2-EHMC undergoes during exposure to UV radiation, the separation of the photoproducts and their identification by using spectroscopic and chromatographic techniques. The photodimerisation of 2-EHMC was further investigated by resolving the fractions of each dimer chromatographically prior to analysis with Fourier transform infrared and nuclear magnetic resonance spectroscopy.

In addition, theoretical studies using computational methods have been carried out to determine the lowest energy geometrical structures of some of the photoproducts and hence their relative stabilities. This aspect is discussed in Chapter 6.

4.2 Experimental

4.2.1 Materials

All reagents and solvents were of analytical or HPLC-grade. Methanol and acetonitrile were purchased from BDH HiperSolv Chemicals Ltd. The sample of *trans*-2-EHMC of 98% purity

was obtained from BASF and was kept in the dark to avoid any photochemical reactions. Deionised water was obtained from a Milli-Q[50] water purification system (Millipore, Bedford, MA, USA) and was used in all procedures.

4.2.2 Irradiations

The irradiation experiments were carried out by using an Osram HBO 500W/2 high pressure mercury lamp as the irradiation source. This was ideal, since the Osram HBO lamp contains a specific amount of mercury in a pressurised atmosphere of an inert gas. It is an intense light source that consists of mercury emission spectral lines extending from the middle ultraviolet to the infrared regions (Figure 50). This made it suitable for the irradiation work, since most of the active chemical absorbers in commercial sunscreens that were investigated absorb in this region.

Since the lamp has a very high intense source and because of the energy of UV radiation it emits, plus the high pressure contained therein, it was operated in an enclosed purpose-built housing. The lamp was housed in an insulated box constructed out of mild steel and connected to a ventilation system (i.e. an extractor), a Schreiber power supply and an igniter. The extractor leads to the outside of the building. This serves to remove any ozone formed by UV radiation and also to provide some ventilation around the lamp. The lamp was placed vertically in front of a circular aperture fitted with an external bracket onto which a shutter gate, a filter holder and a cell holder were attached. The cell holder was designed to hold either 1 mm or 1 cm pathlength irradiation cells. A portable fan was placed in front of the lamp housing to cool and prevent heat build-up around the filters. The lamp has a lifetime of about 400 hours during which time its output in light intensity does not vary significantly. The degree of loss of light intensity was monitored by a Black-Ray J221 longwave photovoltaic UV intensity meter. The lamp was normally allowed to warm-up for 15 minutes before starting the irradiation of any sample.

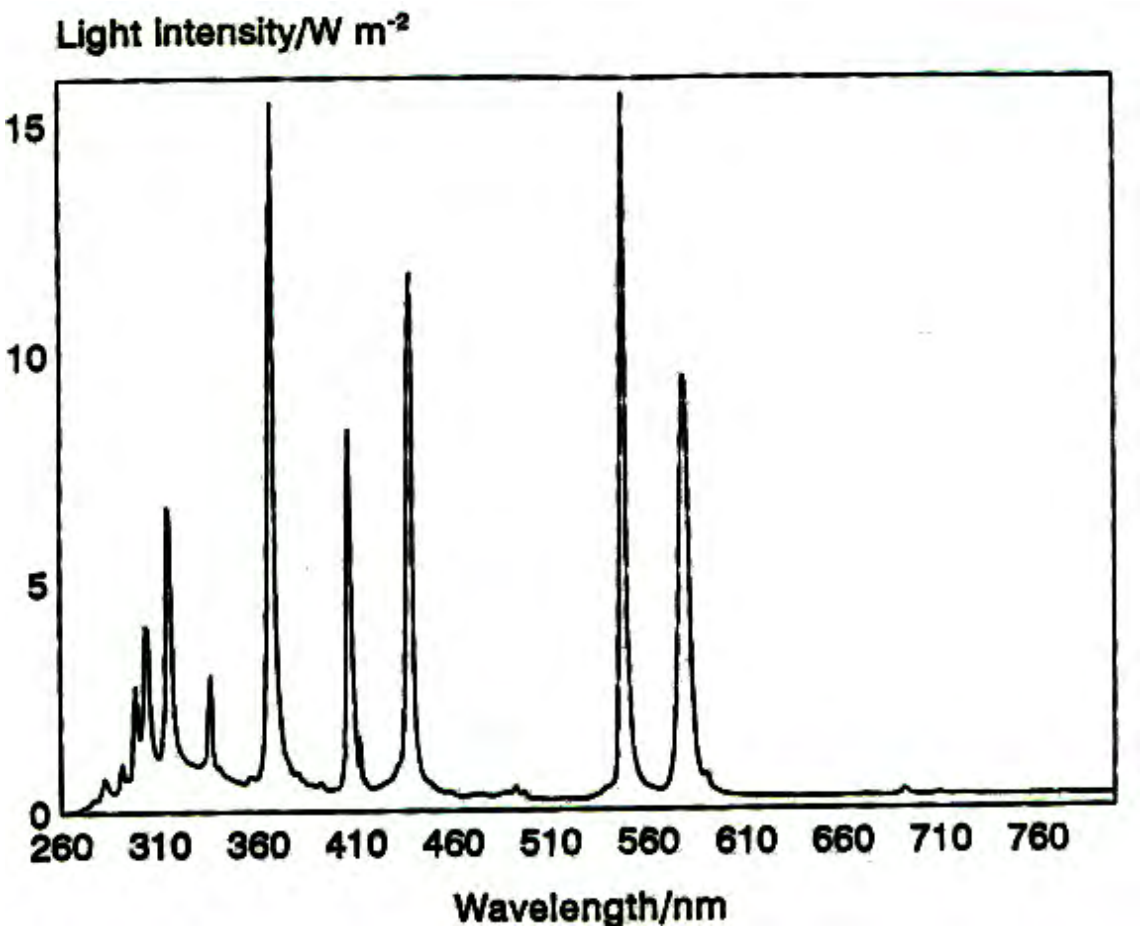

Figure 50 Output of the Osram HBO 500W/2 high pressure mercury lamp [18].

Since the radiation from the Osram HBO lamp spans over a wide wavelength range of 260 nm to 700 nm, it was important to isolate those wavelengths of interest by choosing an appropriate filter. The filter used in this study was a 10 mm thick Pyrex filter. This filter has a short wavelength cut-off of about 300 nm and therefore allows only those wavelengths greater than 300 nm to pass through as shown in Figure 51. The filtered optical output of the for the HBO mercury lamp is now shown in Figure 52. This was ideal for irradiation experiments because it allowed the simulation of natural sunlight incident on the surface of the earth. The minimum cut-off wavelength of solar UV radiation at sea level is 290 nm [42]. A 10 mm or 1 mm quartz photolysis cell was used in most of the irradiation experiments depending on the amount and concentration of the sample. For the case of dilute and large samples, 10 mm pathlength quartz cuvettes were used especially when monitoring the formation of photoproducts.

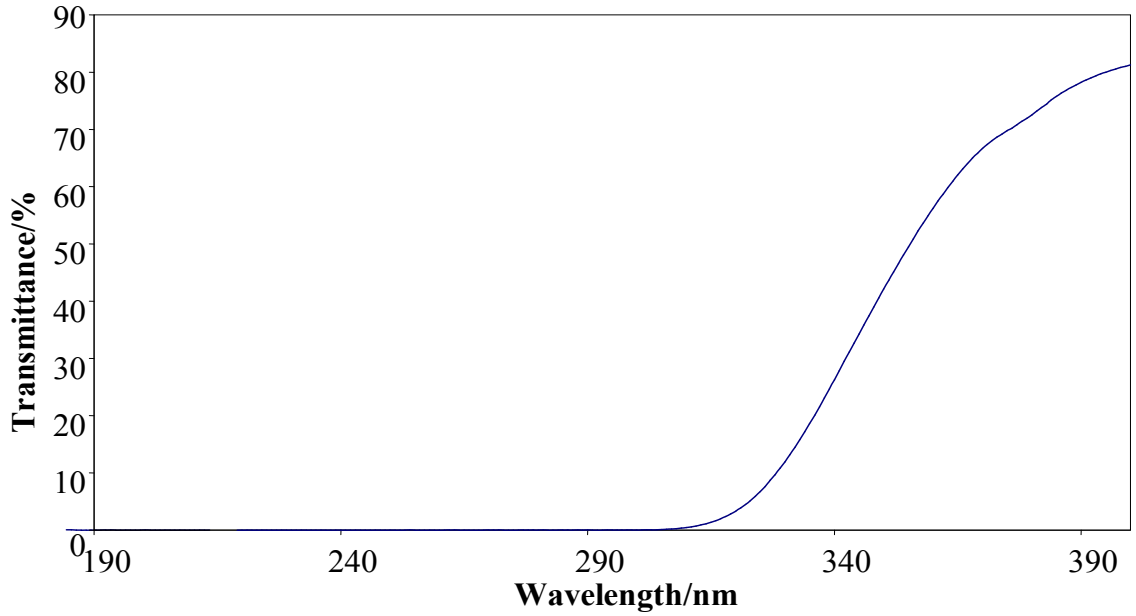

Figure 51 The transmission spectrum of the 10 mm thick Pyrex filter.

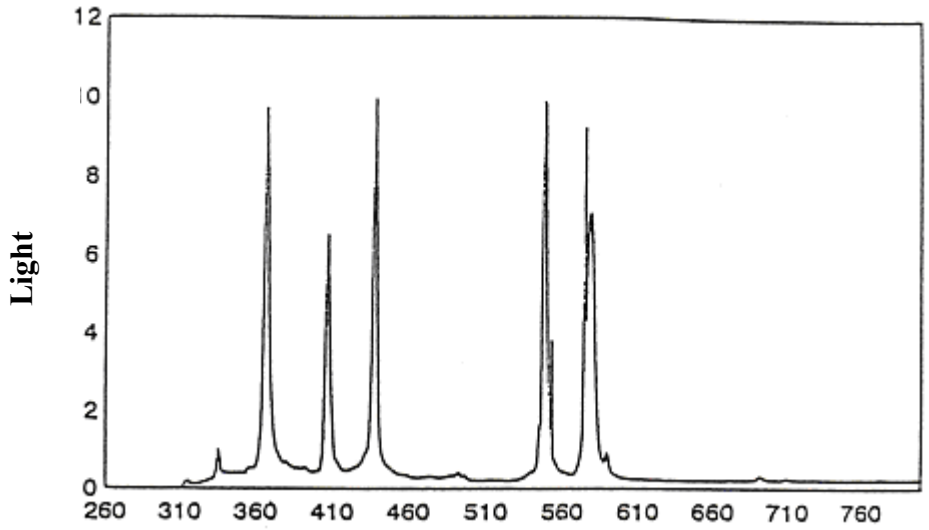

Figure 52 Output of the Osram HBO 500W/2 high pressure mercury lamp in combination with a 10 mm thick Pyrex filter [18].

4.2.3 UV-spectral analyses of 2-EHMC

The absorption spectra were acquired with a Perkin Elmer Lambda 35 double-beam UV-visible spectrophotometer at a constant spectral bandwidth of 1.0 nm using a matched pair of 1 x 1 cm quartz cells. Pure HPLC methanol was used as a blank. The UV spectra were used as an identification and purity check of the compounds separated by high performance liquid chromatography. UV spectroscopy was also used to establish the photostability of 2-EHMC by monitoring the spectra and the absorbance at the wavelength of maximum absorbance on exposure to UV radiation.

4.2.3.1 Determination of the molar absorptivity (ε) of cis-2-EHMC

A pure sample of *cis*-2-EHMC was separated from a mixture of irradiated *trans*-2-EHMC by fraction collection by semi-preparative HPLC. A 1 x 10^{-3} M stock solution of *cis*-2-EHMC in methanol was prepared by mass. This solution was then serially diluted to give different concentrations of *cis*-2-EHMC. The absorbance readings were obtained with a Perkin Elmer Lambda 35 double-beam UV-visible spectrophotometer at a constant spectral bandwidth of 1.0 nm using a matched pair of 1 x 1 cm quartz cells. The molar absorptivity of the *cis*-2-EHMC isomer was determined from the Beer-Lambert law ($A = \varepsilon cl$, where A is the absorbance, l is the path length in cm, c is the concentration in mol dm^{-3} and ε is the molar absorptivity in $dm^3\ cm^{-1}\ mol^{-1}$).

4.2.4 High performance liquid chromatographic analysis of 2-EHMC solutions

Two types of systems were used for high performance liquid chromatographic analyses in this study. These were an analytical and a preparative system. In the analytical mode, a Waters 600 multisolvent delivery system was connected to Waters 996 photodiode array (PDA) UV detector and also attached was a Perkin-Elmer 2000 series autosampler. The PDA detector allows for the acquisition of the absorbance at every wavelength within the 190 to 900 nm range and therefore a UV spectrum of any component eluting from the column can be obtained. The ability to monitor the entire absorbance spectrum of an eluting peak is useful information for the identification of the components eluting from the system. The

preparative instrument consisted of a Waters Delta Prep 4000 preparative chromatography system, a Waters 486 UV variable wavelength detector and Rheodyne 7010 injector. Both these systems were connected to a De'Mark Pentium II personal computer controlled by using Waters Millennium Version 4.00 software.

4.2.4.1 Chromatographic conditions

Separations were usually performed on reversed-phase columns of modified silica gel such as octadecylsilica (C18). A reversed-phase Nucleosil C100 C18 column of 250 mm length, 4.6 mm internal diameter and 5 μm particle size stationary phase was used for the analytical work. A Waters Guard-Pak μ-Bondapak C_{18} pre-column guard was used to protect the analytical column. The photoproducts were separated and collected as fractions on a Spherisorb S5 ODS (250 mm length, 10 mm internal diameter and 5 μm particle size) semi-preparative column. The mobile phases used in the separations were aqueous mixtures of either methanol or acetonitrile. The mobile phase was normally prepared by measuring out separately the appropriate amounts of methanol or acetonitrile and water in a measuring cylinder before mixing. This was to avoid inconsistencies in the eluent composition that result from the contraction of solvent, for example of methanol-water mixtures [43]. The solvent was filtered through a Millipore 0.45 μm filter before subsequently feeding it into the reservoir. This was then degassed with helium at the rate of 30 mL min^{-1}. The flow rate of the eluent was 1 mL min^{-1} for the analytical work and 4 mL min^{-1} for the preparative work.

4.2.4.2 Sample preparation

A solution of approximately 0.1 M *trans*-2-EHMC was prepared by measuring out 1 mL of pure *trans*-2-EHMC into a 25 mL volumetric flask. This was diluted to the mark with HPLC-grade methanol. The concentration was calculated from the weighed mass of pure *trans*-2-EHMC. This would give approximately 5% (m/v) of 2-EHMC in solution. This is within the permissible limits in a sunscreen formulation which falls below the maximum limit of 10%. Hence this concentration was felt most appropriate for our analysis. An aliquot of sample was transferred into a 400 μL quartz photolysis cuvette by means of a Volac micropipette and the cuvette was sealed with a stopper and polythene plastic film to prevent evaporation of the solvent during irradiation. Solutions of 2-EHMC were irradiated at wavelengths greater than

300 nm by using the Osram HBO 500W/2 high pressure mercury lamp and the 10 mm Pyrex filter combination. The irradiations were carried out in a dark room to ensure that any formation of photoproducts is wholly attributed to a known quantity of light from the lamp. All the solutions were light protected before and after irradiation by wrapping the flask or the cuvette containing the sample with aluminium foil. The solutions were kept in a refrigerator while covered with aluminium foil to keep off any further light interference prior to HPLC analysis.

4.2.4.3 Sample analysis

Unirradiated and irradiated samples were filtered by passing them through 0.45 μm Millex syringe filters to ensure that no particulate matter was introduced into the HPLC column. The samples were then diluted appropriately before injecting into the HPLC column. An injection volume was a 20 μL aliquot of the sample. The flow rate was maintained at 1 mL min^{-1}. A mobile phase of 85:15 % v/v methanol-water was used as this was found to give a good separation within a reasonable time of less than 30 minutes. The chromatogram was detected at 310 nm which is the wavelength of maximum absorbance for 2-EHMC. The identity of the compounds separated was determined from the wavelength of maximum absorbance in the UV spectra obtained from the PDA detector. The extent of photodegradation was determined by comparing the peak areas of *trans*-2-EHMC from the irradiated samples with those obtained by analysis of an equivalent amount of the unirradiated sample. All experiments were performed at room temperature.

4.2.5 High performance liquid chromatography separation of photoproducts of irradiated 2-EHMC

From UV spectral analysis it was evident that 2-EHMC undergoes photodegradation in methanol upon UV irradiation. Therefore to investigate this further a pure sample of *trans*-2-EHMC was irradiated for twenty four hours with a HBO 500W/2 high-pressure mercury lamp combined with a 10-mm Pyrex filter. This sample was diluted in methanol and an aliquot of 100 μL of the sample was then injected into the HPLC. The photoproducts were collected as fractions on the semi-preparative HPLC system. The eluent system was 93% (v/v) methanol/water at a flow rate of 4 mL min^{-1}. The fractions collected were further

characterised by FTIR and NMR. The sample of *cis*-2-EHMC was used to determine its molar absorptivity (ε).

4.2.6 High performance liquid chromatographic – mass spectroscopic studies

An Agilent HPLC 1100 series (Agilent Technologies, San Jose, CA) comprising a quatenary solvent delivery system, an on-line degasser, an autosampler, a column thermostat and interfaced to an Agilent LC/MSD Trap 1100 series mass detector was used. The column was an Agilent Zorbax Eclipse XDB-C18 reversed-phase column (5 μm, 50 x 4.6 mm). The sample injection volume was 5 μL and the eluent flow rate was 1 mL min^{-1}. Liquid chromatographic – mass spectroscopic analysis was performed in the isocratic mode (85:15% v/v MeOH/H_2O). Mass spectra were recorded between 100 and 1000 m/z in the atmospheric pressure chemical ionization (APCI) positive mode. The heated capillary temperature was set at 155 ^oC and the APCI vaporizer temperature at 300 ^oC. The capillary voltage was 3500 V and the spray voltage 5 kV.

4.2.7 Column chromatographic for the separation of 2-EHMC photoproducts

Gravitational column chromatography was carried out by using glass columns wet packed with silica gel of particle size of 230-400 mesh ASTM (Merck). This was done in order to separate the photoproducts of 2-EHMC formed upon UV irradiation. The mobile phases used were varying ratios of hexane, dichloromethane, ethyl acetate and methanol. The solvent that gave a good separation was 50% v/v dichloromethane /hexane. Separations and purifications were monitored by thin layer chromatography (TLC). TLC was carried out by using aluminium sheets pre-coated with silica gel (Merck, 60 F254) with layer thickness of 0.2 mm. After eluting with the same solvent system as used for the column, the plates were visualised under UV light (at 254 and 366 nm). This was followed by spraying the plates with an anisaldehyde reagent (prepared by mixing 100 mL of methanol, 1.25 mL anisaldehyde and 2.5 ml of concentrated sulphuric acid).

4.2.8 Fourier transform infrared analysis of photoproducts

The potassium bromide (KBr) discs were made by the pressed disc technique. The disc was then carefully layered between the two dies in the die holder and developed under pressure by using a 15 ton manual hydraulic press to produce transparent discs. The infrared spectra of *trans*-2-EHMC and its photoproducts were obtained by spreading a small sample on transparent KBr discs. The sample was then placed in a sample holder. The analysis was carried out between the wavenumber ranges of 400 - 4000 cm^{-1}. The instrument used was a Nicolet Impact 410 spectrophotometer with Omnic FT-IR as the operating software.

4.2.9 Analysis of photoproducts with nuclear magnetic resonance spectroscopy

The chemical structure of the isolated compounds from preparative HPLC was determined by nuclear magnetic resonance spectroscopy (NMR). ^{1}H-NMR spectra were measured on a Varian Gemini 300 MHz instrument. The isolated samples were dissolved in deuterated methanol (CD_3OD) containing tetramethylsilane (TMS) as an internal standard. The effect of UV irradiation on a sample of *trans*-2-EHMC was monitored with NMR. The pure sample of *trans*-2-EHMC was dissolved in deuterated methanol and the NMR spectrum was recorded. An irradiated sample was also run in deuterated methanol and its respective spectrum was recorded. ^{1}H NMR spectra of the photodimers of 2-EHMC were analyzed and the spectral parameters and the coupling constants were obtained. The NMR absorption pattern of the cyclobutyl protons may have a diagnostic value for the stereochemical assignments.

4.3 Results and Discussion

4.3.1 UV spectral behaviour of *trans*-2-EHMC upon irradiation

UV spectra of a 3 x 10^{-6} M solution of *trans*-2-EHMC were obtained before and after exposure to UV irradiation for one hour. Figure 53 shows the resultant UV spectra which depict a change in absorbance of *trans*-2-EHMC indicating that either photoisomerisation and/or photodegradation have taken place.

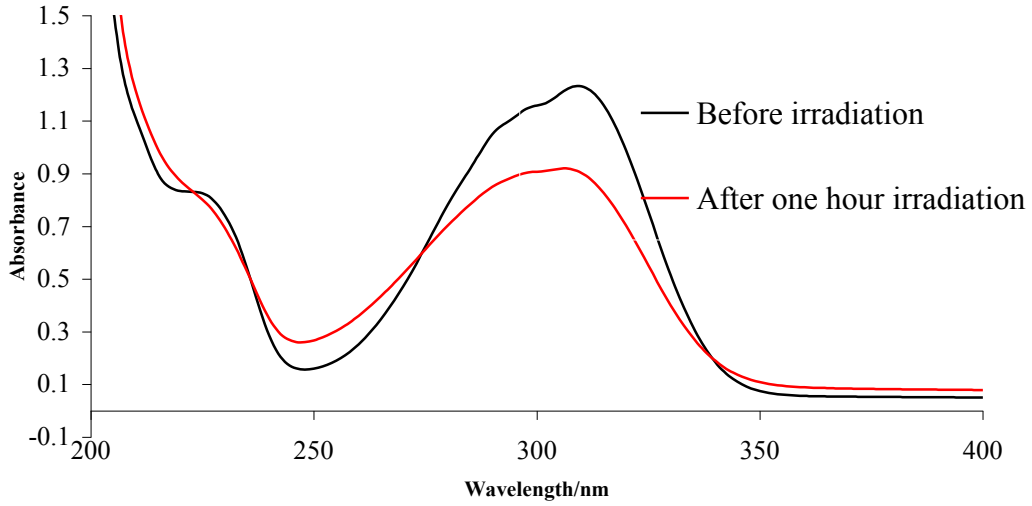

Figure 53 Changes in the UV absorption spectrum of *trans*-2-EHMC on irradiation**.**

There was a substantial decrease in absorbance at wavelength of 310nm from a value of 1.23 to 0.86 which is approximately a 30% decrease in just one hour of irradiation. This therefore means that the efficiency of *trans*-2-EHMC as a UVB absorber is compromised [44]. The spectra obtained in this study are similar to those of other members in our research group [1, 19, 31]. Morliere *et al.* [9] also obtained a similar result where *trans*-2-EHMC was found to photodegrade substantially in just 40 minutes. The identity of the photoproduct was confirmed by obtaining HPLC-MS (see Section 4.3.3). The photoproduct was indeed a *cis*-isomer.

4.3.2 Effect of irradiation time on the photoisomerisation of 2-EHMC

The effect of irradiation time on the photoisomerisation of *trans*-2-EHMC was investigated by irradiating a 3 x 10^{-6} M solution of 2-EHMC dissolved in methanol and recording the UV spectra after set irradiation periods. The spectra were obtained from 190 nm to 400 nm at time intervals of 30 minutes. Figure 54 displays these spectra and show a continuous decrease in absorbance. The observed spectral behaviour suggested that 2-EHMC underwent some photochemical changes as is evidenced with the gradual decrease in the absorbance. After a period of 3 hours of exposure to UV radiation, a photostationary state of the *trans-cis* equilibrium was attained. Since the UVB absorbance of the *cis*-isomer is less than that of the

trans-isomer [1], the resulting absorbance of the photostationary *cis-trans* mixture is lower than that of the initial *trans*-isomer.

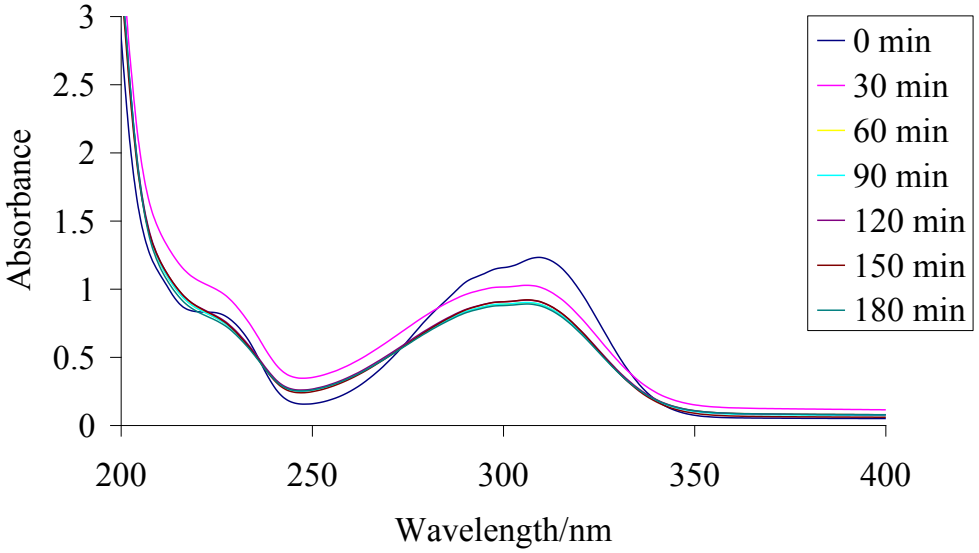

Figure 54 The changes in the UV absorption spectra of *trans*-2-EHMC obtained at different times of UV irradiation.

The solution was also analysed by HPLC before and after irradiation. The analysis by HPLC showed the appearance of a new peak at a shorter retention time attributed to the *cis*-isomer and a closer analysis showed an increase in the formation of the *cis*-isomer with time until a photostationary state was attained. Although Broadbent [18] observed that after the establishment of a photostationary state, the *cis*-isomer is in excess this aspect was not observed. This could be due to the high concentration of 2-EHMC (80%) that was initially irradiated by Broadbent. It could also be due to different irradiation systems. The formation of the isomers is concentration dependent and is explained in Section 4.3.3. In this work an almost 50:50 % ratio of the two isomers was obtained.

An increase in the formation of *cis*-2-EHMC with increasing irradiation time means that a lower absorbance is obtained. The degree of photodegradation was measured by comparing the peak areas of both the *trans*-2-EHMC and *cis*-2-EHMC from the irradiated sample. The peak area of an equivalent amount of the unirradiated sample was also obtained. The peak areas of the chromatograms were considered as these are directly proportional to the

concentrations of the respective isomers. It was surmised that only the two isomers are formed in the dilute solution as has been shown by previous workers in our laboratory [18, 31]. The percentage ratio of the photoproduct peak areas was also used to evaluate the extent of photodegradation. The results of this analysis are shown in Figure 55 which shows the increase in concentration of the *cis* isomer upon irradiation of *trans*-2-EHMC. The photoisomerisation alters the absorption spectrum of *trans*-2-EHMC resulting in a loss of its protective capacity. This is because the *cis*-isomer has a lower molar absorption coefficient than the *trans*-isomer [45].

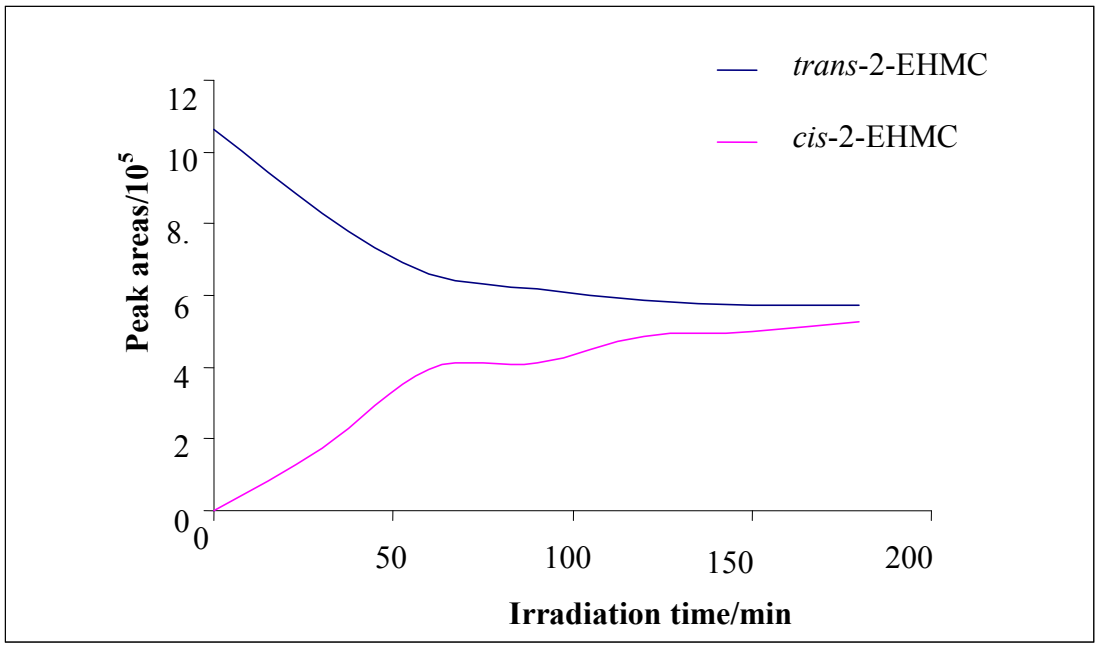

Figure 55 A plot showing the photoisomerisation of *trans*-2-EHMC to *cis*-2-EHMC with increasing time of irradiation.

It was apparent that the dimers were not seen in diluted solutions of 2-EHMC. These results are consistent with other studies involving the photochemical dimerisation of cinnamic acids and their esters [21]. The formation of the cyclobutane ring at the ethylenic double bond is well established. Photochemical cyclodimerisation of cinnamic acid derivatives is highly inefficient in dilute solutions due to a very rapid competing *trans-cis* photoisomerisation [22]. This has been supported by studies carried out on the irradiation of dilute solutions of cinnamic esters in the presence of several Lewis acids resulting in selective *trans*- to *cis*-photodimerisation to yield photostationary states enriched in the *cis*-isomers [46].

4.3.3 Effect of concentration of 2-EHMC on photoproduct formation

The formation of photoproducts upon UV irradiation of 2-EHMC was investigated for different concentrations of *trans*-2-EHMC ranging from 1 x 10^{-6} M to pure 2-EHMC. An aliquot of each sample was irradiated for 24 hours with the Osram HBO 500W/2 high pressure mercury lamp in combination with the 10 mm thick Pyrex filter. These were analysed by HPLC. HPLC chromatograms were obtained for both unirradiated and irradiated samples of 2-EHMC. Figure 56 shows the chromatogram of a sample of 1 x 10^{-6} M *trans*-2-EHMC dissolved in methanol before irradiation. The UV spectrum for the only peak which appears in the HPLC chromatogram shows a wavelength of maximum absorption of 310 nm which identifies this as the *trans*-isomer. Upon irradiation for 24 hours with UV light at wavelengths greater than 300 nm, a second peak appears at a shorter retention time. This peak exhibits a wavelength of maximum absorption at 304 nm which identifies it as the *cis*-isomer (Figure 57).

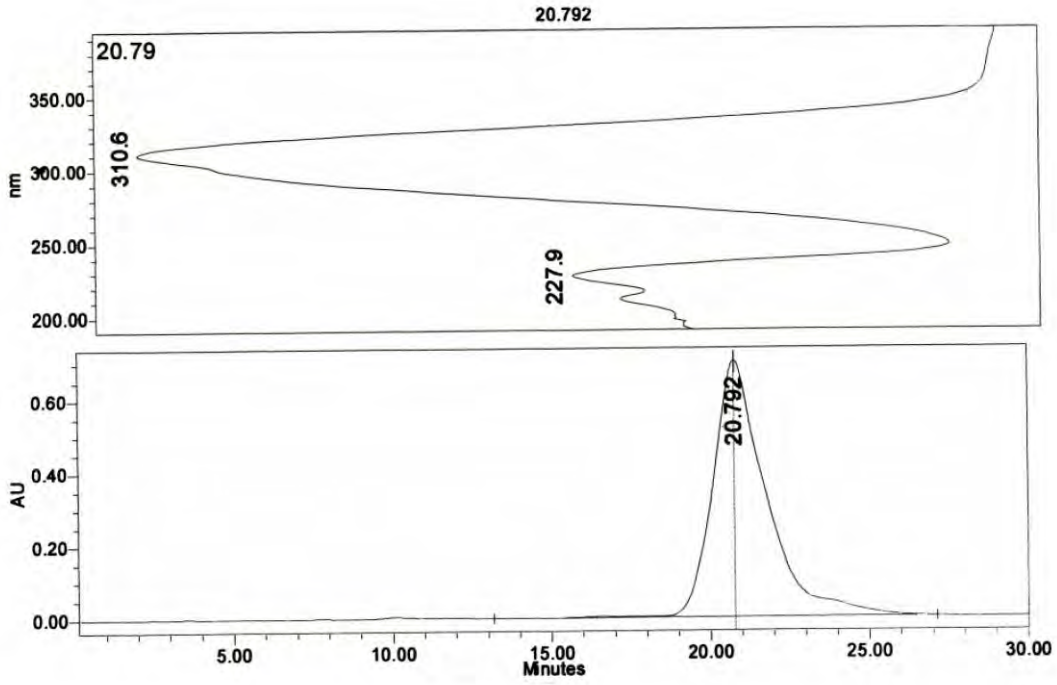

Figure 56 The HPLC chromatogram of 1 x 10^{-6} M 2-EHMC before irradiation obtained by elution on a Nucleosil 100 C18 column. The eluent was methanol/water (90% v/v) at a flow rate 1 mL min^{-1} , injection volume – 10 µL The detection wavelength was 310 nm.

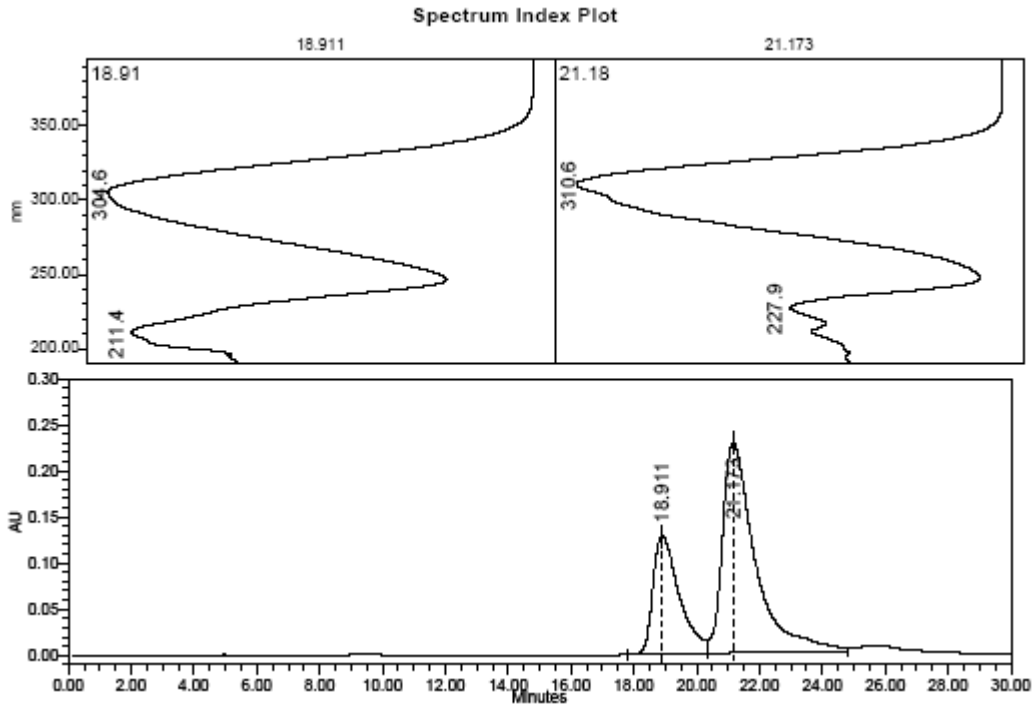

Figure 57 The HPLC chromatogram of 1 x 10^{-6} M 2-EHMC after irradiation obtained by elution on a Nucleosil 100 C18 column. The eluent was methanol/water (90% v/v) at a flow rate 1 mL min^{-1} , injection volume – 10 µL The detection wavelength was 310 nm.

This observation is consistent with other studies related to 2-EHMC containing products [1, 14, 17]. The identity of this second peak was confirmed by HPLC-MS studies. The corresponding HPLC chromatogram and the mass spectra are shown in Figure 58 and Figure 59 respectively. The peaks labelled E1 and E2 shows the presence of the *cis*- and *trans*-isomers respectively. This corresponds to those marked similarly in the mass spectra. Both the spectra gave a protonated molecular peak $[CH_3OC_6C_4{=}CHC(O)C_8H_{18}]H^+$ at m/z of 291. This similarity between the mass spectra confirmed that the two peaks indeed are isomers. The peak at m/z of 179 is due the protonated methoxy cinnamic acid $[CH_3OC_6H_4{=}CH(O)OH]H^+$ resulting from fragmentation at the ester bond.

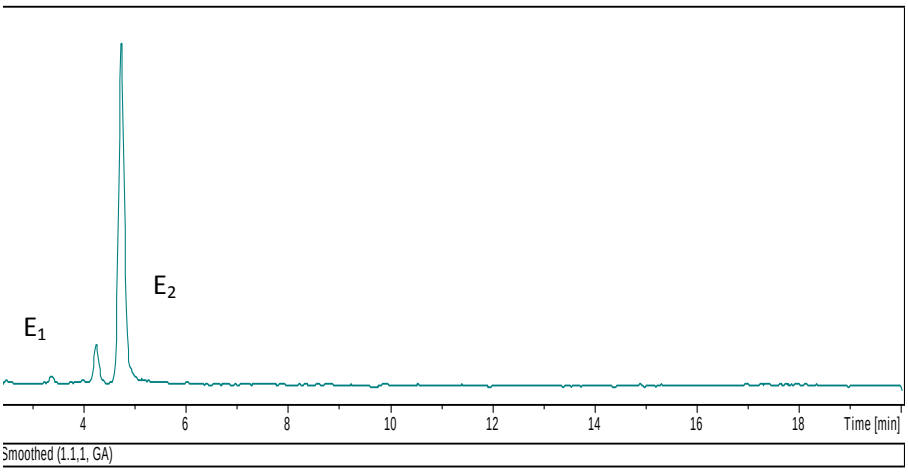

Figure 58 HPLC chromatogram of irradiated 1 x 10^{-6} M *trans*-2-EHMC analysed on the Agilent Zorbax Eclipse XDB-C18 column by isocratic elution at a flow rate 1 mL min^{-1} , injection volume – 5 µL with the Agilent 1100 Series HPLC with UV detection at 310 nm. The order of elution was *cis*-2-EHMC (E_1) and *trans*-2-EHMC (E_2).

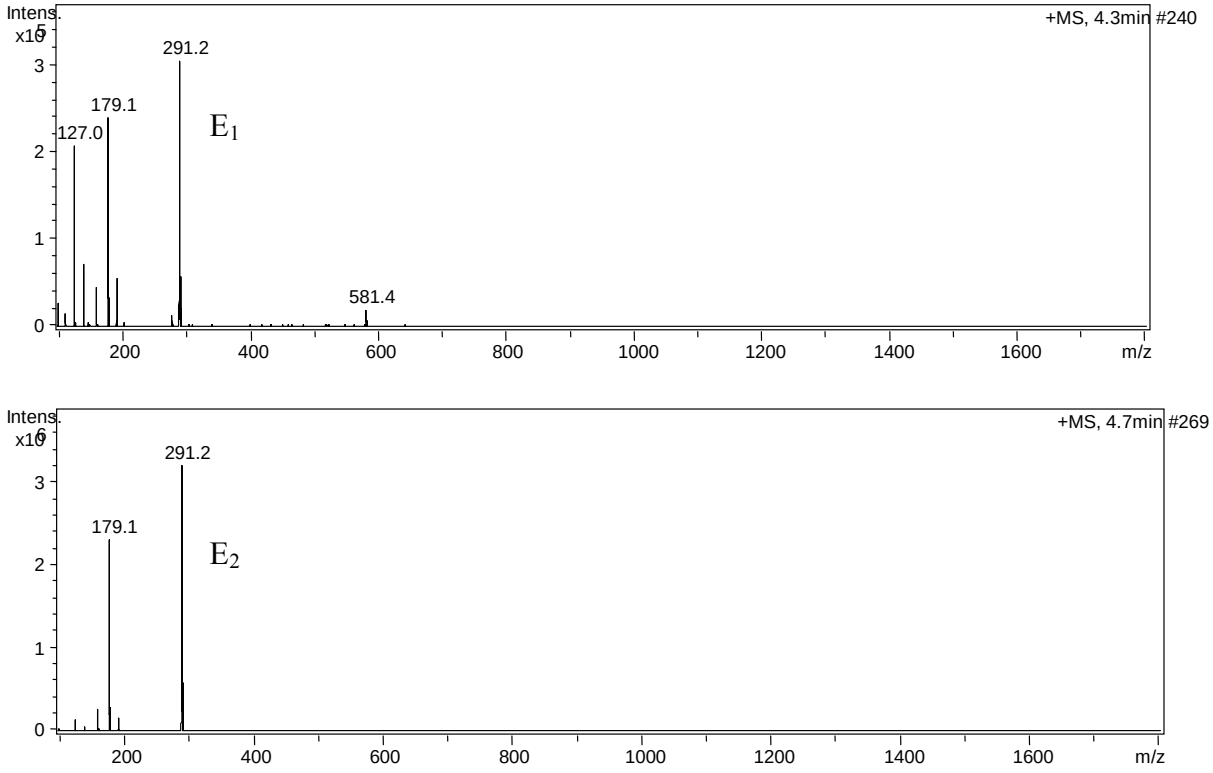

Figure 59 Mass spectra of the peaks labelled E_1 and E_2 in Figure 58.

This result is in agreement with studies carried out by Pattanaargson *et al.* [47] which showed the existence of the two isomers. A pure sample of *cis*-2-EHMC was separated and

collected as a fraction on the Waters Delta Prep 4000 semi-preparative chromatographic system. Figure 60 shows the chromatogram of the *cis*-isomer with its respective UV spectrum as a confirmation that indeed a pure *cis*-isomer was successfully isolated.

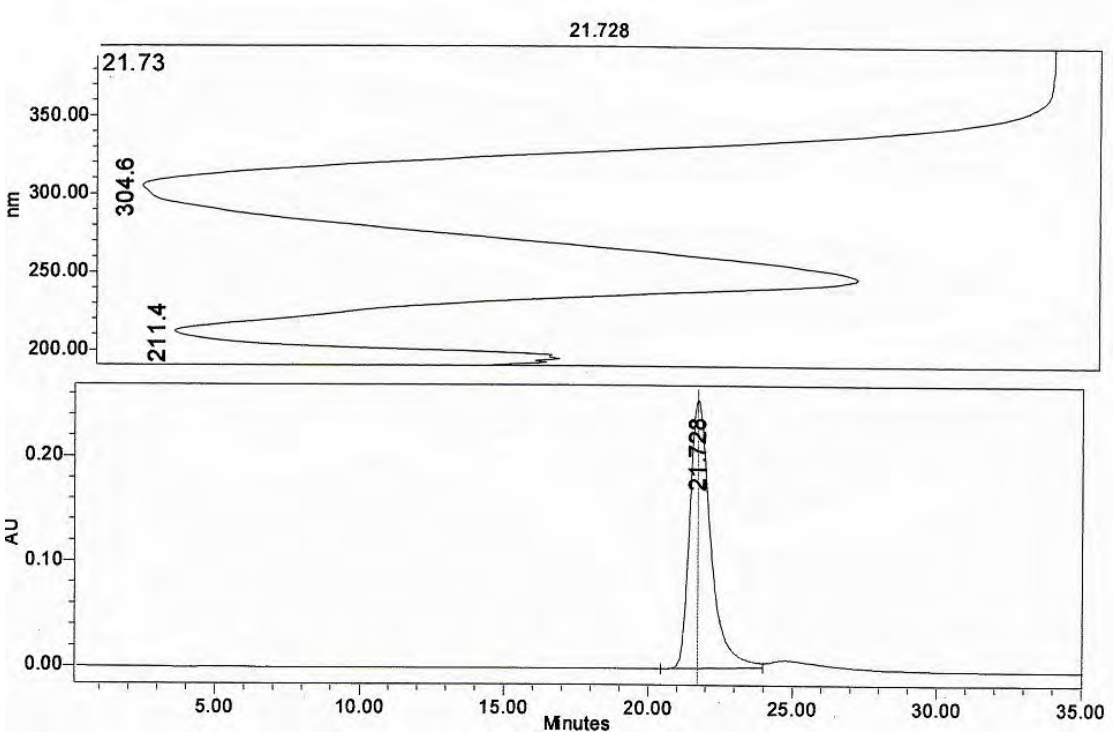

Figure 60 The HPLC chromatogram of pure *cis*-2-EHMC obtained by elution on a Nucleosil 100 C18 column. The eluent was methanol/water (85% v/v) at a flow rate 1 mL min^{-1} injection volume – 20 µL. The detection wavelength was 310 nm.

A UV spectrum of the *cis*-isomer was obtained on the UV/vis spectrophotometer and is shown in Figure 61. The wavelength of maximum absorption is 304 nm showing a hypsochromic shift from *trans*-2-EHMC (310 nm). The molar absorptivity of a pure sample of the *cis*-isomer was determined at 304 nm which is the wavelength of maximum absorption. A stock solution of 1 x 10^{-3} M *cis*-isomer was prepared in methanol and appropriate concentrations obtained by serial dilution. UV spectra were obtained for six concentrations. The absorbance was plotted against the various concentrations from which the molar absorptivity was calculated (Figure 62). A value of 1.805 x 10^4 dm^3 mol^{-1} cm^{-1} was obtained and this is lower than that of *trans*-2-EHMC which is 2.33 x 10^4 dm^3 mol^{-1} cm^{-1} at 311 nm in methanol [48]. The lower value therefore means that the *cis*-isomer is indeed a less efficient UVB absorber.

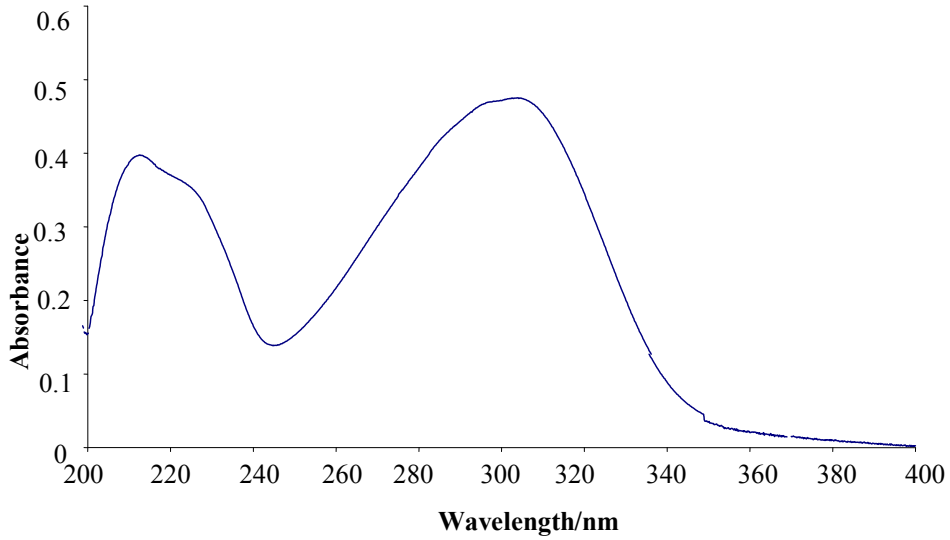

Figure 61 UV spectrum of pure *cis*-2-EHMC dissolved in methanol.

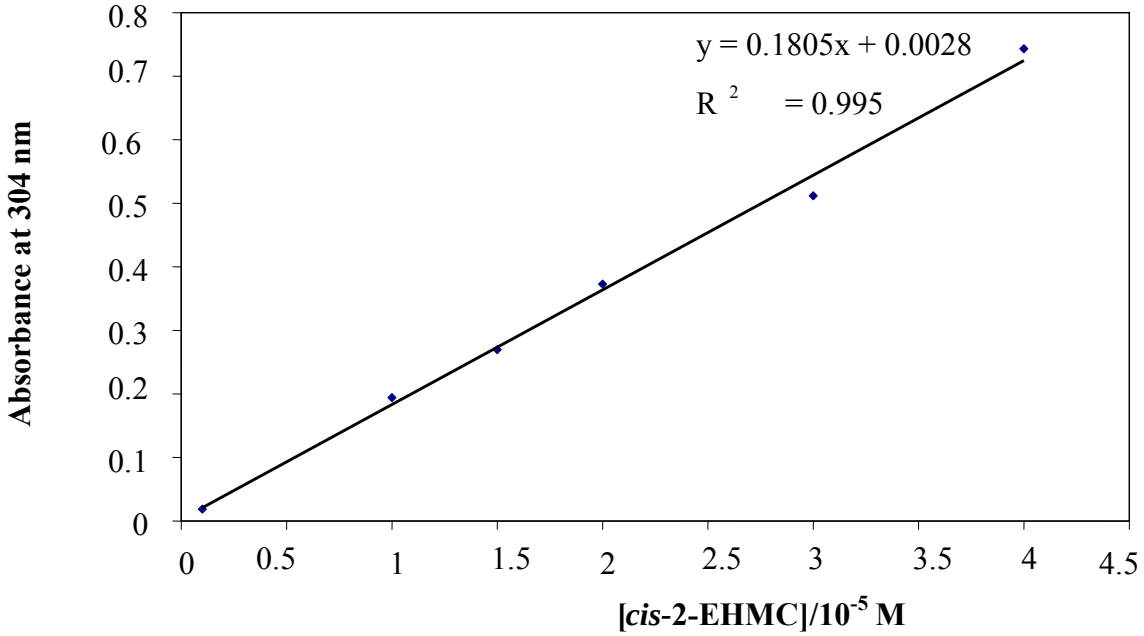

Figure 62 Calibration curve for the determination of the molar absorptivity of *cis*-2-EHMC in methanol at 304 nm.

The formation of dimers was detectable in concentrated solutions of irradiated 2-EHMC. Figures 63, 64, 65 and 66 show the chromatograms obtained at different concentrations after UV irradiation. The formation of dimers is concentration dependent. It was observed that at low concentration of 1 x 10^{-6} M of 2-EHMC no dimers form. But as the concentration was increased from 1 x 10^{-3}M, dimers were observed.

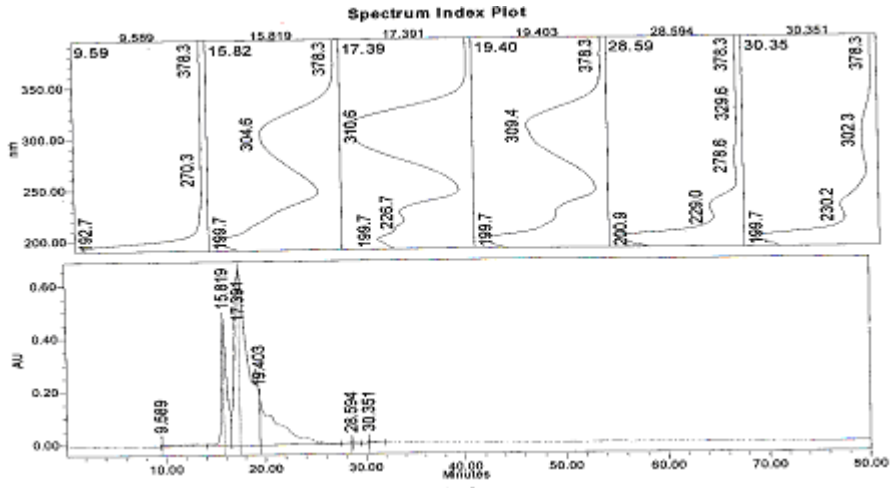

Figure 63 The HPLC chromatogram of an irradiated 1 x 10^{-3} M solution of *trans*-2-EHMC obtained by elution on a Spherisob 5S ODS column. The eluent was methanol/water (93% v/v) at a flow rate of 4 mL min^{-1}., injection volume – 20 µL**.** The detection wavelength was 310 nm.

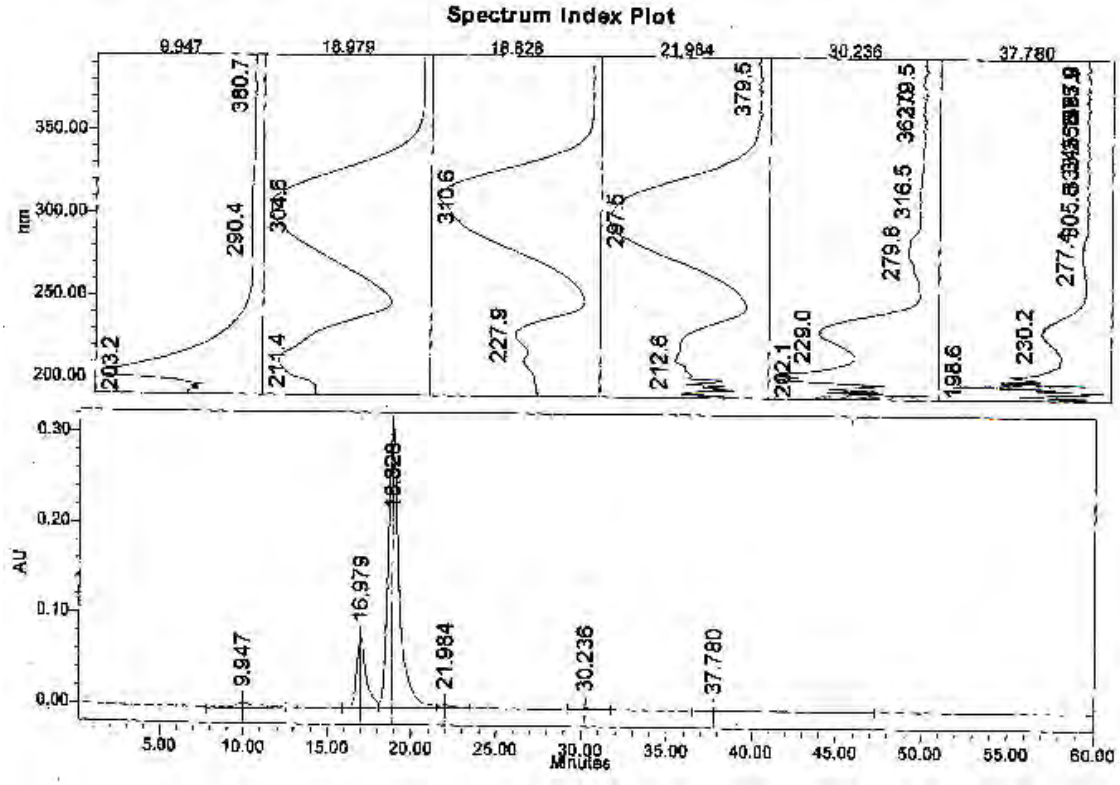

Figure 64 The HPLC chromatogram of an irradiated 1 x 10^{-2} M solution of *trans*-2-EHMC obtained by elution on a Spherisob 5S ODS column. The eluent was methanol/water (93% v/v) at a flow rate 4 mL min^{-1}, injection volume – 20 µL. The detection wavelength was 310 nm.

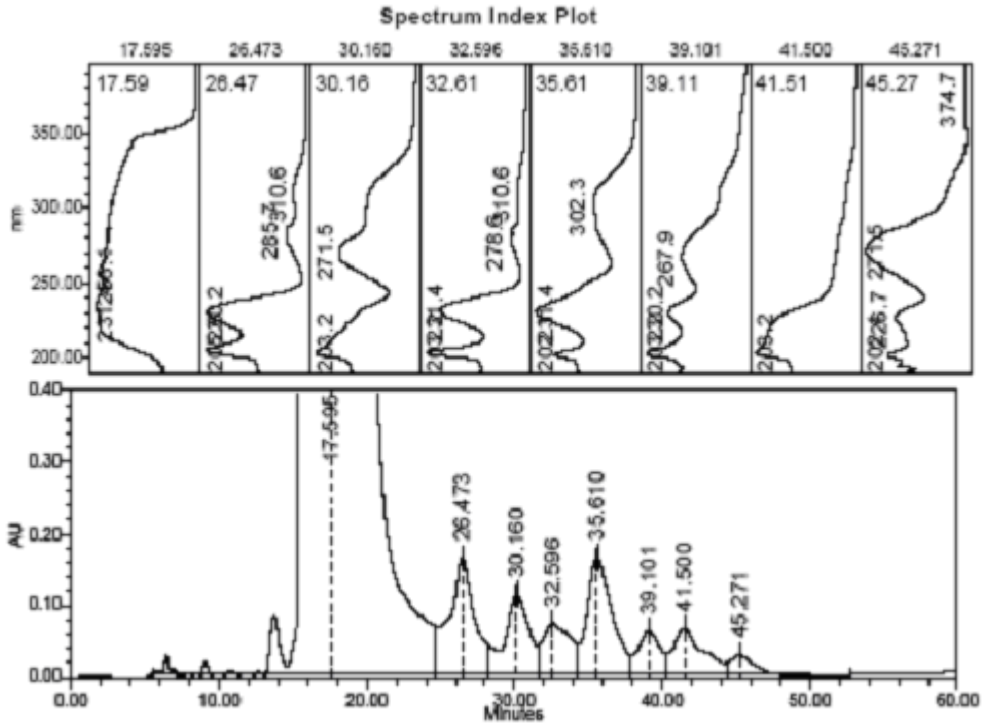

Figure 65 The HPLC chromatogram of an irradiated concentrated solution of *trans*-2-EHMC obtained by elution on a Spherisob 5S ODS column. The eluent was methanol/water (93% v/v) at a flow rate 4 mL min^{-1}, injection volume – 20 µL. The detection wavelength was 310 nm.

The dimers were found to elute much later than the isomers. This is due to structural differences since the dimers have twice the molecular mass and size of the isomers. In addition, due to the bulky ethylhexyl alkyl group, these dimers may be considered to be more hydrophobic and non-polar. It is therefore these structural characteristics that make them elute after the isomers on a reversed-phase column. This is consistent with reversed-phase HPLC in which non-polar compounds are expected to stay longer on the stationary phase and elute much later than polar compounds. The presence of these dimers was confirmed with HPLC-MS studies. The corresponding HPLC chromatogram and the mass spectra are shown in Figure 66 and Figure 67 respectively. Apart from the molecular masses associated with the protonated ion $[M + H]^+$ *trans/cis* isomers at m/z of 291 there were additional peaks with m/z of 581. This value is double that of the single isomer which indicated the formation of dimers.

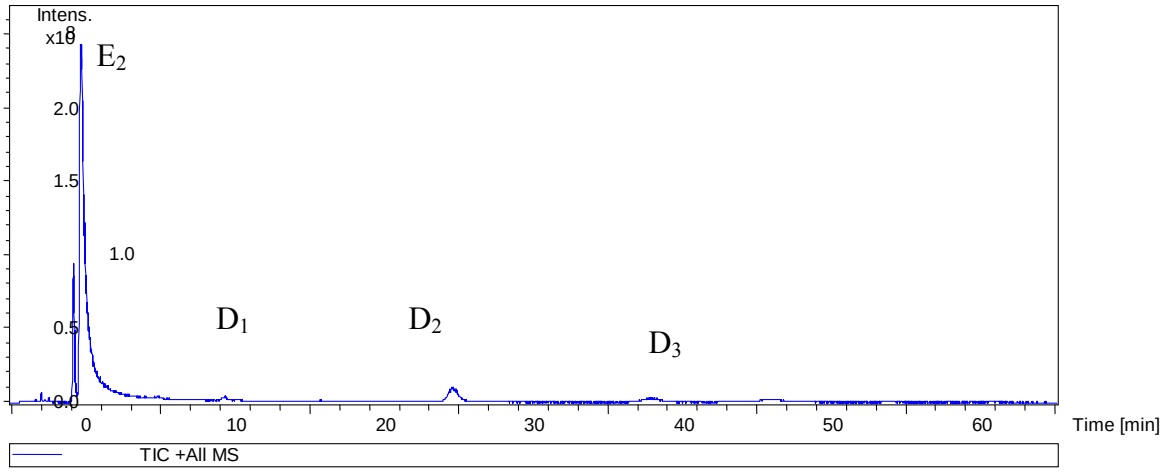

Figure 66 HPLC chromatogram of irradiated *trans*-2-EHMC analysed on the Agilent Zorbax Eclipse XDB-C18 column by isocratic elution at a flow rate 1 mL min^{-1} , injection volume – 5 µL with the Agilent 1100 Series HPLC with UV detection at 310 nm. The order of elution was *cis*-2-EHMC (E_1), *trans*- 2-EHMC (E_2) and the dimers (D_1, D_2, D_3).

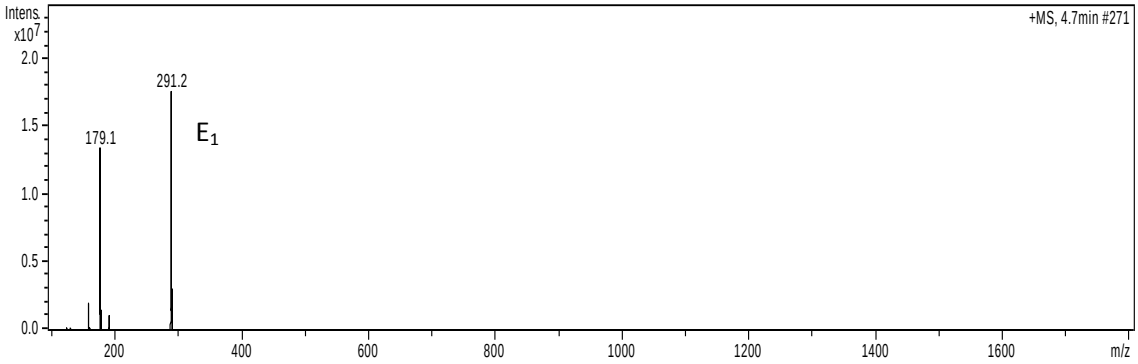

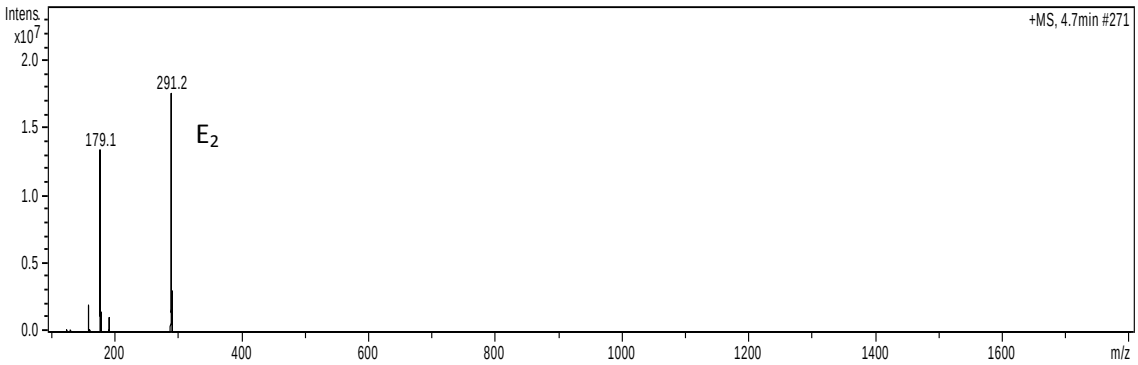

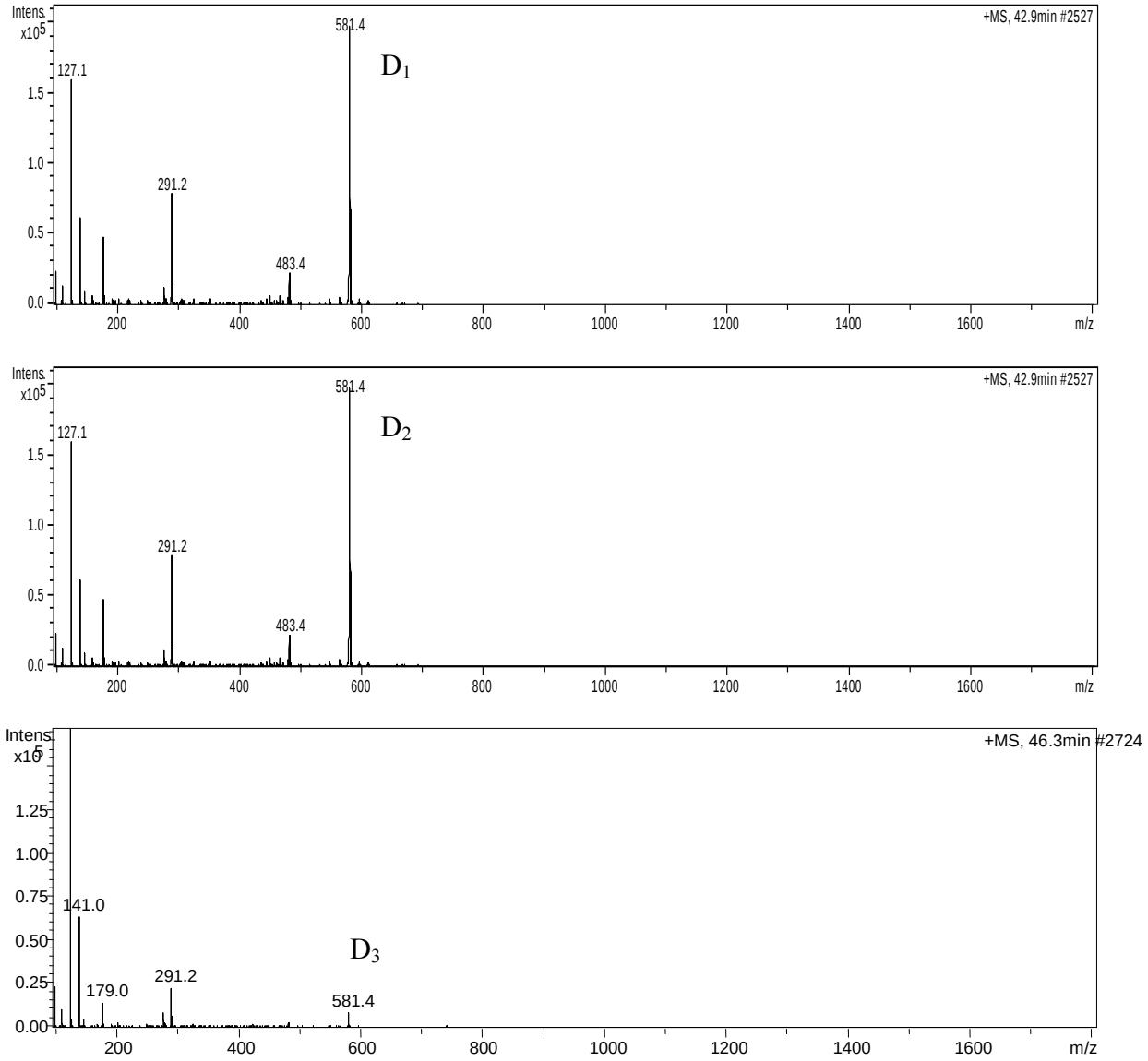

Figure 67 Mass spectra of the peaks labelled E_1, E_2, D_1, D_2 and D_3 in Figure 66.

4.3.4 Column chromatography for the separation of 2-EHMC photoproducts

Gravity column chromatography was attempted to separate the photoproducts of 2-EHMC that were formed during UV irradiation. Although this system showed a complex mixture of products as was observed by TLC analysis, they were difficult to separate. This was due to the very low concentration of the dimers that are formed after irradiation of 2-EHMC with UV light. However, the major products (*trans/cis*) were successfully isolated and characterised by ^{1}H NMR.

4.3.5 FTIR analysis of the isomers of 2-EHMC

A sample of irradiated 2-EHMC was separated on a semi-preparative HPLC column and the fractions collected. The infrared spectra of *trans*- and *cis*- 2-EHMC were obtained in the region of 700 - 4000 cm^{-1} and are shown in Figures 68 and 69 respectively. Both show strong absorption bands at around 1710 cm^{-1} associated with the conjugate ester C=O stretching band while the conjugate C=C stretching band shows at around 1600 $cm^{-1.}$ Another distinct feature is the bands observed from 2860 to 2960 cm^{-1} which are due to the presence of the ethylhexyl side chain. Although the fingerprint region is generally similar for the two isomers the peak occurring at 983 cm^{-1} was only detectable in the *trans*-isomer. This peak corresponds to the CH rocking deformation vibration of the Ph-CH=CH which is only seen in the *trans*-configuration [49].

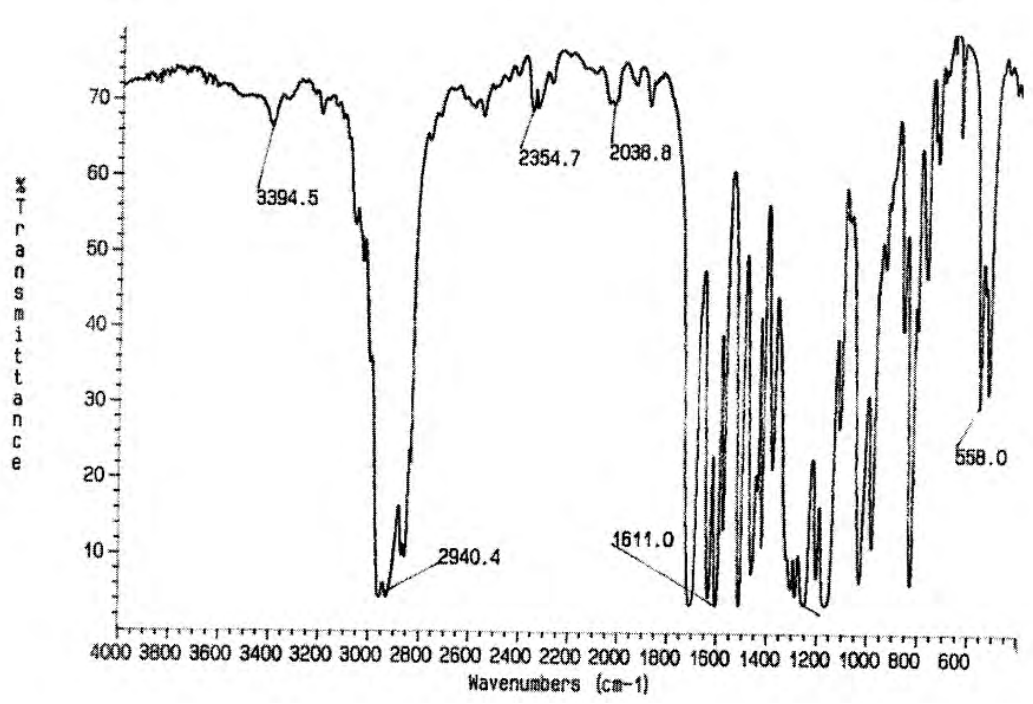

Figure 68 An infrared spectrum of *trans*-2-EHMC recorded as a thin film on a KBr disc.

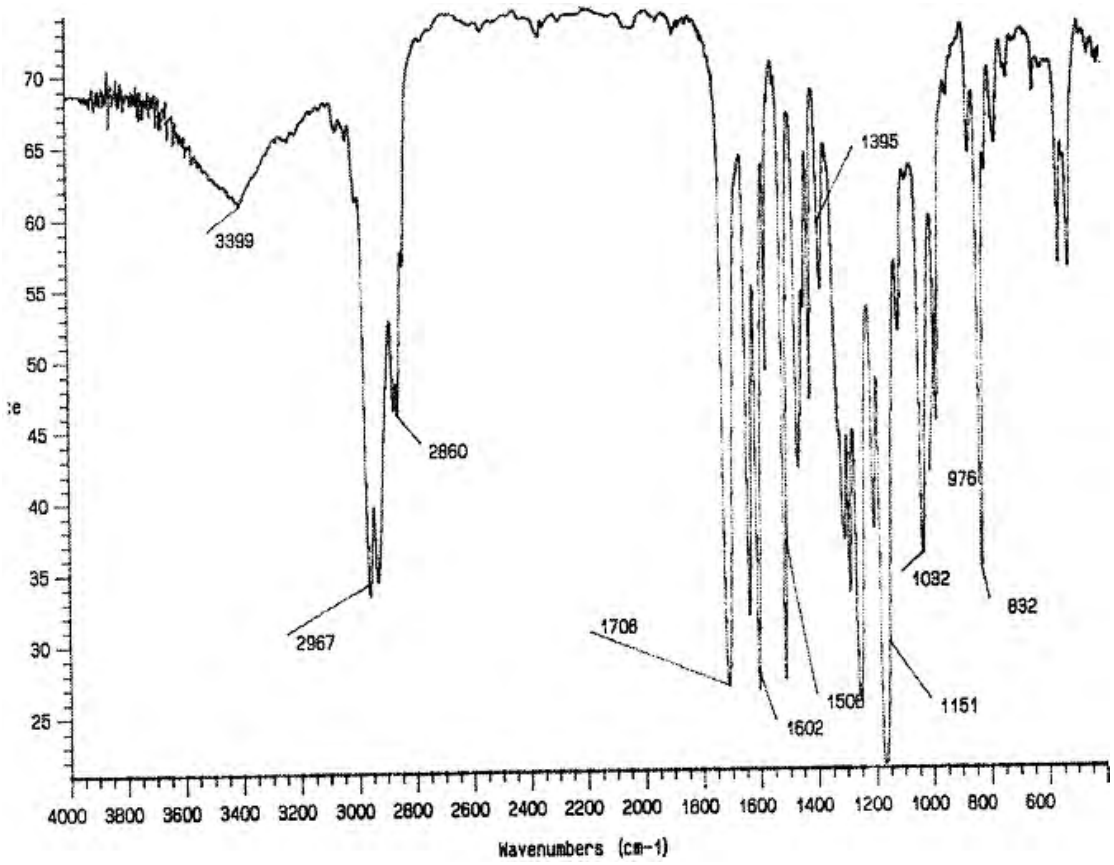

Figure 69 An infrared spectrum of *cis*-2-EHMC recorded as a thin film on a KBr disc.

4.3.6 NMR Analysis of the photoproducts of 2-EHMC

The isomers and the dimers of 2-EHMC were separated on the semi-preparative HPLC and collected as fractions. They were then analyzed by using NMR.

A comparison of the proton NMR of *cis*–2-EHMC (Figure 71) with that of the *trans*-isomer (Figure 70) shows a different chemical shift in the region where the aromatic hydrogens resonate. The peaks of the *cis*-product are shifted upfield as compared with those of *trans*-2-EHMC. The aromatic hydrogens appear at 6.9 and 7.6 ppm. The two sets of doublets arising from the *cis*-ethylenic hydrogens appear at 5.8 and 6.95 ppm as compared with those of the *trans*-ethylenic hydrogens appearing at 6.4 and 7.6 ppm. The NMR spectral data acquired are summarised in Table 18.

Table 18 ^{1}H NMR spectral data for *trans*- and *cis*-2-EHMC.

	Trans-isomer	cis-isomer
Position	δH/ppm	δH/ppm
1	3.82 (3H, s)	3.81 (3H, s)
3	6.87 (2H, d, J = 8.7 Hz)	6.80 (2H, d, J = 7 Hz)
4	7.45.(2H, d, J = 8.7Hz)	7.66 (2H, d, J = 7 Hz)
6	7.64 (1H, d, J = 16Hz)	6.80 (1H, d, J = 12 Hz)
7	6.32 (1H, d, J = 16Hz)	5.82 (1H, d, J = 12 Hz)
9	4.08 (2H, d, J = 5Hz)	4.09 (2H, d, J=6 Hz)
10	1.63(1H, br m)	1.63 (1H, br m)
11	1.34 (2H, br m)	1.34 (2H, br m)
12	0.91 (3H, br t)	0.91 (3H, br t)
13	1.36 (2H, m)	1.36 (2H, m)
14	1.41 (2H, m)	1.41 (2H, m)
15	1.34 (2H, br m)	1.34 (2H, br m)
16	0.94 (3H, t)	0.94 (3H, t)

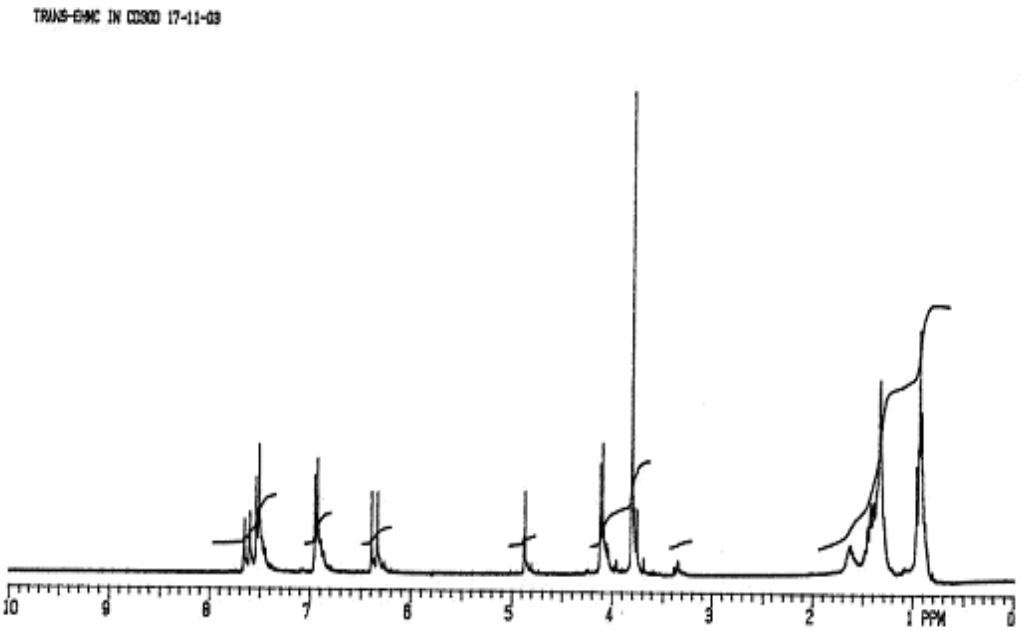

Figure 70 Proton NMR spectrum of *trans*-2-EHMC acquired in CD_3OD.

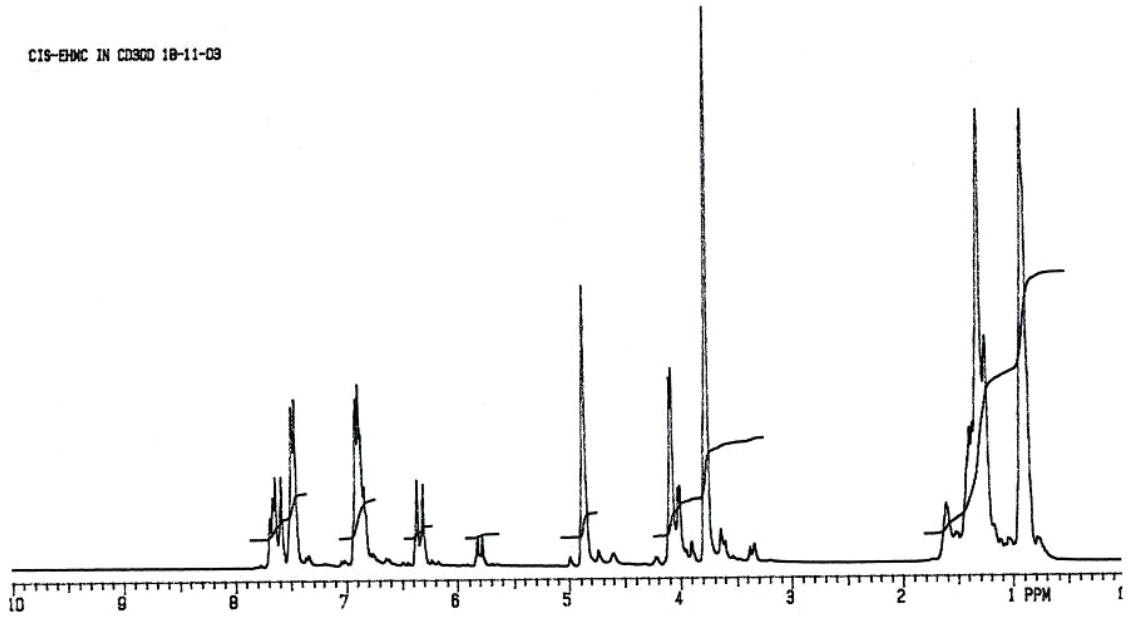

Figure 71 Proton NMR spectrum of *cis*-2-EHMC acquired in CD_3OD.

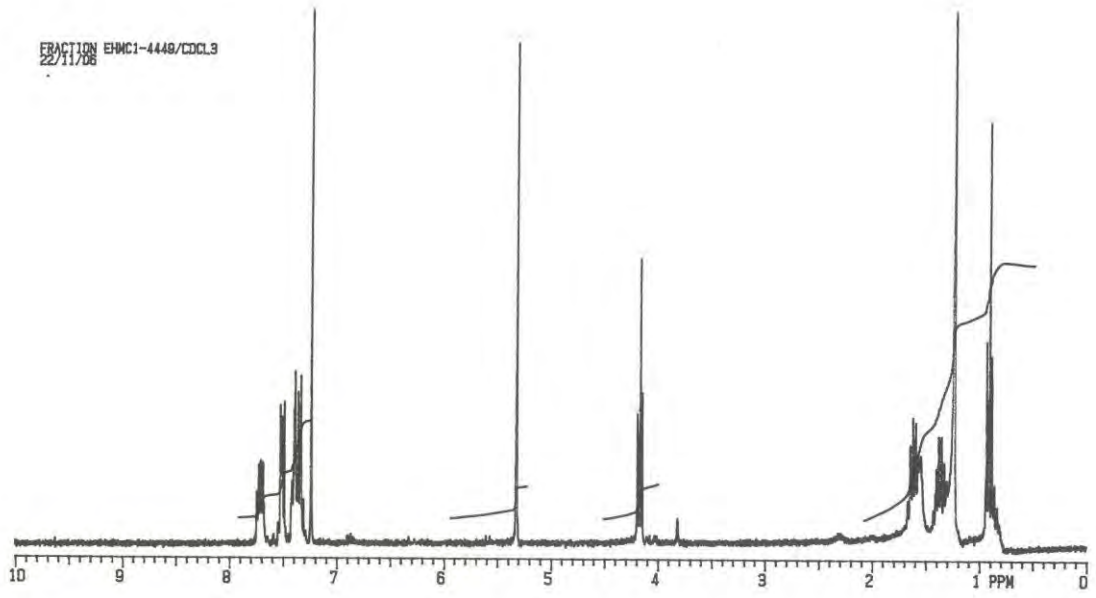

Figure 72 Proton NMR spectrum of the dimer of 2-EHMC acquired in CD_3OD.

Unfortunately, the quantities of the dimers were quite small and they were not effectively separated by either gravity column chromatography or the semi-preparative HPLC. A mixture of the dimers was instead obtained. Nevertheless, the NMR spectra show a loss of double bonds, which is indicative of the formation of the cyclobutane ring. The photodimerisation process resulting in the formation of cyclobutane rings was confirmed by the IR and NMR spectral changes with the disappearance of the aliphatic carbon–carbon double bonds and appearance of aliphatic single carbon–carbon bonds. The UV spectra of the dimers (see Figure 65) show that they absorb at a much shorter wavelength predominantly in the UVC region. This is in conformity with the absorption of a non-conjugated benzene nucleus. This is also in agreement with the knowledge that products resulting from the cycloaddition reaction of cinnamate molecules using double bonds effectively cancel the conjugation responsible for the absorption of the cinnamates [50]. The photodimerisation of 2-EHMC yields cyclobutane derivatives of different stereochemistry [21, 46]. The *trans*-ethylenic hydrogens appear as doublets at 6.32 and 7.64 ppm. The coupling constant is 16 Hz which is consistent with *trans* ethylenic hydrogens [51]. The ortho-coupled aromatic hydrogens can be seen to resonate as doublets at 6.87 and 7.45 ppm. The three methoxy hydrogens give a strong singlet at 3.82 ppm and the two hydrogens belonging to the $–OCH_2-$ group resonate as a doublet at 4.08 ppm. The hydrogens of the 2-ethylhexyl group occur as a multiplet in the 0.9 to 1.7 ppm region, whereas the signals due to the two $-CH_3$ groups appear at 0.9 ppm. The methylene hydrogens, the four $–CH_2$ groups appear at 1.27 ppm and those due to the singlet –CH at 1.6 ppm. The peak at 4.9 ppm is due to the deuterated methanol.

Due to the extremely low yields of the dimers resulting from UV irradiation and in the difficulties experienced in separation, computational studies were carried out in order to elucidate the stereochemistry, the lowest energies and hence the relative stabilities of the different photoproducts. This aspect is discussed in Chapter 6.

4.4 Conclusion

UV irradiation of 2-EHMC causes it to photodegrade either through photoisomerisation or photodimerisation. Since the *cis*-isomer absorbs UV radiation less efficiently than *trans*-2-EHMC, the photoinduced isomerisation of the sunscreen agent decreases its UV-protective

capacity. If the absorption decreases while the shape of absorption curve remains the same, then there will be an increase in the intensity or flux of UV radiation, but of the same spectrum, reaching the basal epidermal cell layers. If the shape of the absorption spectrum also changes by moving to shorter wavelengths then the situation becomes more complicated. This can lead to a higher UVB and UVA exposure than expected [13].

The formation of dimers was found to be concentration dependent as dimerisation was observed at concentrations greater than 1 x 10^{-3} M solutions of 2-EHMC. The dimerisation occurs via a [2 + 2]-cycloaddition reaction across the ethylenic double bond. The dimers were found to absorb at wavelengths mostly in the UVC region which is consistent with cyclobutane type of compounds and hence photodimerisation of 2-EHMC is another cause for its loss in absorbance upon irradiation.

Since there is an increasing demand by dermatologists for use of sunscreen agents even in non-sunscreen products there is therefore a need to examine the toxic potential of UV-induced degradation products. Sunscreens are applied topically on large parts of the human body. The photodegradation of the sunscreen agent under UV radiation whereby reactive radicals, isomers and even photoadducts are formed may or may not penetrate human skin. However, the photochemical degradation, although occurring to only a small extent could have a cytotoxic effect on the human skin. Future studies should therefore focus on the toxicological properties of the photoproducts with the aim of achieving a further improvement in cosmetic product safety.

REFERENCES

1. Broadbent, J.K., Martincigh, B.S., Raynor, M.W., Salter, L.F., Moulder, R., Sjoberg, P., Markides, K.E., *Capillary supercritical fluid chromatography combined with atmospheric pressure chemical ionisation mass spectrometry for the investigation of photoproduct formation in the sunscreen absorber 2-ethylhexyl-p-methoxycinnamate.* Journal of Chromatography A, 1996, **732,** (1), 101-110.
2. Hayden, C.G.J., Roberts, M.S., Benson, H.A.E., *Sunscreens: are Australians getting the good oil?* Australian and New Zealand Journal of Medicine, 1998, **28,** (5), 639-646.
3. Lowe, N.J., Shaath, N.A., *Sunscreens: Development, Evaluation and Regulatory Aspects*, ed. N.A. Shaath. 1990, New York: Marcel Dekker, Inc. USA. pp 222-232.
4. Schneider, S., Deckardt, K., Hellwig, J., Kuttler, K., Mellert, W., Schulte, S., *Octyl methoxycinnamate: Two generation reproduction toxicity in Wistar rats by dietary administration.* Food and Chemical Toxicology, 2005, **43**, 1083–1092.
5. Diffey, B., Stokes, R.P., Forestier, S., Mazilier, C., Rougier, A., *Suncare product photostability: a key parameter for more realistic in vitro efficacy evaluation.* European Journal of Dermatology, 1997, **7**, 226-228.
6. Matthieu, L., Meuleman, L., Van Hecke, E., Blondeel, A., Dezfoulian, B., Constandt, L., Goossens, A., *Contact and photocontact allergy to ketoprofen. The Belgian experience*, Contact Dermatitis., 2004, **50**, 238-241.
7. Hayden, C.G.J., Cross, S.E., Anderson, C., Saunders, N.A., Roberts, M.S., *Sunscreen penetration of human skin and related keratinocyte toxicity after topical application.* Skin Pharmacology and Physiology, 2005, **18,**(4), 170-174.
8. Hayden, C.G., Roberts, M. S., Benson, H.A.E., *Systemic absorption of sunscreen after topical application,* Lancet, 1997, **350**, 863–864.
9. Morliere, P., Avice, O., Melo, T.S.E., Dubertret, L., Giraud, M., Santus, R., *A Study of the Photochemical Properties of Some Cinnamate Sunscreens by Steady-State and Laser Flash-Photolysis.* Photochemistry and Photobiology, 1982, **36,** (4), 395-399.
10. Kammeyer, A., Westerhof, W., Bolhuis, P.A., Ris, A.J., Hische, E A., *The Spectral Stability of Several Sunscreening Agents on Stratum-Corneum Sheets.* International Journal of Cosmetic Science, 1987, **9,**(3), 125-136.

11. Deflandre, A., Lang, G., *Photostability Assessment of Sunscreens - Benzylidene Camphor and Dibenzoylmethane Derivatives.* International Journal of Cosmetic Science, 1988, **10,**(2), 53-62.
12. Serpone, N., Salinaro, A., Emeline, A.V., Horikoshi, S., Hidaka, H., Zhao, J.C., *An in vitro systematic spectroscopic examination of the photostabilities of a random set of commercial sunscreen lotions and their chemical UVB/UVA active agents.* Photochemical and Photobiological Sciences, 2002, **1,** (12), 970-981.
13. Tarras-Wahlberg, N., Stenhagen, G., Larko, O., Rosen, A., Wennberg, A.M., Wennerstrom, O., *Changes in ultraviolet absorption of sunscreens after ultraviolet irradiation.* Journal of Investigative Dermatology, 1999, **113,** (4), 547-553.
14. Pattanaargson, S., Munhapol, T., Hirunsupachot, N., Luangthongaram, P., *Photoisomerization of octyl methoxycinnamate.* Journal of Photochemistry and Photobiology A: Chemistry, 2004, **161,** (2-3), 269-274.
15. Agrapidispaloympis, L.E., Nash, R.A., Shaath, N.A., *The Effect of Solvents on the Ultraviolet Absorbency of Sunscreens.* Journal of the Society of Cosmetic Chemists, 1987, **38,** (4), 209-221.
16. Beyere, L., Yarasi, S., Loppnow, G.R., *Solvent effects on sunscreen active ingredients using Raman spectroscopy.* Journal of Raman Spectroscopy, 2003, **34,** (10), 743-750.
17. Huong, S.P., Andrieu, V., Reynier, J.P., Rocher, E., Fourneron, J.D., *The photoisomerization of the sunscreen ethylhexyl p-methoxy cinnamate and its influence on the sun protection factor.* Journal of Photochemistry and Photobiology A: Chemistry, 2007, **186,**(1), 65-70.
18. Broadbent, J.K., *Photochemical studies of sunscreen constituents;* M.Sc. Dissertation, University of Natal, Durban, South Africa, 1994.
19. Ingouville, N.A., *The photochemical behaviour of the sunscreen absorber 2-ethylhexyl-p-methoxycinnamate;* M.Sc. Dissertation, University of Natal, Durban, 1995.
20. Robinet, G., Devillers, J., Debourayne, C., Riviere, M., Barthelat, M., *Photodimerization of Cinnamate Derivatives in Microemulsions - Investigation by Molecular Mechanics of the Conformations and Relative Energies of Some Isomers of the Methyl Cinnamate Dimer.* New Journal of Chemistry, 1987, **11,** (1), 51-59.
21. Egerton, P.L., Hyde, E.M., Trigg, J., Payne, A., Beynon, P., Mijovic, M.V., Reiser, A., *Photocycloaddition in Liquid Ethyl Cinnamate and in Ethyl Cinnamate Glasses - the Photoreaction as a Probe into the Micro-Morphology of the Solid.* Journal of the American Chemical Society, 1981, **103,** (13), 3859-3863.

22. Lewis, F.D., Oxman, J.D., Gibson, L.L., Hampsch, H.L., Quillen, S.L.J, *Lewis acid catalysis of photochemical reactions. 4.Selective isomerization of cinnamic esters.* Journal of the American chemical society, 1986, **108**, 3005.

23. Cohen, M.D., Schmidt, G.M.J., *Topochemistry. Part 1. A survey.* Journal of Chemical Society, 1964, **2**, 1996-2000.

24. Smith, G.J., Miller, I.J., *The effect of molecular environment on the photochemistry of p-methoxycinnamic acid and its esters.* Journal of Photochemistry and Photobiology A: Chemistry, 1998, **118**, 93-97.

25. Lanebrown, M.M., Gallagher, C.H., Greenoak, G.E., Reeve, V.E., Baker, R.S., Bonin, A., *Sunscreens and UV Carcinogenesis.* Medical Journal of Australia, 1980, **2,**(8), 463-463.

26. Bonin, A.M., Arlauskas, A.P., Angus, D.S., Baker, R.S.U., Gallagher, C.H., Grenoak, G., Lane Brown, M.M., Meher-Homji, K.M., Reeve, V., *UV-absorbing and other sun-protecting substances: genotoxicity of 2-ethylhexyl p-methoxycinnamate.* Mutation Research, 1982, **105**, 303 -308.

27. Mohammad, T., Baird, W.M., Morrison, H., *Photochemical covalent binding of p-methoxycinnamic acid to calf thymus DNA.* Bioorganic Chemistry, 1991, **19**, 88-100.

28. Martincigh, B.S., Kowlaser, K., Raynor, M.W., *Photoproducts of 2-ethylhexyl-para-methoxycinnamate.* Photochemistry and Photobiology, 1999, **69**, 64S-64S.

29. Seidlova-Wuttke, D., Jarry, H., Christoffel, J., Rimoldi, G., Wuttke, W., *Comparison of effects of estradiol (E2) with those of octylmethoxycinnamate (OMC) and 4-methylbenzylidene camphor (4MBC) - 2 filters of UV light - on several uterine, vaginal and bone parameters.* Toxicology and Applied Pharmacology, 2006, **210,** (3), 246-254.

30. Setlow, R.B., Wookhead, A.D., Grist, E., *Animal model for UV-radiation induced melanoma: platyfish-swordtail hybrid.* Proceedings of the National Academy of Sciences of the United States of America, 1989, **86,** (22), 8922-8926.

31. Kowlaser, K., *Photoproduct formation in the irradiated sunscreen absorber 2-ethylhexyl-p-methoxycinnamate;* M.Sc., Dissertation, University of Natal, Durban, 1998.

32. Aliwell, S.R., Martincigh, B.S., Salter, L.F., *Para-Aminobenzoic Acid-Photosensitized Dimerization of Thymine .2. in Puc19 Plasmid DNA.* Journal of Photochemistry and Photobiology A-Chemistry, 1993, **71,** (2), 147-153.

33. Sutherland, J.C., Griffin, K.P., *Para-Aminobenzoic Acid Can Sensitize the Formation of Pyrimidine Dimers in DNA - Direct Chemical Evidence.* Photochemistry and Photobiology, 1984, **40,** (3), 391-394.

34. Salim, A.M., *The effect of antioxidants on the para-aminobenzoic acid photosensitised formation of thymine dimer and singlet molecular oxygen;* PhD Thesis, University of KwaZulu-Natal, Durban, 2005.

35. Bolton, K., Martincigh, B.S., Salter, L.F., *The Potential Carcinogenic Effect of Uvinul-Ds49 - a Common UV Absorber Used in Cosmetics.* Journal of Photochemistry and Photobiology A-Chemistry, 1992, **63,** (2), 241-248.

36. Aliwell, S.R., Martincigh, B.S., Salter, L.F., *Photoproducts Formed by near-UV Irradiation of Thymine in the Presence of P-Aminobenzoic Acid.* Journal of Photochemistry and Photobiology A: Chemistry, 1994, **83,** (3), 223-228.

37. Gonzenbach, H., Hill, T.J., Truscott, T.G., *The Triplet Energy-Levels of UVA Sunscreens and UVB Sunscreens.* Journal of Photochemistry and Photobiology B: Biology, 1992, **16,**(3-4), 377-379.

38. Butt., S.T., Christensen, T, *Phototoxicity of sunscreens.* Radiation Protection Dosimetry, 2000, **91**, 283-286.

39. Janjua, N.R., Mogensen, B., Andersson, A.M., Petersen, J.H., Henriksen, M., Skakkebaek, N. E., Wulf, H.C., *Systemic absorption of the sunscreens benzophenone-3, octyl-methoxycinnamate, and 3-(4-methyl-benzylidene) camphor after whole-body topical application and reproductive hormone levels in humans.* Journal of Investigative Dermatology, 2004, **123,** (1), 57-61.

40. Schlumpf, M., Cotton, B., Conscience, M., Haller, V., Steinnmann, B., Lichtensteiger, W., *In Vitro and in vivo estrogenicity of UV screens.* Environmental Health Perspectives, 2001, **109**, 239-244.

41. Allen, J.M., Gossett, C.J., Allen, S.K., *Photochemical formation of singlet molecular oxygen in illuminated aqueous solutions of several commercially available sunscreen active ingredients.* Chemical Research in Toxicology, 1996, **9,**(3), 605-609.

42. Martincigh, B.S., Allen, J.M., Allen, S.K., *Sunscreen: the molecule and their photochemistry, in: Suncreen photobiology: cellular and physiological aspects*, ed. F.P. Gasparro. 1997: Springer-Verlag and Landes Bioscience. pp 11-45.

43. Christie, W.W., *HPLC and Lipids: A practical guide*. 1987: Pergamon Press, Oxford. pp.35-41.

44. Maier, H., Schauberger, G., Brunnhofer, K., Honigsmann, H., *Change of ultraviolet absorbance of sunscreens by exposure to solar-simulated radiation.* Journal of Investigative Dermatology, 2001, **117,** (2), 256-262.

45. Pattanaargson, S., Hongchinnagorn, N., Hirunsupachot, P., Sritana-anant, Y., *UV absorption and photoisomerization of p-methoxycinnamate grafted silicone.* Photochemistry and Photobiology, 2004, **80,** (2), 322-325.
46. Lewis, F.D., Quillen, S.L., Hale, P.D., Oxman, J.D., *Lewis acid catalysis of photochemical reactions. Photodimerization and cross-cycloaddition of cinnamic esters.* Journal of American Chemical Society, 1988, **110**, 1261 - 1267.
47. Pattanaargson, S., Limphong, P., *Stability of octyl methoxycinnamate and identification of its photodegradation product.* International Journal of Cosmetic Science, 2001, **23**, 153-160.
48. Lowe, N.J., Shaath, N.A., *Sunscreens: Development, Evaluation and Regulatory Aspects*, ed. N.A. Shaath. 1990, New York: Marcel Dekker, Inc. USA. pp505-536.
49. Pangnakorn, P., Nonthabenjawan, R., Ekgasit, S., Thammacharoen, C., Pattanaargson, W.S., *Monitoring 2-ethylhexyl-4-methoxycinnamate photoisomerization on skin using attenuated total reflection Fourier Transform Infrared spectroscopy.* Applied Spectroscopy, 2007, **61,**(2), 193-198.
50. Schrader, A., Jakupovic, J., Baltes, W., *Photochemical studies on trans-3-methylbutyl 4-methoxycinnamate.* Journal of the Society of Cosmetic Chemists, 1994, **45**, 43-52.
51. Clayden, J., Greeves, N., Warren, S., Wothers, P.; *Organic Chemistry*, ed. O.U. Press. 2001, London: Oxford University Press. pp 263-265.

CHAPTER 5

Computational chemistry

5 Introduction

Computational chemistry is a valuable and powerful tool, which simulates chemical structures that enhance our understanding of many complex chemical systems [1]. These model chemical systems can be used to obtain information, which may be difficult or impossible to obtain experimentally. They can be used to calculate reliable equilibrium structures for molecules and can also be used to obtain structures of transition states. Such calculations have become possible because efficient methods have been developed for the calculation of derivatives of the electronic energy with respect to geometrical parameters. These derivatives can then be used in optimization procedures to find the geometry with minimum energy or locate a saddle point on the potential energy surface. The potential energy surface is a mathematical relationship linking molecular structure and the resultant energy. So a complete potential energy surface provides for a given collection of atoms complete information about all possible chemical structures and all isomerisation pathways interconnecting them [2]. Points of interest on the potential energy surface include local minima, which correspond to stable structures including intermediates, and maxima or saddle points. A saddle point is at its simplest a maximum in one dimension and a minimum in the other. Saddle points are important in chemistry because they correspond to transition states [3]. Although experimental methods are starting to probe the transition state, present computational methods offer the only reliable method by which one can routinely determine the structure and energy of a transition state or reaction intermediate [4]. Ccommercially available software calculates the electronic structures of the molecules and then displays the results graphically.

In this work theoretical studies making use of computational methods have been carried out to determine the lowest energy geometrical structures of the photoproducts of 2-EHMC and hence their relative stabilities.

There are two broad areas of computational chemistry available, namely, molecular mechanics or force field derived calculations, and electronic structure methods. A brief discussion of each is given in the respective subsequent sections.

5.1 Molecular orbital theory

Molecular orbital (MO) theory is a molecular quantum mechanics approach which utilizes one-electron functions or orbitals to approximate the full wavefunction [5]. A MO, Ψ (x, y, z), is a function of the Cartesian coordinates of a single electron. This three-dimensional function determines the properties of an individual molecule. The probability of finding an electron in a particular region or space is given by the electron in the square of Ψ (Ψ^2) (or square modulus $|\Psi^2|$ if Ψ is a complex conjugate). In qualitative MO theory one always employs the linear combination of atomic orbitals (LCAO) approximation in which a molecular orbital is written as a linear combination of atomic orbitals centred on the various atoms (Equation 4.1) [6]. The overlap between atomic orbitals is determined by their energy, orientation, symmetry and size.

$$\Psi = \Phi_1\Phi_2\Phi_3 \ldots \Phi_n \qquad [4.1]$$

where Φ_n is a three dimensional function for an individual electron.

Since the wavefunction is a product of spin-orbitals, the spin value, which can take the value of ±½, has to be included. The resulting MO is occupied by up to two electrons of opposite spins that are both attracted by the positive nuclei of the atoms. According to Pauli's Exclusion Principle [7], a MO cannot be occupied by two electrons of the same spin and therefore the orbital may be classified as singly or doubly occupied or empty. Most molecules have an even number of electrons in their ground states and may be represented by orbitals that are either doubly occupied or empty, i.e. closed shell wavefunctions.

To date, MO methods represent the most accurate mathematical description of the wavefunction of a molecule. Solving the wavefunction reveals the position of the atoms as well as the energy associated for the given geometry of the molecule. Solving the

wavefunction is only possible with various approximations and even with severe approximations, only molecules having a limited range of sizes can currently be investigated by MO methods.

Various computational chemistry methods have been developed to obtain information of the geometry, energy and other characteristics of molecules. Some of these MO methods are not used at all. The MO theory is utilized in computational chemistry, with various levels of approximations, as will be discussed below.

5.2. Molecular mechanics

Molecular mechanics (MM) models make use of the laws of classical physics to predict the structures and properties of molecules [8, 9]. A molecule is viewed as composed of atoms held together by bonds and the molecular electronic energy is expressed as the sum of bond-stretch, angle-bending, and other kinds of energies. There exist several MM methods which are characterized individually by a particular force field. A force field is composed of a set of equations which define how the potential energy of a molecule varies with the locations of its component atoms, and a series of atom types, defining the characteristics of an element within a specific chemical context [8]. The atom types describe different characteristics and behaviour for an element depending on its environment. The atom type also depends on the hybridisation, charge and the identities of the other atoms to which it is bonded. Some typical atom types are the sp^3 carbon (carbon bonded to four atoms), non-aromatic sp^2, sp carbon, aromatic carbon, hydrogen bonded to carbon, hydrogen bonded to oxygen, hydrogen bonded to nitrogen, etc. MM does not treat the electrons in the molecule explicitly but rather the calculations are performed based solely on nuclear interactions [1].

The electronic effects are included in the force field through parameterisation. A parameter is a quantity that is constant for a set of circumstances but may vary for other circumstances. This approximation makes MM methods relatively less expensive in terms of computation time and hardware, and it can handle far larger molecular systems than electronic structure models or MO methods. Because of its ability to handle large molecules, MM is widely used to deal with biological molecules. For example, folding of a small protein in solution has been modelled by making use of the AMBER force field [10].

The ability to predict a protein's three-dimensional structure for its amino acid sequence is of major help in areas such as drug design. However, MM methods are limited to problems that do not require knowledge of electronic effects; hence it is not usually utilized for transition state calculations [11, 12]. The latter calculations require electronic effects that lead to bond breaking or formation and the details of orbitals involved in the corresponding interactions. It is therefore clear that MM can actually not be classified as a MO based-method.

5.3 Electronic structure methods

Electronic structure or MO methods of computational chemistry use the laws of quantum mechanics instead of classical physics [8, 9]. They seek to solve the Schrödinger wave equation which describes the behaviour of an atom or molecule in terms of its wave-like (or quantum) nature. This is represented by Equation 4.2 which relates the energy and wavefunction of a system

$$H\Psi = E\Psi \qquad [4.2]$$

where H is the Hamiltonian operator, a differential operator which like the energy in classical mechanics, is representative of the sum of kinetic energy and the potential energy of the molecule, E is the numerical energy of the system and Ψ is the wavefunction of the molecular system.

The Schrödinger wave equation for molecular systems can only be solved approximately. By trying to solve the equation, the energy levels of the system can be calculated. Because of the mathematical rigour involved, the models work well for small molecules. Exact solutions to the Schrödinger equation may only be obtained for simple molecules (e.g. H_2) because of the inter-electronic repulsion terms in the equation, where the motion of each electron depends on the motion of the others. Therefore, approximate methods have to be used for larger molecules such as variation methods and the Hartree-Fock self–consistent field method, where the calculated approximate energies are all equal or greater than the exact energy [5].

The different methods and aspects of computational chemistry namely MM, semi-empirical, *ab initio*, and density functional theory (DFT) are commonly referred to as the „level of theory' applied to calculate the geometry and the energy of a molecule. Both *ab initio* and DFT are concerned with predicting various properties of atomic and molecular systems.

5.3.1 The *ab initio* method

Ab initio methods are derived directly from theoretical principles without including experimental parameters in their calculations. In a more fundamental way *ab initio* methods attempt to calculate structures from first principles, using only the atomic numbers of the atoms present. The calculations are based solely on the laws of quantum mechanics and on the values of a few physical constants: the speed of light, the masses and charges of electrons and nuclei, and Planck's constant [8]. The advantage of *ab initio* methods is that they eventually converge to the exact solution once all the mathematical approximations become sufficiently small. They provide high quality quantitative predictions for a broad range of molecules. However, although modern computational developments (hardware and software) have increased the size of the systems manageable by *ab initio* methods, they are still very expensive in terms of computer resources and time. These methods often take an enormous amount of computer CPU time, memory and disk space.

The *ab initio* methods follow mainly two lines, the Hartree-Fock (HF) approach possibly supplemented by the inclusion of electron correlation via second order Moller-Plesset perturbation theory (MP2) or alternatively a density functional approach [13]. Within the conventional scheme, geometry optimization is usually performed at the HF level and in a subsequent single point calculation electron correlation is taken into account. The MP2 specifies the calculation of the electron correlation energy. Figure 73 illustrates the relationship between some of the *ab initio* methods used [6].

Most of these methods are based on MO methods and the wavefunctions are calculated by a self-consistent field (SCF) method using the HF theory. The HF method assumes that the electrons move independently and does not make an allowance for electron correlation.

However, the effects of electron correlation can be taken into account by configuration interaction (CI) or by many-body perturbation theory (MBPT) which ensures that the treatment is size extensive and size consistent [14]. The incorrect dissociative behaviour of the molecular-orbital wavefunction is a serious deficiency which can be corrected by using the multi-configuration self-consistent field (MC-SCF) method, e.g. generalized valence bond (GVB) and complete active space self-consistent field (CASSCF) methods [6]. Most of the computational chemistry software packages have these methods embedded in the calculation.

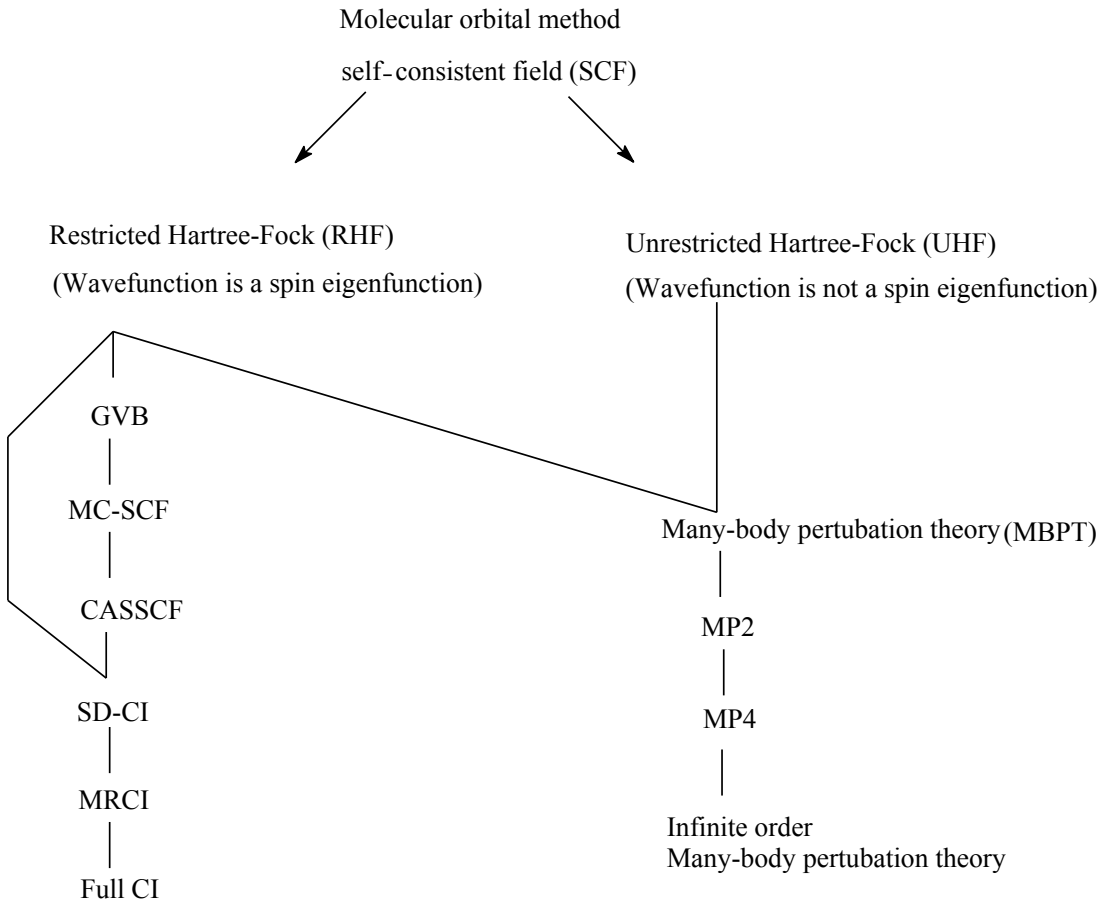

Figure 73 Flow chart showing the relationship between *ab initio* methods [6].

∗GVB – generalized valence bond; MC-SCF – multi-configuration self-consistent field; CASSCF – complete active space self-consistent field; SD-CI – spaced configuration interaction; MRCI – multi reference configuration interaction; CI – configuration interaction, MP – Moller- Plesset.

Unrestricted Hartree-Fock (UHF) and Restricted Hartree–Fock (RHF are commonly named HF) are different approximations of the wavefunction that are used in quantum mechanics calculations. The UHF wavefunctions are those that occur when the spin α-electrons are

allowed to differ from those of spin β (i.e. they are unpaired). Hence, the UHF wavefunction is often used for multiplicities greater than singlets. In RHF calculations the electron spins are by default paired and they also occupy the same spatial orbital; hence the RHF wavefunction is used for singlet electronic states, for example, the ground states of stable organic molecules [15]. Some more theory of this method will be provided below.

5.3.2 Semi-empirical methods

Semi-empirical methods utilise parameters derived from experimental data to simplify the computation. These methods introduce various approximations, which reduce the computational effort characteristic of *ab initio* methods, hence they are much faster. The major approximation of semi-empirical methods is that only the valence electrons are considered in the calculation. The inner shell electrons are treated as part of the nucleus. This is rationalized by the fact that electrons involved in chemical bonding are those in the valence shell. The second approximation is that the basis set is restricted to a minimal representation. This means only a minimal basis set (the number of functions necessary for accommodating the electrons in the neutral atom) is used for the valence electrons. For example, hydrogen has one basis function and all atoms in the second and third rows of the periodic table have four basis functions (one-s and one set of p-orbitals, p_x, p_y and p_z). For transition metals, a set of d-type functions, a s-type function and a set of p-type functions are included, for example $3d_{x2-y2}$, $3d_{z2}$, $3d_{xy}$, $3d_{yz}$, $3d_{xz,}$ 4s, $4p_x$, $4p_y$, 4pz.

A common assumption of semi-empirical methods is the zero differential overlap (ZDO) approximation, which neglects all products of basis functions depending on the same electron coordinates when located on different atoms. Thus some of the elements that respond to the overlap between the atomic orbitals on different atoms are set to zero [1]. However, it is important to include some of the overlaps in even the simplest semi-empirical models. To compensate for some of these approximations the specific method may include parameters that are assigned on the basis of *ab initio* calculations or experimental data. Hence the various semi-empirical methods differ depending upon how many integrals are neglected, and how the parameterization is done.

Semi-empirical methods solve an approximate form of the Schrödinger equation that depends on having appropriate parameters available for the type of chemical system in question. For example, expressions that occur in the Schrödinger equation are set equal to the parameters that have been chosen to lead to the best fit of experimental quantities such as enthalpies of formation [8]. Semi-empirical methods are applicable to a wide range of molecules with almost limitless number of atoms. They can be used, with the exception of modelling transition states, to reproduce a variety of experimental data, such as heats of formation, dipole moments and ionisation potentials. However, accuracy is limited largely because the models are parameterized based upon the results from relatively low level *ab initio* calculations [16]. The most widely used semi-empirical methods are the Austin Method (AM1) [17] and the parametric method (PM3) [18, 19] which are implemented in programs like MOPAC, AMPAC, HyperChem and Gaussian [20]. They usually give satisfactory bond lengths and bond angles hence they can be used to optimize the structure of a starting material. In general, semi-empirical methods are faster than *ab initio* methods but also the results obtained can be unreliable if the molecule is significantly different from the parameterization set utilized in the chosen method.

5.3.3 Density Functional Theory (DFT)

Density functional theory (DFT) [21] based methods are very similar to *ab initio* methods as they require similar resources and provide similar accuracy. DFT methods do account for the effect of electron correlation and are, therefore, a more attractive method than normal *ab initio* calculations that exclude electron correlation. DFT methods owe their origin to the work of Hohenberg and Kohn [22] in which they demonstrated that the ground state energy of any molecule can be described in terms of the total electron density. This means that each molecule has a unique functional form in which the energy and all other properties of a ground state molecule are uniquely determined by the ground state electron probability density. This system is different to the wavefunction approach of *ab initio* techniques, where the complexity of the wavefunctions increases by a factor of 3N for an N-electron system. The complexity of the DFT function is less dependent on the system size since electron density has the same variables [23]. The advantage of DFT methods is that only the total electron density needs to be considered rather than the wavefunction Ψ. A set of orbitals is used to obtain a better approximation to the electron

density and the process is repeated until the density and the energy are constant within some tolerance. The gradient-corrected functions involve both the values of the electron spin densities and their gradients. Becke [24] has introduced functionals consisting of a mixture of HF theory and DFT combined with a gradient-corrected correlation. A widely used gradient-corrected correlation functional is the Lee, Yang and Parr (LYP) that combines with Becke to form BLYP [24, 25]. In general, gradient-corrected or hybrid calculations give more accurate results.

In addition to these traditional wavefunction approaches, theoretical calculations based on DFT methods have achieved a significant breakthrough during the last decade and they are now used worldwide to study the molecular structure and reactivity of chemical systems. The advantages of DFT include less demanding computation effort, less computer time and, in some cases, better agreement with experimental values. For example, Diels-Alder reactions and related cycloadditions have been the subject of several DFT studies showing that those that include gradient corrections and a hybrid functional, such as B3LYP together with the 6-31+G basis set, lead to potential energy barriers (PEBs) in good agreement with experimental results [11]. Despite many successes, DFT does have some drawbacks. The major criticism against DFT is that it does not approach the experimental answer in a systematic manner by reducing the approximations employed even after using a higher level of theory and better basis sets as is the case in *ab initio* methods [5].

The present study relied heavily on transition state calculations and was limited to RHF and DFT calculations.

5.3.4 Hartree-Fock Theory

As described above, HF theory is the basis for MO or electronic structure methods. Below follows a short discussion of the principles involved with this theory.

HF theory makes the fundamental approximation that each electron moves in the static field created by all other electrons [2]. This approximation involves the replacement of the many electron wavefunction by a product of one-electron wavefunctions, namely, the spin orbitals. Therefore, there is no allowance made for electron correlation. Each spin orbital is

written as a molecular orbital with one of two possible spin parts, α or β. According to the Pauli Exclusion Principle only two electrons may occupy a given molecular orbital of a ground state molecule and they must be of opposite spin [7]. The orbitals for all the electrons are then optimized in a self-consistent fashion subject to a variational constraint. The resulting wavefunction, when operated upon by the Hamiltonian, delivers as its expectation value the lowest possible energy for a single determinant wavefunction formed from the chosen basis set [2].

The HF level of theory is the entry level of *ab initio* techniques. It is very useful for providing initial, first level predictions for many systems. The structures and the vibrational frequencies of stable molecules and some transition states can be reasonably computed. As such it is a good base level of theory. There are better levels of theory such as DFT (not strictly a HF method), MP2, MP4, etc., but they are more expensive with regard to hardware resources and time. However, HF theory also has limitations arising principally from the fact that effects of electron correlation are neglected making it unsuitable for some purposes. For example, it is insufficient for accurate modelling of the energetics of reactions and bond dissociation [8].

When fewer approximations are used (i.e. higher level of theory and bigger/or better basis sets), then the computed data are in agreement with or approach experimental data. This is because larger basis sets impose few constraints on electrons and more accurately approximate exact molecular orbitals. For example, the coupled cluster and quadric configuration interaction (QCI) methods represent a higher level treatment of electrons beyond MP4 usually providing even greater accuracy [8]. However, they require more computational resources.

5.3.5 Basis sets

A basis set is a mathematical description of the orbitals within a system used to perform the theoretical calculation [6, 8]. The wavefunction, Ψ, can be expanded in terms of a set of atomic orbitals, $x_{\mu,}$ in the linear combination of atomic orbitals (LCAO) method, to give (Equation 4.3) [9]

$$\Psi = \sum c_\mu x_\mu \qquad [4.3]$$

where c_μ is the molecular orbital expansion coefficient, and x_μ is the basis function of the atomic orbital. The linear combination of atomic orbitals is a basis function. The basis functions are collectively called basis sets [9]. The coefficient c_μ is varied to obtain the wavefunction Ψ, which will give the lowest energy in the Schrödinger wave equation. The more variational parameters used to describe an individual orbital, the lower the energy. However, a situation is reached when the energy is no longer decreased when the number of vibrational parameters is increased and then the best single determinant wavefunction is obtained. When this occurs, changing the wavefunction Ψ by an infinitesimal amount will not alter the energy. The number and the quality of the atomic orbitals x_μ determine the quality of the molecular orbital expansion coefficient c_μ. If there are many electrons in a molecule then the number of atomic integrals required increases rapidly and can be as many as several million for quite small molecules. For this reason a fast computer which has large storage capacity is essential.

The two types of atomic basis functions are the Slater-type atomic orbitals (STOs) and the Gaussian-type atomic orbitals (GTOs). The former are not well-suited to numerical work, and their use in practical MO calculations has been limited. For example, the use of STOs as basis functions in polyatomic molecule calculations produces integrals that are very time-consuming to evaluate. Therefore, most molecular quantum-mechanical calculations use Gaussian functions instead of STOs as the basis functions [26]. These basis sets, in which each orbital is made up of a number of Gaussian probability functions, have considerable advantages over STOs. The Gaussian series of programs deals, as the name implies, almost exclusively with Gaussian-type orbitals. There are different types of basis sets which are discussed in the following sections.

5.3.5.1 Minimal basis sets

This is the simplest type of basis set that contains the minimum number of basis functions needed for each atom [8]. Only enough functions are employed to contain all the electrons of the neutral atoms. In the case of methane (CH_4), for example, a minimal basis set would include 1s, 2s and 2p functions on the carbon atom and 1s functions on each of the hydrogen atoms. They use fixed-sized (contracted) atomic-type orbitals, e.g. Slater type

orbitals (STOs) and Gaussian type orbitals (GTOs). The most common minimal basis set is called STO-3G, where a linear combination of three Gaussian type atomic orbitals (GTO-type) are fitted into Slater-type atomic orbitals (STO) [23]. The STO-3G basis yields properties that are reasonably close to limiting values and in view of the relative computational times of various expansions, it is this level that has been selected as an optimum compromise for widespread application. The individual GTOs are called primitive orbitals while the combined functions are called contracted functions. Some other commonly used STO-nG basis sets are STO-4G and STO-6G where the STO is fitted onto 4 and 6 GTOs respectively.

5.3.5.2 Split valence basis sets

In these types of basis set, the number of basis functions per atom are increased which make the basis set larger and increases its flexibility [5]. Split valence sets such as 3-21G and 6-31G have two sizes of basis function for each valence orbital. As for the case of methane there will be two 1s functions for hydrogen and two 1s, two 2s and two 2p functions for the carbon atom. By doubling the number of functions, there tends to be a significant improvement in the accuracy obtained. Such a basis set is usually described as a valence double zeta (ζ) basis [27]. The nomenclature is a guide to the contraction scheme. The first number indicates the number of primitives used in the contracted core functions. The numbers after the hyphen indicate the numbers of primitives used in the valence functions.

5.3.5.3 Polarised basis sets

Polarised basis sets add polarisation functions into the split valence basis set [5]. Split valence basis sets only expand the virtual size of the orbitals but do not change their shapes. Polarized basis sets remove this limitation by adding orbitals corresponding to one quantum number of higher angular momentum than the valence orbitals. They add d functions for the main group atoms like C, N and O, some add p functions to hydrogen atoms and f functions to transition metals. It is important to note that the d functions that are added to C, N and O atoms have similar sizes to 2p orbitals, and p functions in hydrogen atoms are also similar in size to the 1s orbital, and so on [27, 28]. The primary purpose of the polarization functions (d and p functions) is to give additional angular

flexibility to the linear combination of atomic orbitals (LCAO) process in forming bonding orbitals between pairs of valence atomic orbitals (1s, 2s, 2p, etc.). Polarization functions are essential in strained ring compounds because they provide the angular flexibility needed to direct the electron density into regions between bonded atoms. They can also be used in unstrained compounds for accuracy. An important nomenclature point is that most basis sets are defined to use five spherical d functions, except 6-31G (d) which uses six Cartesian d functions. The six Cartesian d functions are d_{x2}, d_{y2}, d_{z2}, d_{xy}, d_{xz}, d_{yz} and pure spherical d functions are $d_{z2\text{-}r2}$, $d_{x2\text{-}y2}$, d_{xy}, d_{xz}, d_{yz}. Examples of polarized basis sets include 6-31G(d) and 6-31G(d, p). In other words, polarization functions remove the approximation of a perhaps practical limitation on the size of the orbital, by awarding more virtual space to the orbital and allowing the mathematical algorithm to "decide" if to use the additional space or not. By doing so the calculation requires a bit more time and resources, but produces a slightly lower energy structure.

5.3.5.4 Basis sets incorporating diffuse functions

The normal basis sets described above are sometimes inadequate. This is particularly true in the case of excited states and in anions where the electron density is more spread out over the molecule (i.e. delocalization). Since the electron affinities of the corresponding neutral molecules are typically quite low, the extra electron in the anion is only weakly bound. Therefore, to account for this anomaly, a model basis function was designed which is more spread out. The spreading out of the basis function is called the diffuse function [5]. Since highest energy molecular orbitals of anions, molecules with lone pairs, highly excited electronic states, and loose supermolecular complexes tend to be much more spatially diffuse than normal molecular orbitals, diffuse functions are needed to minimise errors in the energy of such systems. To minimise this error in energy, standard basis sets like polarized basis sets [3-21G(d), 6-31G(d), etc.] are often augmented with diffuse basis functions, which are indicated by adding „+' in the basis set name [23]. Diffuse functions are typically used as a better treatment for cases where negatively charged species are being studied because the ionic radius of an anion increases significantly as compared with the corresponding neutral species. Diffuse functions are large versions of s- and p-type functions. Thus, 6-31+G(d) indicates that heavy atoms have been augmented with an additional one s and one set of p functions. A second „+' in 6-31++G(d) indicates the presence of s functions on H.

5.4 The Gaussian 98 program

This program belongs to a series of electronic structure computer programs beginning with Gaussian 70 with the latest being Gaussian 03. The Gaussian program contains a hierarchy of procedures corresponding to different approximation methods commonly referred to as different levels of theory. These programs are capable of performing *ab initio* HF molecular orbital as well as DFT calculations dealing mainly with Gaussian type orbitals based on a LCAO approach. It is capable of computing energies, molecular structures and vibrational frequencies in the gas phase or in solution.

5.4.1 The SCAN calculation

A SCAN calculation can be used as an aid to finding an approximate starting structure for a normal transition-state optimization. A relaxed SCAN calculation involves changing the reaction coordinate from reactants to products, in a step-wise manner. The only constraint in this calculation is the required reaction coordinate(s) (i.e. bond length, angle or the dihedral angle). The rest of the molecule is then optimized to find the structure with lowest possible energy, subject to the imposed constraints, after which the reaction coordinate is modified by a prescribed value and in the next step the procedure is repeated. In this study only relaxed SCAN calculations were used. The energy of each step was plotted against the reaction coordinate. By inspecting the different structures at each step of the scan job, the course of the reaction could be followed. The approximate starting structure for a full (non-restrained) transition-state (TS) optimization can be obtained by manually extracting the coordinates of the structure closest to the maxima on the energy versus reaction coordinate plot. The structure is then used as the starting geometry for a full (non-restrained) transition state optimization, followed by a frequency calculation. A frequency calculation of a true transition state produces only one negative eigenvalue that corresponds to the expected movement of atoms involved in the specific transition.

5.4.2 Commands used during a SCAN or TS search

(i) GDIIS

This command is recommended for use with larger systems, tight optimizations and molecules with flat potential energy surfaces utilized in the Gaussian 98 program. It is the default for semi-empirical calculations. This command makes use of a smaller step-size down the potential energy valley. If this feature is not used, one often gets optimizations that overstep the minimum on the potential energy surface, as the default step size is too large. This is prevented by decreasing the default stepsize of the optimization algorithm through the use of the GDIIS command [20].

(ii) MODREDUNDANT or ModRed

Modified Redundant coordinates (ModRed) is used in geometry optimization, e.g. the bond length to be scanned. The specified coordinates are constrained during a SCAN job, while the rest of the structure or coordinates are optimised. The Modred parameters are specified below the Cartesian coordinates.

(iii) TS

This is used as a request for the optimization to use a mathematical search algorithm which aims to find local maxima on the potential energy surface (i.e. a transition state) rather than a local minimum.

(iv) NOEIGENTEST

The default transition state search in Gaussian 98 makes use of the EigenTest. If only one imaginary frequency is found, the calculation continues to find the transition state associated with this negative eigenvalue. If more than one imaginary frequency exists, the default routine is to terminate the calculations. Since it is practically almost impossible to find a starting structure for TS with one and only one negative eigenvalue, the default TS calculation terminates very often. In order to overcome this oversensitive search criterion, one uses the "NoEigenTest''option which overrides the default search criteria in Gaussian 98.

(v) CALCFC

This is a specified force constant computed at the first point using the current methods available for the HF, MP2, CASSCF, DFT, and semi-empirical methods only. By default Gaussian uses a MNDO (semi-empirical) guess for the solution to the wave function of the specified system. The optimization uses this guess as a starting point after which the *ab initio* calculation is „built' on this starting point. Since the MNDO guess is based on a rather crude or inaccurate method, the calculation could sometimes follow a wrong solution for the wavefunction. One observes this by inspecting the geometry of the structure produced by the optimization; there are basically two choices: start with a better structure, i.e. a structure that was optimized at a lower level of theory, or if a better starting structure was already used, use the CalcFc option.

5.4.3 The GaussView Program

This is a graphical user interface that is used in conjunction with Gaussian 98. It is used to build molecules for submission to and for viewing results in the Gaussian 98 program. In this case GaussView was used to verify the animation of the vibrations associated with negative eigenvalues of the different states.

5.5 Transition Structure Modelling

A transition state (TS) is a molecular species that is represented by the maximum on a potential energy curve in two-dimensional reaction co-ordinate diagram. An attractive feature of computational chemistry is its ability to model species that may be too unstable or short-lived to be studied experimentally. Theoritically, it is therefore amenable to study transition states, stabilize them and even increase the reaction rate through a theoretical modification of the structure.

5.5.1 Determination of transition states

Ab initio methods are also well suited to the calculation of the structures of transition states which are characterized by saddle points on the potential energy surface [2]. Although

there are new techniques such as femtosecond pulse laser spectroscopy to help in experimentally predicting transition states they are still limited to specific systems [28]. Therefore the whole process of transition state modelling still relies mainly on computational methods. The search for the potential minima and saddle points can be very efficient if one can calculate derivatives of the energy with respect to changes in geometry. In order to locate maxima (transition states), it is necessary to have fairly accurate initial geometries and matrices of the second derivatives of the energy (e.g. Hessian matrix). The reason for that is because a typical optimization algorithm does a crude guess of the initial solution to the wavefunction of the molecule under investigation. The optimization algorithm then starts a series of iterations to solve the wavefunction. If the initial structure is too far away from the correct transition state, then the initial guess will not locate the correct wavefunction of the specific transition, leading to the wrong solution.

In order to obtain a transition state, it is important to know which parameters represent the reaction coordinates involved in the transition. A program for modelling structures between reactant and product could be used to perform a linear search for the lowest maximum on the energy surface and for this purpose a SCAN job was performed as discussed above. This enables the determination of a suitable starting geometry and a subsequent full TS optimization. A SCAN calculation is a convenient method to obtain an approximate starting structure for a specific transition state at the top of a maximum on the potential energy curve. The SCAN job increases/decreases the bond length, angle and dihedral angle in a stepwise manner. In each step of a SCAN calculation the molecule is optimized while only constraining the specified parameters. The approximate starting structure is then manually extracted and used in a normal non-constrained transition state optimization. A frequency calculation is performed to confirm that the structure obtained is really a transition state and to determine the number of imaginary frequencies. Imaginary frequencies are found in the output file as negative eigenvalues. For a transition state only one imaginary frequency (negative eigenvalue) is accepted, since it is a first-order saddle point.

There are other methods being developed for transition state optimizations. Another manual method (for experienced computational chemists) involves guessing the starting structure of a transition state and performing a full unrestricted transition search (optimization) for it. The course of the movement of atoms during the first part of the

optimization then determines the changes that can be made in order to get a better starting structure. This approach could be faster; however, it requires experience and understanding of the reaction coordinates of a transition state for a specific system. Once a transition state (TS) is located it is important to verify that it is connecting the reactants to products by inspecting the atomic motion of the atoms associated with the negative eigenvalue. An important method that can be useful for proving the correctness of a transition state structure is by using the *intrinsic reaction coordinate* (IRC) method to find the *minimum energy path* (MEP) from the TS to the local minimum. The intrinsic reaction coordinate is defined as the path that would be traced by a classical particle sliding with infinitesimal velocity from the transition structure to the minima corresponding to reactants or products. If one uses Cartesian coordinates the intrinsic reaction coordinate is the path of steepest descent. The intrinsic reaction coordinate can be calculated by taking small steps in the direction of steepest descent. At the saddle point the IRC coincides with the transition vector (i.e. the eigen-vector corresponding to the negative eigenvalue of the Hessian matrix) [29].

In this study an input file for the optimization of the transition state structure was based on a simplified diene complex generated by using the "SCAN" function in Gaussian 98. Hence *ab initio* calculations were carried out by using the Gaussian 98 computer program at the restricted HF level of theory in order to determine the relative stabilities and structures of the 2-EHMC dimers. A variety of starting structures including both the isomers and dimers of 2-EHMC were employed. The calculations were carried out on both singlet and triplet states.

REFERENCES

1. Jensen, F., *Introduction to computational chemistry*. 1999: John Wiley and Sons, U.K. pp 1-5.
2. Cramer, C.J., *Essentials of computational chemistry*. *Theories and Models.* 2004,. John Wiley and Sons, U.K. pp.7-10.
3. Hinchliffe, A., *Chemical modelling from atoms to liquids*, Chechester, England: John Wiley and Sons Ltd. pp 171-175.
4. Atkins, P., de Paula, J., *Elements of physical chemistry*. 1992: W.H. Freeman and Company. pp 371-374.
5. Hehre, W.J., Radom, L., Schleyer, P.V., Pople, J.A., *Ab initio Molecular Orbital Theory*. 1986: John Wiley and Sons, U.S.A, pp 105-110.
6. Hirst, D.M., *A computational approach to chemistry*. 1990, Oxford, London: Blackwell Scientific Publications. pp.12-15.
7. Atkins, P.W., *Physical Chemistry*. 6th ed. 1998, Oxford University Press. pp 362-367.
8. Foresman, J.B., Frisch, A., *Exploring Chemistry with Electronic Structure Methods*. 2nd ed. 1996, Pittsburg, PA: Gaussian, Inc. pp 1-10.
9. Levine, I.N., *Quantum chemistry*. 3rd ed. 1983, Boston Allyn and Bacon. pp.24-27.
10. Duan, Y., Kollman, P.A., *Pathways to a protein folding intermediate observed in a 1-microsecond simulation in aqueous solution.* Science, 1998, **282**, 740-744.
11. Alves, C.N., Camilo, F.F., Gruber, J., da Silva, A.B.F, *A density functional theory study on the molecular mechanism of the cycloaddition between (E)- methyl cinnamate and cyclopendantadiene.* Chemical Physics, 2004, **306**, 35-41.
12. Engler, E.M., Andose, J.D., von R.Schleyer, P., *Critical Evaluation of Molecular Mechanics.* Journal of American Chemical Society, 1973, **95**, 8005-8025.
13. Hobza, P., Sponer, J., *Structure, energetics, and dynamics of the nucleic acid base pairs: nonempirical ab initio calculations*. Chemical Reviews, 1999, **99**, 3247-3276.
14. Bartlett, R.J., *Coupled-cluster approach to molecular structure and spectra: A step toward predictive quantum chemistry.* Journal of Physical Chemistry, 1989, **93**, 1697-1708.
15. HyperChem computational chemistry, Hypercube, Inc., Canada 1996. pp 36-37.
16. Young, D., *Computational Chemistry: A practical Guide for Applying Techniques to real World Problem*. 2001, New York: Wiley-Interscience. pp 10-20.

17. Dewar, J.S., *A new general purpose quantum mechanical molecular model.* Journal of American Chemical Society, 1985, **107**, 3902-3909.

18. Stewart, J.J.P., *Reply to "Comments on a comparison of AM1 with the recently developed PM3 method"* Journal of Computational. Chemistry, 1990, **11**, 543-544.

19. Stewart, J.J.P., *Optimization of parameters for semiempirical methods. III Extension of PM3 to Be, Mg, Zn, Ga, Ge, As, Se, Cd, In, Sn, Sb, Te, Hg, Tl, Pb, and Bi.,* Journal of .Computational .Chemistry, 1991, **12**, 320-341-.

20. Frisch, M.J., Trucks, G.W., Schlegel, H.B., Scuseria, G.E., Robb, M.A., Montgomery, J.A.Jr., Vrenen, T., Kudin, K.N., Burrant, J.C., Millam, J.M., Iyengar, S.S., Tomasi, J., Barone, V., Mennucci, B., Cossi, M., Scalmani, G., Rega, N., Petersson, G.A., Nakatsuji, H., Hada, M., Ehara, M., Toyota, K., Fukuda, R., Hasegawa, J., Ishida, M., T. Nakijima, T., Honda, M., Kitao, O., Nakai, H., Klene, M., Li, X., Knox, J.E., Hratchian, H.P., Cross, J.B., Bakken, V., Adamo, C., Jaramillo, J., Gomperts, R., Stratmann, R.E., Yazyev, O., Austin, A.J., Cammi, R., Pomelli, C., Ochterski, J.W., Ayala, P.Y., Morokuma, K., Salvador, A., Dannenberg, J.J., Zakrzewski, V.G., Dapprich, S., Daniels, A.D., Strain, M.C., Farkas, O., Malick, D.K., Rabuck, A.D., Raghavachari, K., Foresman, J.B., Ortiz, J.V., Cui, Q., Baboul, A.G., Clifford, S., Cioslowski, J., Stefanov,B.B., Liu, G., Liashenko, A., Piskorz, P., Komaromi, I., Martin, R.L., Fox, D.J., Keith, T., Al-Laham, M.A., Peng, C.Y., Nanayakkara, A., Challacombe, M., Gill,P.M.W., Johnson, B., Chen, W., Wong, M.W., Gonzalez, C., Pople. J.A., *Gaussian 03, Revision C.02*. 2004, Wallingford CT, Gaussian.Inc.

21. Seminario, J.M., Politzer, P *Modern density functional theory: A tool for chemistry*. 1998, Amsterdam: Elsevier Science. pp 11-15

22. Hohenberg, P., Kohn, W., *Inhomogeneous Electron Gas.* Physical Review B, 1964, **136,** 864-866.

23. Hehre, W.J., *A Guide to Molecular Mechanics and Quantum Chemical Calculations*. 2003, Irvine, Wavefunction, Inc. pp 458-460.

24. Becke, A.D., *Density-functional thermochemistry III. The role of exact exchange.* Chemical Physics, 1993, **98**, 5648-5652.

25. Lee, C.K., Yang, G., Parr, G., *Development of the Colle-Salvetti correlation-energy formula into a functional of the electron density*. Physical Review B, 1988, **37**, 785-789.

26. Levine, I.N., *Physical Chemistry*. 5th ed. 2002, New York: McGraw-Hill. pp 714-718.

27. Pietro, W.J., Levi, B.A., Henhre, W.J., Stewart, R.F, *Molecular Orbital theory of the properties of inorganic and organometallic compounds. 1. STO-NG Basis sets for third-row Main-Group Elements.* Inorganic Chemistry, 1980, **19**, 2225-2229.

28. Peitro, W.J., Henhre, W.J. *Molecular orbital theory of the properties of inorganic and organometallic compounds. 3. STO-3G basis sets for first- and second-row transition metals* Journal of Computational Chemistry, 1983, **4**, 241-251.

29. Garrett, B.C., Redmon, M.J., Stackler, R., Truhlar, D.G., Baldridge, K.K., Bartol, D., Schmidt, M.W., Gordon, M.S., *Algorithms and accuracy requirements for computing reaction paths by the method of steepest descent*, Journal of Physical Chemistry, 1988, **92**, 1476-1488.

CHAPTER 6

A computational study of the photodimerisation of 2-ethylhexyl-*p*-methoxycinnamate

Walyambillah Waudo, Bice S. Martincigh and H. Gert Kruger

School of Chemistry, University of KwaZulu-Natal, Westville Campus, Private Bag X54001, Durban, 4000, Republic of South Africa

Abstract

Theoretical studies using computational methods have been carried out to determine the lowest energy geometrical structures of some of the photoproducts generated via the photodimerisation of 2-ethylhexyl-*p*-methoxycinnamate and hence their relative stabilities. *Ab initio* molecular orbital calculations have been used to investigate the structures and the transition states of the various dimers resulting from the cycloaddition reactions. Geometry optimizations and energy calculations were performed with the Gaussian 98 program, using the B3LYP density functional and 6-31+G(d) basis set. GaussView was used to visualize the transition state structures. The results show that the process of ultraviolet light-induced cyclodimerisation is through a stepwise mechanism via diradical intermediates. The photochemical reaction pathway involves the lowest excited singlet state of the different ethylene-ethylene molecular arrangements along the reaction coordinate. Due to spin inversion, a triplet radical is formed. The theoretical calculations predicted the most stable dimer forms result from isomers with a *trans-trans* configuration along the cyclobutane ring. These dimers are the most likely that were identified by HPLC analysis where only seven out of a possible thirteen dimers could be separated.

1. Introduction

The most commonly used ultraviolet B (UVB) sunscreen absorber is 2-ethylhexyl-*p*-methoxycinnamate (2-EHMC: Figure 74) which is commercially available as the *trans*-isomer [1]. It is classified as a UVB filter because it absorbs the shorter wavelengths (290-320 nm) of solar UV radiation most effectively, which are regarded as the most harmful to human skin [2, 3]. Therefore, its photochemical behaviour is of fundamental interest. Previous studies have shown that 2-EHMC is photoreactive at wavelengths above 300 nm and isomerizes to its *cis*-isomer [1, 4, 5]. Irradiation of 2-EHMC with a high-pressure mercury lamp and a combination of filters with maximum transmittance greater than 300 nm shows not only the formation of *trans*- and *cis*-isomers but also dimers through self-dimerisation (Figure 74) [1, 6].

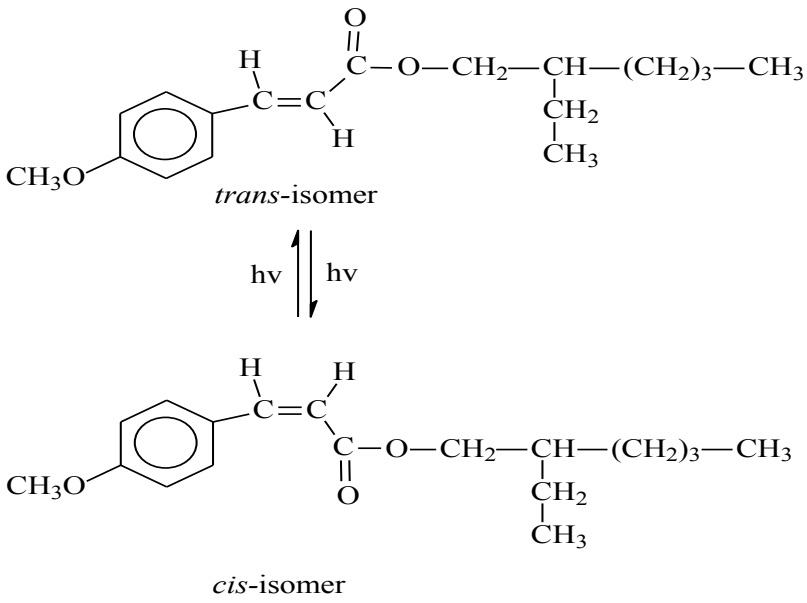

Figure 74 2-EHMC *trans-cis* isomerisation reaction.

When 2-EHMC dimerises 13 possible dimers can potentially form; probably via a [2+2]-cycloaddition reaction mechanism across the ethylenic double bond (as shown in Figure 75). The [2+2]-cycloadditions are concerted reactions that proceed via a cyclic transition state. All bond breaking and bond formation occurs simultaneously, and no intermediates are involved [7].

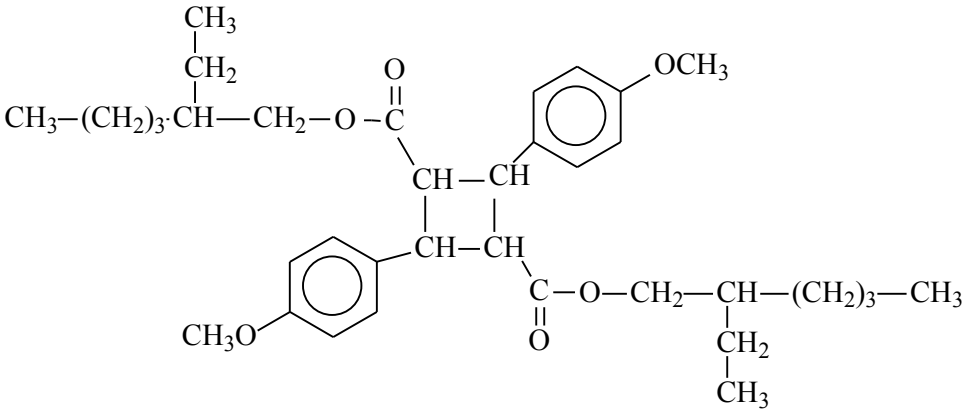

Figure 75 Chemical structure of the 2-EHMC dimer.

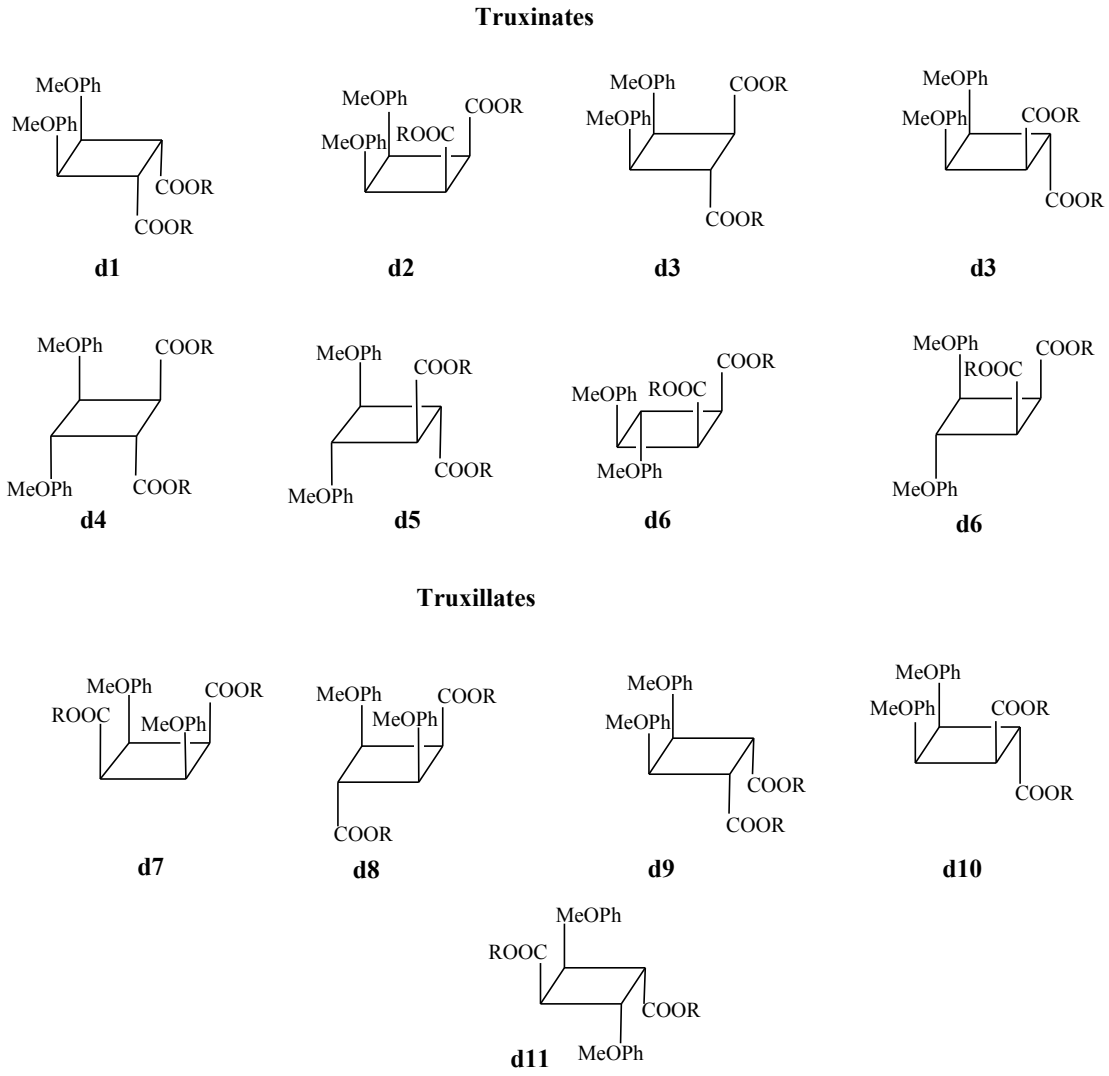

Figure 76 Possible isomeric structures of the 2-EHMC dimer adapted from Robinet *et al.* [12].

The photodimerisation of *trans*-2-EHMC can give rise to different stereoisomers/diastereoisomers that will depend on the spatial orientation of the groups attached to the ethylenic carbon-carbon double bonds. Both isomerisation and dimerisation of 2-EHMC reduce its ability of absorbing ultraviolet radiation [8, 9]. The loss of absorbance is an unfavourable condition as it reduces the actual efficacy of the sunscreen and hence offers less protection to human skin [10, 11].

A high performance liquid chromatographic investigation of the photodimerisation of 2-EHMC has shown the formation of at least seven dimers. As only very small quantities of the dimers of 2-EHMC can be isolated it is very difficult to determine their stereochemistry exclusively by spectroscopic means such as infrared (IR) and nuclear magnetic resonance (NMR) spectroscopy. Therefore, the aim of this work was to gain some understanding of the stereochemistry of these dimers that are formed upon irradiation of 2-EHMC. In addition, the mechanism of this reaction was investigated by using *ab initio* theoretical methods.

Studies by quantum-chemical calculations can provide valuable information about the nature of the transition states and metastable intermediates which cannot be readily characterised by experimental techniques [13]. Such information, as well as details of the thermodynamics and the kinetics of the reaction, thereby allows direct insight into reactions mechanisms providing data that are complementary to and consistent with available experimental results.

No theoretical studies dealing explicitly with the photodimerisation of 2-EHMC have been reported. Therefore a systematic *ab initio* quantum-chemical investigation of the mechanism of the photodimerisation of 2-EHMC when exposed to UV radiation was carried out. A general mechanism could explain the formation of the various dimers and possibly their stereochemistry. Furthermore, a careful theoretical study would give answers to a number of concrete questions. For example:

- Is the formation of the dimers through a stepwise or concerted reaction mechanism?
- What determines the orientation of the substituents on the cyclobutane ring?
- Does the mechanism follow a triplet or singlet transition state?
- What reaction step requires high temperatures to occur, i.e. which is the pathway that is energetically or thermodynamically favourable for the reaction sequence?

- What are the transition states or intermediates that are preferred? That is, how do the geometries of the various intermediates fit into the mechanism?
- The influence of stereochemistry and substitution pattern at the cyclobutane motif on the reactivity.

Beyond these mechanistic questions, 2-EHMC dimers are interesting structures in that they reduce the overall efficacy of *trans*-2-EHMC which is an active ingredient in sunscreen products. Spectral analysis of the dimers does show that they absorb in the UVC region of the UV spectrum which is compatible with the non-conjugated benzene nucleus [14]. It has been proposed that products resulting from the cycloaddition of two cinnamate molecules using double bonds effectively cancel the conjugation responsible for the absorption of the cinnamates [15].

The aim of this work was to develop a model, which would include, as far as possible, all species and reactions of 2-EHMC. The procedure adopted was to consider a simplified molecular model (Figure 77) that would exhibit as close as possible the chemistry of *trans*- and *cis*-2-EHMC isomers. A computational model was used to determine the relative energies of the reactants, transition states, intermediates and products. A simplified model has the benefits of using less computer time and resources. Hence, the purpose of this is to present computations for a model system and thus provide a general basis for future mechanistic discussion and rationalisation of the experimental work.

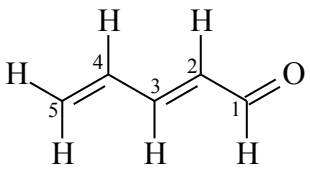

Figure 77 A simplified molecular model for 2-EHMC.

1.1 A proposed reaction mechanism

Figure 78 shows a proposed mechanism for the photodimerisation of 2-EHMC. This mechanism is proposed based on what is known about such reactions from literature [16, 17]. The mechanism accounts for the important intermediates and the reaction steps

anticipated. It starts with the reactants that may form a precomplex. This unsaturated complex can further rearrange through the transition state which eventually forms the product. During the [2 + 2]-cycloaddition photodimerisation reaction, the topochemical principle predicts that a reaction occurs if the reacting double bonds are parallel to each other and their distance in the crystal lattice is less than 4.2 Å [18]. The photodimerisation of cinnamic acids is one of the classical examples of a topologically controlled reaction [19].

The first step of this [2 + 2]-cycloaddition corresponds to the nucleophilic attack of C2 of one monomer to C2′ of the second monomer with the formation of the corresponding intermediate. The second step involves the ring closure of these intermediates to give the final cycloadducts, achieved by the nucleophilic attack of C3 of one monomer to the C3′ position of the second monomer.

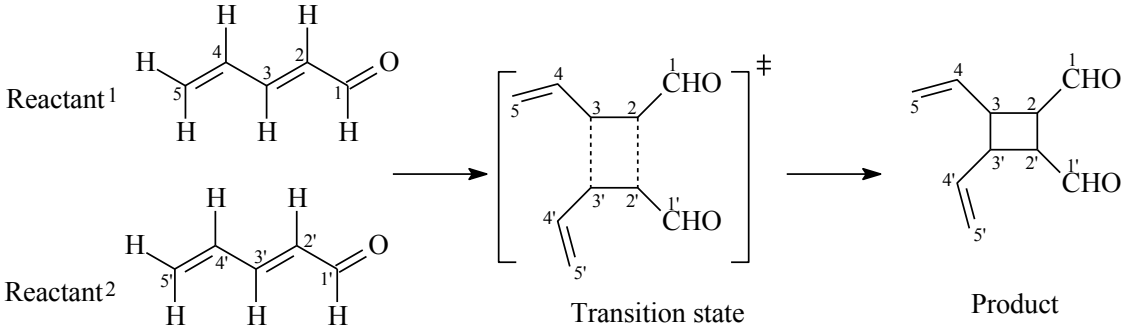

Figure 78 A proposed reaction mechanism for the photodimerisation reaction.

In the present study the proposed mechanism in Figure 78 was systematically investigated with the help of *ab initio* quantum chemical techniques. Both the singlet and triplet potential energy surfaces were studied.

As a first step, the stable conformers of the postulated intermediates were determined and confirmed as true minima on the potential energy surface by means of PM3 calculations. In the second part of the work, the transition states between the energy minima were located and characterised by vibrational frequency calculations of their energies. In this way, a complete reaction profile for the proposed mechanism could be obtained that allows for conclusions about the preferred reaction pathways and the rate- determining steps.

A main characteristic of the present work is a systematic and unbiased approach. For each intermediate all theoretically reasonable conformations were considered in the geometry optimizations. *Ab initio* and density functional theory (DFT) levels of calculations were performed to gain a better understanding of the correlation between the experimental and theoretical results. A systematic DFT study through the localisation of stationary points (reactants, transition structures (TS) and products) was carried out on the molecular model (Figures 79 and 80).

Figure 79 A structure of the working model for the 2-EHMC isomer obtained with the BLYP and 6-31G basis set. The Cartesian coordinates of all optimized structures are available on CD as supplementary material.

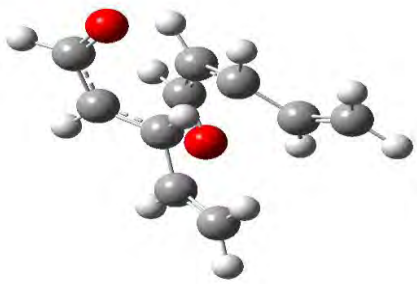

Figure 80 A structure of the transition state model for the 2-EHMC dimer obtained with the BLYP and 6-31G basis set.

Figure 81 is a schematic pathway for the photodimerisation of the simplified proposed model.

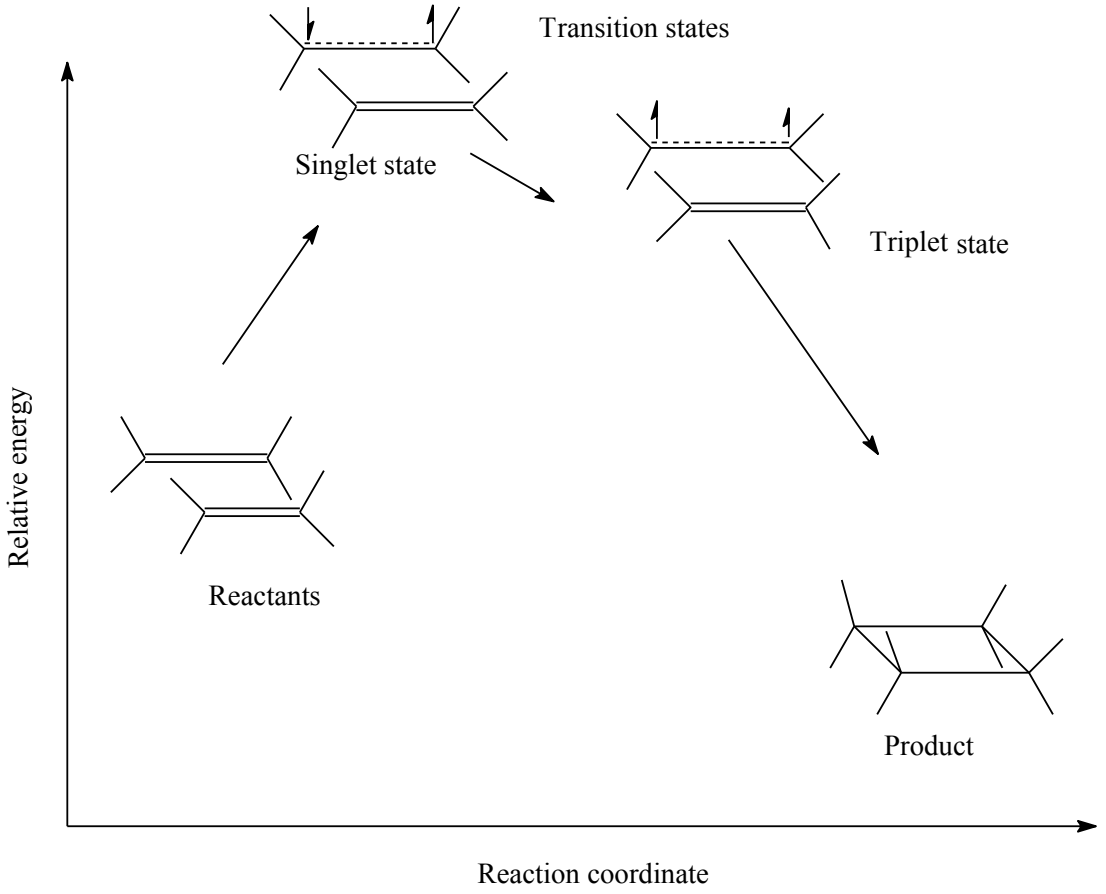

Figure 81 A proposed schematic reaction pathway for the photodimerisation of the molecular model of 2-EHMC as shown in Figure 79.

A singlet transition is initially formed because the electrons are still spin paired. This then undergoes intersystem crossing to a triplet state where now the electron spins are unpaired. The triplet state loses some energy to a form a product (cyclobutane ring adduct).

2. Computational details

The theoretical studies involved two sets of calculations. First, the B3LYP hybrid functional in conjunction with the split valence 6-31G(d) basis set was used to obtain the optimised geometries of the monomers of 2-EHMC. Secondly, frequency calculations were performed at the same level of theory to ensure that the systems represent true minima on

the potential energy surfaces. An *ab initio* study was performed on a series of the thirteen theoretical possible 2-EHMC dimers. Semi-empirical calculations using PM3 were also carried out for comparison with the *ab initio* results. All the calculations were performed by using the Gaussian 98 computer program, implemented on a Unix workstation.

Starting geometries of the dimers were drawn with the Gaussian 98 program and then converted to Gaussian input files. Before running a Gaussian job, the program had to be provided with input. The input section to the Gaussian program consists of the molecular charge and the spin multiplicity, the symbols of the constituent atoms and a definition of the molecular structure, either in the form of Cartesian coordinates or the Z-matrix notation which defines the molecular geometry in terms of bond lengths, bond angles and dihedral angles. It is also very important that the task to be performed, i.e. whether a single-point energy calculation, geometry optimisation or frequency calculation, is specified together with the appropriate basis set and the level of theory.

Precaution was taken to ensure that a low energy conformation for molecules was obtained as a starting structure for the *ab initio* calculations. This was done by manual rotation of side chain dihedral angles, or by a molecular dynamics investigation using a force field method. Geometry optimisations and energy calculations were first performed with PM3 and RHF/6-31+G(d). Geometry optimisations were then performed without restrictions by using B3LYP/6-31+G(d) so as to find the lowest energy structures for the reactants, intermediates, transition states and products.

2.1 Energy optimisation of structures

A full geometry optimisation for each of the thirteen dimer products was performed and their relative energies were calculated. During an optimisation of a structure the following basic mathematical procedure was performed by the computational program. Firstly, the software performed a rough guess (normally at the semi-empirical level of theory) of the solution of the wavefunction associated with the geometry of the input structure. The direction of the steepest descent on the energy surface, its largest energy gradient, was selected, and the bond lengths and angles were changed by an automatic mathematical

algorithm so as to precede one short step down the energy gradient. All the atoms of the molecule were "moved" by the mathematical algorithm so as to obtain the lowest energy position for the specific position of the molecule on the energy surface associated with the specific wavefunction. The mathematical procedure was repeated again and a new lowest energy geometry and energy gradient were found. The entire process was repeated until the energy differences between two calculations were reduced to some predetermined limit. The final geometry was said to have been optimised with respect to the geometry/energy and represents the best molecular parameters that could be obtained from that basis set. The same basic mathematical optimisation algorithm was used for molecular mechanics, semi-empirical and *ab initio* calculations. Gaussian 98 performed the optimisation, initialised by the OPT [20] keyword, of reactants and products using redundant internal coordinates.

The same basic algorithm was also utilised for a transition state optimisation, except that the algorithm was changed to search for a maximum on the energy surface and not a minimum. Some advanced methods were also available which made use of the negative eigenvalues (following them to find a maximum) associated with the wavefunction/transition state. Any transition state is associated with one negative eigenvalue only. The movement of atoms associated with the transition should correlate with the expected transition (i.e. bond breaking/formation, etc.). When the movement of atoms is complicated and it is unclear if the movement of atoms is associated with the specific transition, an intrinsic reaction coordinate (IRC) calculation should be performed to show that the reactants and products are indeed connected through the specific transition.

2.2 Transition-structure modelling of the cinnamates using ab initio methods

In this case an input file for the optimisation of the transition structure based on the simplified diene complex shown in Figure 82 was generated by using the "SCAN" function in Gaussian 98.

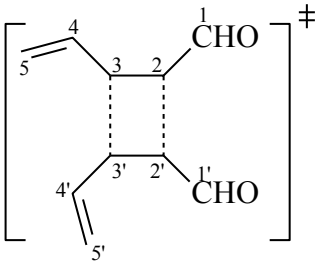

Figure 82 A schematic molecular model of the transition structure as obtained with the BLYP and 6-31G basis set as seen in Figure 79.

Hence, *ab initio* calculations were first carried out by using the Gaussian 98 computer program at the restricted Hartree-Fock level of theory in order to determine the relative stabilities and structures of the dimers. A variety of starting structures including both the isomers and dimers of 2-EHMC were employed. The calculations were carried out on both singlet and triplet states. *Ab initio* molecular orbital calculations were also used to investigate the structures of the transition states of 2-EHMC. *Ab initio* calculations are well suited for the calculation of transition states which are saddle points on the potential energy surface [21].

3 Results and Discussion

In an effort to better understand the mechanism of the photodimerisation of 2-EHMC, we have performed theoretical *ab initio* calculations on model structures possessing different substitution patterns and stereochemistries at the cyclobutane ring. Most calculations were performed by using DFT with B3LYP hybrid functional and the 6-31G(d) basis set. The geometries of all the 2-EHMC dimers and the monomer isomers together with their corresponding energies were optimised. Initially PM3, RHF/3-21+G and RHF/6-31+G(d) were used for geometry optimisations and energy calculations. These results are presented in Table 19. The reactants which had a *cis-cis* configuration along the cyclobutane gave the most stable dimers. The *cis*-isomer is less stable than the *trans* hence it is more reactive. Although the formation of the dimers is a kinetic process, it is possible that not all are thermodynamically stable.

Table 19 The relative energies of the optimized structures of the dimeric products and reactant monomers to that of their respective non-optimized structures.

Reactants Monomers		Product dimer[a]	Optimized energies [b]/kJ mol^{-1} Basis set		
			PM3	RHF/3-21+G	RHF/6-31+G
trans	*trans*	d1(tt)	-55.495	2.936	84.084
cis	*cis*	d2(cc)	-11.108	40.326	124.154
cis	*trans*	d3(ct)	-68.529	-47.545	36.824
cis	*cis*	d4(cc)	-109.482	-136.097	-49.877
trans	*trans*	d5(tt)	-91.792	-55.189	8.954
cis	*trans*	d6(ct)	-84.377	-94.663	-27.944
cis	*trans*	d7(ct)	-84.223	-36.114	41.513
cis	*trans*	d8(ct)	-52.644	-13.891	61.737
cis	*cis*	d9(cc)	-43.744	-21.827	67.611
trans	*trans*	d10(tt)	-101.039	-120.927	-38.433
trans	*trans*	d11(tt)	-76.837	-11.099	57.863
trans-isomer			-0.794	-2694.411	-2708.059
cis-isomer			-0.795	-2694.353	-2708

[a] Nomenclature as depicted in Figure 76.
[b] Approximate heat of formation $\Delta H_f = E_{product} - E_{reactant}$

It was clear that the semi-empirical calculations, although much quicker, produced results that were inconsistent. This prompted the use of the density functional B3LYP/6-31+G which was found more suitable to our system (see Section 3.2).

3.1 The transition structures (TS)

There were no concerted TS that could be obtained. This was for singlet states as well as for triplet states. Therefore, the only TS obtained, as discussed below, for this system was a stepwise triplet state. It was not specified which of the two reactants were to be triplet states, it was left for the calculation to determine that using its optimisation algorithms.

A relaxed scan was carried out between atom 2 and atom 2′ (see Figure 83). The conformational searching was performed by systematically varying the distances (e.g. by 0.05A) between atoms 2 and 2′ with energy minimization at each step. The energy was plotted as a result of the change in reaction coordinate. The energy profile of this relaxed scan gave a maximum at about 2.313 Å (see Figure 84).

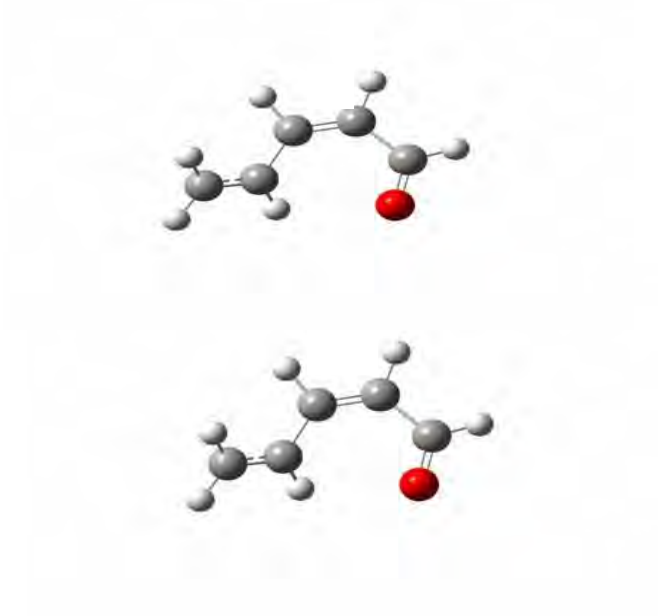

Figure 83 The reactants that were used for the transition state.

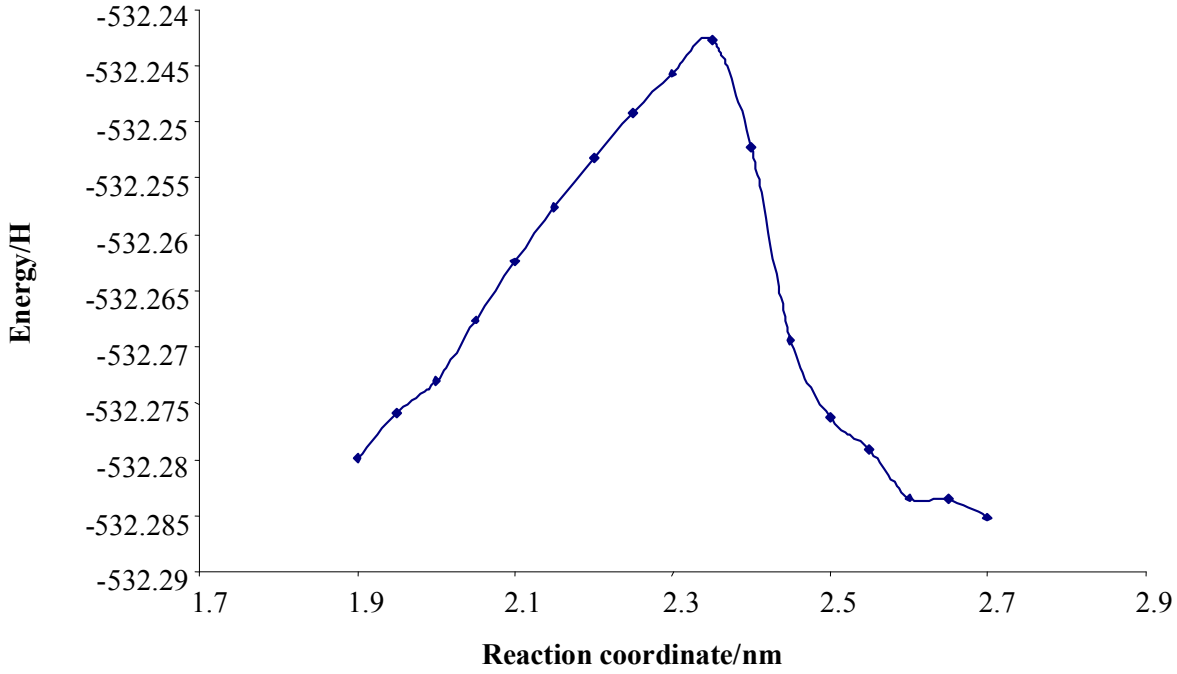

Figure 84 A plot of the energy obtained after each SCAN calculation for different bond lengths between the two molecules during a search for an optimum transition state.

The structure closest to the maximum on the energy profile was manually extracted and used as the input file for a transition state optimisation, followed by a frequency calculation. It is possible that the formations of two cyclic products are associated with each pair of reactants; depending on the relative orientation of the reactants (i.e. whether it is either *trans* or *cis* at the ethylenic bond). Figure 85 shows the position of the carbons at the ethylenic bond. An initial bond can form between C2 and C2′ as the first transition state (TS 1). It is equally possible to have a bond formation between C3 and C3′ as another second transition state (TS 2).Therefore, depending on the substituents on those carbons one could end up with different geometrical products.

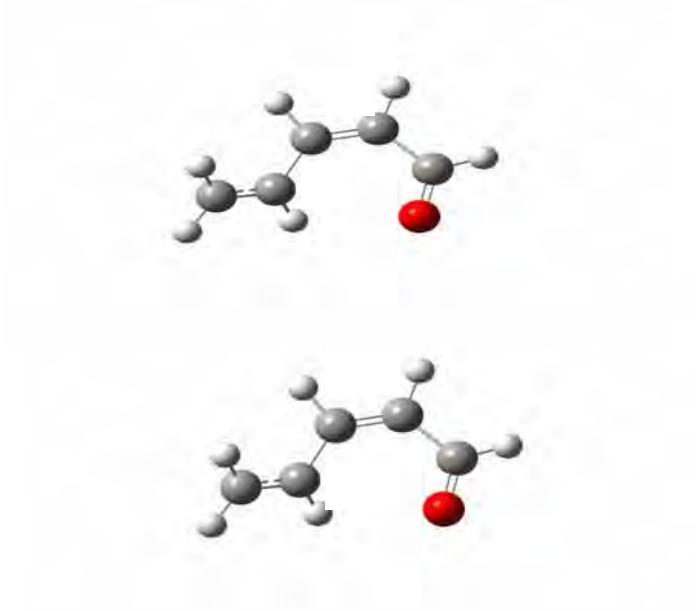

Figure 85 The reactants showing the positions of the carbons at the cyclobutane ring.

During a relaxed energy SCAN between the reaction coordinates of the proposed second (2^{nd}) TS for the triplet state, it was found that a maximum was not observed (see Figure 86). This observation was confirmed by a normal optimisation of a starting structure where the reaction coordinate of the first TS (triplet state with a transition state "bond" length of ~2.3Å) was manually reduced to approximately 1.8 Å (after inversion of the one radical electron to produce a singlet state molecule). The structure was then optimised as a singlet structure by using the normal optimisation algorithm (finding a minimum on the energy surface). The structure collapsed to the product without any delay. One should take into consideration that most optimisation algorithms are sensitive enough to be trapped in local maxima or minima and that the result mentioned above is sufficient proof that no maxima exist between the second transition state (TS 2) and the product.

Table 20 Calculated SCAN energies for the second transition state for the proposed model.

Bond lengths/nm	Energies /H
2.4593	-538.583121
2.2593	-538.5957
2.0593	-538.61114
1.8593	-538.6283
1.6593	-538.64208
1.4593	-538.63672

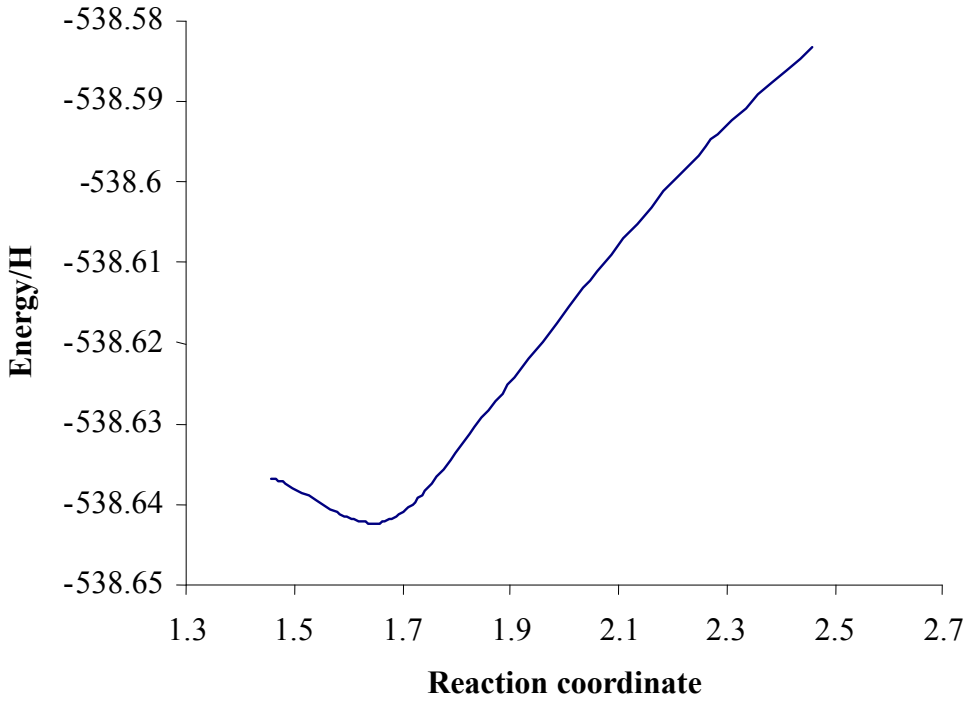

Figure 86 A search for the second transition state.

The proposed mechanism indicates cyclobutane ring formation through a stepwise radical mechanism. In this case, the initial step requires the homolytic cleavage of the double bond of one reactant to form a diradical. In the presence of sunlight, it is surmised there is enough energy to break the double bond, with formation of a single bond between the carbons. This diradical initially has the electron spins in the same direction forming a singlet intermediate. Then spin inversion is possible in which a triplet radical results. This intermediate radical is expected to be highly reactive, which results in rapid carbon-carbon bond formation. This reaction, which proceeds in a stepwise fashion via diradical intermediates, can be graphically represented as shown in the reaction profile given in Figure 81. The reaction profile shows the various stages which a reaction goes through whereby the molecule is a precomplex state of singlets before a spin inversion to a triplet state.

3.2 Energy calculations of the products

Ab initio molecular orbital calculations were performed on structures of reactants, transition states and products of the 2-EHMC model. These were done at the Hartree-Fock

level by using the Gaussian 98 program. The 3-21G and 6-31G basis sets were used. Although the 3-21G basis set produces inferior results in terms of structure accuracy and energy, it was initially used to get the starting stuctures. The starting structures were further optimised at the higher level of theory RHF/6-31+G (see Table 21 for the energies). However, the density functional B3LYP/6-31+G(d) was found more suitable for our system. The most stable dimers that can possibly form have a *trans-trans* configuration along the cyclobutane ring. This can be seen from the low energies, for example, of d1(tt), d2(tt) and d5(tt) except d6 (ct) which showed also a stable dimer. Those dimers that had *cis-cis* configuration gave relatively less stable products. This could be due to steric hindrance between the groups along the cyclobutane ring. Table 21 shows the relative energies calculated for the reactants, transition states and the products.

Table 21 Relative energies calculated for the various isomeric dimers and the reactants.

Dimer[a]	Relative energies[b] [B3LYP/6-31+G(d)] /(kJ mol^{-1})		
	Transition states		Product
	1[c]	1[d]	
d1 (tt)	152.013	152.013	-395.337
d2 (tt)	154.019	154.019	-393.337
d3 (ct)	184.619	184.619	-396.247
d4 (cc)	134.385	134.385	-375.821
d5 (tt)	171.137	171.137	-398.962
d6 (ct)	171.567	175.998	-395.337
d7 (ct)	185.576	185.576	-393.337
d8 (ct)	186.122	240.634	-396.247
d9 (cc)	177.273	177.273	-375.821
d10 (cc)	186.536	186.536	-375.886
d11 (tt)	160.235	215.344	-389.859
trans-isomer (t)	-	-	0
cis-isomer (c)	-	-	0.005

[a] Nomenclature as depicted in Figure 76
[b] Approximate heat of formation $\Delta H_f = E_{product} - E_{reactant}$
[c] First transition state
[d] Second transition states

Figure 87 is a graphic representation of the reaction profile of the reactants. Since the formation of dimers is a kinetic process, however it is possible that all are not thermodynamically stable.

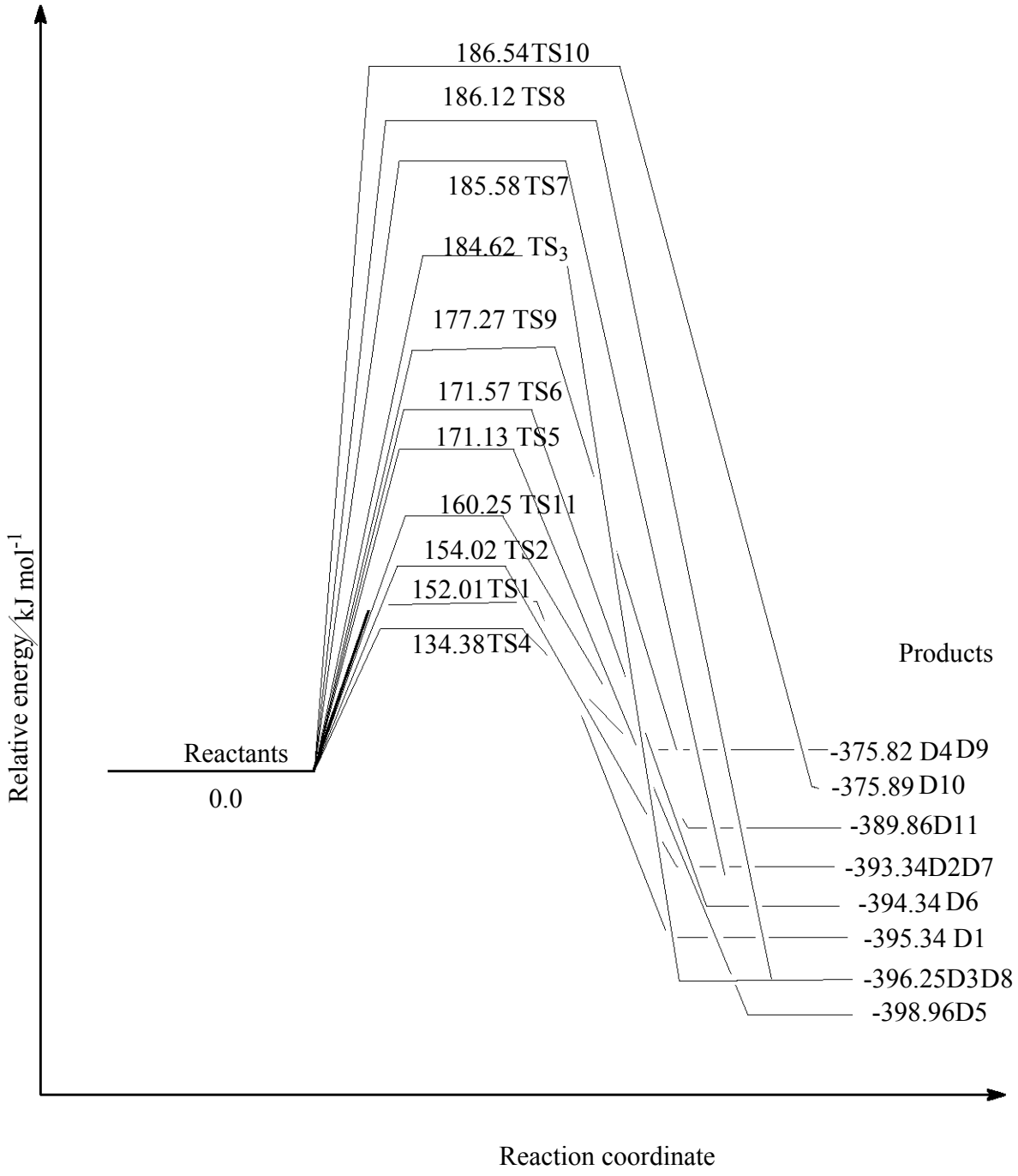

Figure 87 Reaction profiles for the formation of dimers D1 to D11.

4 Conclusions

Direct irradiation of *trans*-2-EHMC yields a mixture of photoproducts which include *cis*- and *trans*-isomers and dimers. Because of the difficulties in isolating the dimer photoproducts, investigations on the mechanism of formation and relative stabilities of the possible dimer structures were carried out by computational methods. Computational studies shed some light on the preferred most stable structures and possible reaction mechanism.

Although the formation of the products is a kinetic process, it is possible that not all are thermodynamically stable. This could be the reason why only seven dimers out of a possible eleven were seen in the HPLC analysis. The most stable dimers that can possibly form have a *trans-trans* configuration along the cyclobutane ring.

- The photochemical reaction pathway involves the lowest excited singlet state of the different ethylene-ethylene molecular arrangements along the reaction coordinate. Due to spin inversion, a triplet radical appears. It is from the triplet state that the final products form.
- This intermediate triplet radical is expected to be highly reactive which subsequently results in rapid closure with another radical. The biradical intermediate is the determinant in the formation of the product as exhibited by the energy of their formation. For example, d1(tt), d2(tt), and d5(tt) resulted in much more stable products.
- The *trans-trans* reactants gave more stable products as compared with *cis-cis* reactants. This is due to a conformation with the least steric hindrance.
- The results provide valuable insight into a process of ultraviolet light-induced cyclodimerisation through a stepwise mechanism via diradical intermediates. This is supported by the fact that no concerted transition state could be determined for either singlet or triplet states.

In summary, the theoretical studies have provided many interesting results on geometries, energies and other properties of these model systems. The results can either be used directly in combination with experimental approaches such as NMR spectroscopy, for

example, or they can lead to a better understanding of the underlying principles of 2-EHMC structures. A challenge for future quantum-chemical studies is the treatment of larger molecular systems. The results presented are sufficient to show that the computation procedure gives consistent results comparable with the experimental ones. The HPLC analysis showed only seven dimers from a possible eleven. It can be argued that these are the ones that are thermodynamically possible since they have the lowest energies of formation.

REFERENCES

1. Broadbent, J.K., Martincigh, B.S., Raynor, M. W., Salter, L.F., Moulder, R., Sjoberg, P., Markides, K.E., *Capillary supercritical fluid chromatography combined with atmospheric pressure chemical ionisation mass spectrometry for the investigation of photoproduct formation in the sunscreen absorber 2-ethylhexyl-p-methoxycinnamate.* Journal of Chromatography A, 1996, **732,** (1), 101-110.
2. De Gruijl, F.R., *Skin cancer and solar UV radiation.* European Journal of Cancer, 1999, **35,** (14), 2003-2009.
3. Taylor, J.S., *DNA, Sunlight, and Skin cancer.* Symposium on Molecular Architecture, 1990, **67,** (10), 835-841.
4. Pattanaargson, S., Munhapol, T., Hirunsupachot, N., Luangthongaram, P., *Photoisomerization of octyl methoxycinnamate.* Journal of Photochemistry and Photobiology A: Chemistry, 2004, **161,** (2-3), 269-274.
5. Maier, H., Schauberger, G., Brunnhofer, K., Honigsmann, H., *Change of ultraviolet absorbance of sunscreens by exposure to solar-simulated radiation.* Journal of Investigative Dermatology, 2001, **117,** (2), 256-262.
6. Kowlaser, K., *Photoproduct formation in the irradiated sunscreen absorber 2-ethylhexyl-p-methoxycinnamate;* M.Sc Dissertation, University of Natal, Durban, South Africa, 1998.
7. Durbeej, B., Eriksson, L. A., *Reaction mechanism of thymine dimer formation in DNA induced by UV light.* Journal of Photochemistry and Photobiology A-Chemistry, 2002, **152,** (1-3), 95-101.
8. Broadbent, J.K., *Photochemical studies of sunscreen constituents;* M.Sc. Dissertation, University of Natal, Durban, South Africa, 1994.
9. Serpone, N., Salinaro, A., Emeline, A.V., Horikoshi, S., Hidaka, H., Zhao, J.C., *An in vitro systematic spectroscopic examination of the photostabilities of a random set of commercial sunscreen lotions and their chemical UVB/UVA active agents.* Photochemical and Photobiological Sciences, 2002, **1,** (12), 970-981.
10. Gasparro, F.P., Mitchnick, M., Nash, J.F., *A review of sunscreen safety and efficacy.* Photochemistry and Photobiology, 1998, **68,** (3), 243-256.
11. Morliere, P., Avice, O., Melo, T. S. E., Dubertret, L., Giraud, M., Santus, R., *A Study of the Photochemical Properties of Some Cinnamate Sunscreens by Steady-State and Laser Flash-Photolysis.* Photochemistry and Photobiology, 1982, **36,** (4), 395-399.

12. Robinet, G., Devillers, J., Debourayne, C., Riviere, M., Barthelat, M., *Photodimerization of Cinnamate Derivatives in Microemulsions - Investigation by Molecular Mechanics of the Conformations and Relative Energies of Some Isomers of the Methyl Cinnamate Dimer.* New Journal of Chemistry, 1987, **11,** (1), 51-59.
13. Jensen, F., *Introduction to computational chemistry*. 1999: John Wiley and sons, U.K. pp 1-5.
14. Huong, S.P., Andrieu, V., Reynier, J.P., Rocher, E., Fourneron, J.D., *The photoisomerization of the sunscreen ethylhexyl p-methoxy cinnamate and its influence on the sun protection factor.* Journal of Photochemistry and Photobiology A: Chemistry, 2007, **186,**(1), 65-70.
15. Schrader, A., Jakupovic, J., Baltes, W., *Photochemical studies on trans-3-methylbutyl 4-methoxycinnamate.* Journal of the Society of Cosmetic Chemists, 1994, **45**, 43-52.
16. Marchand, A.P., Power, T. D., Kruger, H. G., *Ab initio theoretical investigation of a formal alkene-enedione intramolecular [2+2] photocyclization.* Croatica Chemica Acta, 2001, **74,** (2), 265-270.
17. Woodward R.B., Hoffmann; R. *The Conservation of Orbital Symmetry*. 1970, Chemie, Weinheim Verlag. pp 25-30.
18. Cohen, M.D., Schmidt, G. M. J., *Topochemistry. Part 1. A survey.* Journal of Chemical Society, 1964, **2**, 1996 -2000.
19. Lewis, F.D., Quillen, S.L., Hale, P. D., Oxman, J.D., *Lewis acid catalysis of photochemical reactions. Photodimerization and cross-cycloaddition of cinnamic esters.* Journal of American Chemical Society, 1988, **110**, 1261 - 1267.
20. Foresman, J.B., Frisch, A., *Exploring Chemistry with Electronic Structure Methods*. Second ed. 1996, Pittsburg, PA: Gaussian, Inc. pp 1-10
21. Hehre, W.J., *A Guide to Molecular Mechanics and Quantum Chemical Calculations*. 2003, Irvine, Wavefunction, Inc., pp 458-460.

CHAPTER 7

Conclusions

Sunscreen products have become an integral part of our daily lives. They are no longer just for protection of the skin from sunburn but have found use in other personal care formulations including facial and body care products. A safe and effective sunscreen product is recognised as performing an even important role in protecting us from premature skin ageing and skin cancer. An ideal sunscreen should present a high photostability since the UV-induced decomposition may decrease its UV light absorption efficacy. The prevention of photodegradation would decrease the formation of potentially toxic photoproducts and their derivatives, thereby improving the safety of sunscreen formulations.

The photostability and the broad-spectrum protection of Australian commercial sunscreens have been assessed by using both chromatographic and spectroscopic methods. High performance liquid chromatography was used to identify and quantitate the active chemical ingredients. UV spectrophotometry was used to monitor the spectral absorbance before and after UV exposure of the preparations. All together 25 different sunscreen products currently available on the Australian market were investigated. This is among one of the few studies that have been carried out on off-the-shelf ready-to-use commercial products.

The results obtained in this investigation show that some of the photoactive chemical absorbers commonly being used in sunscreens are unstable upon UV radiation. It was noted that upon absorption of UV radiation some of the sunscreens showed formation of photoproducts as revealed by high performance liquid chromatography. This shows the importance of using complementary analytical techniques as one is able to monitor the changes in the UV filters and determine any photoproducts formed. The formation of photoproducts was mainly due to either photodegradation and/or photoisomerisation of the three chemical absorbers, 2-ethylhexyl-*p*-methoxycinnamate, avobenzone and 4-methylbenzylidene camphor. Also there were changes in the absorption of UVA/B radiation which implies a reduction in the expected photoprotection against deleterious

solar radiation. The loss is more noticeable in the UVA region where most of the sunscreens, especially those containing avobenzone in their formulation, were photounstable. Unfortunately, avobenzone is the most commonly used UVA absorber. The addition of other sunscreen absorbers in the formulation such as 4-methylbenzylidene camphor or octocrylene, which are thought to photostabilise avobenzone, did not prevent its photodegradation. As it has been shown in this study avobenzone is highly photounstable and therefore upon UV exposure the sunscreen loses its broad-spectrum protection. This has also been confirmed by critical wavelength and UVA/UVB ratio analyses. The loss of protection in the UVA region is a major concern as the consumer is exposed to more UVA radiation which is known to play a significant role in the induction of malignant melanoma skin cancer [1, 2]. All the sunscreens showed good photostability in the UVB range. This further showed that a mere complex filter combination was not a deterrent to the photoinactivation of the suncare products. In total eight of the twenty five of the assayed sunscreens were found to be photounstable.

The broad-spectrum protection of the sunscreens was assessed by two *in vitro* methods, namely: the critical wavelength and UVA/UVB ratio. While there was general agreement between the methods on the overall status of the sunscreen, it was observed that the UVA/UVB ratio would classify some of the sunscreens as being broad-spectrum protective even though they did not contain UVA absorbers. Eleven of the sunscreens out the twenty five gave broad-spectrum protection. This apparent anomaly could be due to the low threshold critical wavelength assigned by this system. This would call upon formulators to review and harmonise the two systems so that there is no ambiguity in interpretation of results.

All the sunscreens investigated contained 2-ethylhexyl-*p*-methoxycinnamate as a UVB absorber. Therefore, this study also involved an investigation of the photochemistry of 2-EHMC. Solutions of 2-EHMC in methanol were irradiated at wavelengths greater than 300 nm for different irradiation times and were analysed for the formation of photoproducts by various analytical techniques. UV-vis spectrophotometry was used to monitor the photostability of 2-EHMC. It was observed that 2-EHMC showed a loss in the absorbance with increasing irradiation time. This is in agreement with previous studies carried out by other researchers in our laboratory [3-5]. This decrease is due to the photoisomerisation reaction to the *cis*-isomer. A photostationary state was reached with a solution of 1×10^{-6}

M in which *trans*-2-EHMC was in excess of the *cis*-isomer. This is contrary to other studies that show the *cis*-isomer present in larger quantities than the *trans*-isomer at the photostationary state. For example, Broadbent [4], using 80% 2-EHMC showed *cis*-isomer to be in excess. This decrease in absorbance reduces the efficacy of *trans*-2-EHMC since the *cis*-isomer is a less efficient UVB absorber [6].

A pure *cis*-isomer was obtained by fraction collection on HPLC and its identity was confirmed by HPLC-MS, NMR and FTIR techniques. Spectral data were collected for the *cis*-isomer and used to determine its molar absorption coefficient (ε). A value of 1.805 x 10^4 dm^3 mol^{-1} cm^{-1} at 304 nm was obtained and this is lower than that of *trans*-2-EHMC which is 2.33 x 10^4 dm^3 mol^{-1} cm^{-1} at 311 nm in methanol [7]. The lower value therefore means that the *cis*-isomer is indeed a less efficient UVB absorber. The loss in absorbing efficiency is attributed to the photostationary equilibrium between the *trans*- and *cis*-isomers attained during the photoisomerisation process [8].

The formation of photoproducts upon UV irradiation of 2-EHMC was investigated for the different concentrations of *trans*-2-EHMC ranging from 1 x 10^{-6} M to pure 2-EHMC. The formation of several high molecular mass compounds, suspected to be dimers, was only detectable in solutions of 1 x 10^{-3} M or greater of irradiated 2-EHMC implying that the process is diffusion-controlled. Seven dimers were identified by HPLC although theoretically a possible thirteen dimers can form [9]. These results are consistent with other studies of the photochemical dimerisation of cinnamic acids and their esters [10, 11]. The dimers elute much later than the isomers. This is due to structural differences whereby the dimers have twice the molecular mass and size of the isomers. In addition, due the bulky ethylhexyl alkyl group, these dimers can be considered to be more hydrophobic and non-polar. It is therefore these structural characteristics that make them elute after the isomers on a reversed-phase column. This is consistent with reversed-phase HPLC in which non-polar compounds are expected to stay longer on the stationary phase and elute much later than polar compounds. The fractions of the photoproducts were collected by semi-preparative HPLC. However, due to the low yields of the dimers it was difficult to separate them successfully. The presence of these dimers was confirmed with HPLC-MS studies. However, it should be emphasized that photoisomerisation is the main photochemical process when solutions of 2-EHMC are irradiated with UV light. This phenomenon can be

observed by spectrophotometry or by HPLC but the determination of the UV spectrum of the *cis*-form is easier by coupling both methods.

An attempt to characterise the dimers was carried out by using FTIR and NMR. The NMR spectra did show the loss of the peaks associated with the ethylenic double bond present in the monomers. Due to the extremely low yields of the photoproducts the NMR results obtained were not adequate to characterise the dimers as either truxinates or truxillates. Hence, *ab initio* and density functional theory (DFT) level of calculations were performed to provide a better understanding between the experimental results and the theoretical ones. A systematic DFT study through the localization of stationary points for reactants, transition states (TS) and products was carried out on a simplified model of 2-EHMC. The formation of dimers depends on the orientation of the substituents on the cyclobutane ring. The *trans-trans* configuration along the cyclobutane ring gave relatively more stable products than the *cis-cis* configuration of the reactants. This is due to less steric hindrance. Although it is kinetically possible for all the dimers to form, they might not be thermodynamically stable. This could be the reason that we are able to see only seven dimers by HPLC analysis. The formation of the photoproducts is by a stepwise reaction mechanism via diradical intermediates rather than a concerted mechanism.

Despite the low yields, the presence of these photoproducts on the human skin would be of major concern. This would be an interesting area of future study to investigate the toxicological potency of these sunscreen filter substance degradation products with the aim of achieving a further improvement in cosmetic safety. It might be that the cyclobutane systems will not likely penetrate the skin due to their molecular size and conformation.

Presently there is no topical or systematic drug or treatment that is available that is capable of completely reversing chronic damage due to sunscreen exposure. Although the use of topical sunscreens can be an effective strategy for reducing the amount of ultraviolet exposure and sunburn, alternative preventive measures have been suggested. In this respect, campaigns promoting sun avoidance and sun protection have recently gained significant attention. However, some persons because of the nature of their work cannot avoid exposure to the sun. Others continue to expose their bodies to the sun for the aesthetic value of a golden tan. Therefore, preventive measures will remain for the near

future the mainstay of coping with the problem of photoageing as well as with the worldwide dramatic increase in the incidence of skin cancer.

One such approach to reduce UVB light-induced photodamages is through chemoprevention which by definition is a means of cancer control in which the occurrence of the disease can be entirely prevented, slowed or reversed by topical or oral administration of naturally occurring or synthetic compounds or their mixtures [12]. These chemopreventive compounds are known to be anti-mutagenic, anti-carcinogenic and non-toxic and have the ability to exert striking inhibitory effects on diverse cellular events associated with multistage carcinogenesis. Skin care products supplemented with botanicals, in conjunction with the use of sunscreens and educational efforts may be an effective approach for reducing UVA-generated ROS-mediated photodamage, inflammatory responses and skin cancers in humans. Because of the role of UVB in cutaneous damage, the agents that can protect against this radiation could be ideal photochemoprotective agents for the skin.

It is hoped that the knowledge gained through the studies of photoinduced reactions of the sunscreens, in turn, may be relevant to the solution of a number of pending problems such as the development of organic filters possessing unusual stability properties. This knowledge will enhance the capacity in the development of protective strategies against UV-induced skin damage. Although encapsulation techniques [13-15] are being used to stabilise sunscreen products none so far have been completely successful in preventing photodegradation. The strategy is to remove ingredients that are unstable and incorporate those that are known to improve photostability. Consequently, it is imperative that the consumer is provided with reliable information regarding the level of actual sun protection being provided by the product he or she is purchasing. This can be accomplished by continuing to standardise the current methods being used to determine the efficacy and photostability of sun care products.

REFERENCES

1. Wang, S.Q., Setlow, R.; Berwick, M., Polsky, D., Marghoob, A.A., Kopf, A.W., Bart, R. S., *Ultraviolet A and melanoma: A review.* Journal of the American Academy of Dermatology, 2001, **44,** (5), 837-846.
2. Setlow, R.B., Wookhead, A.D., Grist, E., *Animal model for UV-radiation induced melanoma: platyfish-swordtail hybrid.* Proceedings of the National Academy of Sciences of the United States of America, 1989, **86,** (22), 8922-8926.
3. Broadbent, J.K., Martincigh, B.S., Raynor, M.W., Salter, L.F., Moulder, R., Sjoberg, P., Markides, K.E., *Capillary supercritical fluid chromatography combined with atmospheric pressure chemical ionisation mass spectrometry for the investigation of photoproduct formation in the sunscreen absorber 2-ethylhexyl-p-methoxycinnamate.* Journal of Chromatography A, 1996, **732,** (1), 101-110.
4. Broadbent, J.K., *Photochemical studies of sunscreen constituents;* M.Sc. Dissertation, University of Natal, Durban, South Africa, 1994.
5. Ingouville, N.A., *The photochemical behaviour of the sunscreen absorber 2-ethylhexyl-p-methoxycinnamate;* M.Sc. Dissertation, University of Natal, Durban, 1995.
6. Martincigh, B.S., Allen, J.M., Allen, S.K., *Sunscreen: the molecule and their photochemistry, in: Sunscreen photobiology: cellular and physiological aspects*, ed. F.P. Gasparro. 1997: Springer-Verlag and Landes Bioscience. pp 11-45.
7. Lowe, N.J., Shaath, N.A., *Sunscreens: Development, Evaluation and Regulatory Aspects*, ed. N.A. Shaath. 1990, New York: Marcel Dekker, Inc. USA. pp 505-536.
8. Kowlaser, K., *Photoproduct formation in the irradiated sunscreen absorber 2-ethylhexyl-p-methoxycinnamate;* M.Sc. Dissertation, University of Natal, Durban, 1998.
9. Robinet, G., Devillers, J., Debourayne, C., Riviere, M., Barthelat, M., *Photodimerization of Cinnamate Derivatives in Microemulsions - Investigation by Molecular Mechanics of the Conformations and Relative Energies of Some Isomers of the Methyl Cinnamate Dimer.* New Journal of Chemistry, 1987, **11,** (1), 51-59.
10. Lewis, F.D., Quillen, S.L., Hale, P. D., Oxman, J.D., *Lewis acid catalysis of photochemical reactions. Photodimerization and cross-cycloaddition of cinnamic esters.* Journal of American Chemical Society, 1988, **110**, 1261-1267.
11. Egerton, P.L., Hyde, E.M., Trigg, J., Payne, A., Beynon, P., Mijovic, M.V., Reiser, A., *Photocycloaddition in Liquid Ethyl Cinnamate and in Ethyl Cinnamate Glasses - the*

Photoreaction as a Probe into the Micro-Morphology of the Solid. Journal of the American Chemical Society, 1981, **103,** (13), 3859-3863.

12. Afaq, F., Adhami, V.M., Mukhtar, H., *Photochemoprevention of ultraviolet B signaling and photocarcinogenesis.* Mutation Research-Fundamental and Molecular Mechanisms of Mutagenesis, 2005, **571,**(1-2), 153-173.
13. Perugini, P., Simeoni, S., Scalia, S., Genta, I., Modena, T., Conti, B., Pavanetto, F., *Effect of nanoparticle encapsulation on the photostability of the sunscreen agent, 2-ethylhexyl-p-methoxycinnamate.* International Journal of Pharmaceutics, 2002, **246,**(1-2), 37-45.
14. Scalia, S., Tursilli.,R., Iannuccelli, V.; *Complexation of the sunscreen agent, 4-methylbenzylidene camphor with cyclodextrins: Effect on photostability and human stratum corneum penetration.* Journal of Pharmaceutical and Biomedical Analysis 2007, **44**, 29–34.
15. Scalia, S.; Tursilli, R.; Bianchi, A.,Lo Nostro; P.; Bocci, E.; Ridi, F.; Baglioni, P. *Incorporation of the sunscreen agent, octyl methoxycinnamate in a cellulosic fabric grafted with -cyclodextrin.* International Journal of Pharmaceutics, 2006, **308** 155–159.

APPENDIX A

Materials

The chemicals used for the purposes of this study are listed below together with the manufacturers' names and where relevant, the grade of chemical.

A1 Chemicals used for the quantitation of UV filters by HPLC

Methanol (99.8%)	BDH HiperSolv^{TM} Chemicals, Ltd.
Acetonitrile (99.9%)	BDH HiperSolv^{TM} Chemicals, Ltd.
Tetrahydrofuran (99.8%)	Lab-Scan Analytical Sciences, Ltd.
Chloroform (99%)	Waters Division of HPLC Pvt, Ltd.
Dichloromethane (99%)	Saarchem
Isopropanol (99.5%)	Sigma-Aldrich
MBC	Merck
Benz-3	BASF
AVO	BASF
EHMC	BASF
PBSA	Merck
HS	Haamann & Reimer
OCT	BASF
OT	BASF

APPENDIX B

Equipment

All the equipment used during this study is listed below.

B1 Equipment for HPLC analysis

Equipment	Manufacturer
600 multisolvent delivery system	Waters
U6K Variable Injector	Waters
Autosampler Series 2000	Perkin-Elmer
600 Photodiode Array Detector	Waters
996 Photodiode Array Detector	Waters
7010 Rheodyne Injector	Waters
Pentium II 600 MHz Personal Computer	De′ Marc
APCCII Personal Computer	NEC
950C DeskJet printer	Hewlett Packard
Guard-Pak μ-Bondapak C_{18} precolumn insert	Waters
HPLC Columns: Spherisorb 5ODS(2)	Phenomenex
Ultracarb 5ODS(20)	Phenomenex
Nucleosil 100 C_{18} 250 x 4.6 mm	Grom Analytik
100 μl Airtight Syringe	Hamilton Company, Nevada, USA
Ultrasonic bath	Ultrasonic Manufacturing Company (UMC 20)
Milli-Q^{50} ultra pure water apparatus	Millipore
Durapore® 0.45 μm membrane filters	Millipore
Millex-LCR Hydrophilic PFTE 0.45 μm syringe filters	Millipore

B2 Irradiation Equipment

Equipment	Manufacturer
HBO 500 W high pressure mercury lamp	Osram
Powerpack for HBO lamp	Schrieber
500 mL Photochemical reactor vessel with 200 W medium pressure mercury lamp and powerpack	Hanovia
J-221 longwave UV intensity meter	Blak-Ray
10 mm thick pyrex filter	

B3 Equipment for UV-spectroscopy

Equipment	Manufacturer
Lambda 35 UV/Vis Spectrophotometer	Perkin-Elmer
Quartz Cells, 1 and 10 mm pathlength	Pecsa Analytical

B4 Equipment for IR-spectroscopy

15.011 ton manual hydraulic press	Specac
Impact 400D spectrophotometer	Nicolet
7440 Colour Pro plotter	Hewlett Packard

APPENDIX C

Calibration data

The tables below present the calibration data for all the active ingredients quantified in this study. The calibration curve for each active ingredient is presented in Appendix D.

Table C1: Calibration data for the determination of AVO.

[Conc] /mol dm^{-3}	3.24 x10^{-4}	2.43 x10^{-4}	1.62 x10^{-4}	8.11 x10^{-5}	4.06 x10^{-5}	2.03 x10^{-5}	1.01 x10^{-5}	5.07 x10^{-6}
Peak areas	119176546	90801865	56489202	36321490	12191197	6266153	3403214	2151413
	124496979	89499096	62661009	30389596	12215012	6281009	3338895	2173036
	119620317	90389516	57802918	33416213	12957746	6543803	3504065	2100281
	122764483	91990398	51998003	34394958	12975891	6304862	3394958	2179281
	119118332	85785198	56122919	34096774	12503044	6469043	3044405	2265496
	122957705	91125035	56904312	35186337	12577095	6458018	3343402	2198132
	114216875	91869225	58911687	33526437	12184503	6590120	3540650	2256465
	125030744	90296219	59146982	33923893	12048920	6578591	3495107	2204393
	122526437	91434014	58659465	34061082	12256465	6908018	3169213	2127407
Mean	121100935	90354507	57632944	33924087	12434430	6488846	3359323	2183989
STD	3399266	1888936	2875834	1601554	343176.4	201561.7	162576.6	54685.91
RSD/%	2.81	2.09	4.99	4.72	2.76	3.11	4.84	2.50

Table C2: Calibration data for the determination of 2-EHMC.

[Conc] /mol dm^{-3}	6.37 x10^{-4}	5.46 x10^{-4}	4.55 x10^{-4}	3.64 x10^{-4}	1.82 x10^{-4}	9.09 x10^{-5}	4.5 x10^{-5}	2.27 x10^{-5}
Peak areas	169792963	147564939	122332065	96609967	52242298	31571191	17567091	14764012
	168997631	147978959	123453821	99843553	53983248	32585125	18325405	14677109
	169659115	147887949	122875093	98791804	53908739	32714205	17622398	14790105
	166297182	147424893	121948781	101907381	49924453	33064647	18662246	14976837
	169233109	148789106	118562246	103592354	49283455	33906963	18684393	14285509
	167985934	149060993	119048324	100852829	50630217	33021704	19028966	14393736
	168306557	147392906	122651239	96998224	53609063	33473857	17265439	14043721
	169923769	147594316	123207310	99334506	52980096	31912974	17076818	14091771
	170918045	149008559	124376865	96991998	53800956	32500729	18050083	14123511
Mean	169012701	148078069	122050638	99435846	52262503	32750155	18031427	14460701
STD	1344562	687104.4	1969484	2394894	1849731	725961.6	688029.9	348674
RSD/%	0.80	0.46	1.61	2.41	3.54	2.22	3.82	2.41

Table C3: Calibration data for the determination of MBC.

[Conc] /mol dm^{-3}	1.40 $x10^{-4}$	9.29 $x10^{-5}$	4.65 $x10^{-5}$	2.32 $x10^{-5}$	1.16 $x10^{-5}$	5.81 $x10^{-6}$	2.9 $x10^{-6}$	1.45 $x10^{-6}$
Peak areas	68130064	46483759	22852244	11106897	5294105	2430865	1393811	592490
	68540416	46672916	22853588	11209670	5325874	2445444	1426896	598458
	68620871	46803573	23036567	11303352	5351199	2457331	1448033	586921
	70145680	48403417	23489057	12636065	4984481	2455364	1377633	569318
	71978515	48659269	24541365	11376590	4911917	2373575	1295947	578716
	71661098	48019529	24625486	11617616	5009413	2411580	1338086	579005
	68411437	46637354	22986214	11291506	5379123	2480614	1482923	595991
	70664743	47100643	23433326	11146488	5240043	2508917	1470984	597088
	68267735	46862594	23999112	12086764	5301489	2515061	1436632	589997
Mean	69602284	47293673	23535218	11530550	5199738	2453195	1407883	587553.8
STD	1531608.29	833561.1	699093.9	512534.4	179343.5	45188.24	62176.29	9971.57
RSD %	2.20	1.76	2.97	4.45	3.45	1.84	4.42	1.69

Table C4: Calibration data for the determination of Benz-3.

[Conc]/ mol dm^{-3}	4.39 $x10^{-4}$	2.92 $x10^{-4}$	2.19 $x10^{-4}$	1.09 $x10^{-4}$	5.49 $x10^{-5}$	2.74 $x10^{-5}$	1.37 $x10^{-5}$	6.86 $x10^{-6}$
Peak areas	50421773	35010010	24907677	12362996	5832621	2496507	1300511	550226
	51300640	37010700	25285281	13853477	5951657	2524290	1324525	556338
	50890107	35230561	25970007	14134253	5691422	2294522	1281043	577055
	51676065	35633988	23290079	12295705	5645944	2596641	1327377	547126
	52661098	35771747	24748330	12503044	5692586	2646592	1413424	566132
	50597859	35142574	25955368	12449699	5766108	2532884	1300181	567581
	50680145	35328846	24198811	12400505	5600762	2467735	1314539	560287
	50984772	35446316	23761208	12526036	5616647	2595831	1325288	563735
	51226027	34032114	25653746	12496656	5731192	2514133	1319734	567324
Mean	51159832	35400762	24863390	12780263	5725438	2518793	1322958	561756
STD	683606.9	783636.2	959599.5	695466.5	111962.9	101229.5	37202.67	9357.811
RSD/%	1.33	2.21	3.86	5.44	1.96	4.01	2.81	1.67

Table C5: Calibration data for the determination of PBSA.

[Conc.] /mol dm^{-3}	9.85×10^{-4}	4.93×10^{-4}	2.46×10^{-4}	1.23×10^{-4}	6.16×10^{-5}	3.08×10^{-5}	1.54×10^{-5}	$7.7\ 0 \times 10^{-5}$
Peak areas	12273253	6344534	2971230	1394014	641425	304604	149474	66149
	12184532	6285659	2968132	1415929	659899	311170	154135	67617
	12260321	6287857	3061498	1420595	663882	305255	153282	67042
	12358346	6213031	3403219	1406437	665985	320527	151311	69196
	12514093	6288029	3332583	1449238	675891	326489	166839	63972
	12512082	6191719	3176108	1443969	650146	333520	159111	64098
	12298323	6264681	3168972	1411383	632155	321409	149349	66066
	12420093	6466109	3198954	1436437	644512	336337	156375	67109
	12277508	6492133	3285785	1467705	676549	320093	154168	68756
Mean	12344283	6314861	3174053	1427301	656716	319933.8	154893.8	66667.22
STD	115717	103401.6	152885.7	23574.38	15562.72	11327.22	5469.489	1819.703
RSD %	0.94	1.64	4.82	1.65	2.37	3.54	3.53	2.73

Table C6: Calibration data for the determination of OCT.

[Conc] /mol dm^{-3}	3.04×10^{-4}	2.28×10^{-4}	1.52×10^{-4}	7.62×10^{-5}	3.81×10^{-5}	1.9×10^{-5}	9.5×10^{-6}
Peak areas	4793018	3409277	2295760	1176663	569708	287612	137890
	4711138	3428393	2234091	1121669	564167	280321	136044
	4719307	3452643	2272852	1139416	569982	285701	136966
	4932138	3474096	2240654	1204997	568976	290577	138976
	4912082	3500116	2341560	1192839	570695	289437	139840
	5088116	3465496	2300885	1199693	569026	299572	139027
	4941207	3479287	2289076	1195707	576638	292196	140526
	4965496	3464372	2264937	1185838	569437	290307	138093
	4918013	3421113	2292133	1190321	565633	298075	141171
Mean	4886724	3454977	2281328	1178571	569362.4	290422	138725.9
STD	123012.4	29875.52	32828.43	28738.38	3470.99	5901.902	1658.404
RSD %	2.52	0.86	1.44	2.44	0.61	2.03	1.19

Table C7: Calibration data for the determination of OT.

[Conc] /mol dm^{-3}	1.35×10^{-4}	1.01×10^{-4}	6.76×10^{-5}	3.38×10^{-5}	1.69×10^{-5}	8.45×10^{-6}	4.23×10^{-6}	2.11×10^{-6}
Peak areas	18966188	14266027	9508809	4735641	2374406	1188601	592655	296798
	18887709	14305364	9543937	4799697	2419881	1198450	594682	304621
	18907459	14293816	9604027	4810529	2369120	1204892	589762	300544
	18900876	14330467	9608972	4781111	2395416	1156456	589885	299753
	19061208	14406740	9637629	4743969	2346290	1169373	592893	289969
	18985496	14364536	9705109	4804337	2446997	1199577	596366	299193
	18987670	14488633	9593379	4796432	2392506	1169205	597653	298920
	18928883	14593969	9569210	4800762	2421402	1171131	606437	312950
	18918776	14496443	9583938	4893835	2398976	1178006	602383	290067
Mean	18949363	14393999	9595001	4796257	2396110	1181743	595857.3	299201.7
STD	55709.68	111116.3	55951.28	45360.14	30613.46	16794.02	5604.042	7027.028
RSD %	0.29	0.77	0.58	0.95	1.28	1.42	0.94	2.35

Table C8: Calibration data for the determination of HS.

[Conc] /mol dm^{-3}	2.02×10^{-4}	1.52×10^{-4}	1.01×10^{-4}	5.06×10^{-5}	2.53×10^{-5}	1.26×10^{-5}	6.3×10^{-6}	3.2×10^{-6}
Peak areas	2043099	1519936	986742	509514	259698	124235	65266	32715
	2124210	1544860	995960	516372	250434	120480	66717	33408
	2132838	1547203	989343	519609	258136	123732	66433	33593
	2299571	1646640	1109564	498021	262085	119247	66910	34680
	2193020	1591997	1099770	509473	267574	116694	66049	35009
	2280805	1599546	1108332	506690	259790	120811	66864	35115
	2159650	1597732	1097812	510490	262125	129997	68048	34405
	2093730	1585897	1128411	519004	260541	128932	67914	34761
	2112459	1592505	1091733	588027	267224	129020	68179	34086
Mean	2159931	1580702	1067519	519688.9	260845.2	123683.1	66931.11	34196.89
STD	84779.65	37726.24	58568.9	26487.16	5091.607	4785.931	975.9842	813.3802
RSD%	3.93	2.39	5.49	5.10	1.95	3.87	1.46	2.38

Table C9: Calibration data for the determination of ODM-PABA.

[Conc] /mol dm^{-3}	8.64×10^{-5}	7.2×10^{-5}	5.76×10^{-5}	4.32×10^{-5}	2.16×10^{-5}	1.08×10^{-5}	5.4×10^{-6}	2.7×10^{-6}
Peak areas	94534386	76866996	62870840	46418932	25982384	16468766	9568766	5056911
	95576345	78107834	62562842	46250984	27156932	16551639	9596149	5019980
	96995668	79385204	62967204	46061385	27895337	16597304	9375430	5100291
	93104061	78035015	62808821	48212860	27115860	16293156	9653337	5130462
	94849473	80859526	61655757	47731132	27087445	16373071	9604843	5030440
	97054301	81056552	62922141	48057564	26980732	16295526	9756684	5192081
	96296755	79420139	62828865	46139159	27360551	16892994	9803342	5129459
	96760617	78107365	62606250	46278555	27956267	16973626	9596061	5096774
	98598513	79956224	62930214	46503171	27363828	17091329	9662797	5089908
Mean	95974458	79088317	62683659	46850416	27211037	16615268	9624157	5094034
STD	1641401	1411115	410338.16	881098.6	576543.9	300555.9	121909.5	53811.17
RSD/%	1.71	1.78	0.65	1.88	2.12	1.81	1.27	1.056357

APPENDIX D

Calibration curves and residual plots

The following are the respective calibration curves and the residual plots for the various active ingredients analysed in this study. The data used to construct these graphs is given in Appendix C

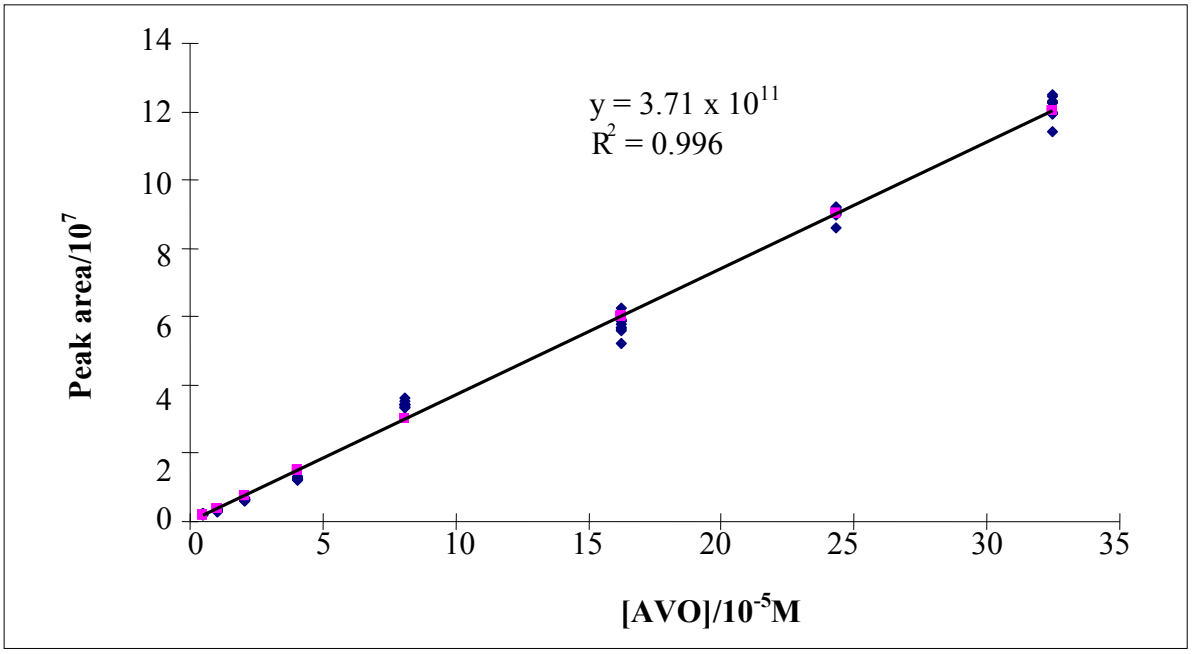

Figure D1 HPLC calibration curve for the determination of AVO. The chromatographic conditions used were: Nucleosil C100 C18 column, eluent 85% (v/v) MeOH/H_2O, flow rate 1 mL min^{-1}, injection volume – 10 µL. Detection wavelength at 360 nm.

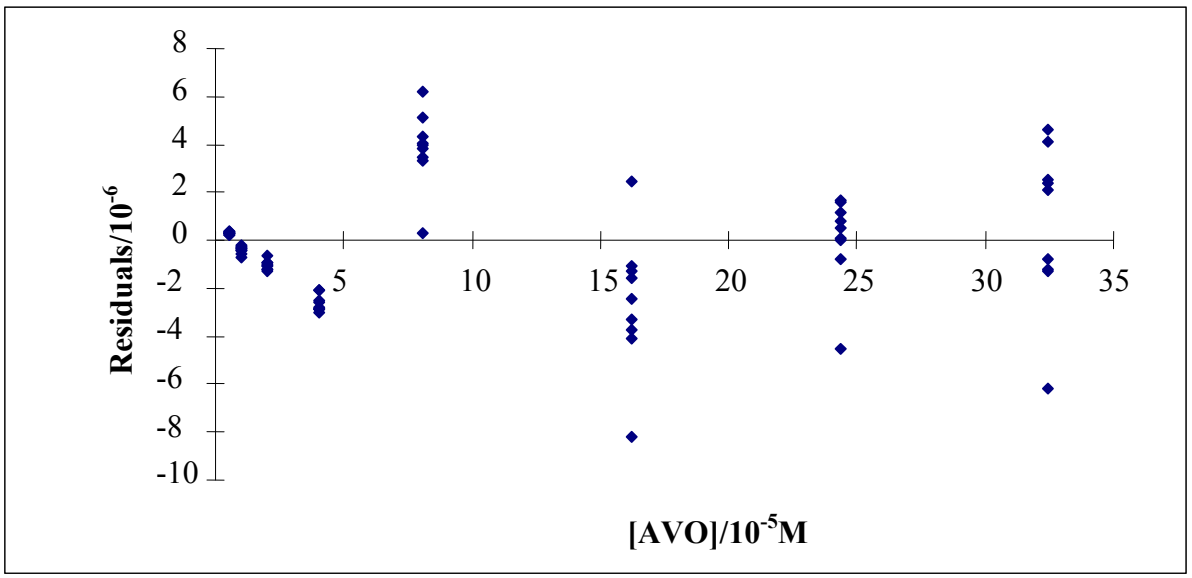

Figure D2 Residual plot for the calibration curve of AVO.

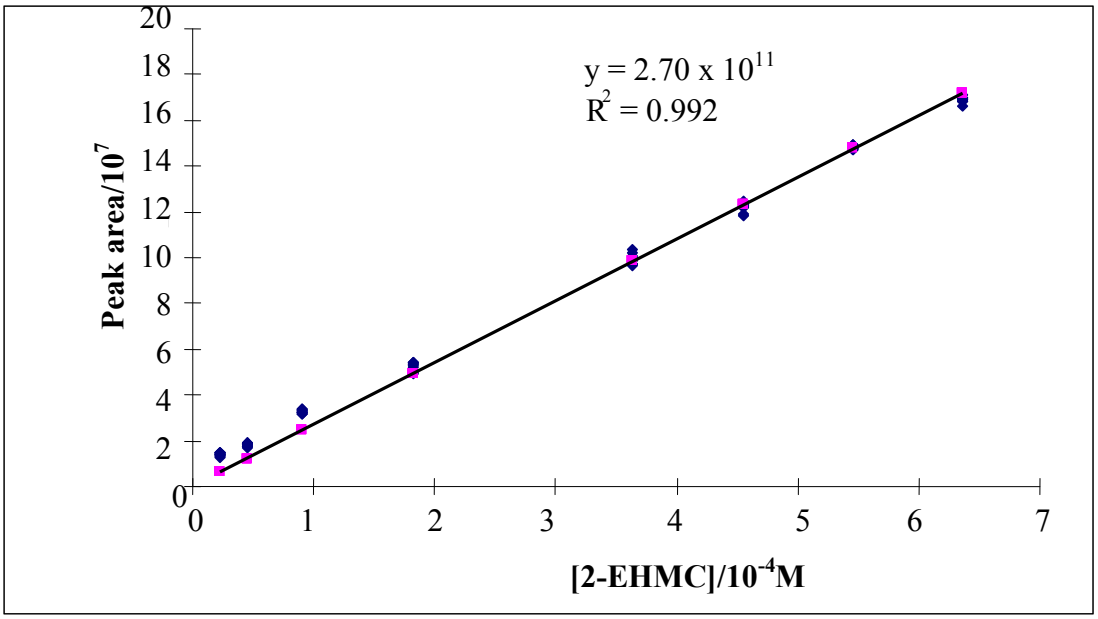

Figure D3 HPLC Calibration curve for the determination of 2-EHMC. The chromatographic conditions used were: Nucleosil C100 C18 column, eluent 85% (v/v) MeOH/H_2O, flow rate 1 mL min^{-1}, injection volume – 10 µL. Detection wavelength at 310 nm.

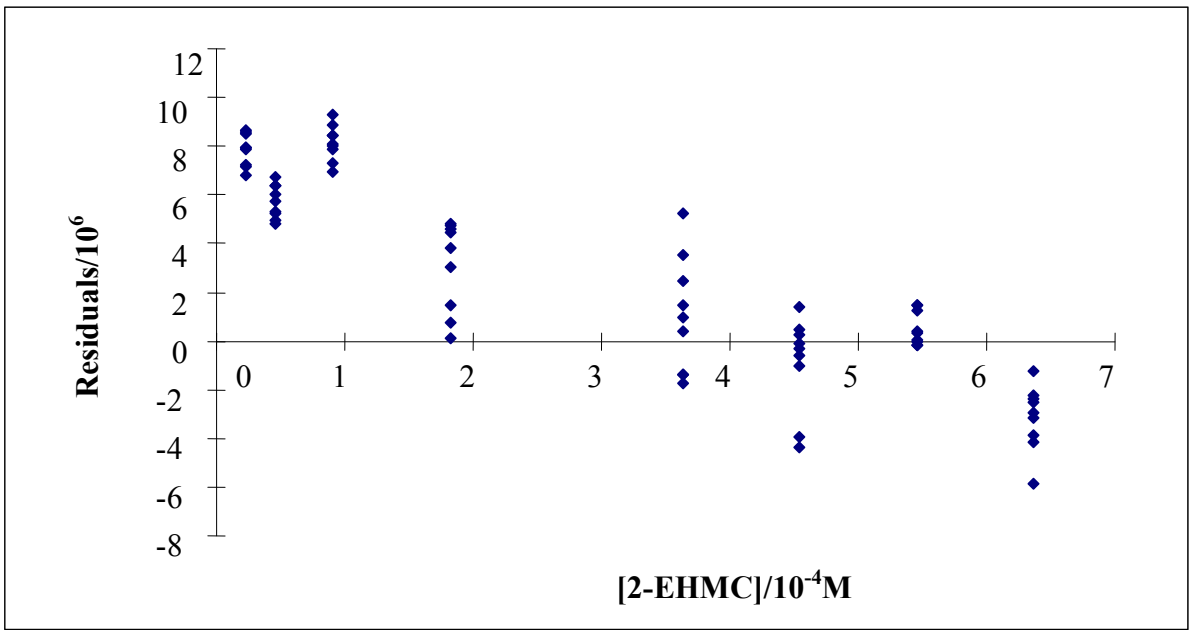

Figure D4 Residual plot for the calibration curve of 2-EHMC.

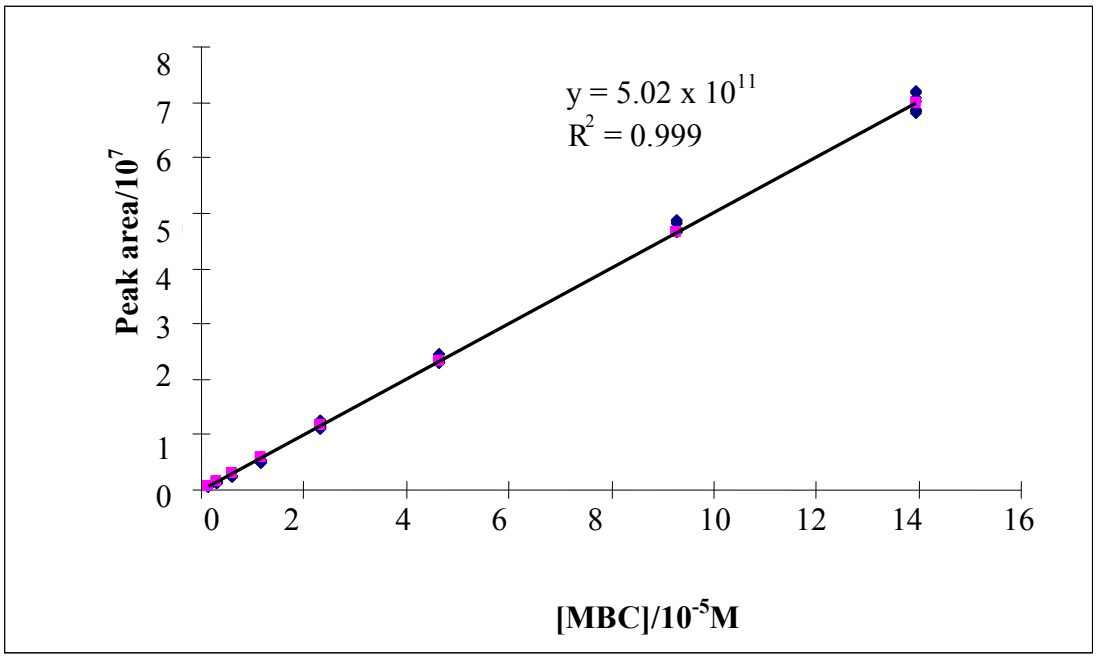

Figure D5 HPLC Calibration curve for the determination of MBC. The chromatographic conditions used were: Nucleosil C100 C18 column, eluent 85% v/v MeOH/H_2O, flow rate of 1 mL min^{-1}, and injection volume – 10 µL. Detection wavelength at 310 nm.

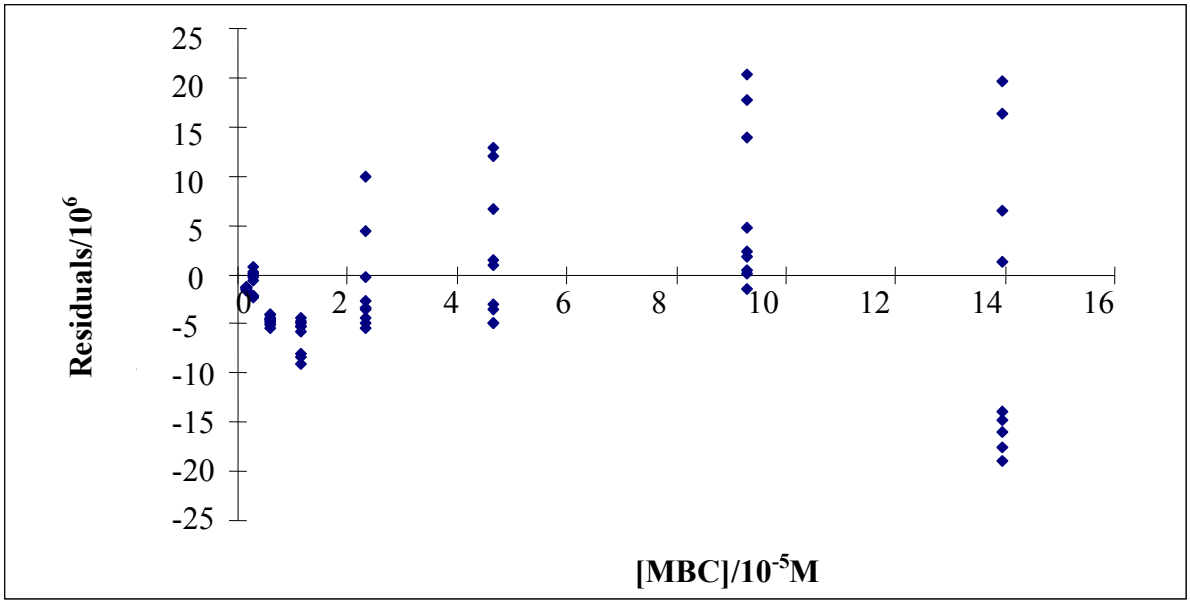

Figure D6 Residual plot for the calibration curve of MBC.

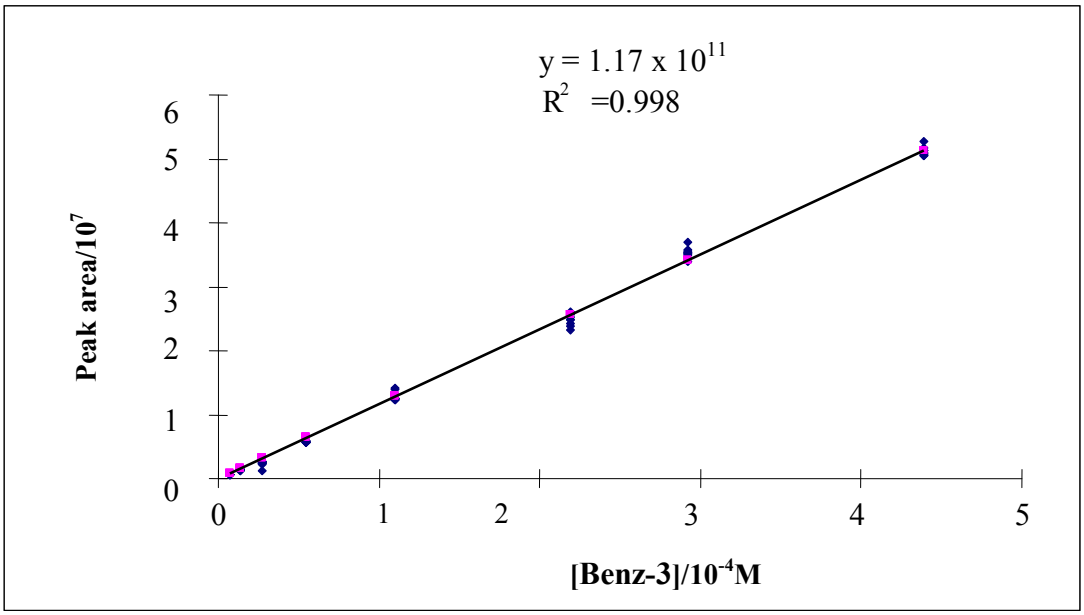

Figure D7 HPLC calibration curve for the determination of Benz-3. The chromatographic conditions used were: Nucleosil C100 C18 column, eluent 85% v/v MeOH/ flow rate of 1 mL min^{-1}, and injection volume – 10 µL. Detection wavelength at 310 m.

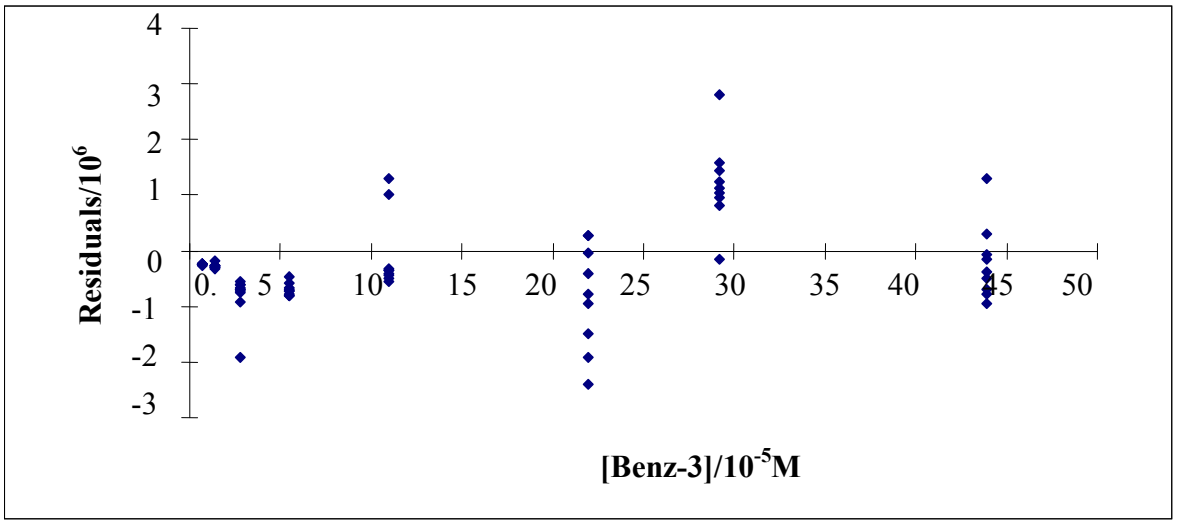

Figure D8 Residual plot for the calibration curve of Benz-3.

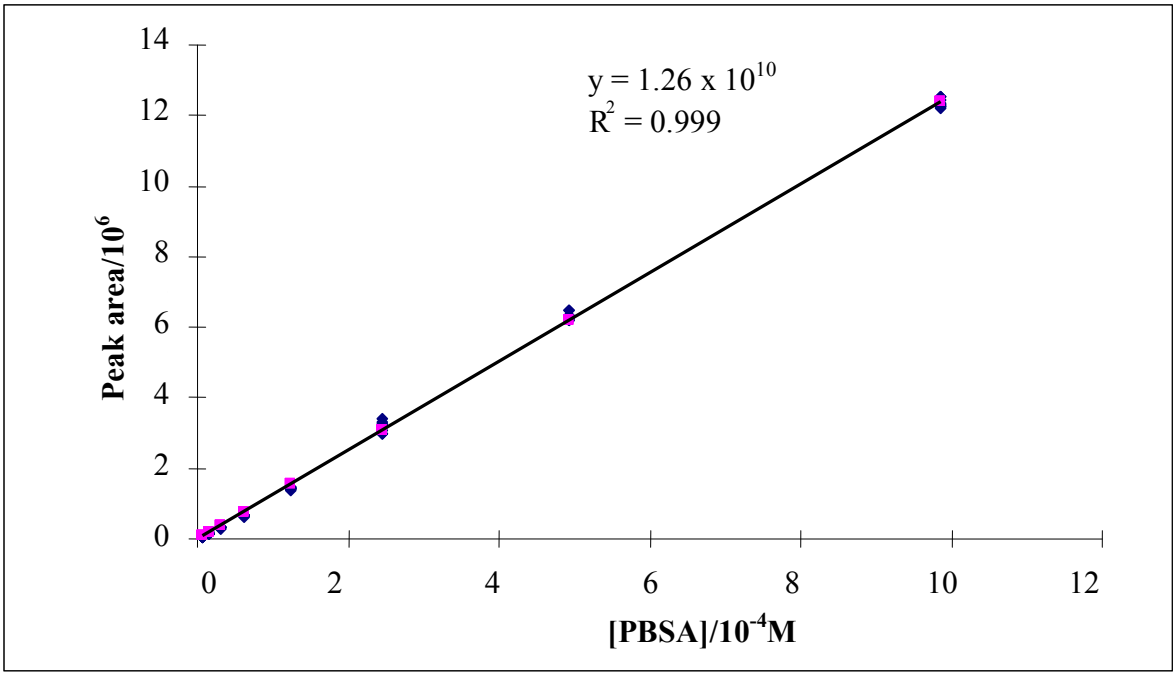

Figure D9 HPLC Calibration curve for the determination of PBSA. The chromatographic conditions used were: Nucleosil C100 C18 column, eluent 85% v/v MeOH/H_2O flow rate of 1 mL min^{-1}, and injection volume – 10 µL. Detection wavelength at 310 nm.

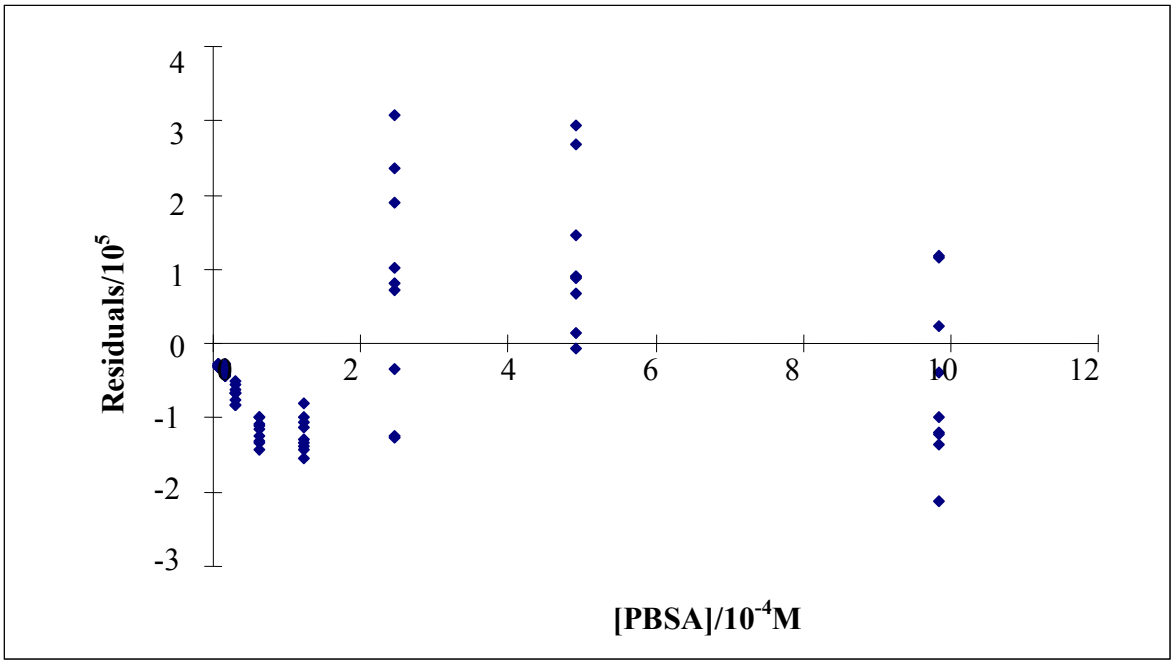

Figure D10 Residual plot for the calibration curve of PBSA.

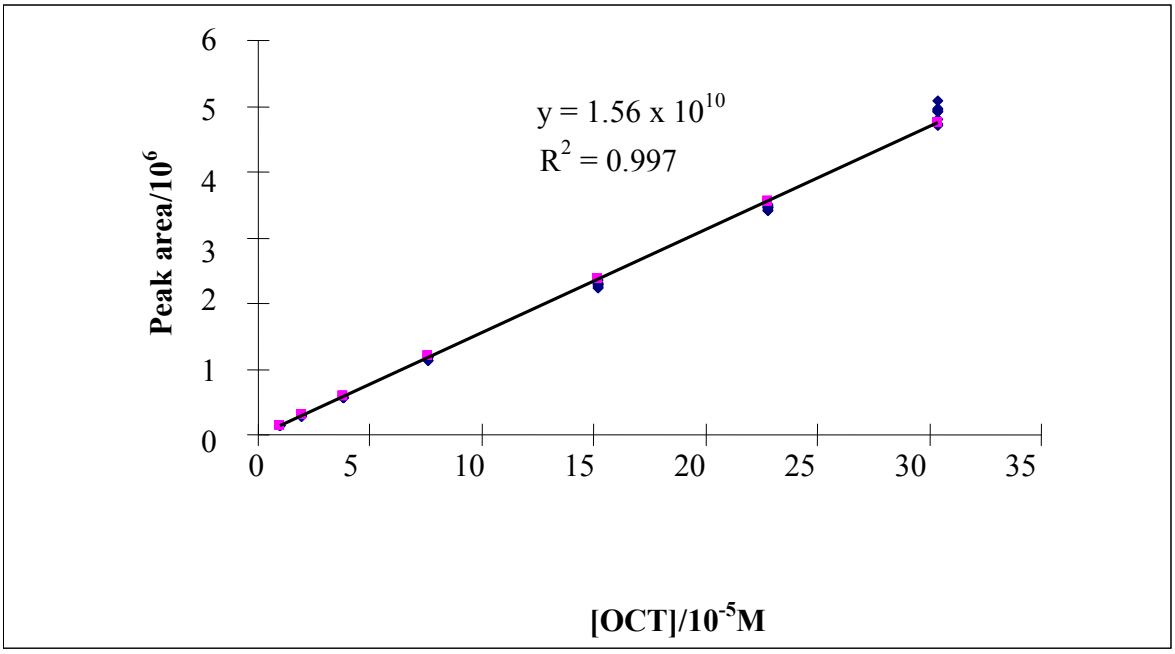

Figure D11 HPLC calibration curve for the determination of OCT. The chromatographic conditions used were: Nucleosil C100 C18 column, eluent 85% v/v MeOH/H_2O flow rate of 1 mL min^{-1}, and injection volume – 10 µL. Detection wavelength at 310 nm.

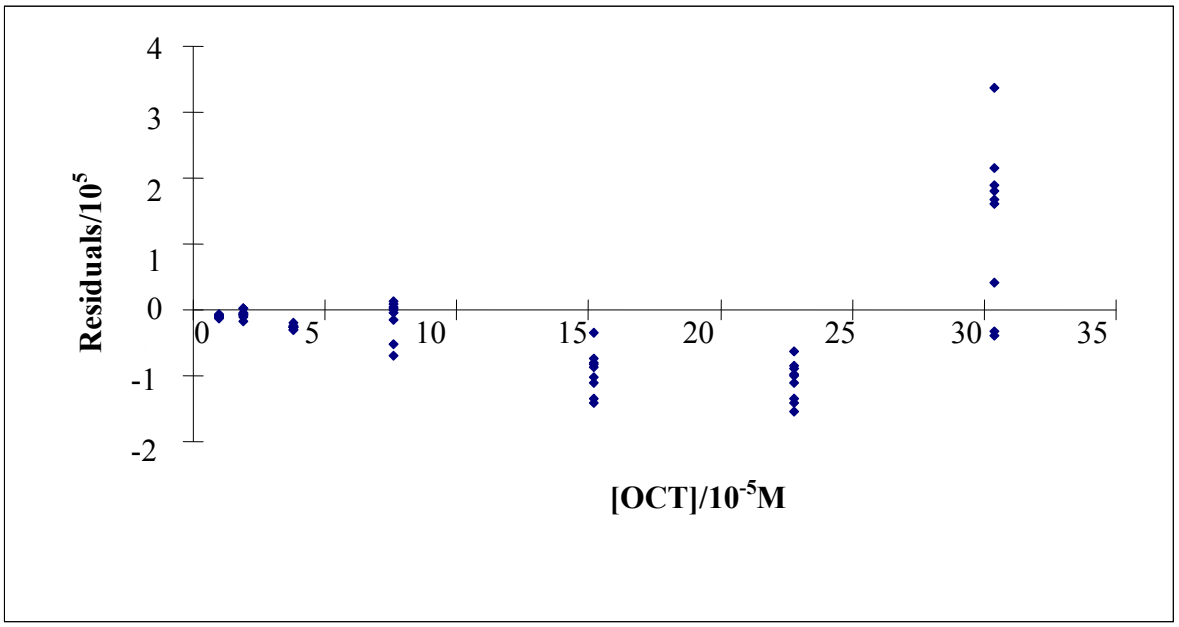

Figure D12 Residual plot for the calibration curve of OCT.

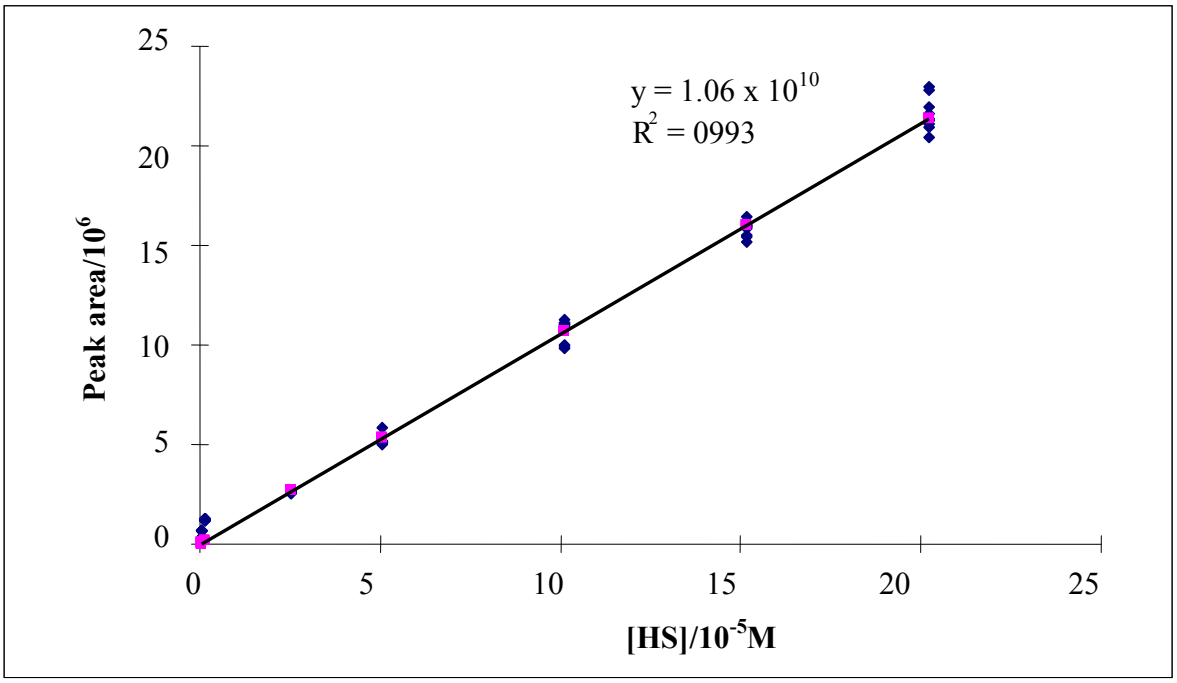

Figure D13 HPLC calibration curve for the determination of HS. The chromatographic conditions used were: Nucleosil C100 C18 column, eluent 85% v/v MeOH/H_2O flow rate of 1 mL min^{-1}, and injection volume – 10 µL. Detection wavelength at 310 nm.

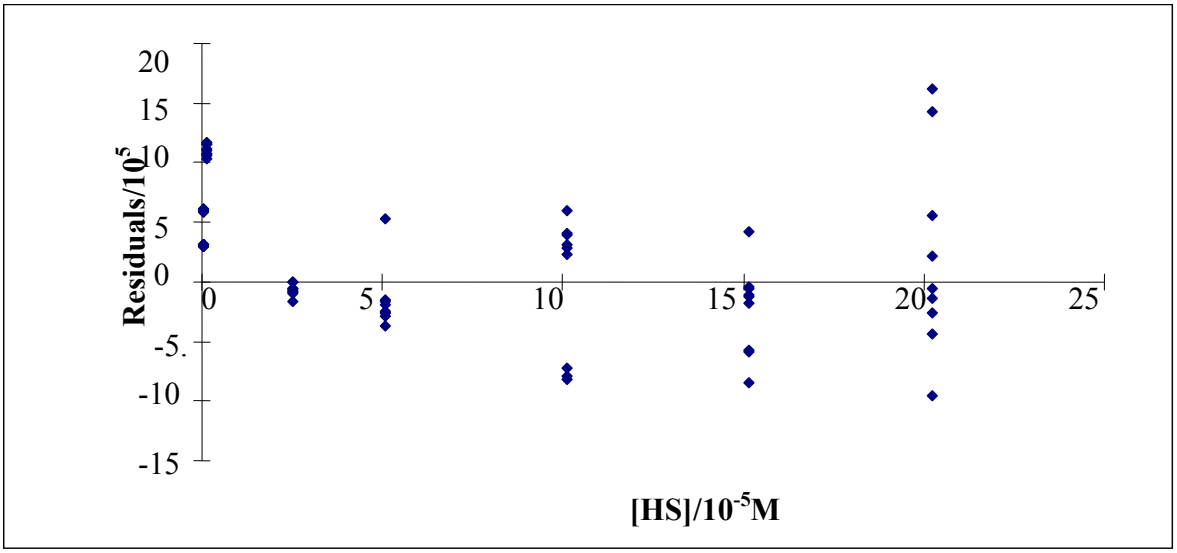

Figure D14 Residual plot for the calibration curve of HS.

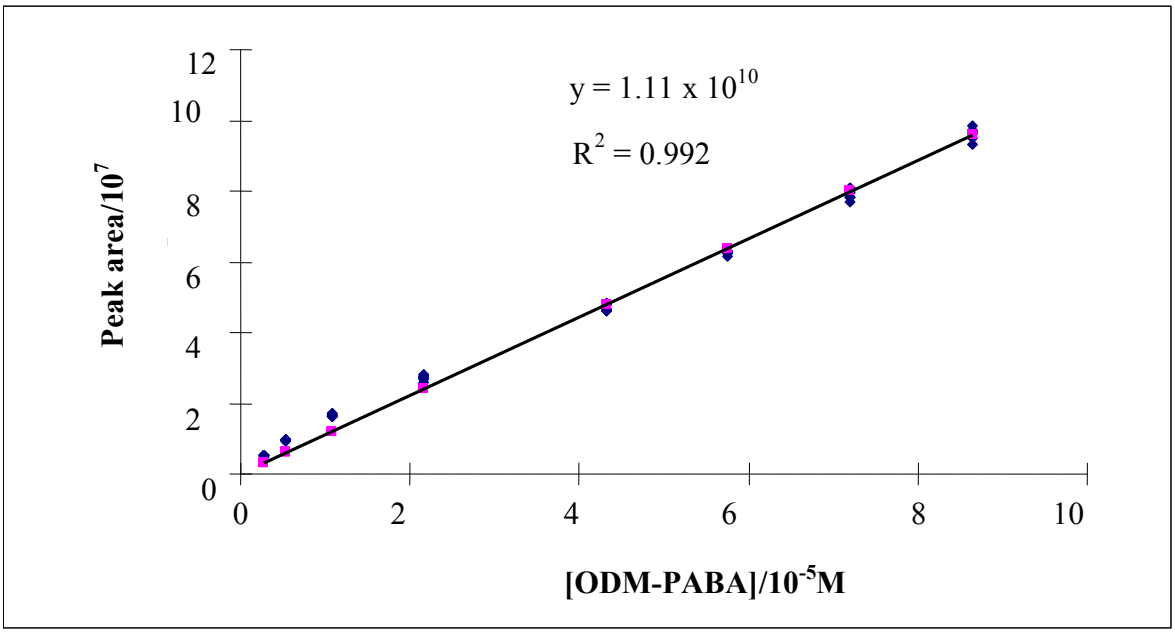

Figure D15 HPLC calibration curve for the determination of ODM-PABA. The chromatographic conditions used were: Nucleosil C100 C18 column, eluent 85% v/v MeOH/H_20, flow rate of 1 mL min^{-1}, and injection volume – 10 µL. Detection wavelength at 310 nm.

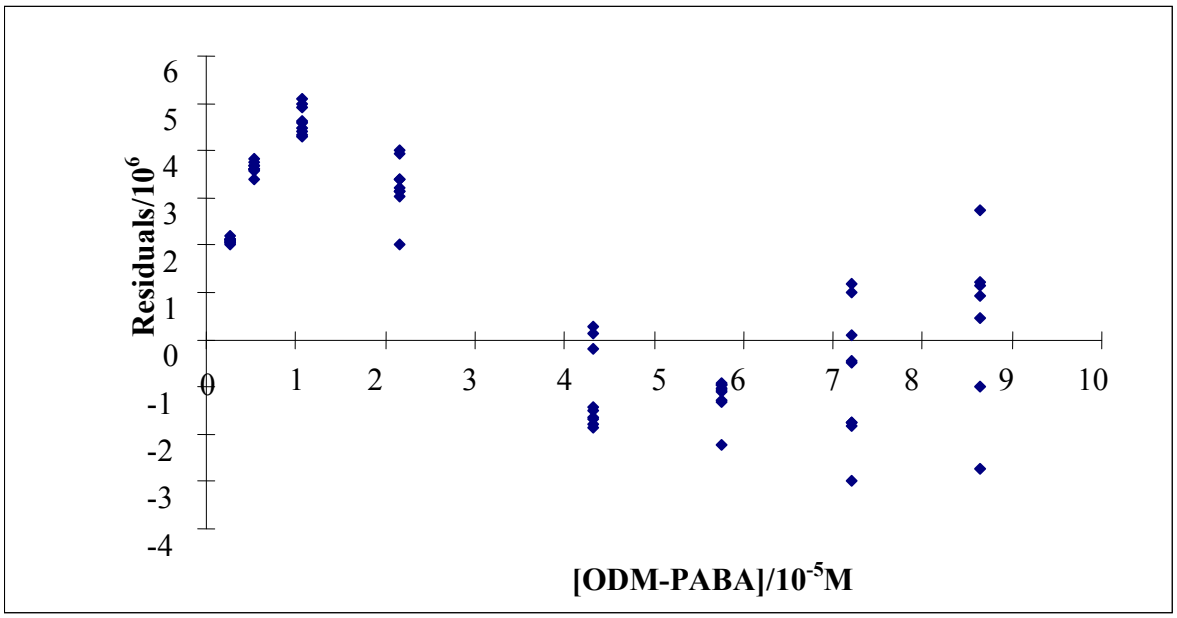

Figure D16 Residual plot for the calibration curve of OD-PABA.

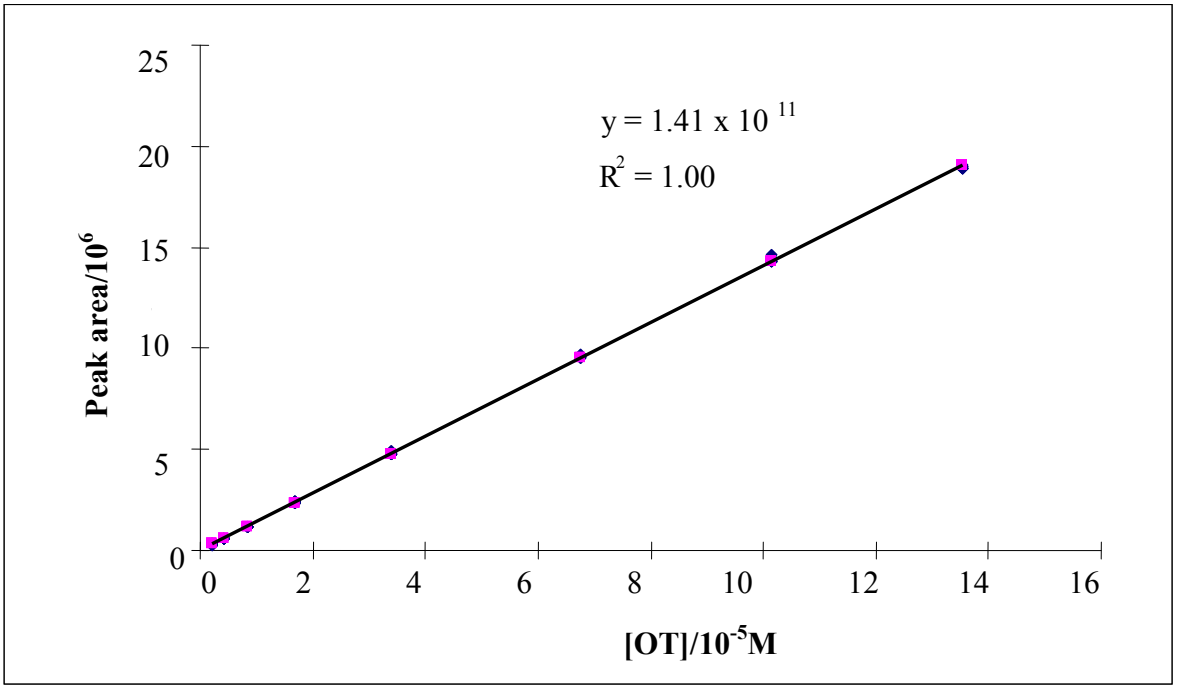

Figure D17 HPLC calibration curve for the determination of OT. The chromatographic conditions used were: Nucleosil C100 C18 column, eluent 85% v/v MeOH/H_20 flow rate of 1 mL min^{-1}, and injection volume – 10 µL. Detection wavelength at 310 nm.

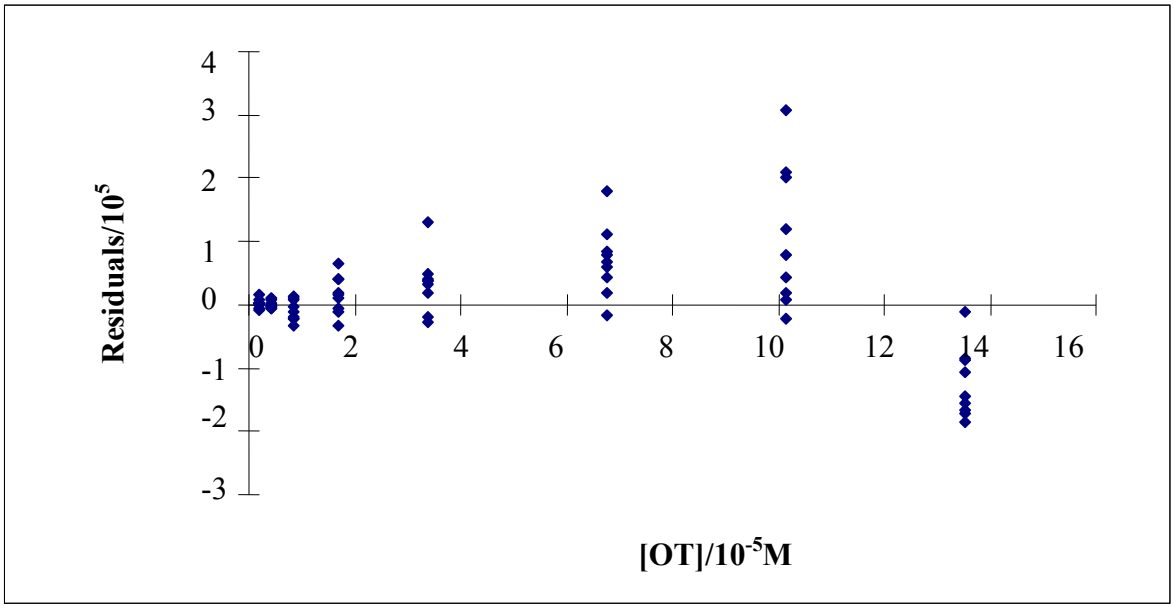

Figure D18 Residual plot for the calibration curve of OT.

APPENDIX E

UV transmission spectra

This appendix shows the UV transmission spectra (in duplicate) of the 25 Australian sunscreen products investigated. They are grouped according to the filter combination that they contain.

Filter combination: 2-EHMC and AVO

Samples: AU11 and AU25

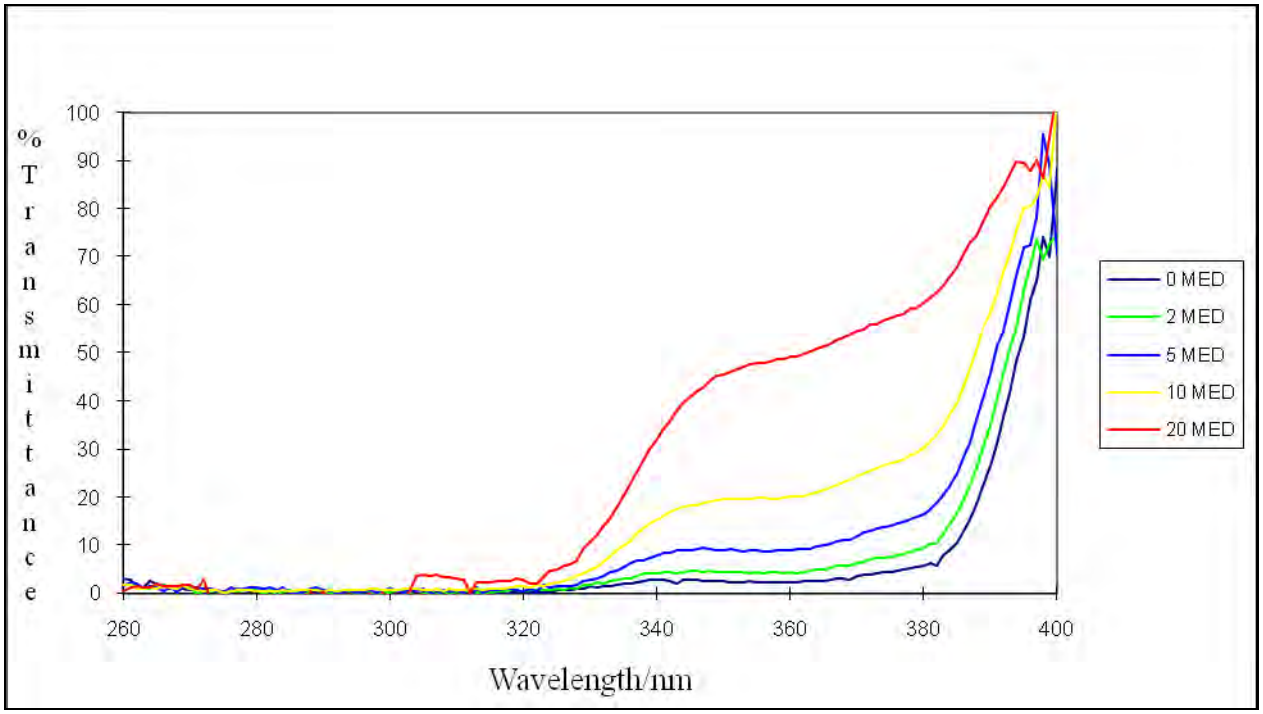

Figure E1 The UV transmission spectra of sample AU11 with increasing doses of UV radiation.

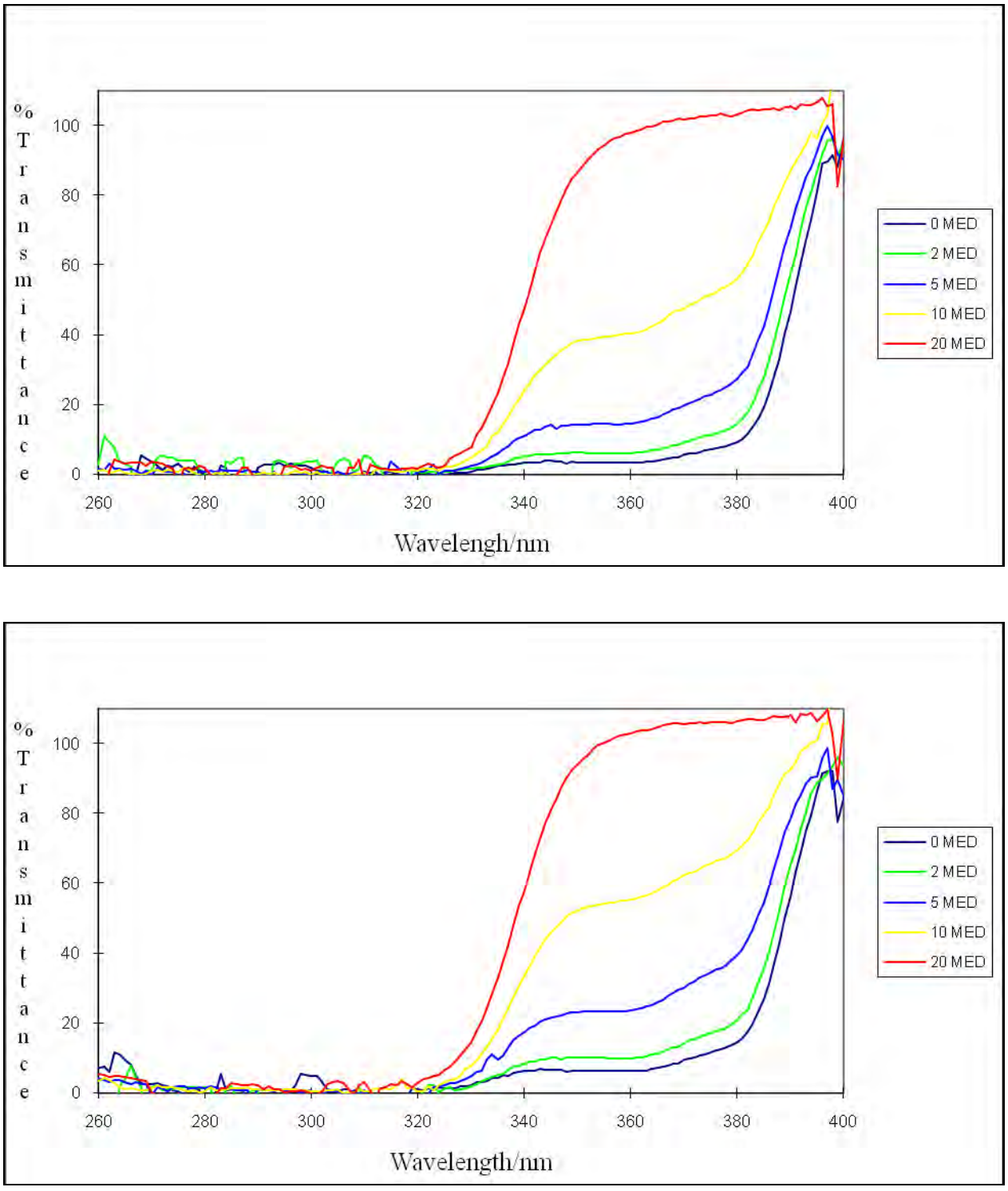

Figure E2 The UV transmission spectra of AU25 with increasing doses of UV radiation.

Filter combination: 2-EHMC and Benz-3

Samples: AU23

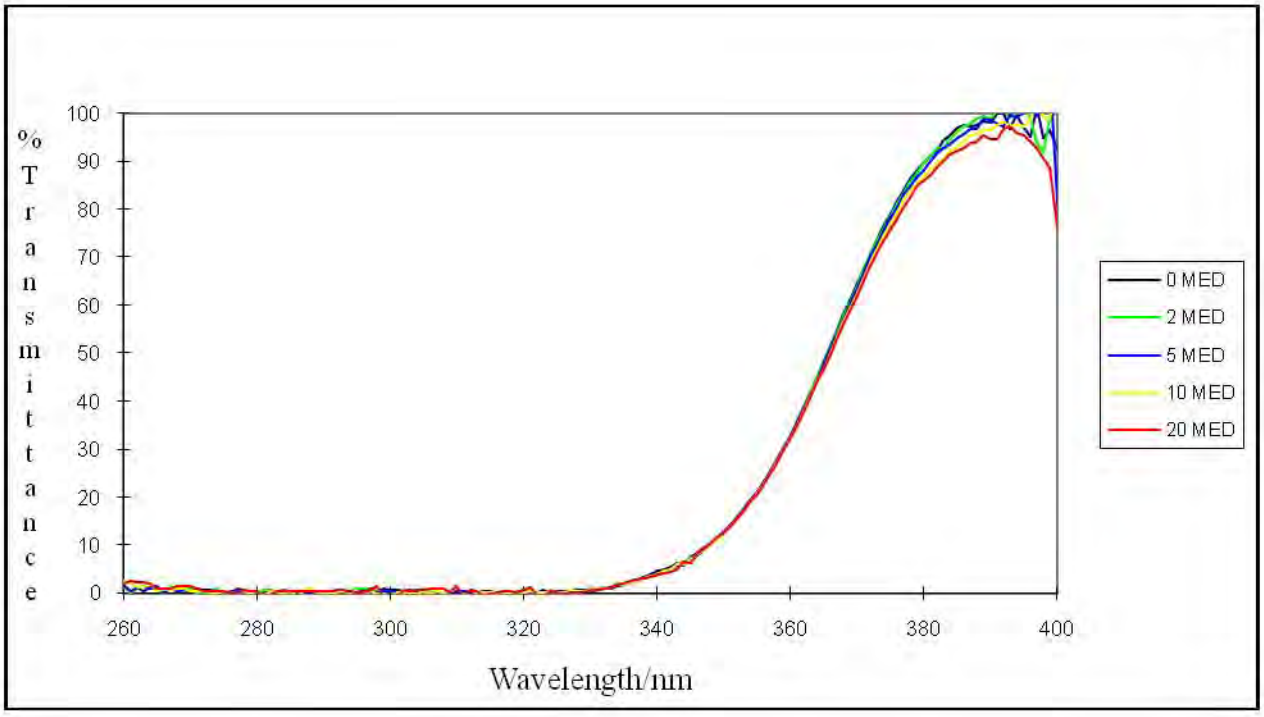

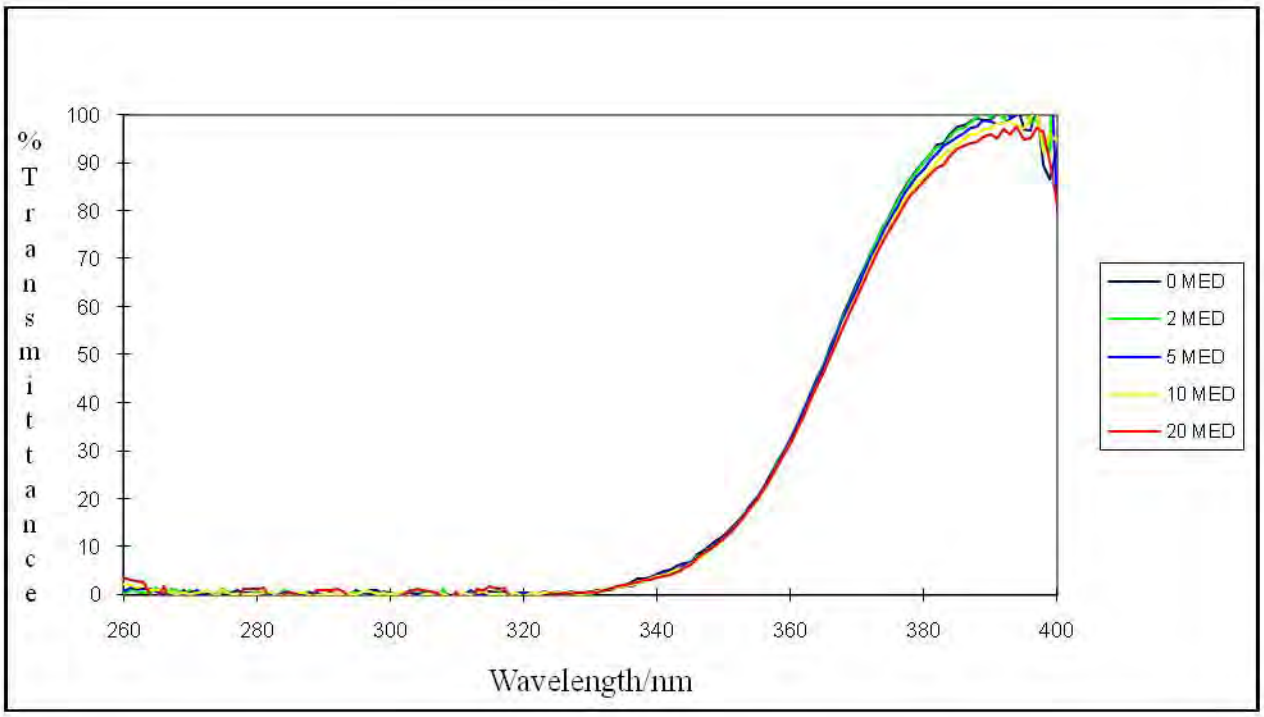

Figure E3 The UV transmission spectra of sample AU23 with increasing doses of UV radiation.

Filter combination: 2-EHMC, MBC and AVO

Samples: AU1, AU10 and AU18

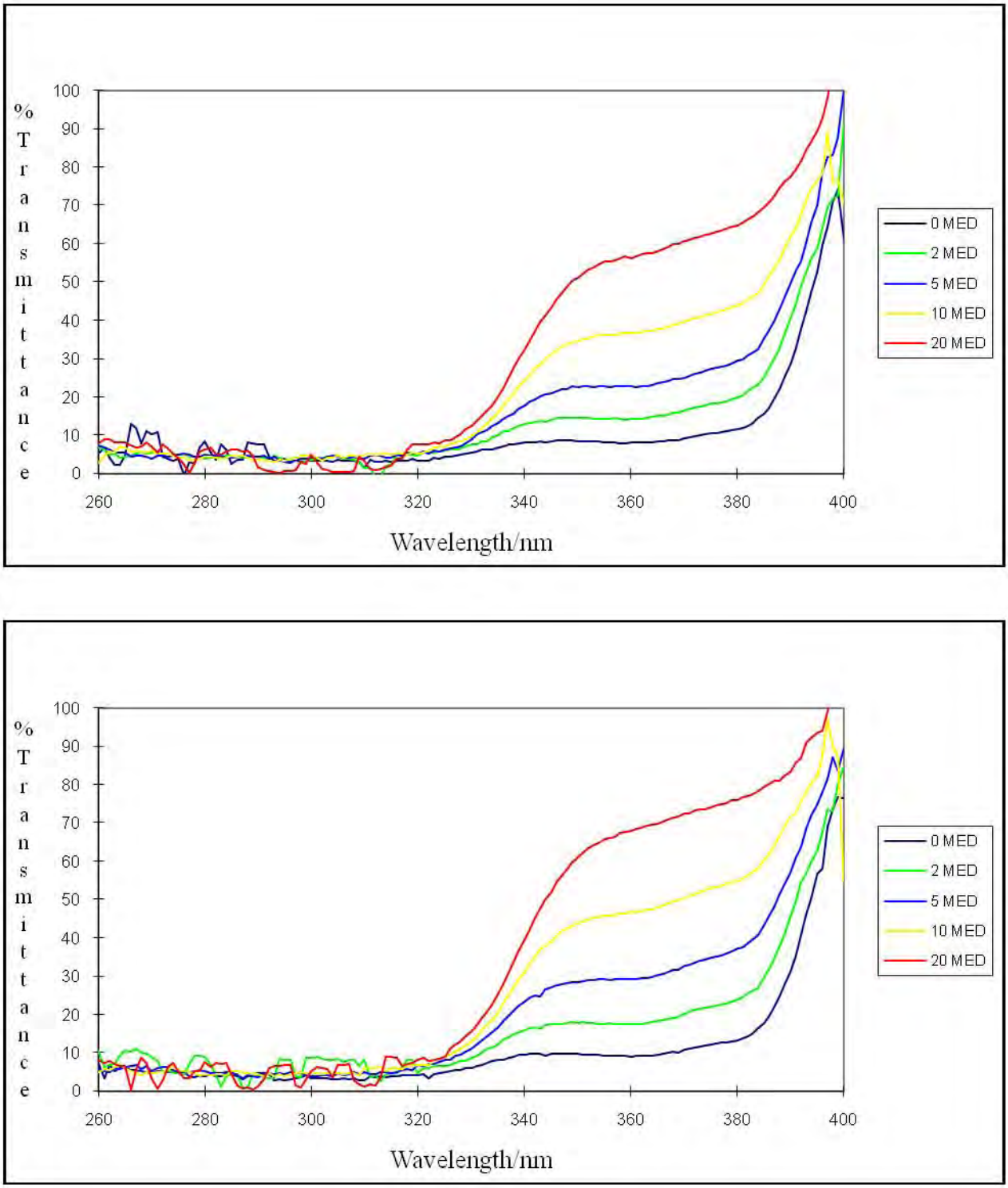

Figure E4 The UV transmission spectra of AU1 with increasing doses of UV radiation.

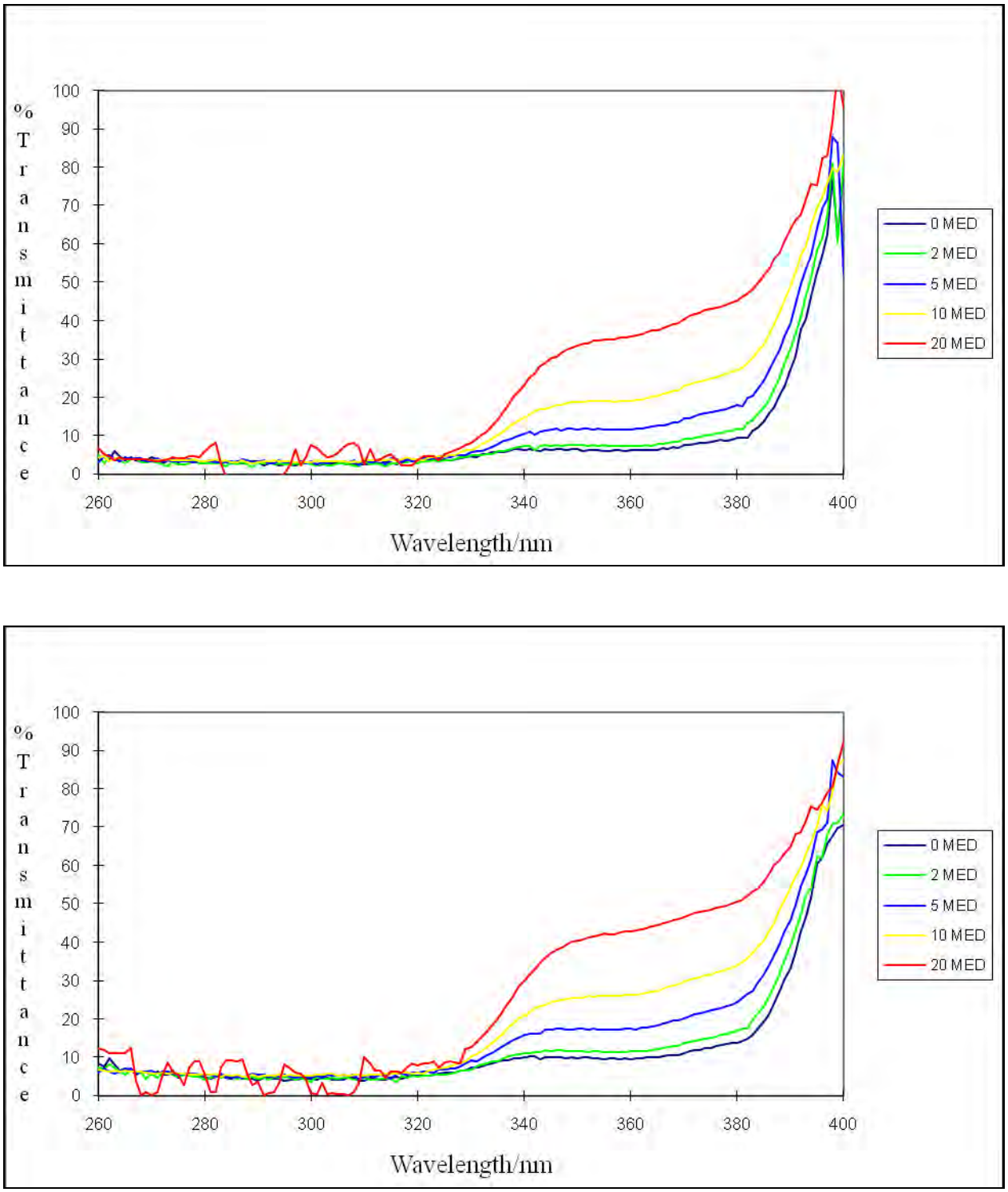

Figure E5 The UV transmission spectra of AU10 with increasing doses of UV radiation.

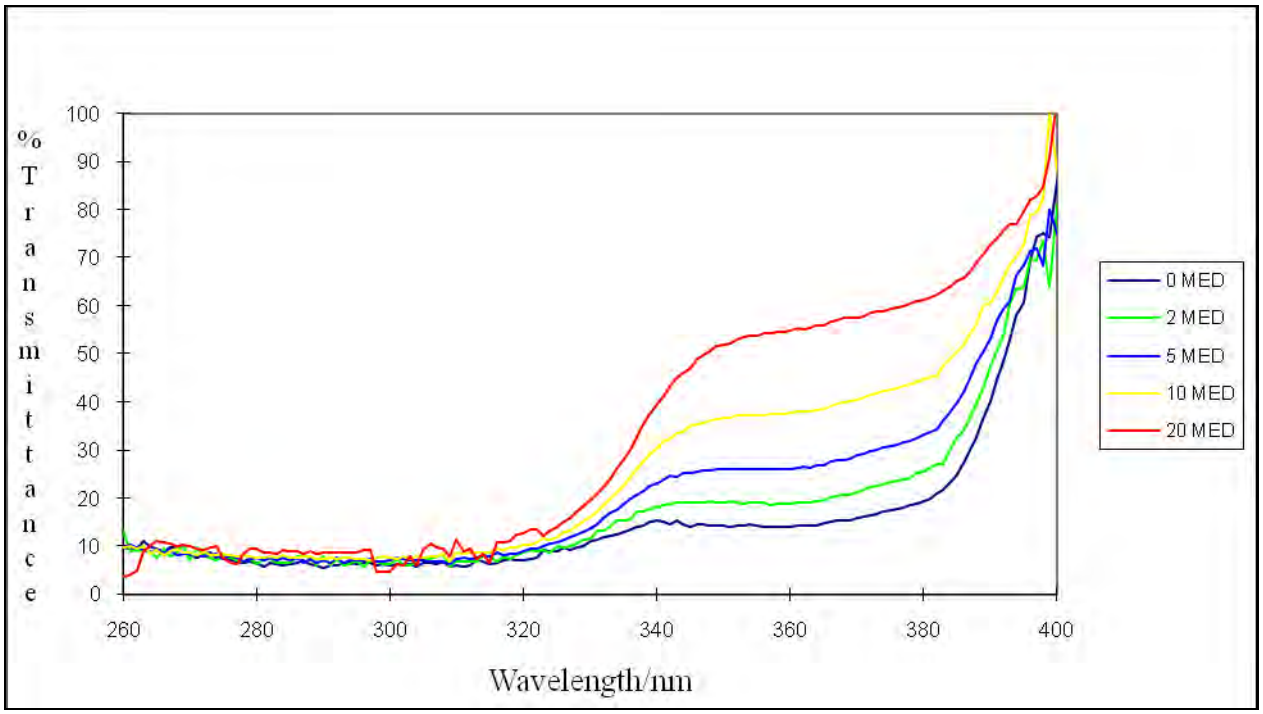

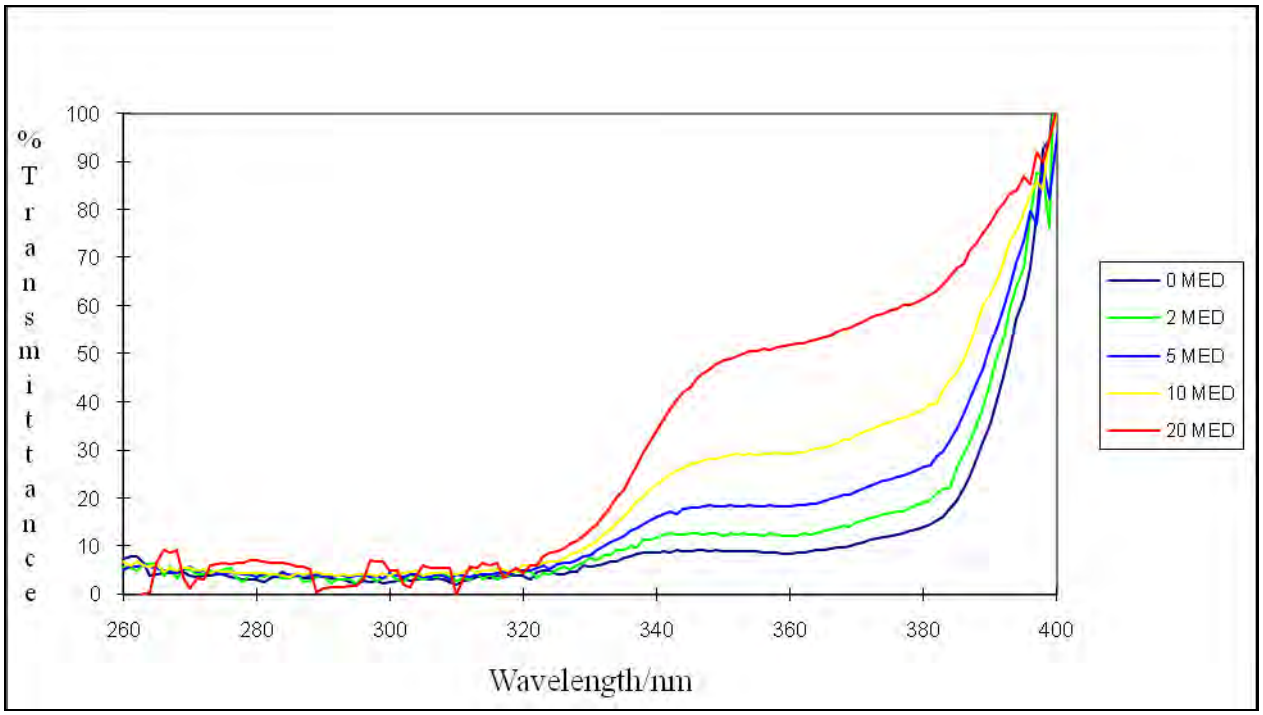

Figure E6 The UV transmission spectra of sample AU18 with increasing doses of UV radiation.

Filter combination: 2-EHMC, Benz-3 and AVO

Samples: AU2

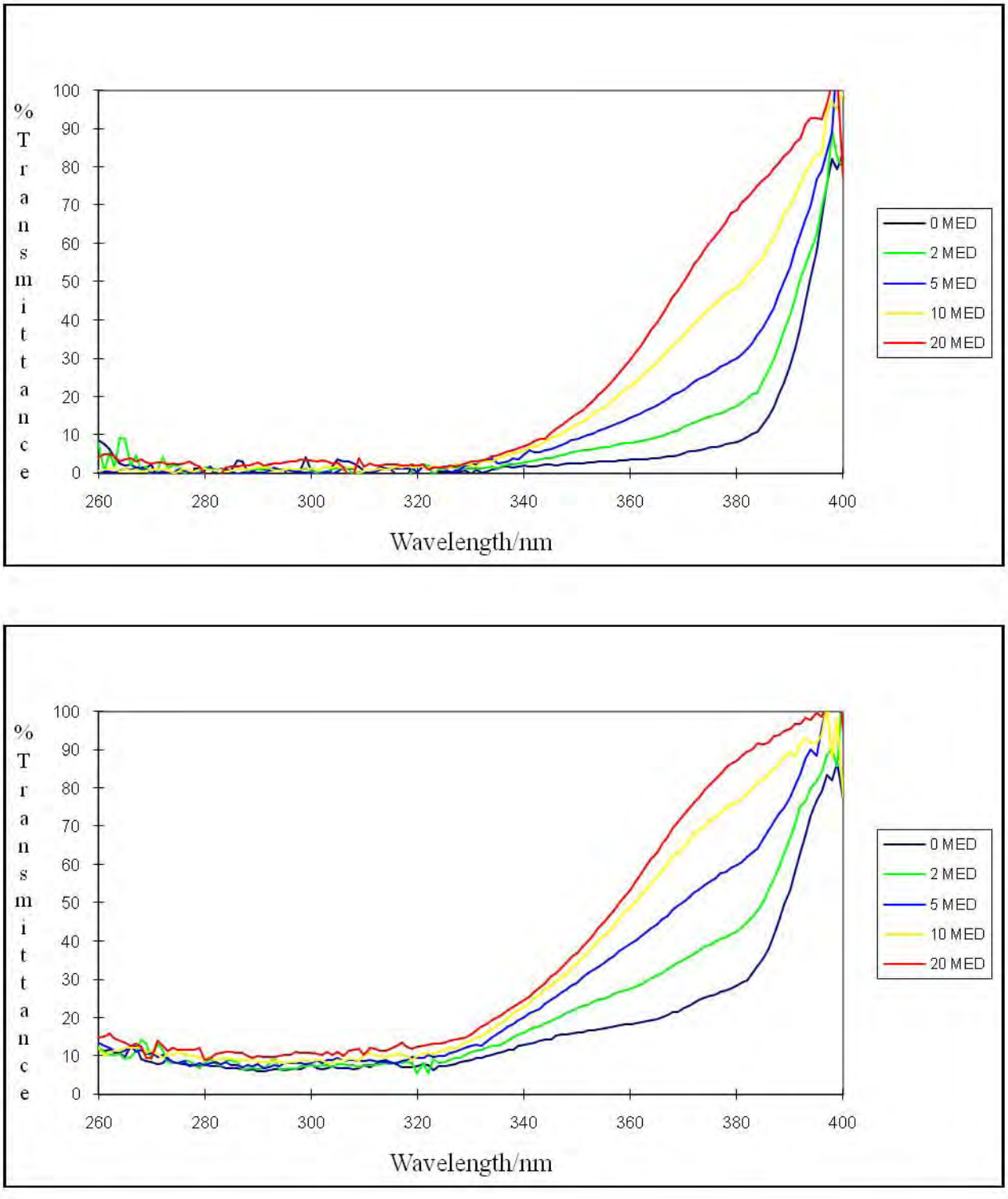

Figure E7 The UV transmission spectra of sample AU2 with increasing doses of UV radiation.

Filter combination: 2-EHMC, MBC, ZnO

Samples: AU5, 6,8,12,14,16,17 and 19

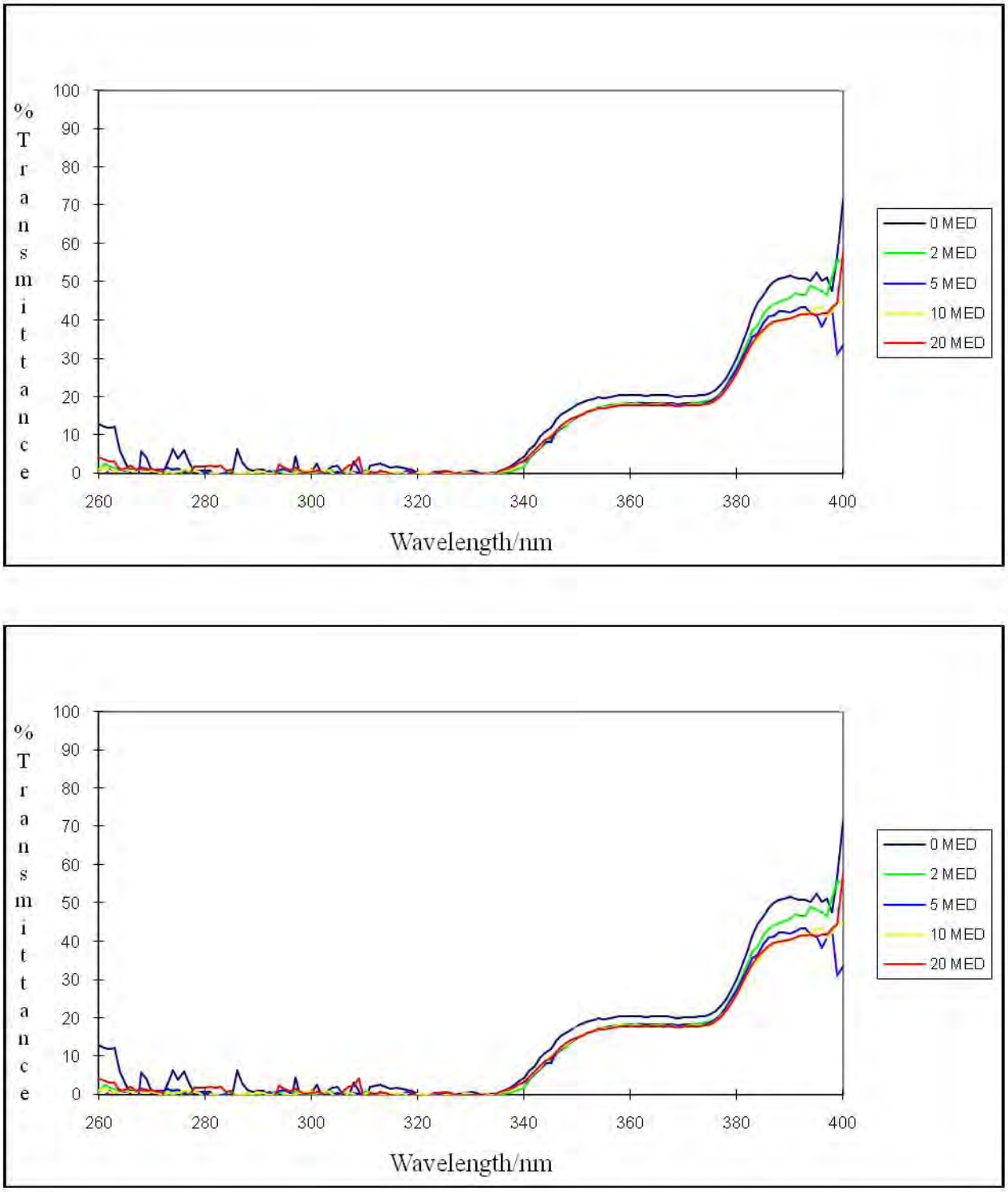

Figure E8 The UV transmission spectra of AU5 with increasing doses of UV radiation.

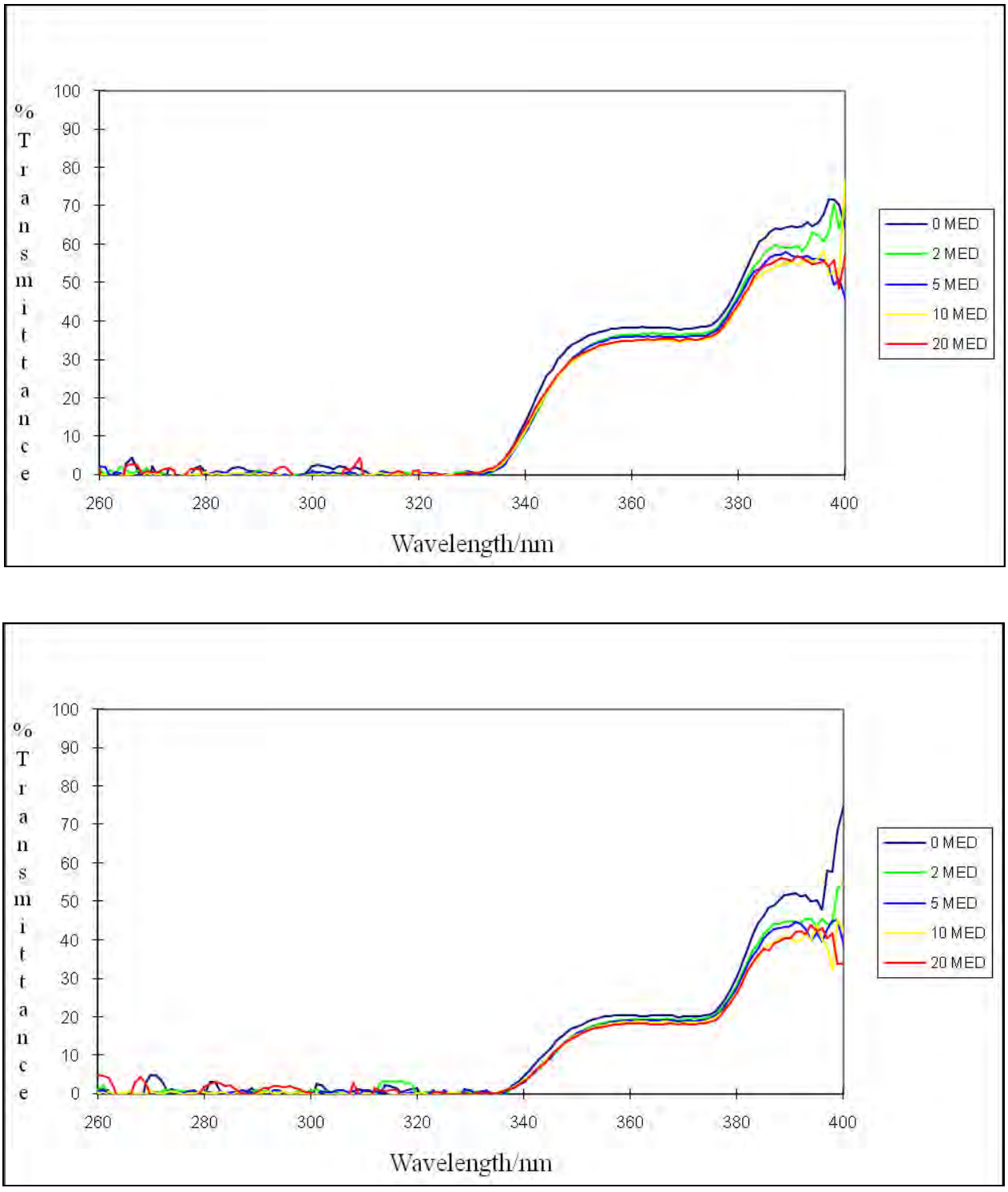

Figure E9 The UV transmission spectra of AU6 with increasing doses of UV radiation.

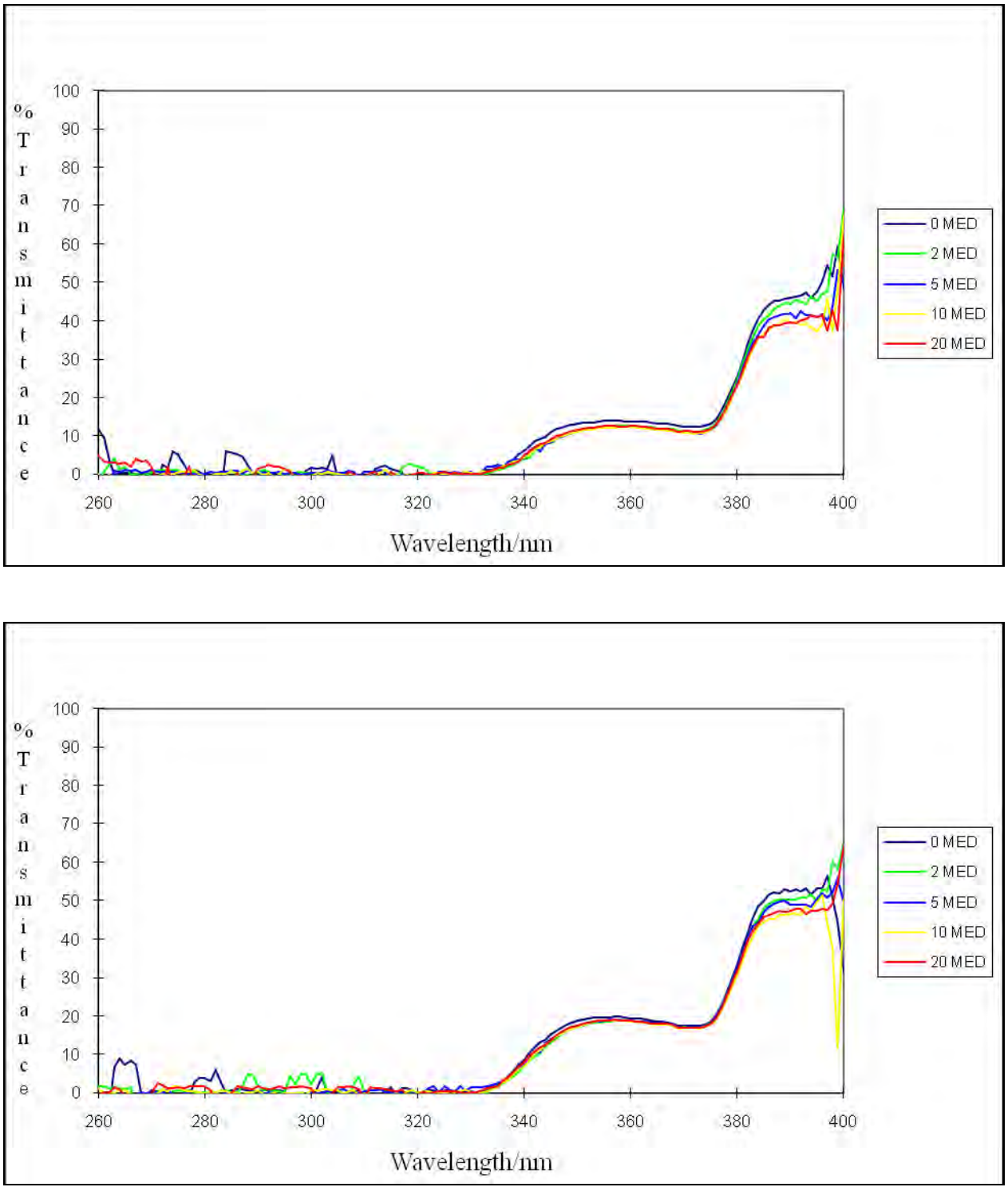

Figure E10 The UV transmission spectra of sample AU8 with increasing doses of UV radiation.

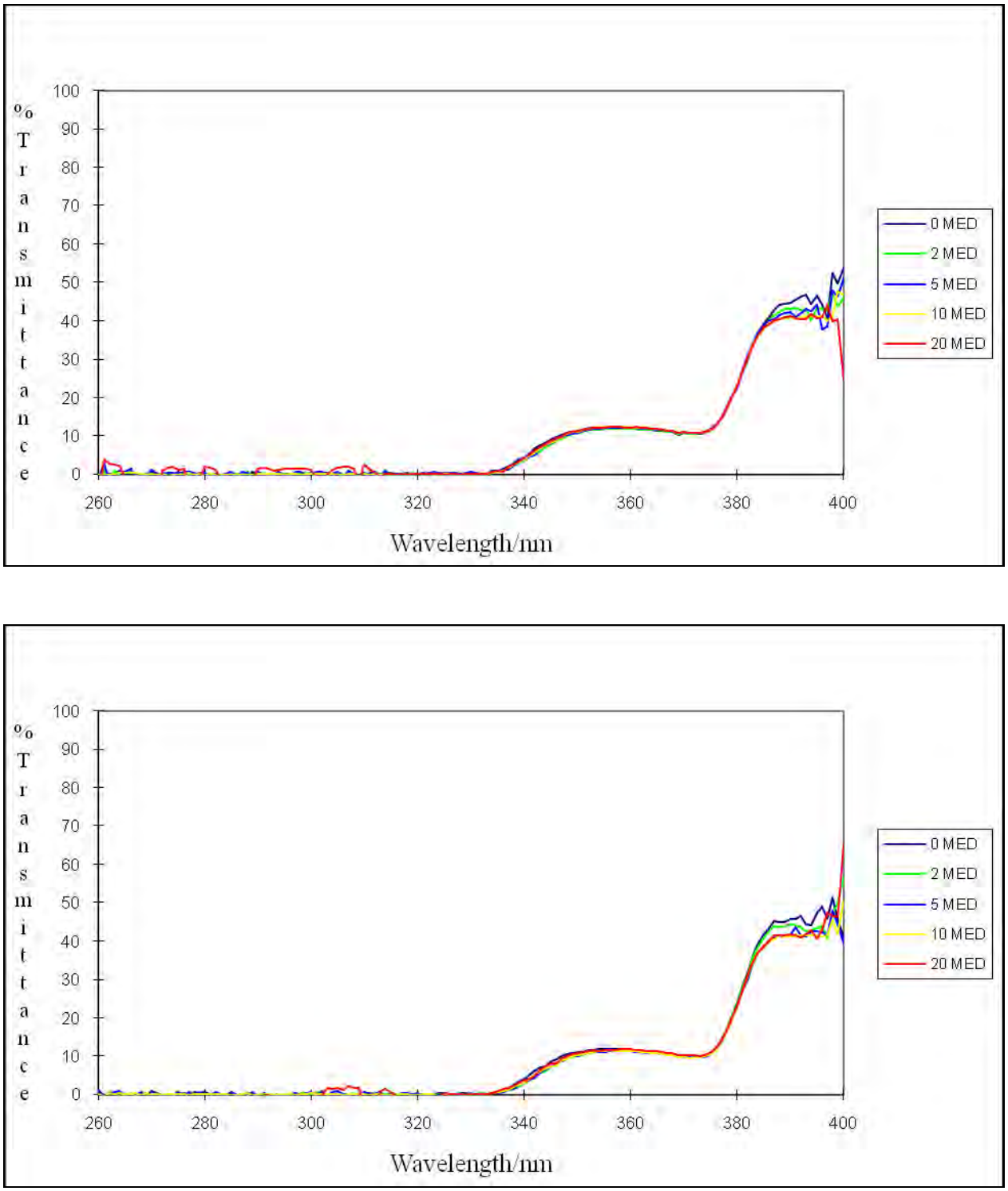

Figure E11 The UV transmission spectra of sample AU12 with increasing doses of UV radiation.

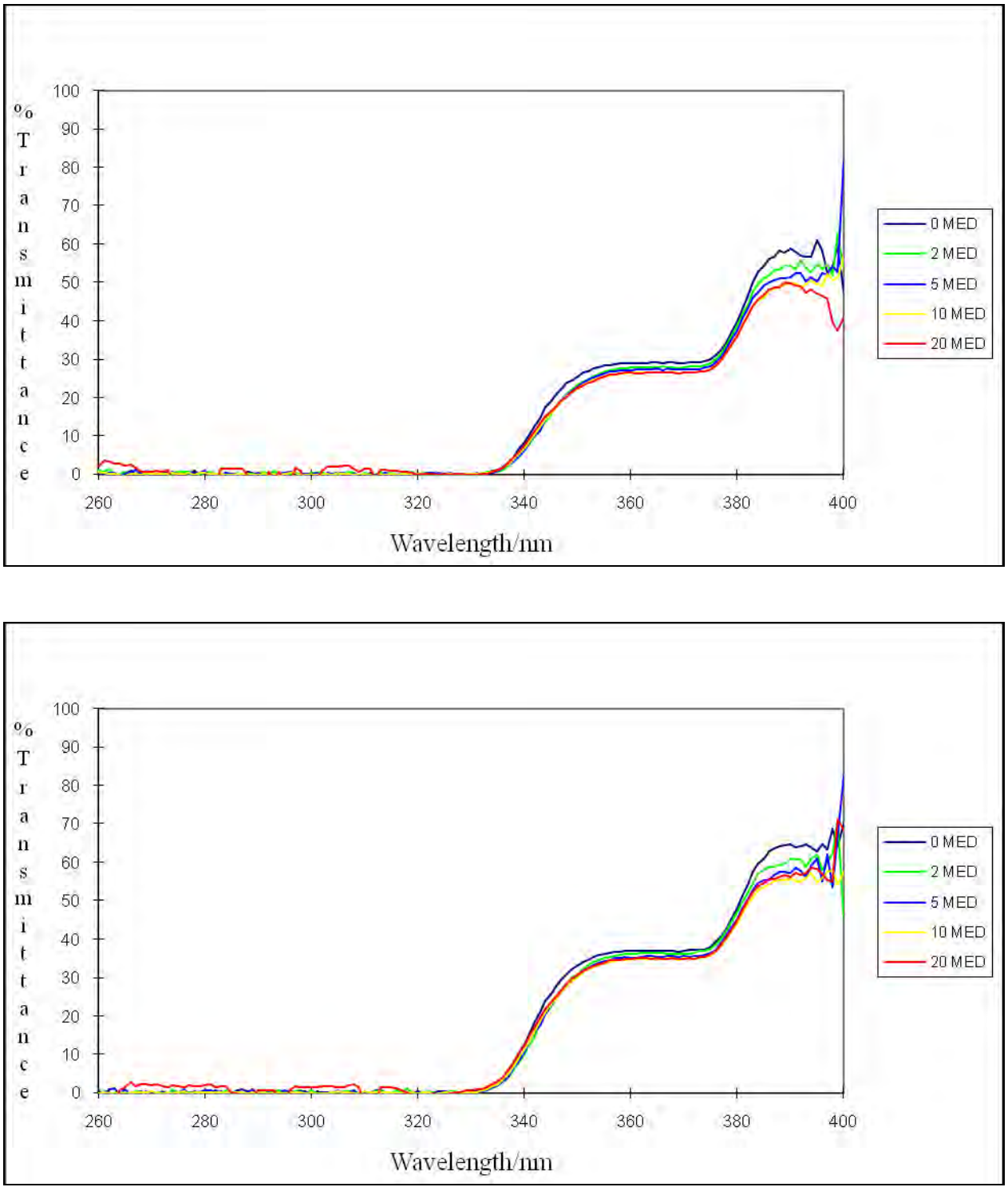

Figure E12 The UV transmission spectra of sample AU14 with increasing doses of UV radiation.

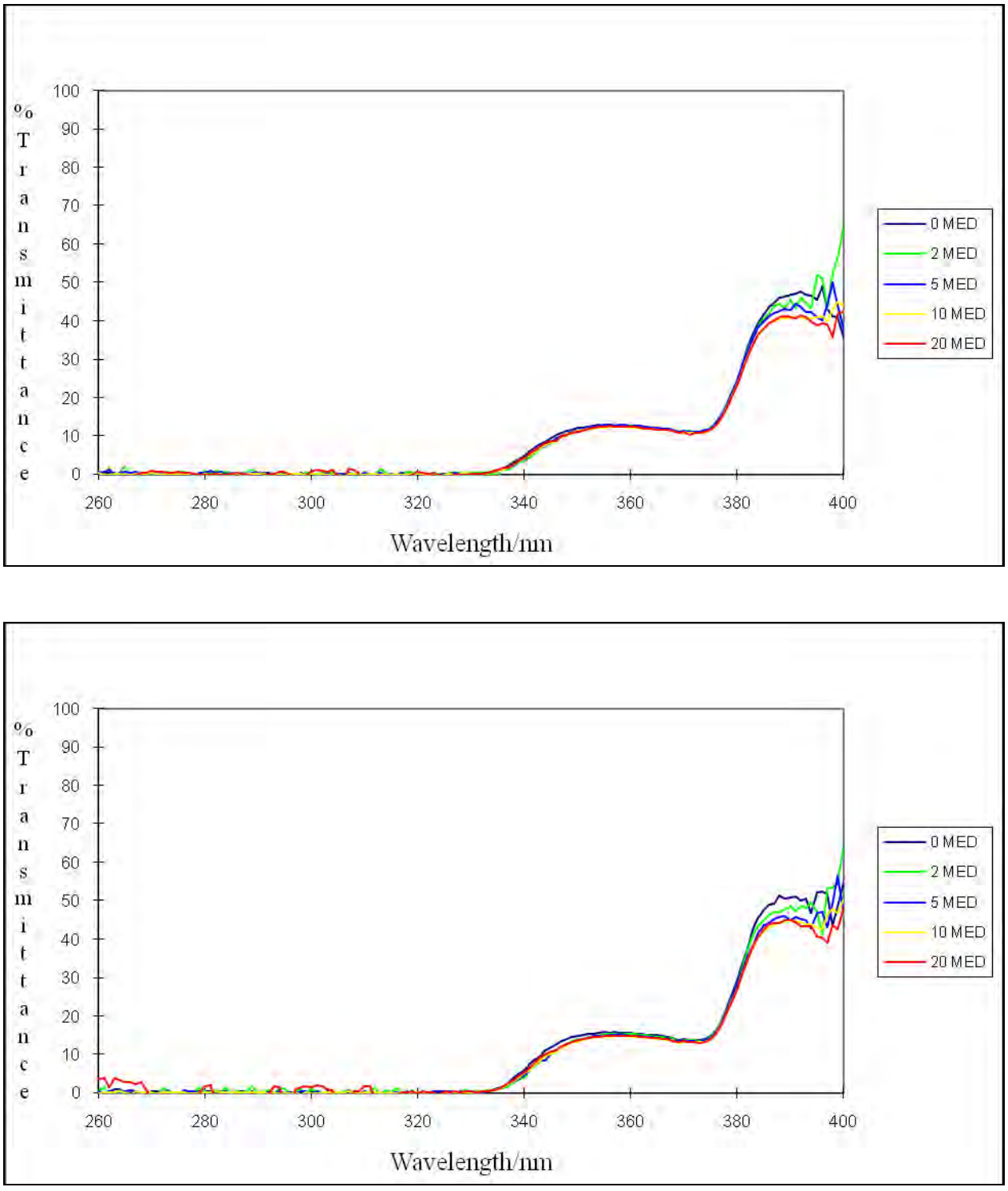

Figure E13 The UV transmission spectra of sample AU16 with increasing doses of UV radiation.

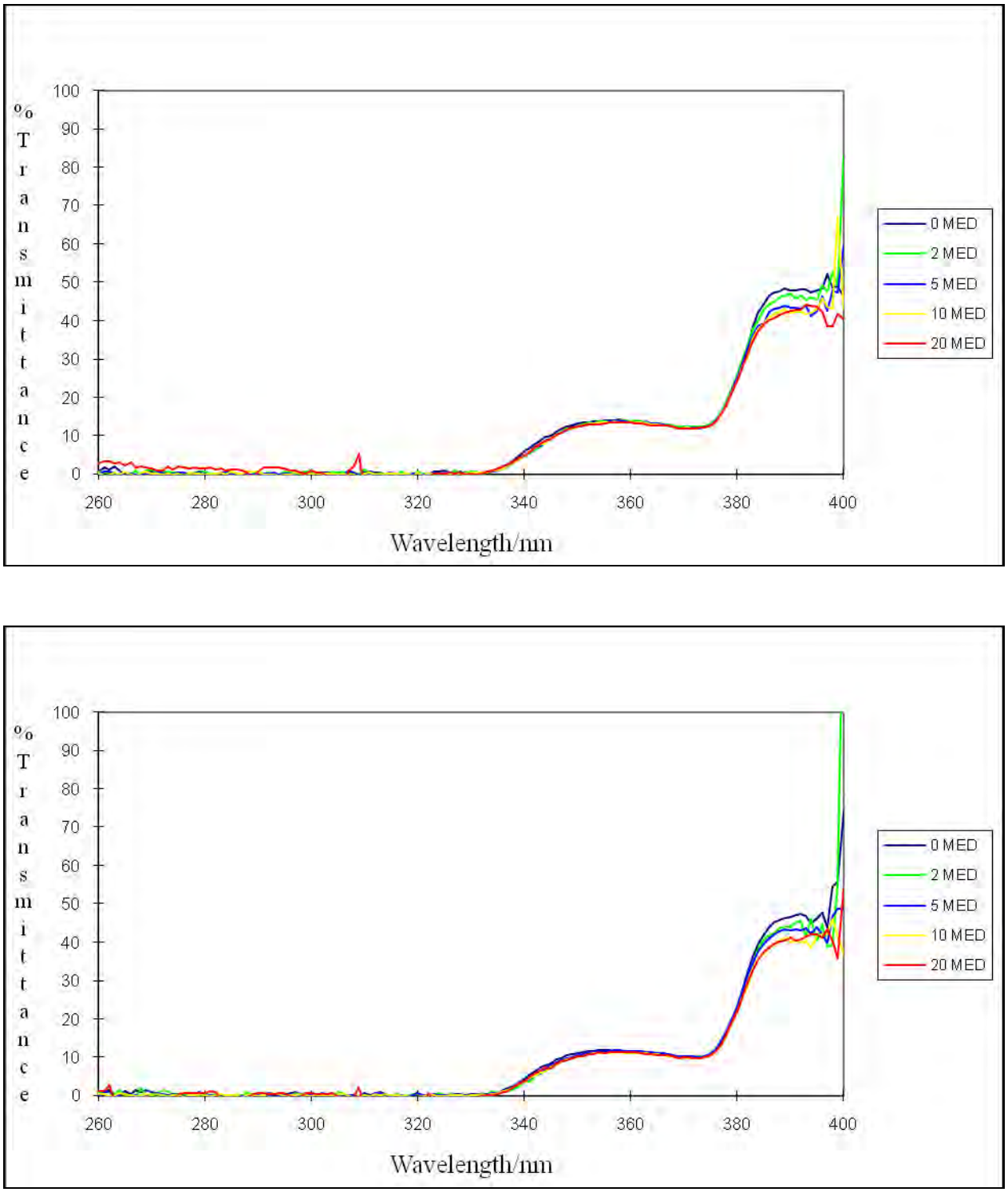

Figure E14 The UV transmission spectra of sample AU17 with increasing doses of UV radiation.

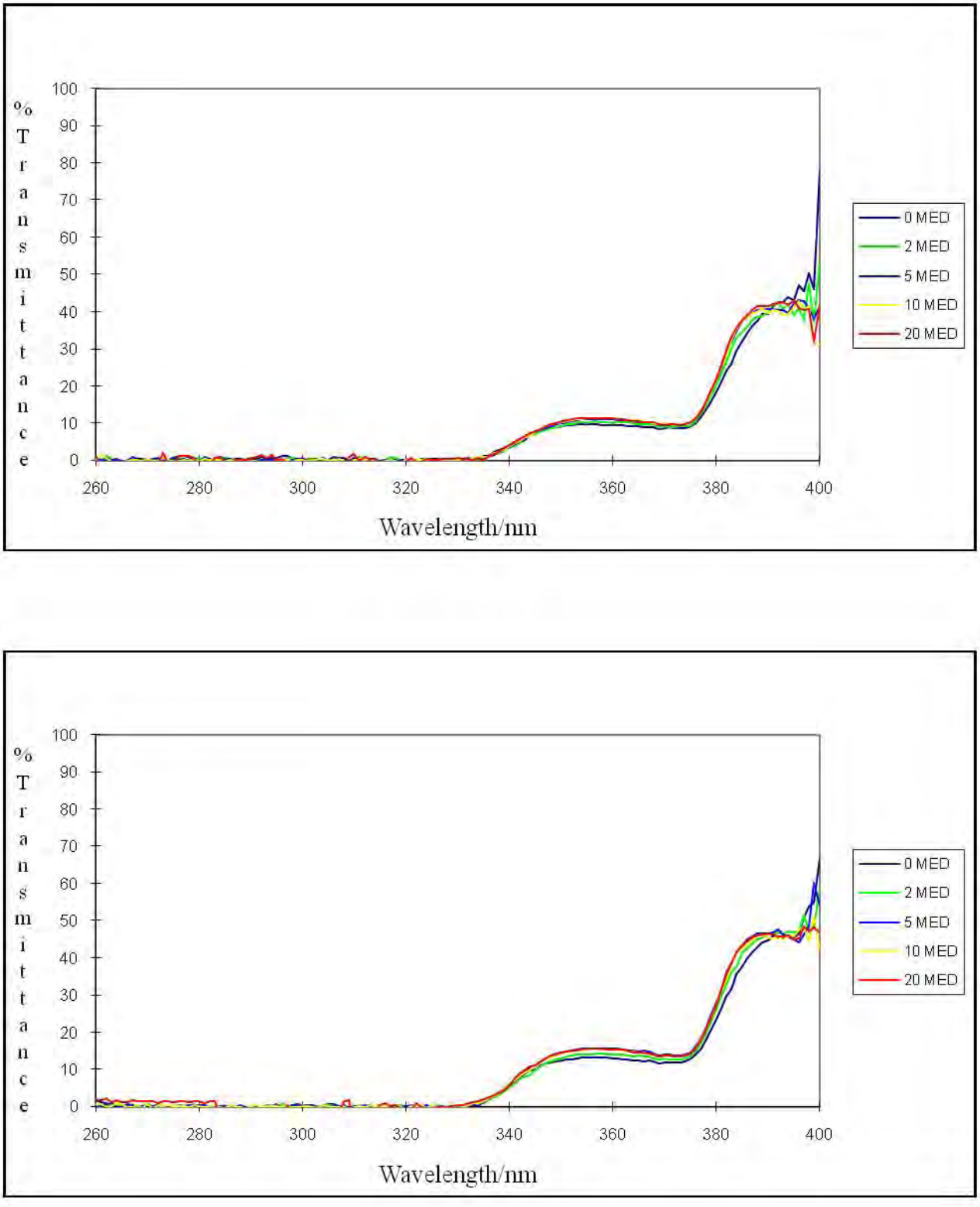

Figure E15 The UV transmission spectra of sample AU19 with increasing doses of UV radiation.

Filter combination: 2-EHMC, PBSA, TiO_2

Samples: AU3

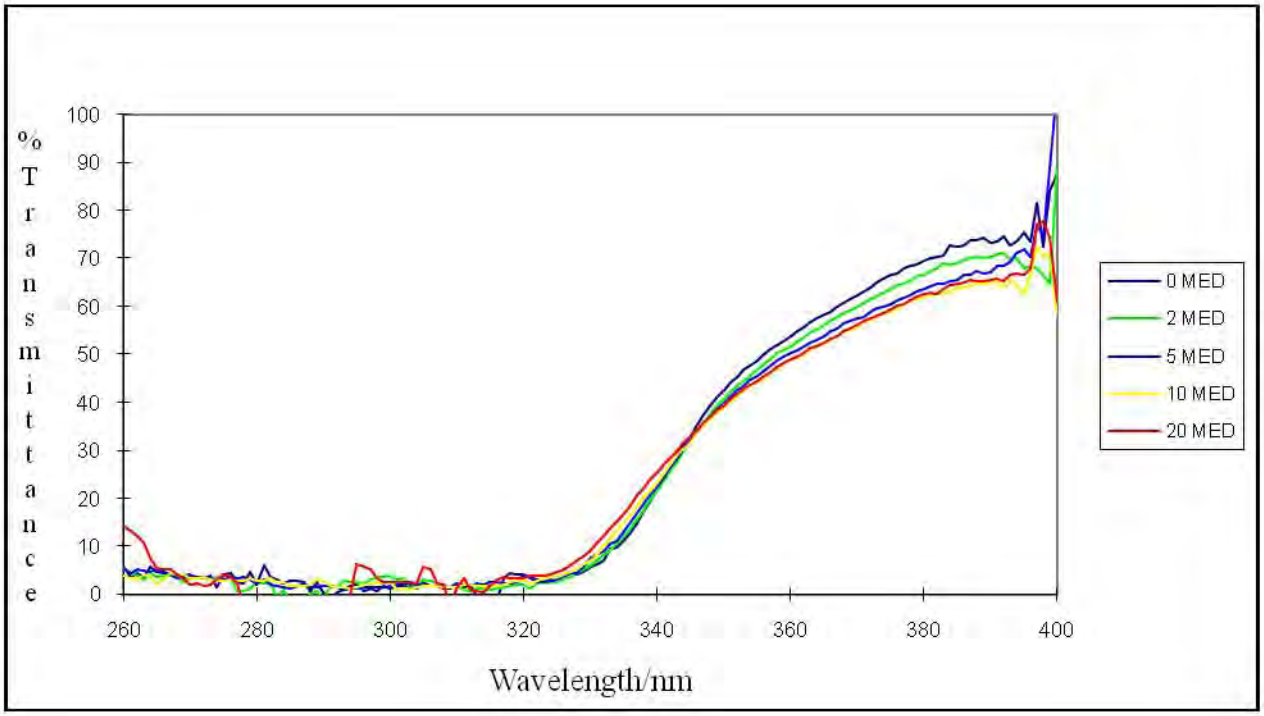

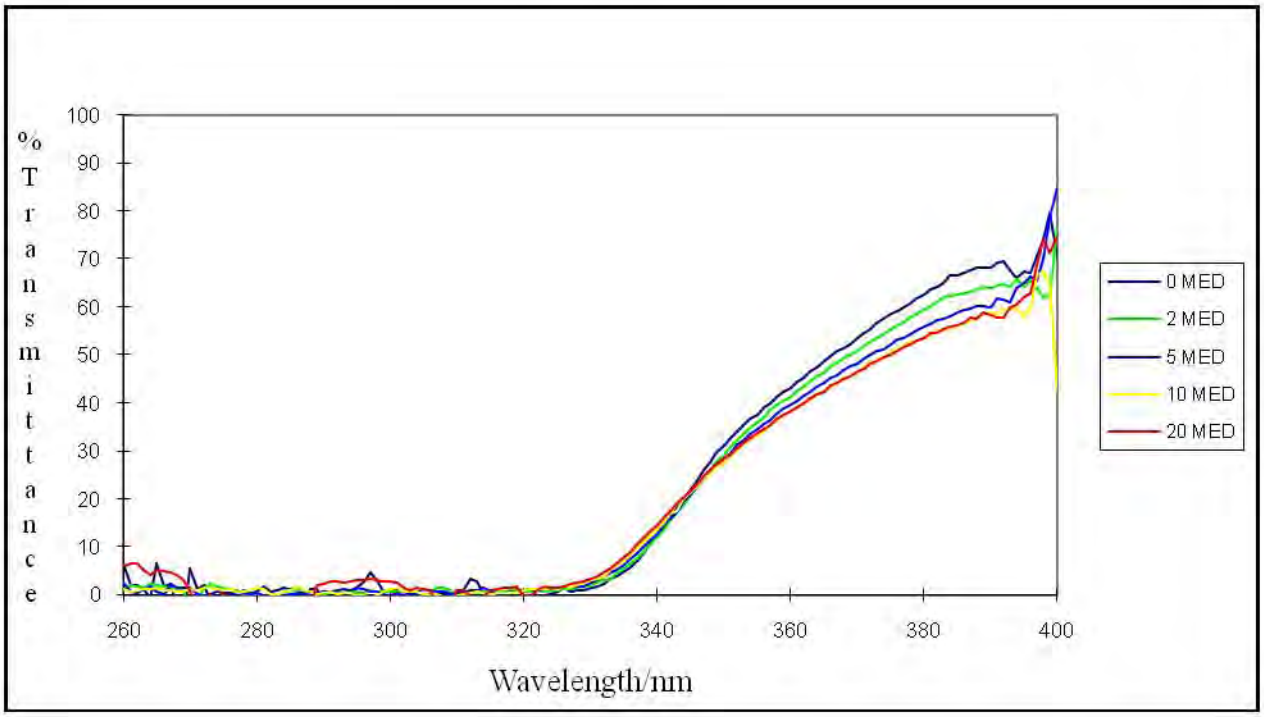

Figure E16 The UV transmission spectra of sample AU3 with increasing doses of UV radiation.

Filter combination: 2-EHMC, OCT, ZnO

Samples: AU4, AU21, AU22

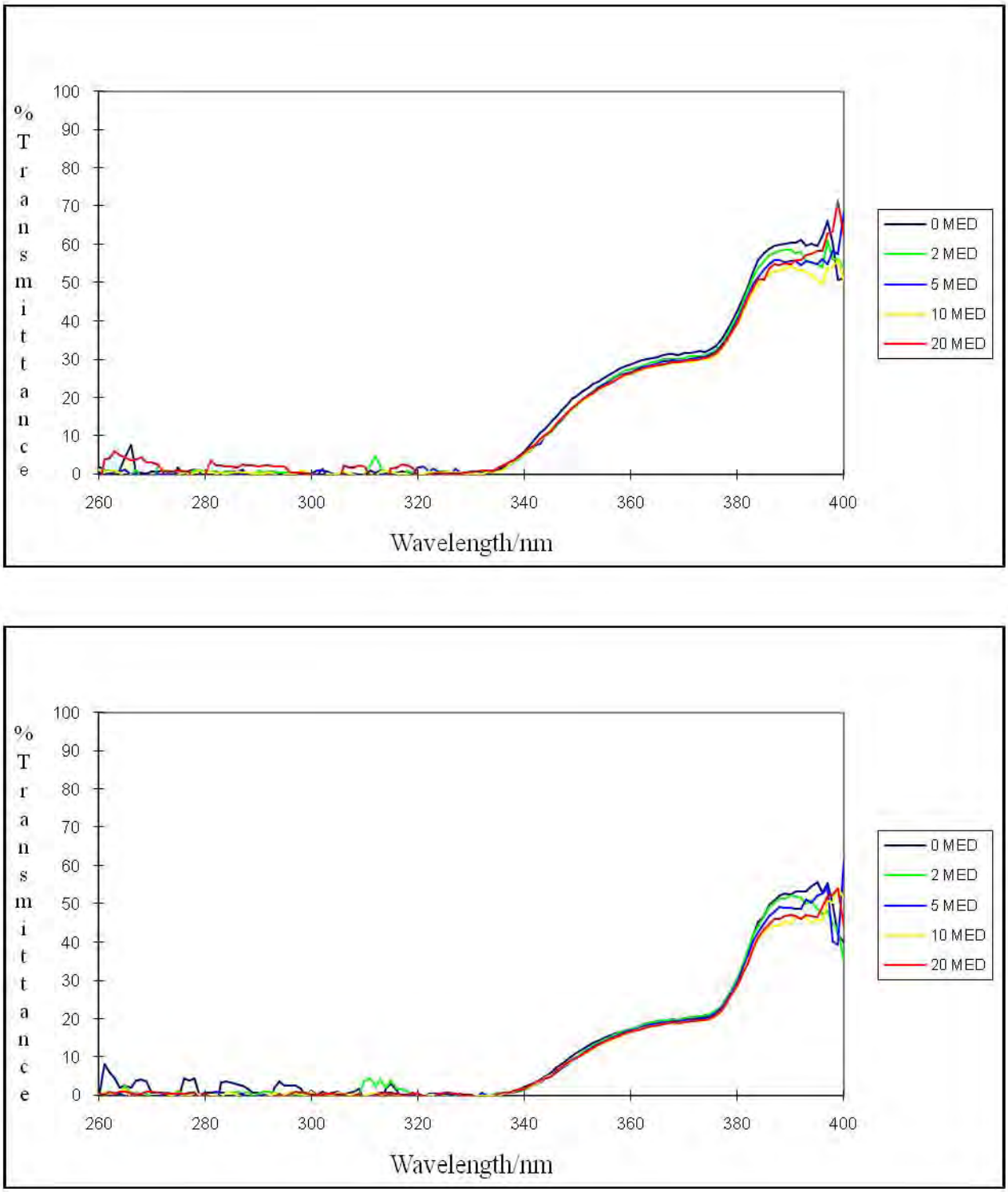

Figure E17 The UV transmission spectra of sample AU4 with increasing doses of UV radiation.

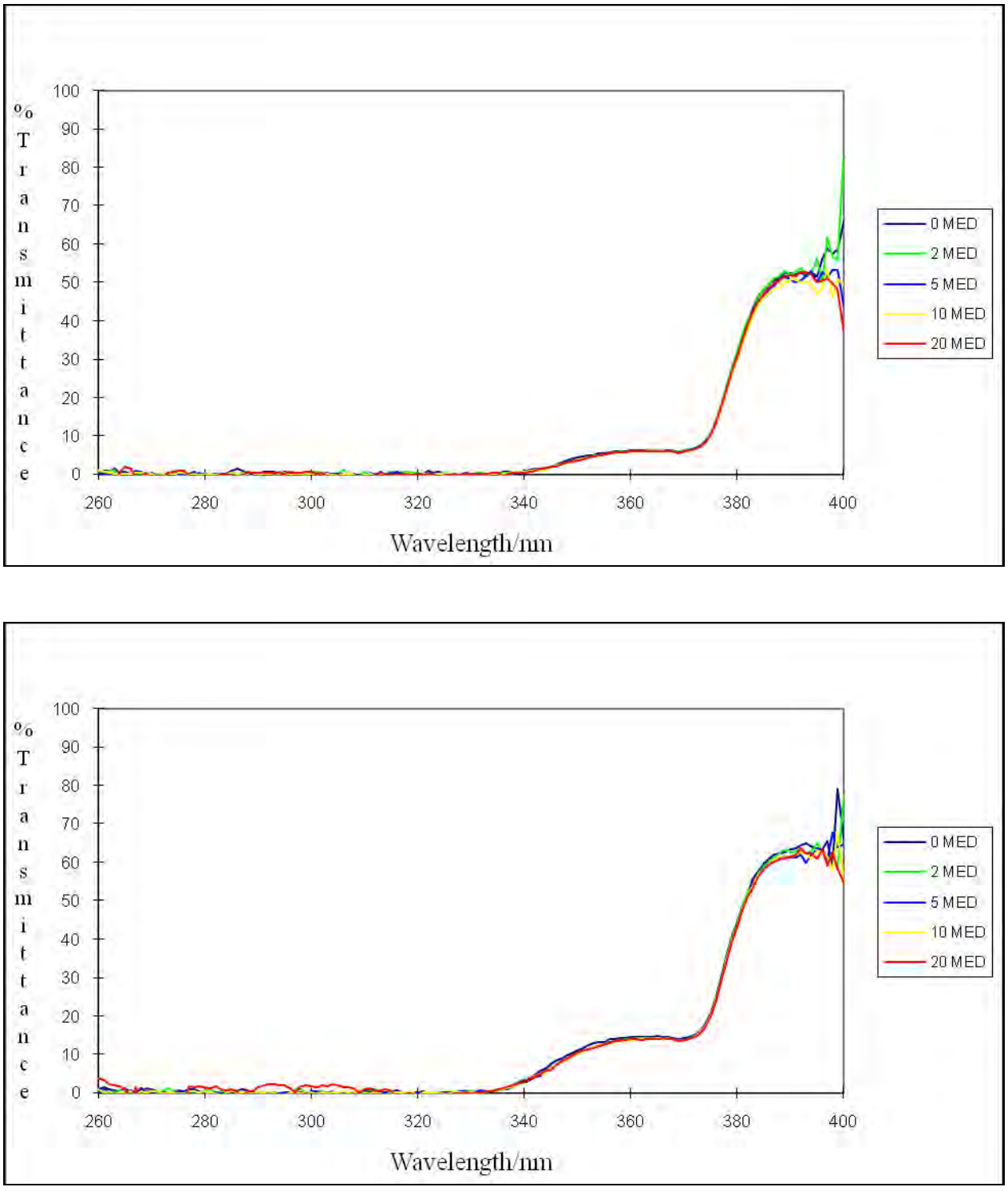

Figure E18 The UV transmission spectra of sample AU21 with increasing doses of UV radiation.

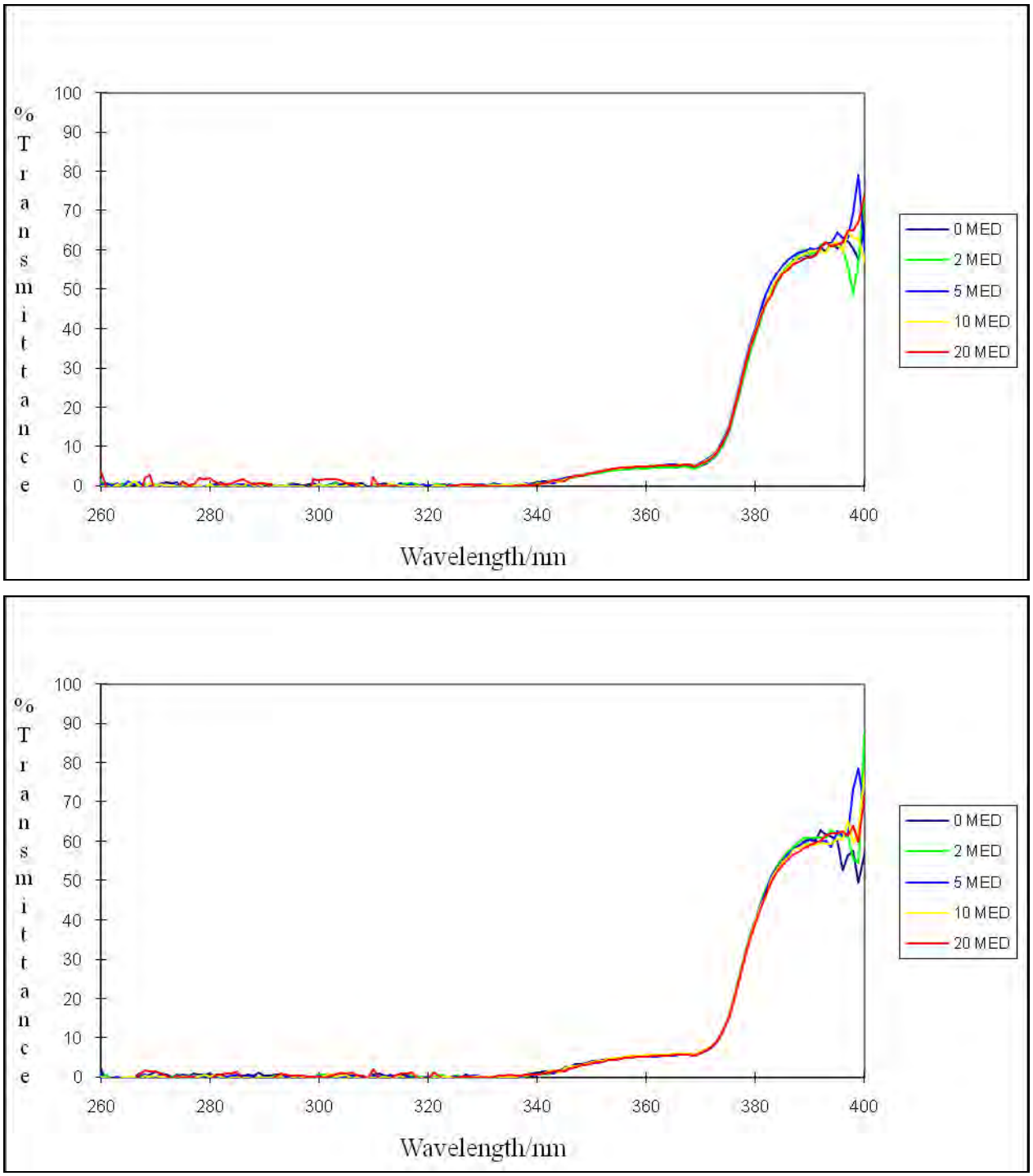

Figure E19 The UV transmission spectra of AU22 with increasing doses of UV radiation.

Filter combination: 2-EHMC, Benz-3, TiO_2

Samples: AU9 and AU13

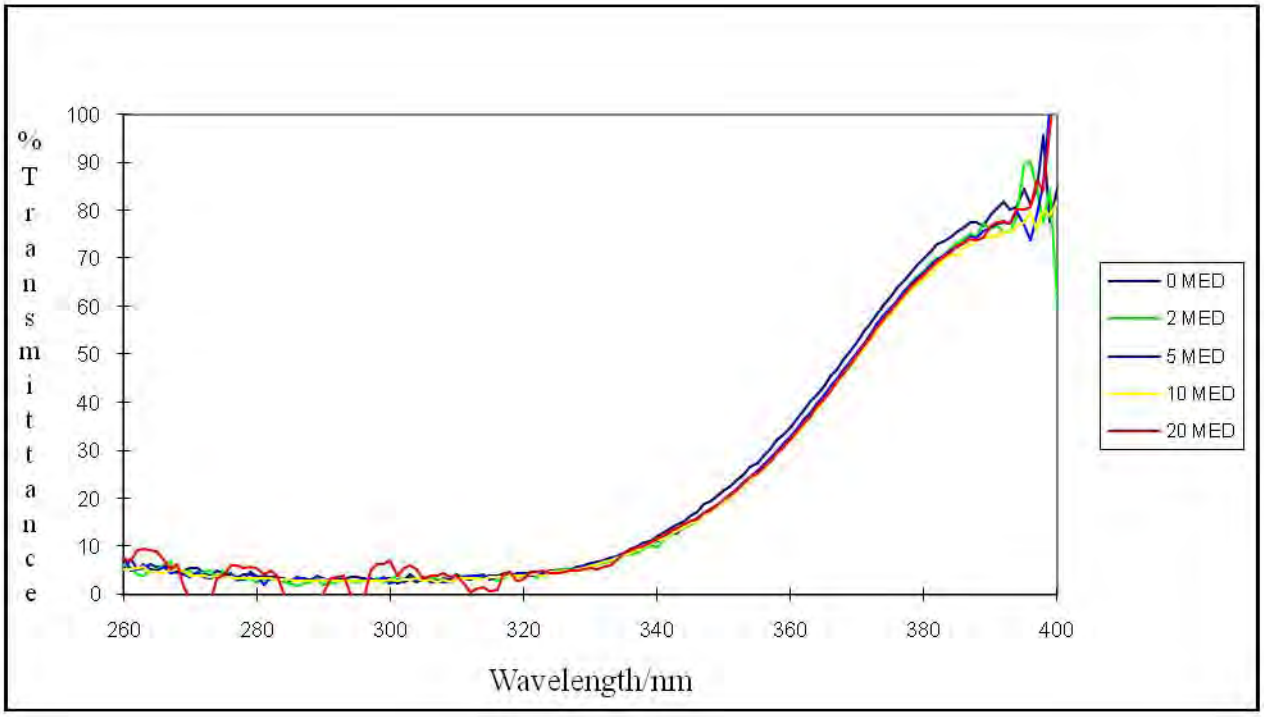

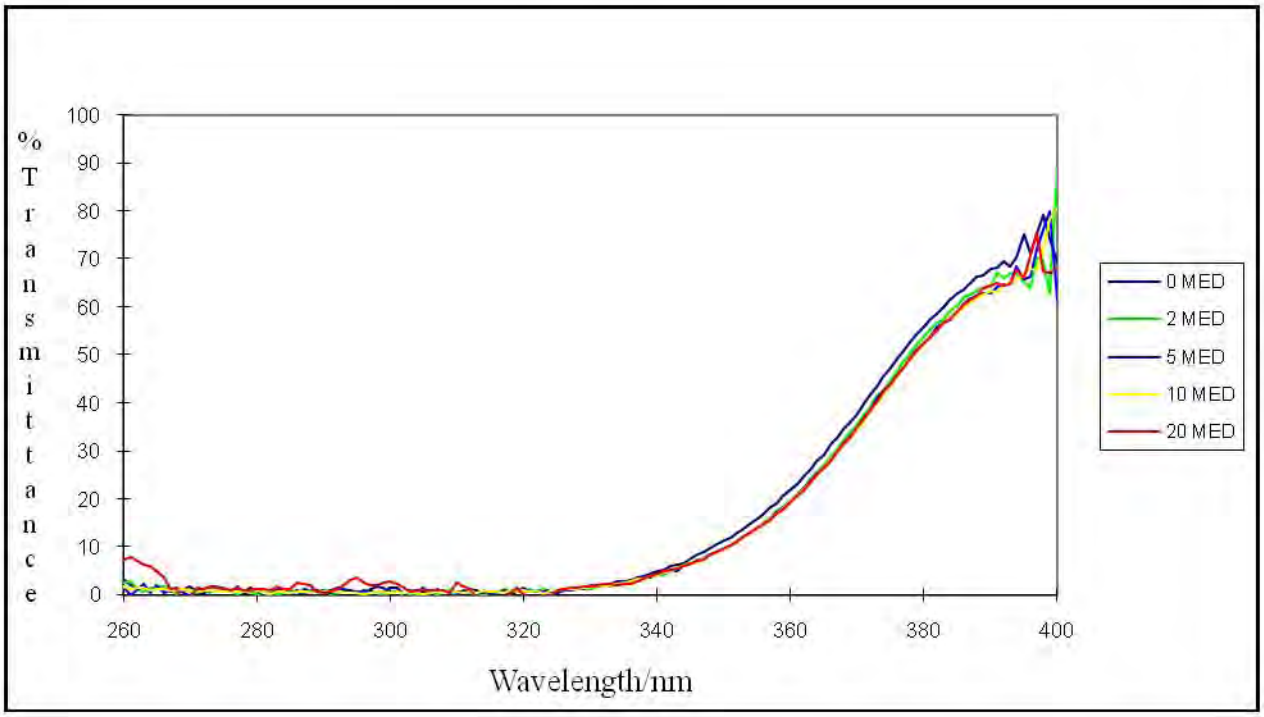

Figure E20 The UV transmission spectra of sample AU9 with increasing doses of UV radiation.

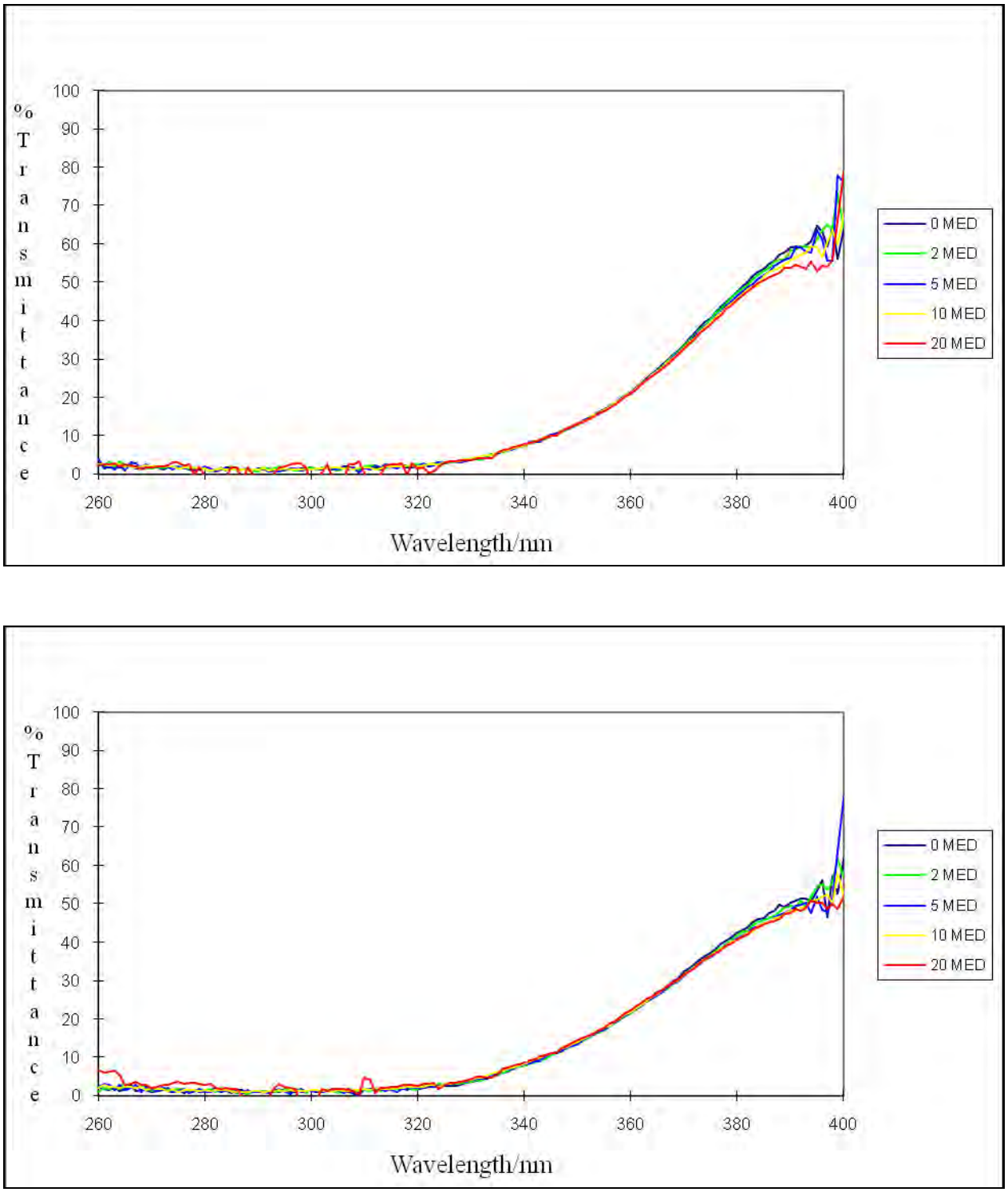

Figure E21 The UV transmission spectra of sample AU 13 with increasing doses of UV radiation.

Filter combination: 2-EHMC, AVO and OT

Samples: AU15

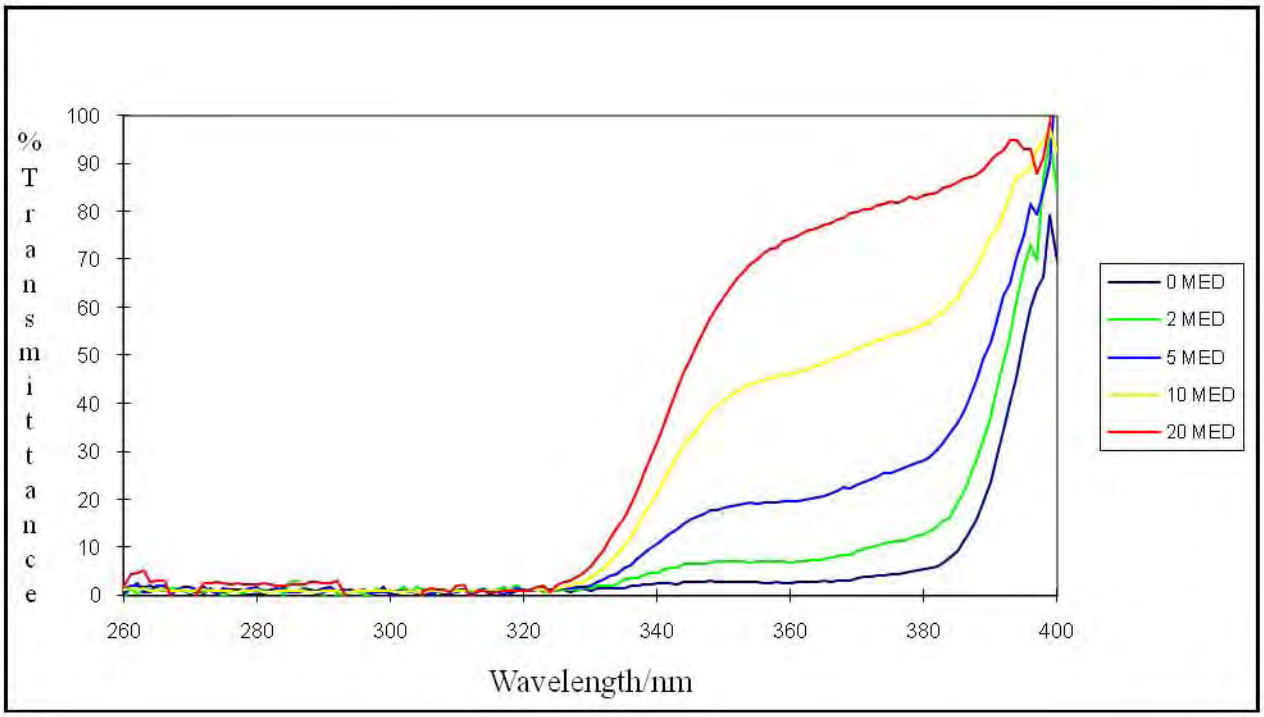

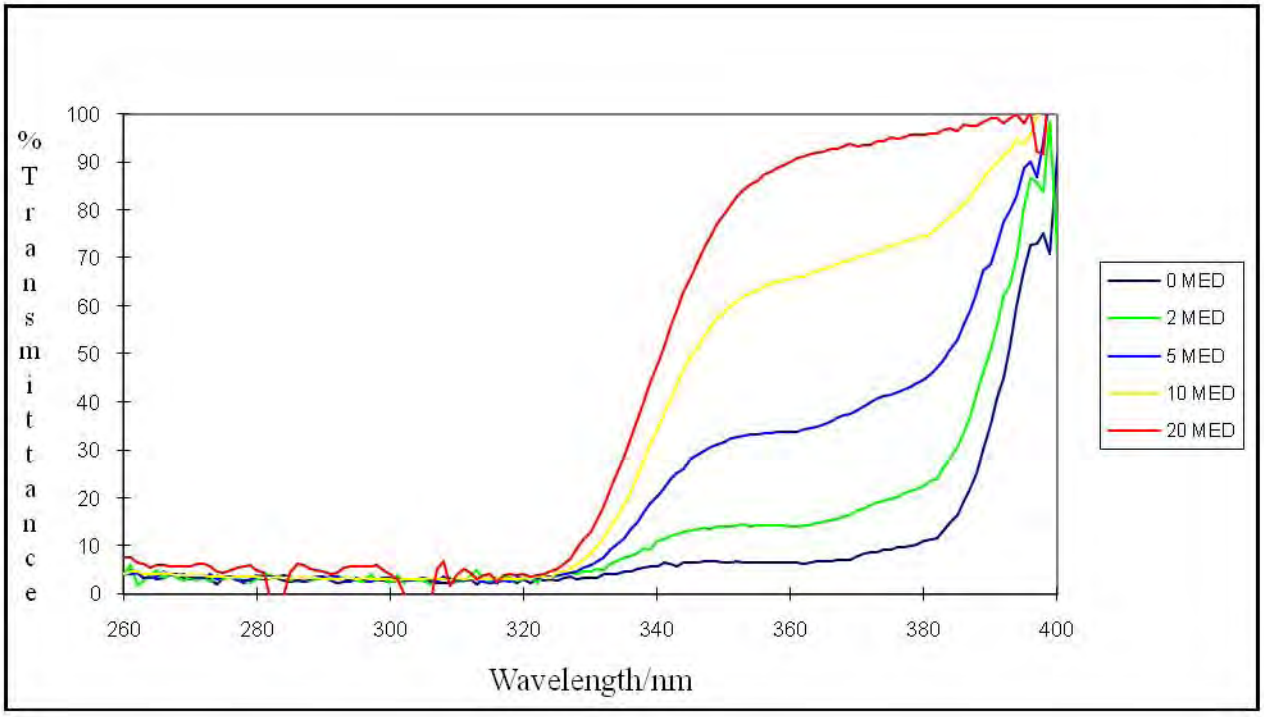

Figure E22 The UV transmission spectra of sample AU15 with increasing doses of UV radiation.

Filter combination: 2-EHMC, AVO, Benz-3 and TiO_2

Samples: AU24

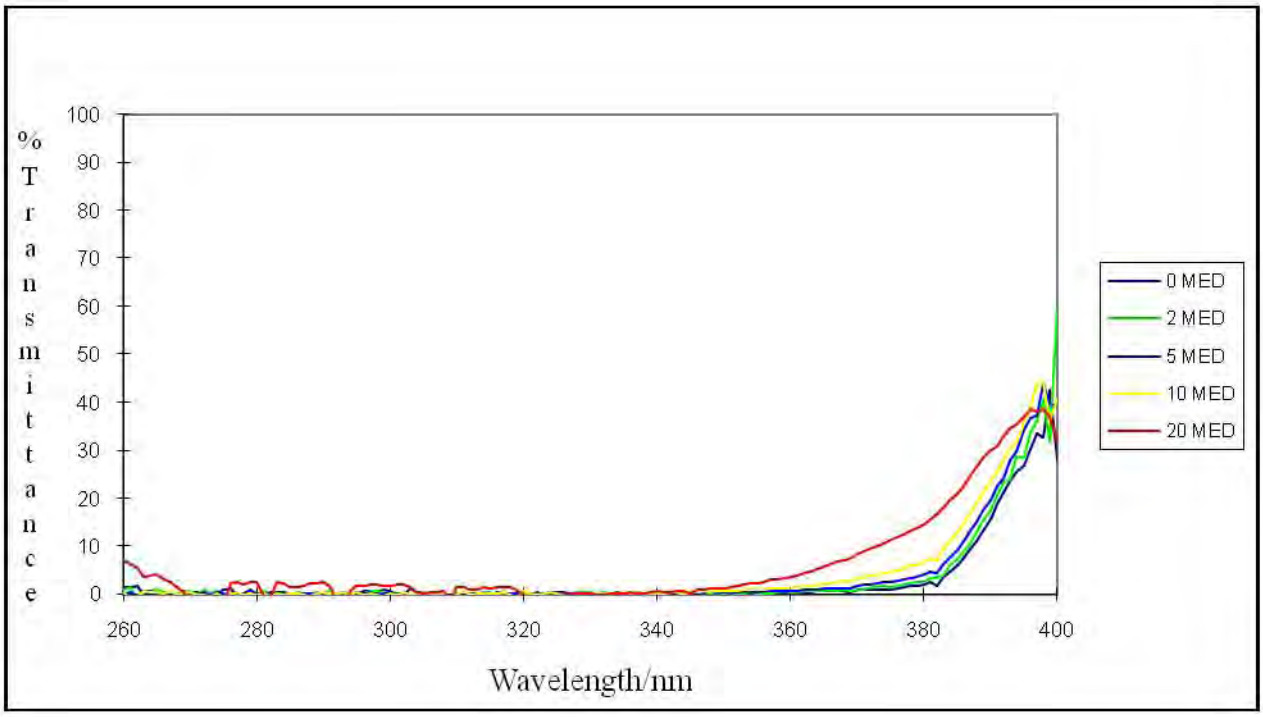

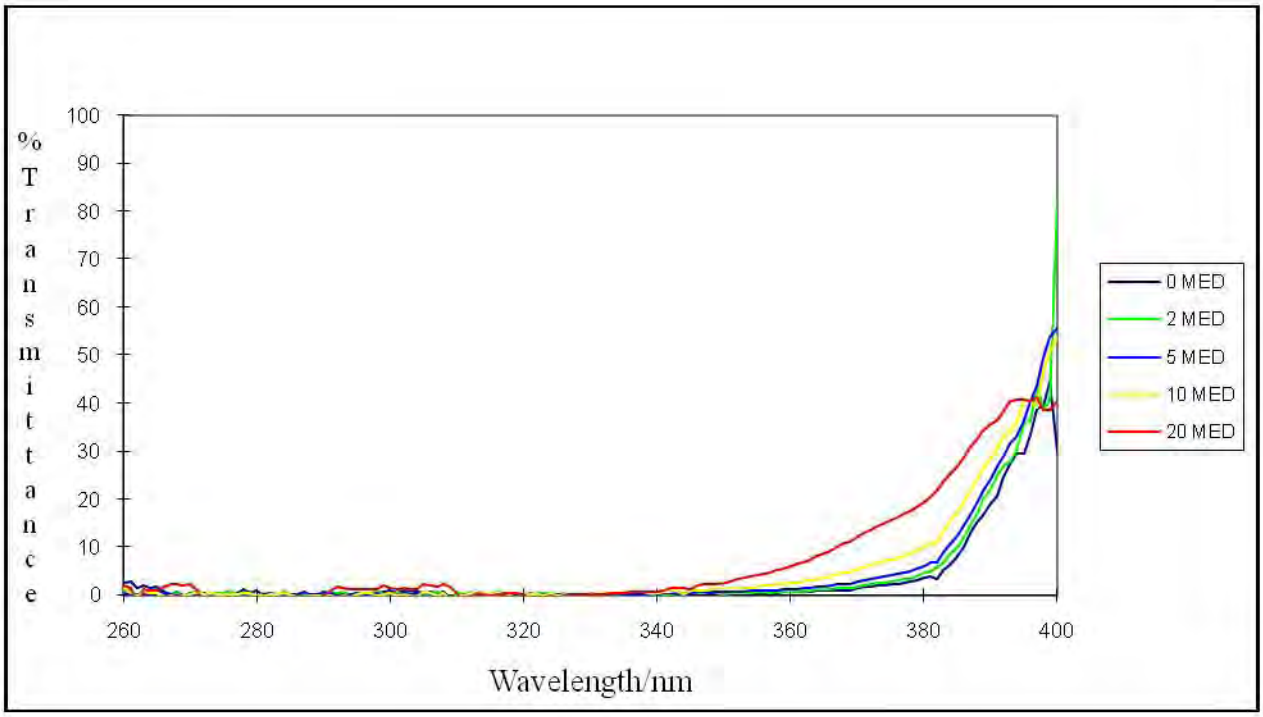

Figure E23 The UV transmission spectra of sample AU24 with increasing doses of UV radiation.

Filter combination: 2-EHMC, AVO, MBC and OT

Samples: AU7

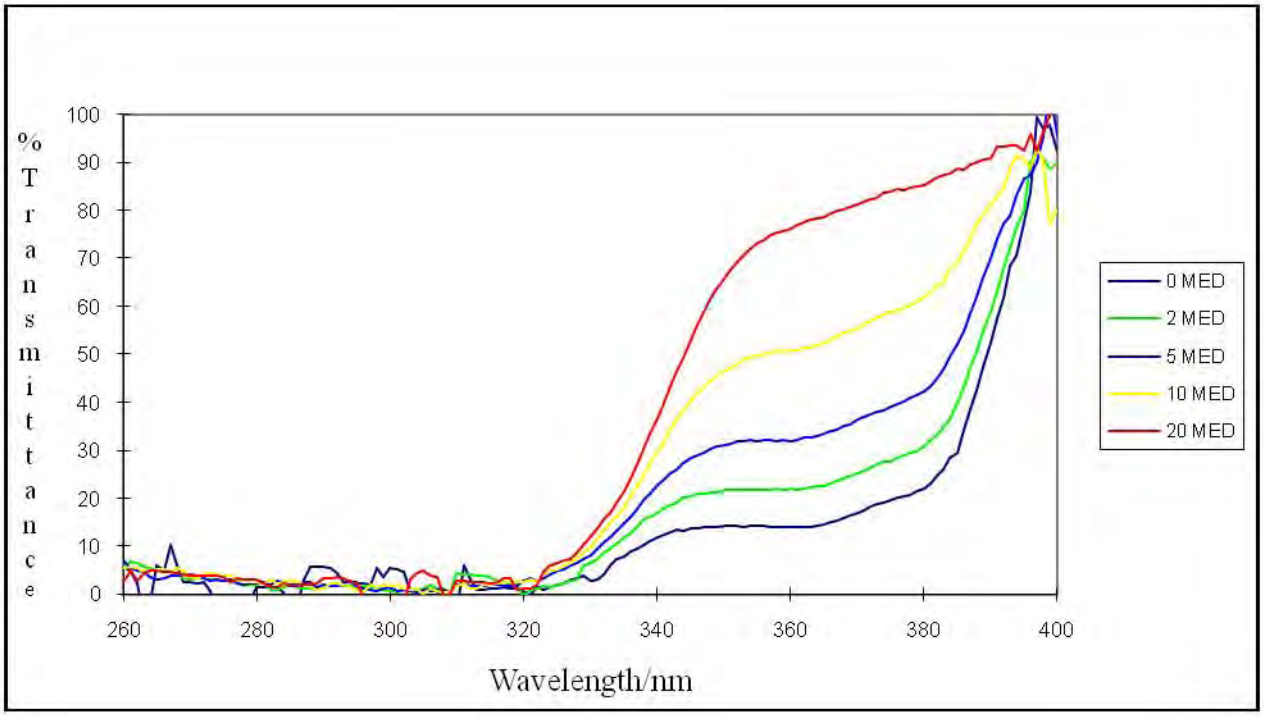

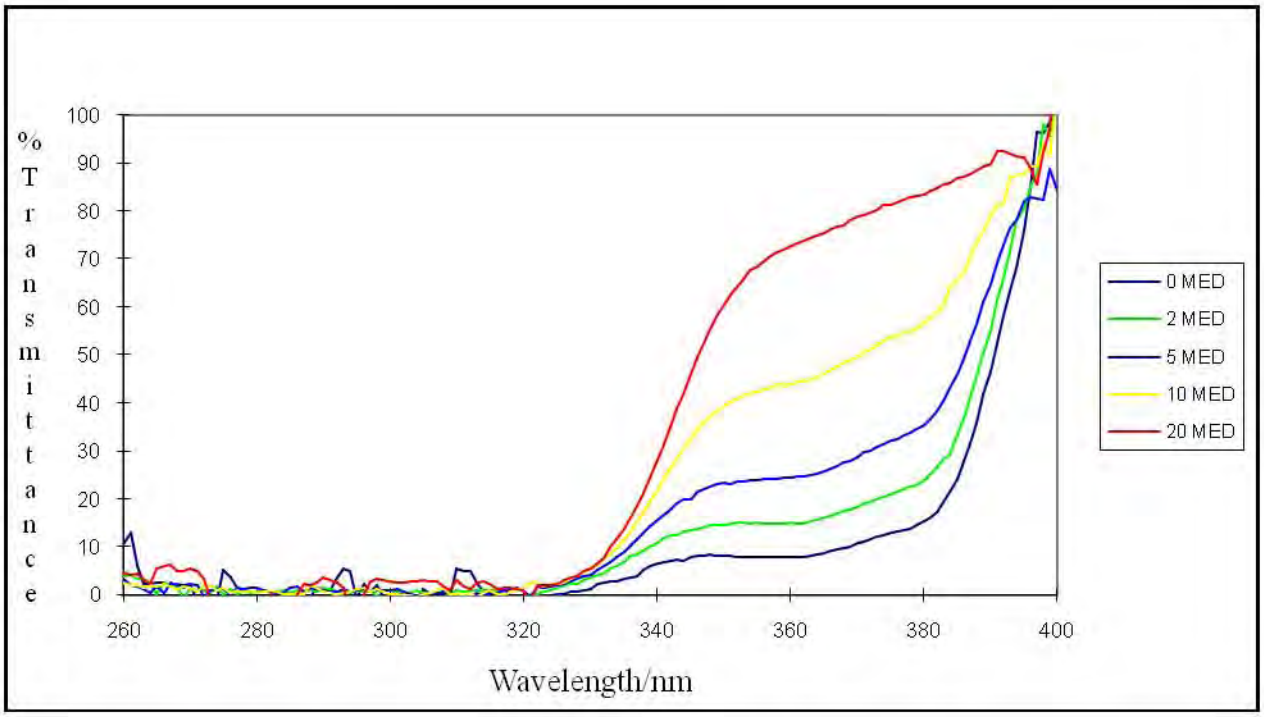

Figure E24 The UV transmission spectra of sample AU7 with increasing doses of UV radiation.

Filter combination: 2-EHMC, Benz-3, HS and ODM-PABA

Samples: AU20

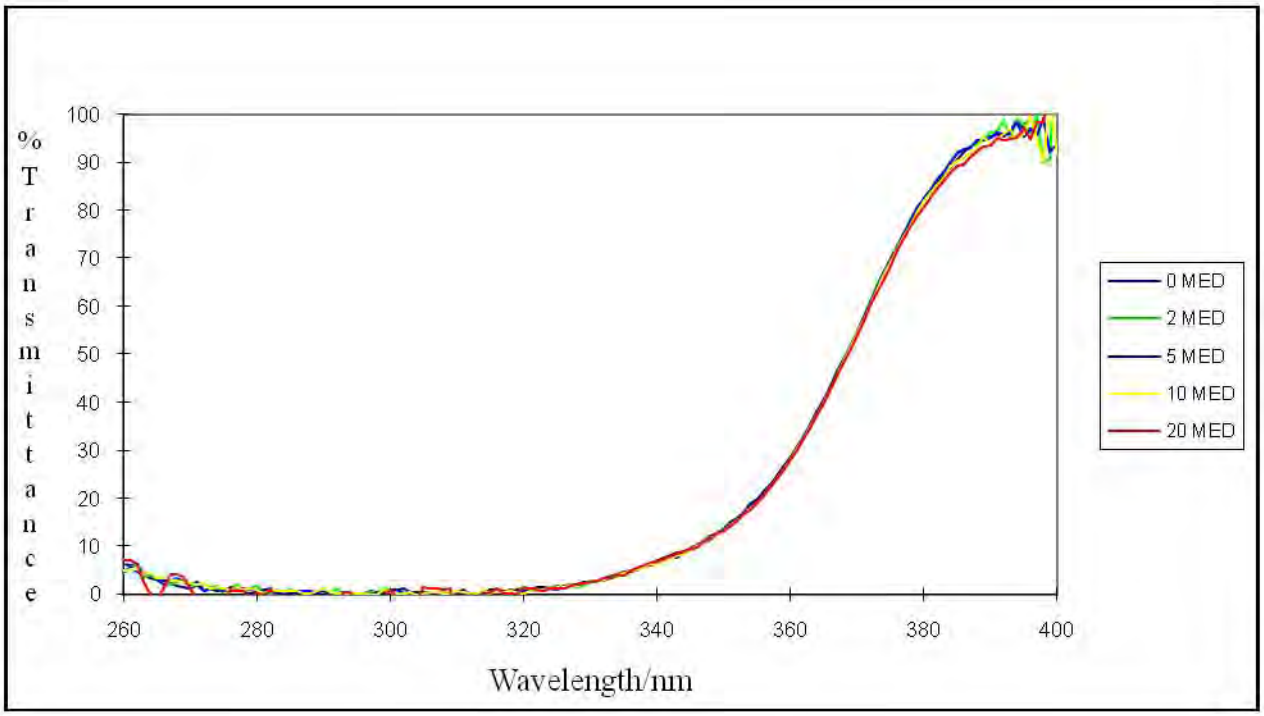

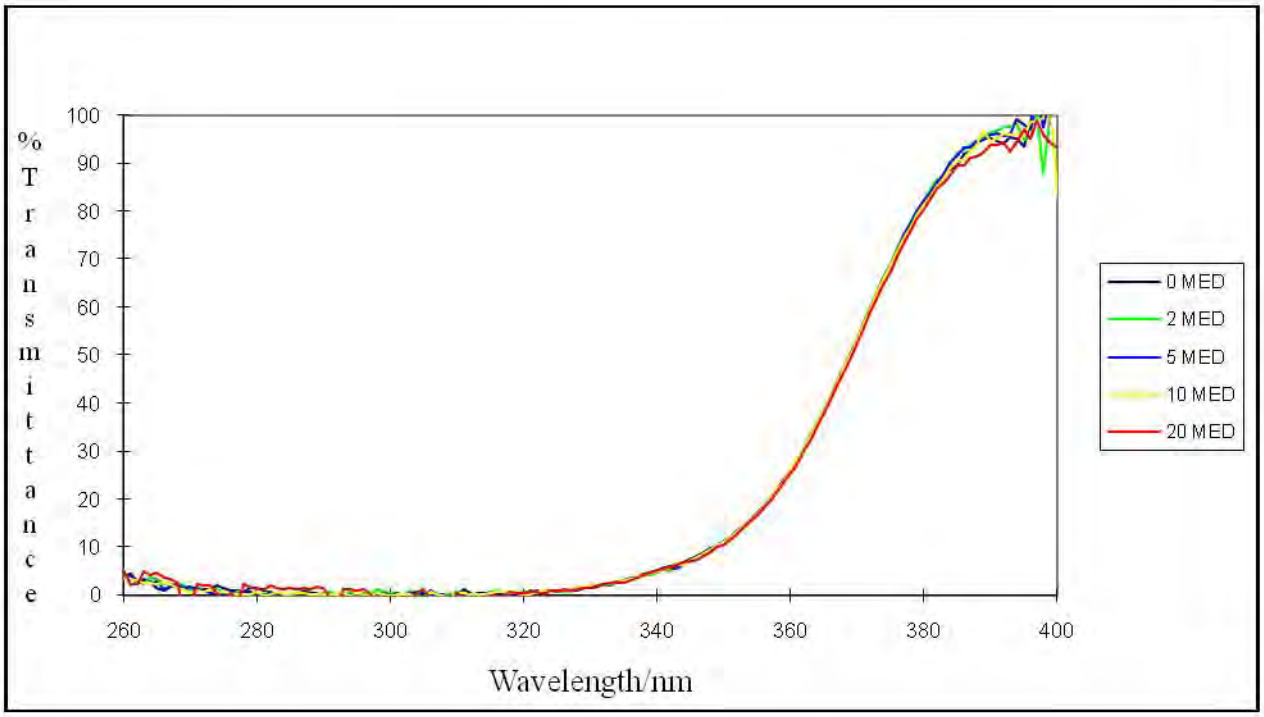

Figure E25 The UV transmission spectra of AU20 with increasing doses of UV radiation.

APPENDIX F

HPLC chromatograms for suncare products

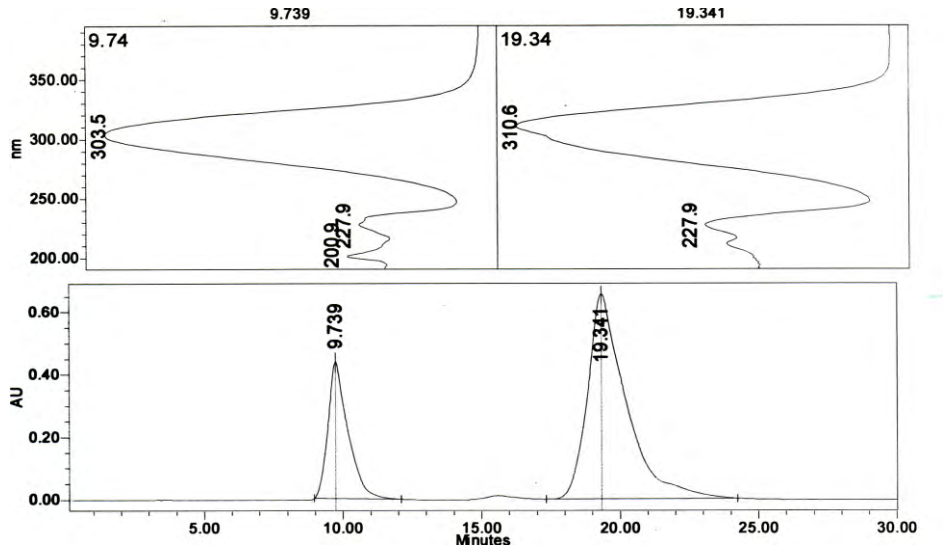

Figure F1 HPLC chromatogram of irradiated AU 1 separated on a Nucleosil C100 C_{18} column, eluent: 85% MeOH/H_2O, flow rate: 1 mL min^{-1}, injection volume: 10 µL and detection wavelength: 310 nm. The order of elution is MBC, and *trans*-2-EHMC.

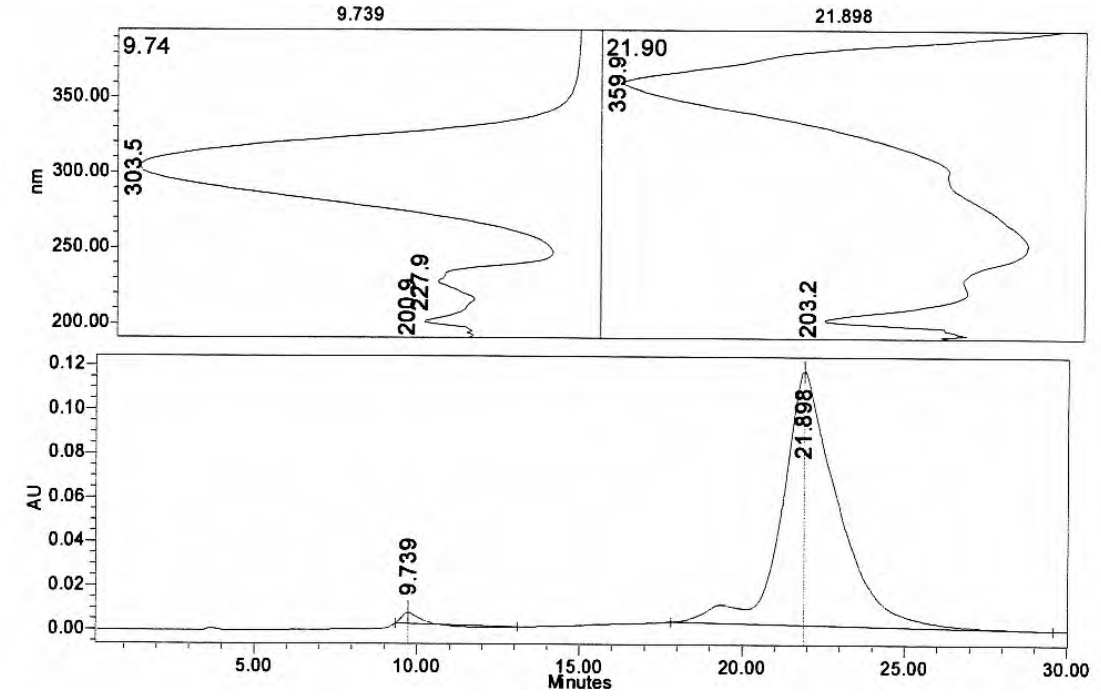

Figure F2 The HPLC chromatogram of unirradiated AU1 separated on Nucleosil C100 C_{18} column, eluent: 85% MeOH/H_2O, flow rate: 1 mL min^{-1}, injection volume: 10 µL and detection wavelength: 360 nm. The order of elution is MBC, *trans*-2-EHMC and AVO.

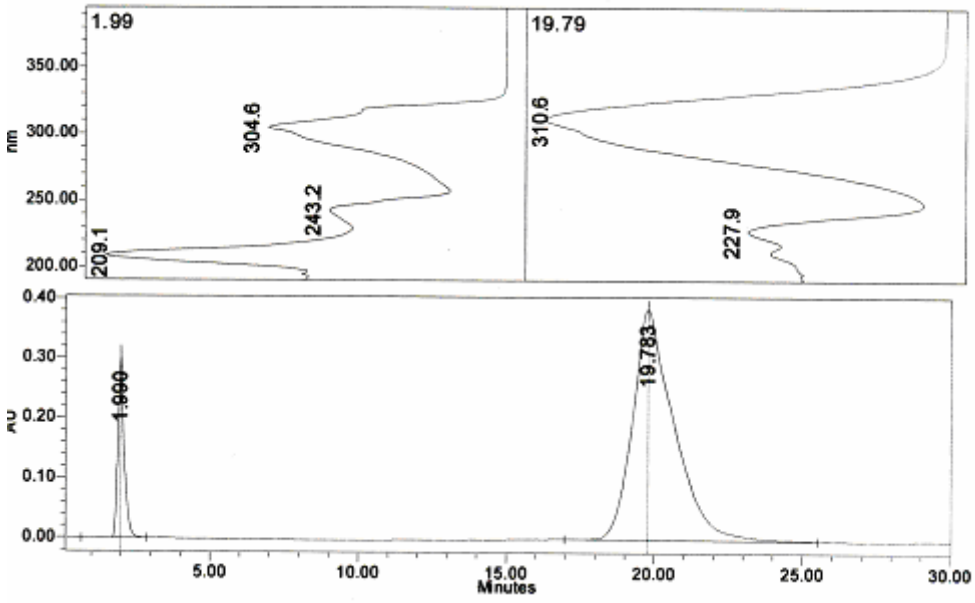

Figure F3 HPLC chromatogram of irradiated AU 3 separated on a Nucleosil C100 C_{18} column, eluent: 85% MeOH/H_2O, flow rate: 1 mL min^{-1}, injection volume: 10 µL and detection wavelength: 310 nm. The order of elution is PBSA and *trans*-2-EHMC.

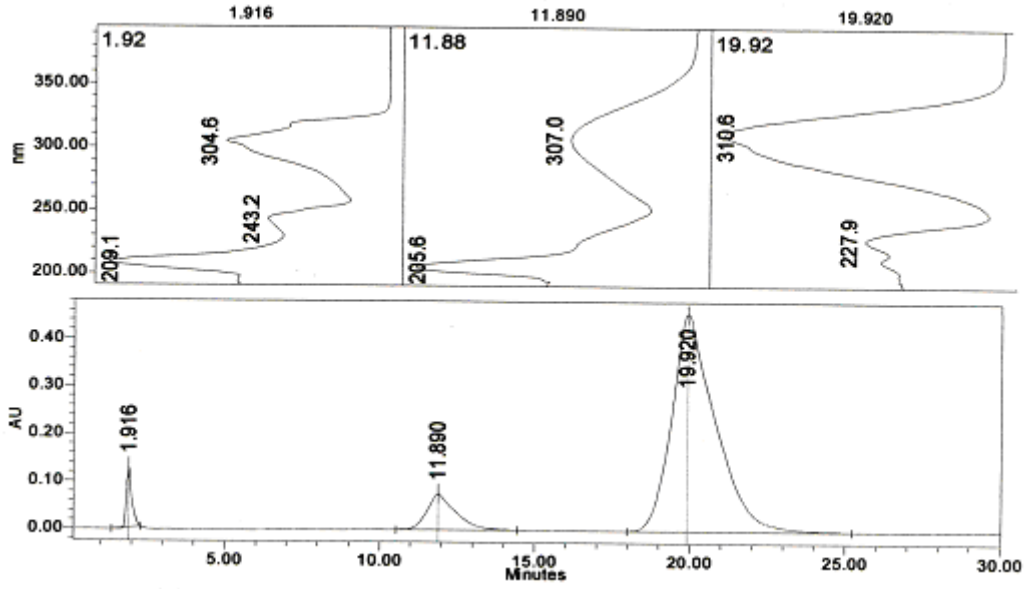

Figure F4 HPLC chromatogram of irradiated AU 4 separated on a Nucleosil C100 C_{18} column, eluent: 85% MeOH/H_2O, flow rate: 1 mL min^{-1}, injection volume: 10 µL and detection wavelength: 310 nm. The order of elution is OCT, and *trans*-2-EHMC.

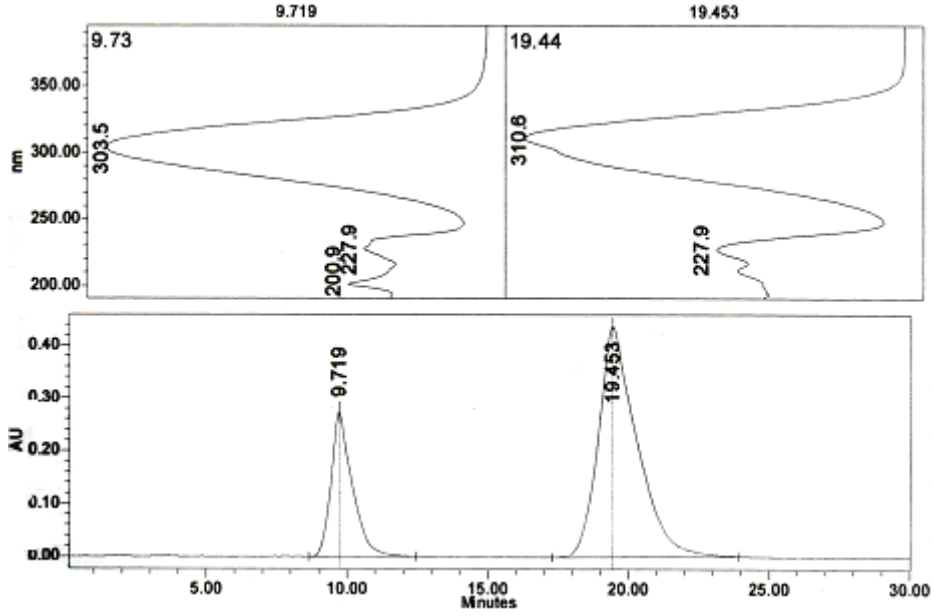

Figure F5 The HPLC chromatogram of unirradiated AU5 separated on Nucleosil C100 C_{18} column, eluent: 85% MeOH/H_2O, flow rate: 1 mL min^{-1}, injection volume: 10 µL and detection wavelength: 310 nm. The order of elution is MBC and *trans*-2-EHMC

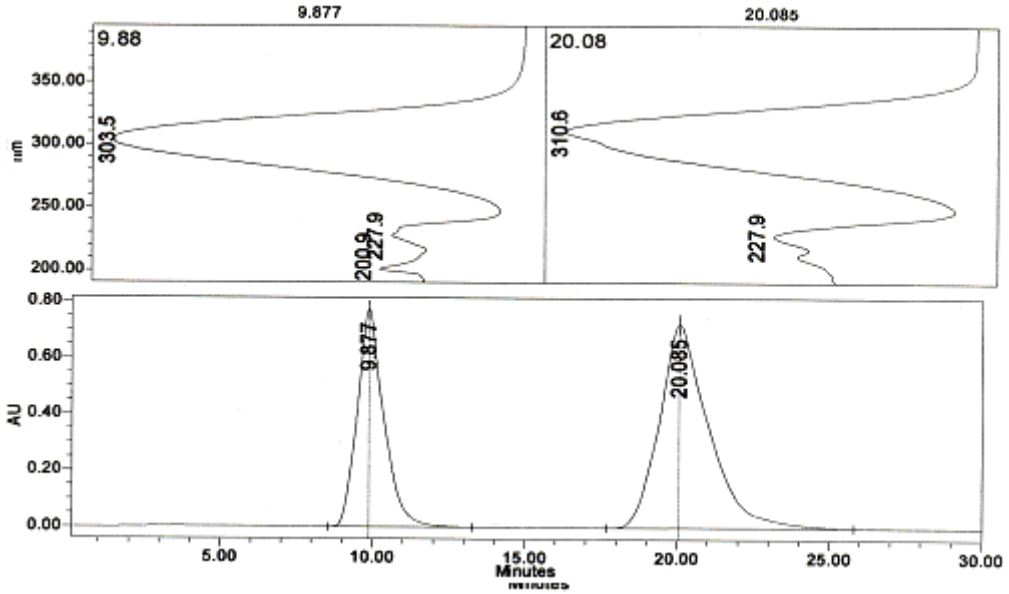

Figure F6 The HPLC chromatogram of unirradiated AU6 separated on Nucleosil C100 C_{18} column, eluent: 85% MeOH/H_2O, flow rate: 1 mL min^{-1}, injection volume: 10 µL and detection wavelength: 310 nm. The order of elution is MBC and *trans*-2-EHMC.

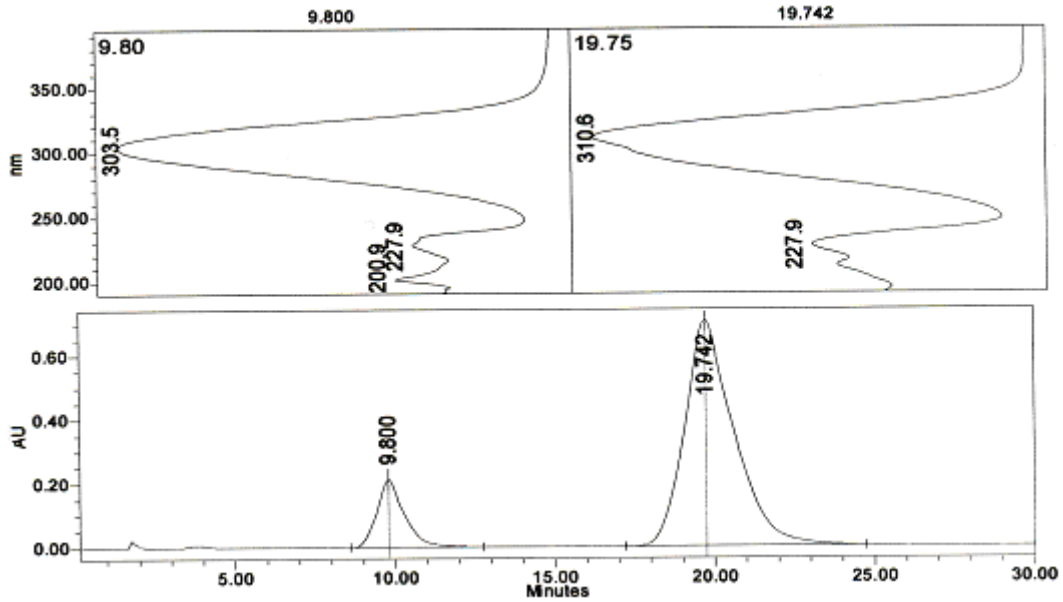

Figure F7 HPLC chromatogram of unirradiated AU 8 separated on Nucleosil C100 C_{18} column, eluent: 85% MeOH/H_2O, flow rate: 1 mL min^{-1}, injection volume: 10 µL and detection wavelength: 310 nm. The order of elution is MBC, and *trans*-2-EHMC

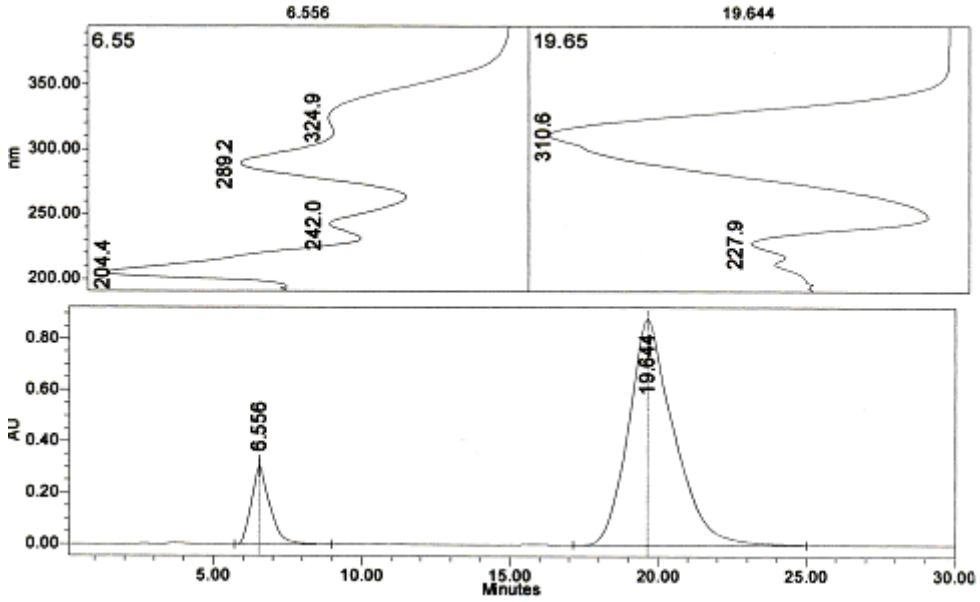

Figure F8 HPLC chromatogram of unirradiated AU9 separated on Nucleosil C100 C_{18} column, eluent: 85% MeOH/H_2O, flow rate: 1 mL min^{-1}, injection volume: 10 µL and detection wavelength: 310 nm. The order of elution is Benz-3 and *trans*-2-EHMC.

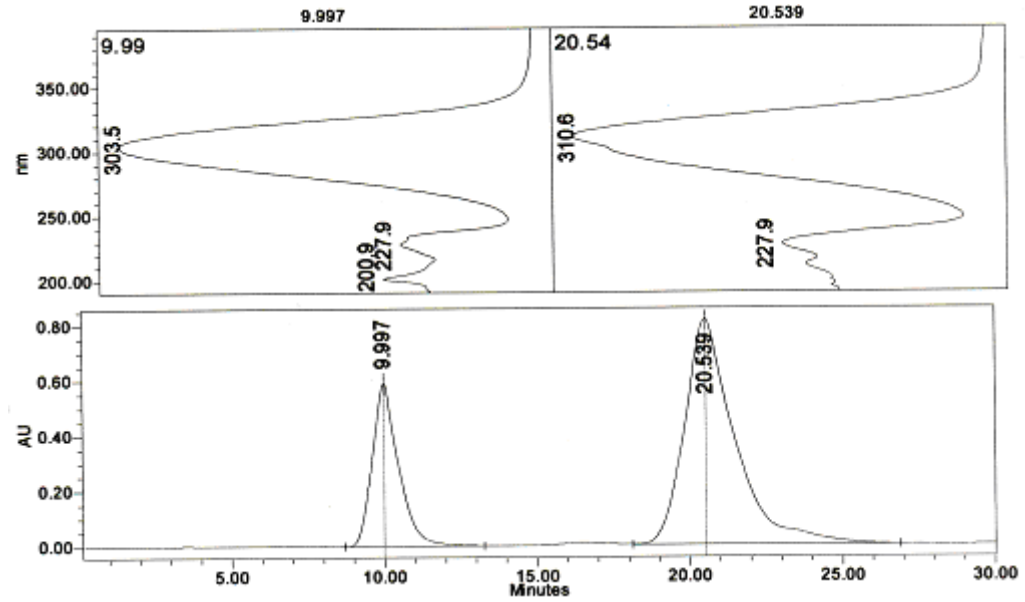

Figure F9 HPLC chromatogram of unirradiated AU10 separated on Nucleosil C100 C_{18} column, eluent: 85% MeOH/H_2O, flow rate: 1 mL min^{-1}, injection volume: 10 µL and detection wavelength: 310 nm. The order of elution is *trans*-MBC, *trans*-2-EHMC and AVO.

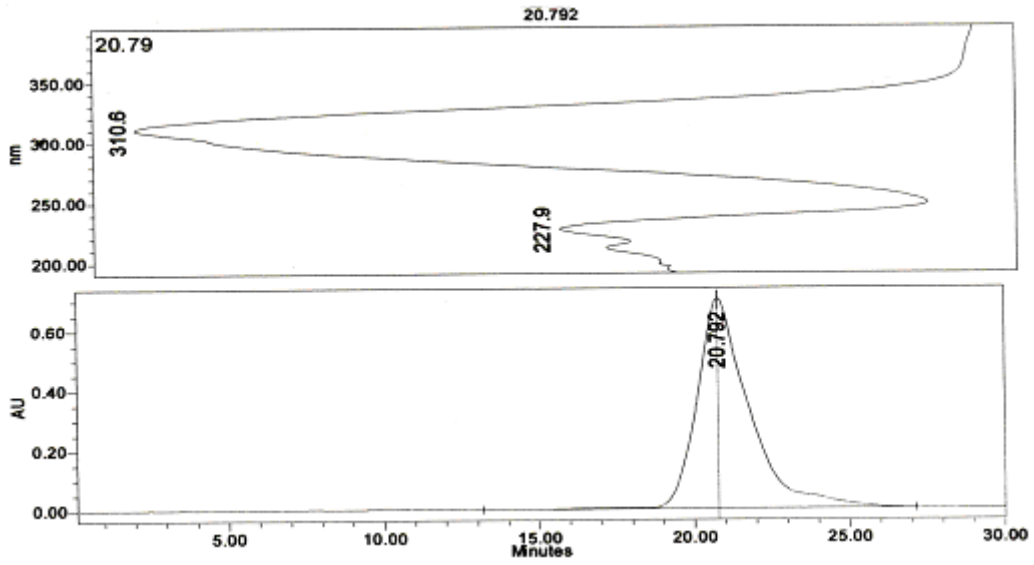

Figure F10 HPLC chromatogram of unirradiated AU10 separated on Nucleosil C100 C_{18} column, eluent: 85% MeOH/H_2O, flow rate: 1 mL min^{-1}, injection volume: 10 µL and detection wavelength: 360 nm. The order of elution is *trans*-2-EHMC and AVO

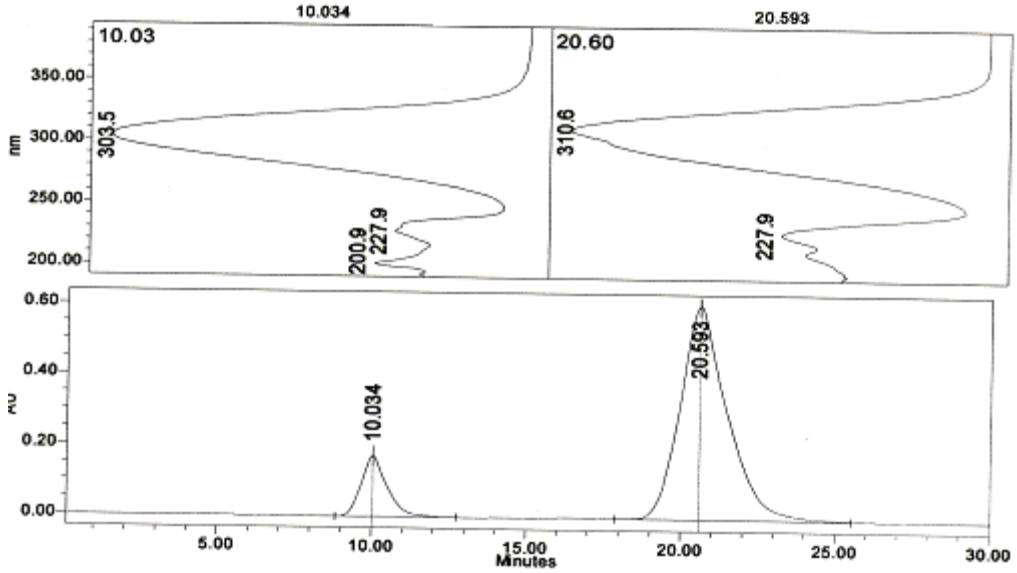

Figure F11 HPLC chromatogram of unirradiated AU12 separated on Nucleosil C100 C_{18} column, eluent: 85% MeOH/H_2O, flow rate: 1 mL min^{-1}, injection volume: 10 µL and detection wavelength: 310 nm. The order of elution is MBC and *trans*-2-EHMC.

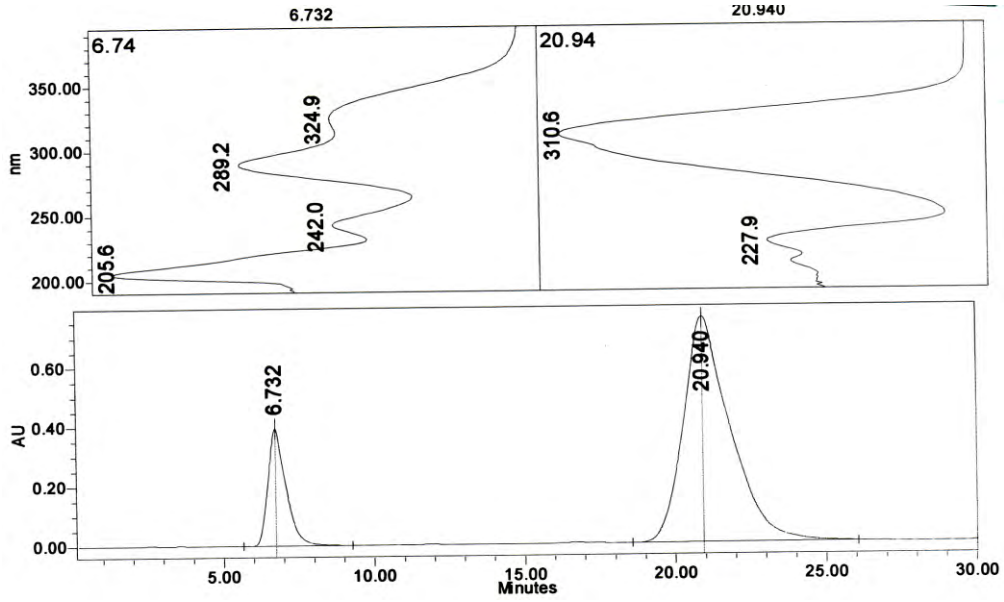

Figure F12 HPLC chromatogram of unirradiated AU13 separated on Nucleosil C100 C_{18} column, eluent: 85% MeOH/H_2O, flow rate: 1 mL min^{-1}, injection volume: 10 µL and detection wavelength: 310 nm. The order of elution is Benz-3 and *trans*-2-EHMC.

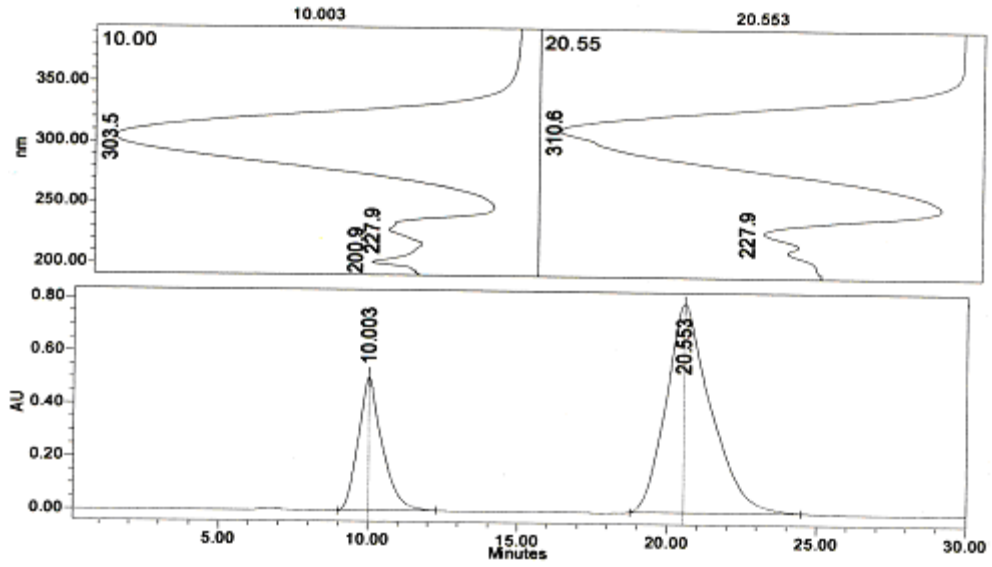

Figure 13 HPLC chromatogram of unirradiated AU14 separated on Nucleosil C100 C_{18} column, eluent: 85% MeOH/H_2O, flow rate: 1 mL min^{-1}, injection volume: 10 µL and detection wavelength: 310 nm. The order of elution is MBC and *trans*-2-EHMC.

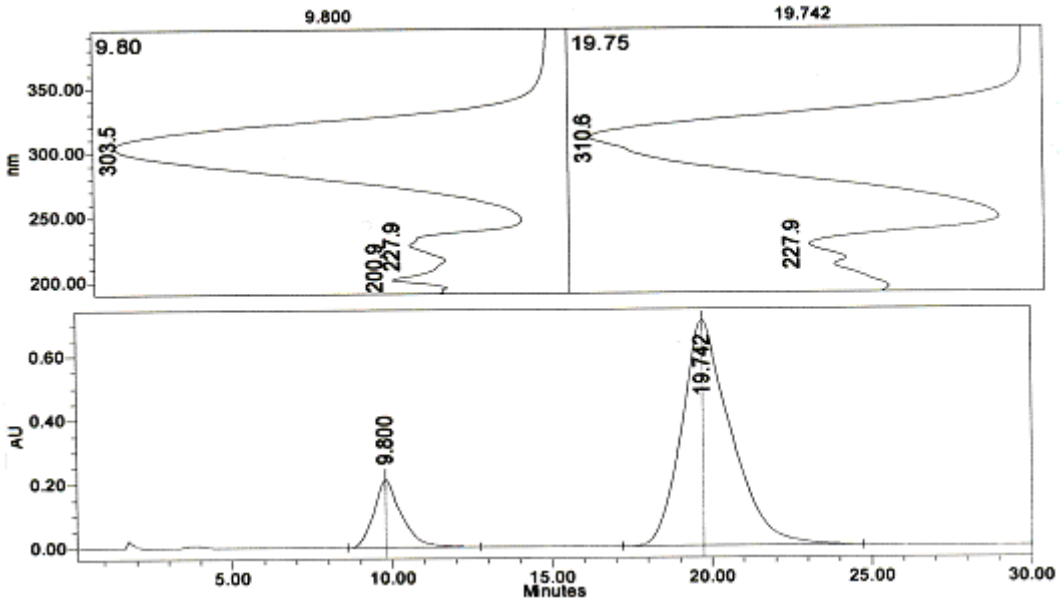

Figure F14 HPLC chromatogram of unirradiated sample AU16 separated on Nucleosil C100 C_{18} column, eluent: 85% MeOH/H_2O, flow rate: 1 mL min^{-1}, injection volume: 10 µL and detection wavelength: 310 nm. The order of elution is MBC and *trans*-2-EHMC.

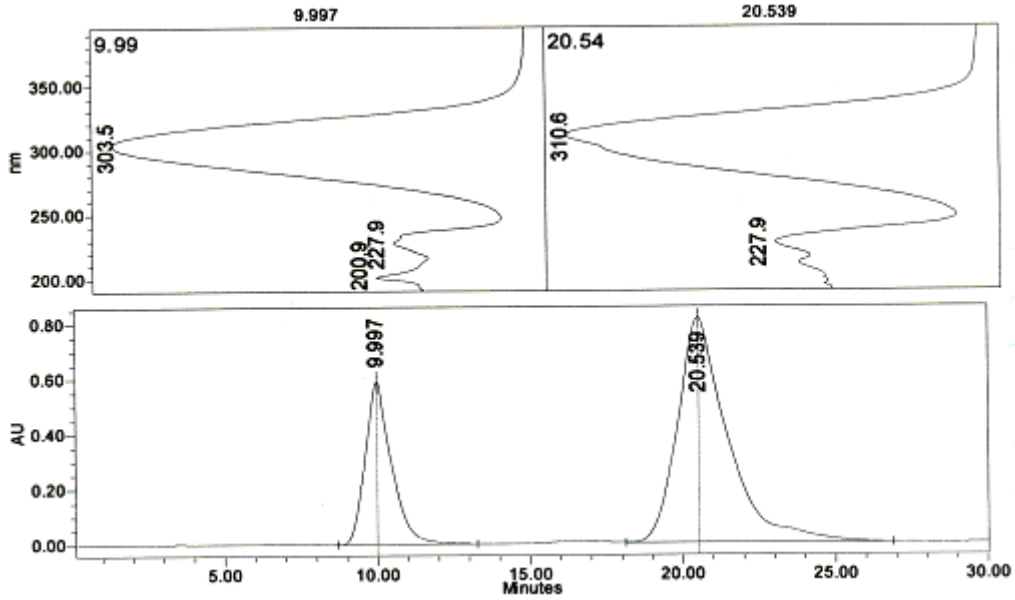

Figure F15 HPLC chromatogram of unirradiated sample AU15 separated on Nucleosil C100 C_{18} column, eluent: 85% MeOH/H_2O, flow rate: 1 mL min^{-1}, injection volume: 10 µL and detection wavelength: 310 nm. The order of elution is OT, *trans*-2-EHMC and AVO.

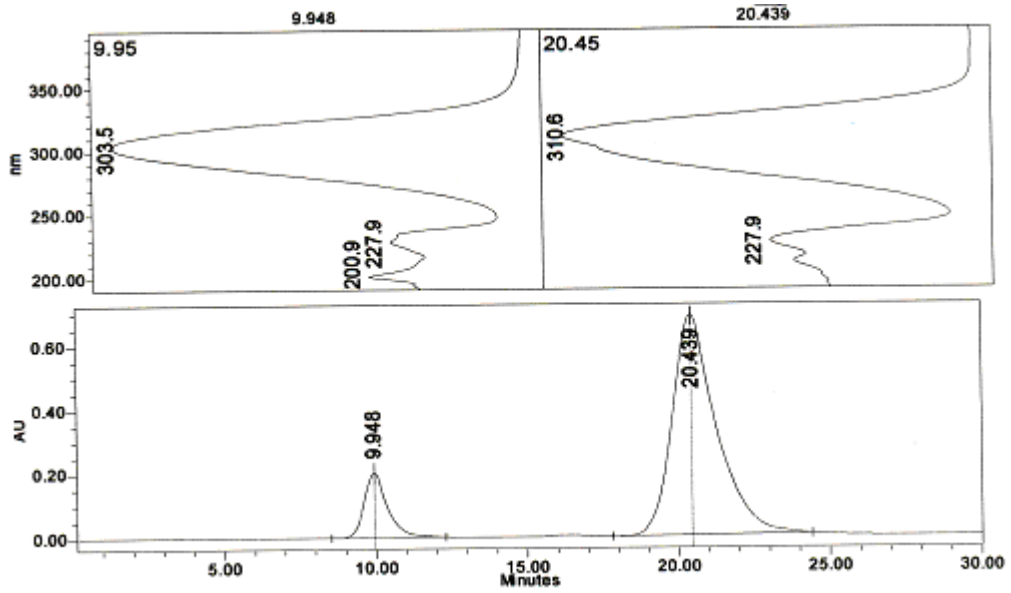

Figure F16 HPLC chromatogram of the unirradiate AU19 separated on Nucleosil C100 C_{18} column, eluent: 85% MeOH/H_2O, flow rate: 1 mL min^{-1}, injection volume: 10 µL and detection wavelength: 310 nm. The order of elution is MBC, and *trans*-2-EHMC.

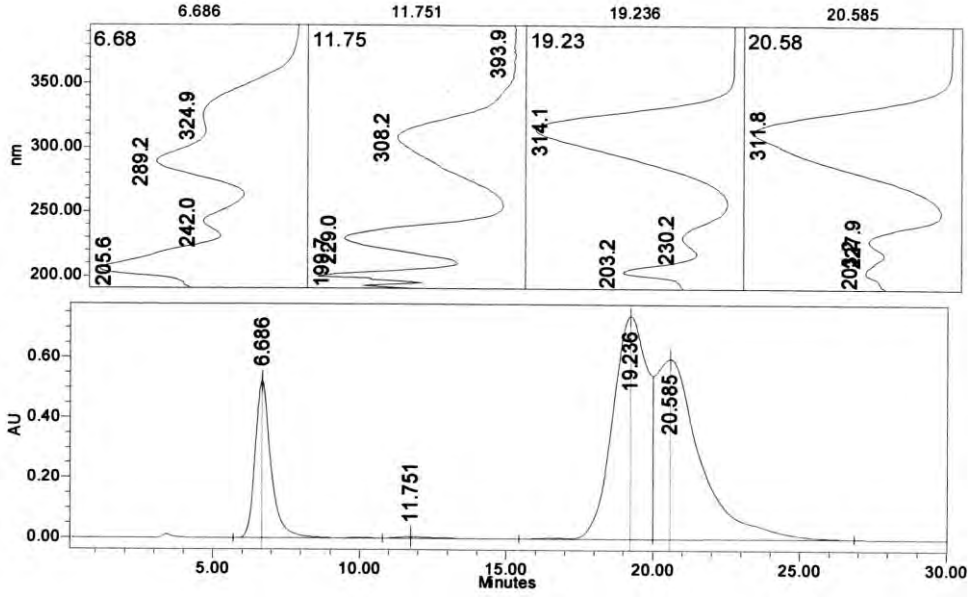

Figure F17 HPLC chromatogram of unirradiated AU20 separated on Nucleosil C100 C_{18} column, eluent: 85% MeOH/H_2O, flow rate: 1 mL min^{-1}, injection volume: 10 µL and detection wavelength: 310 nm. The order of elution is Benz-3, ODM-PABA, HS and *trans*-2-EHMC.

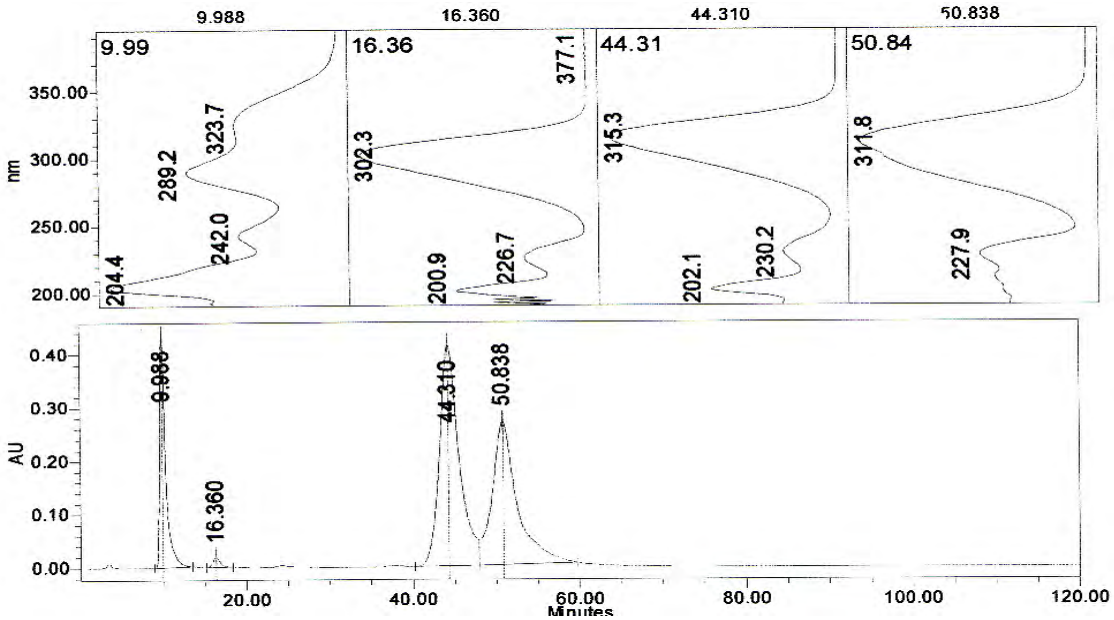

Figure F18 HPLC chromatogram of irradiated AU20 separated on Nucleosil C100 C18 column, eluent: 75% (v/v) MeOH/H_2O, flow rate: 1 mL min^{-1}, injection volume: 10 µL and detection wavelength: 310 nm. The order of elution is Benz-3, HS, ODM-PABA and *trans*-2-EHMC.

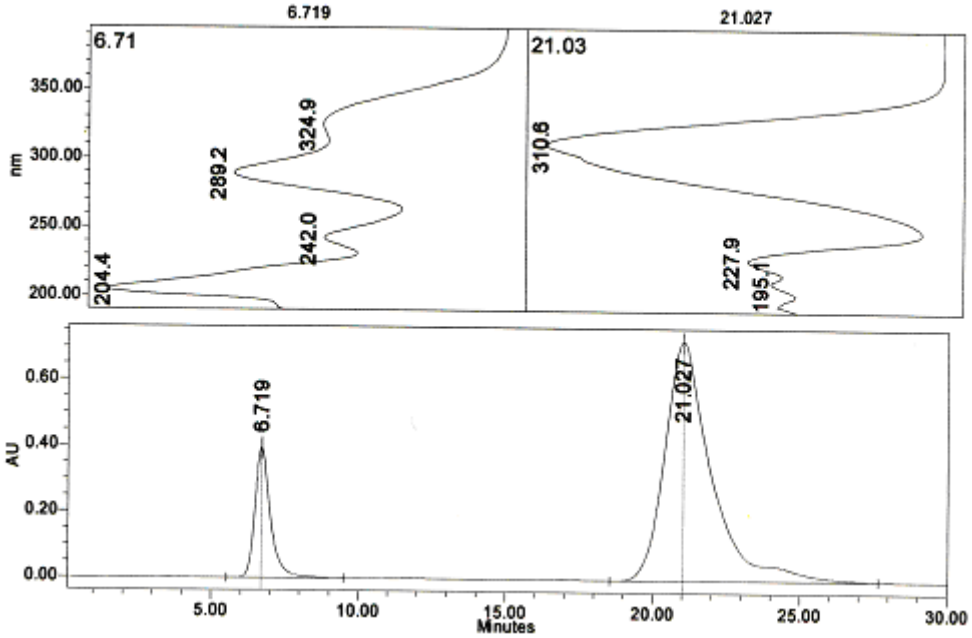

Figure F19 HPLC chromatogram of unirradiated AU24 balm separated on Nucleosil C100 C_{18} column, eluent: 85% MeOH/H_2O, flow rate: 1 mL min^{-1}, injection volume: 10 µL and detection wavelength: 310 nm. The order of elution is Benz-3, *trans*-2-EHMC and AVO.

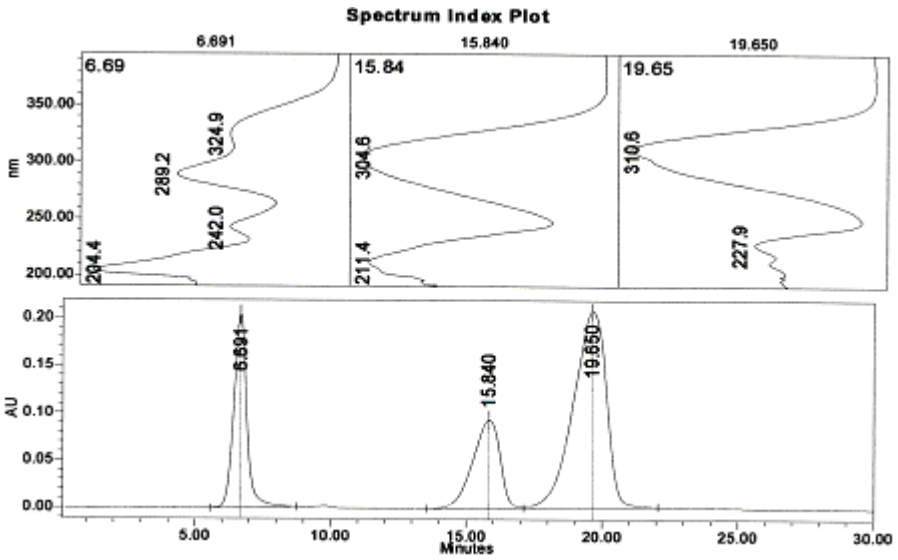

Figure F20 HPLC chromatogram of irradiated sample AU25 separated on Nucleosil C100 C_{18} column, eluent: 85% MeOH/H_2O, flow rate: 1 mL min^{-1}, injection volume: 10 µL and detection wavelength: 310 nm. The order of elution is Benz-3, *cis*-EHMC and *trans*-2-EHMC

APPENDIX G

HPLC-MS spectra for some irradiated suncare products

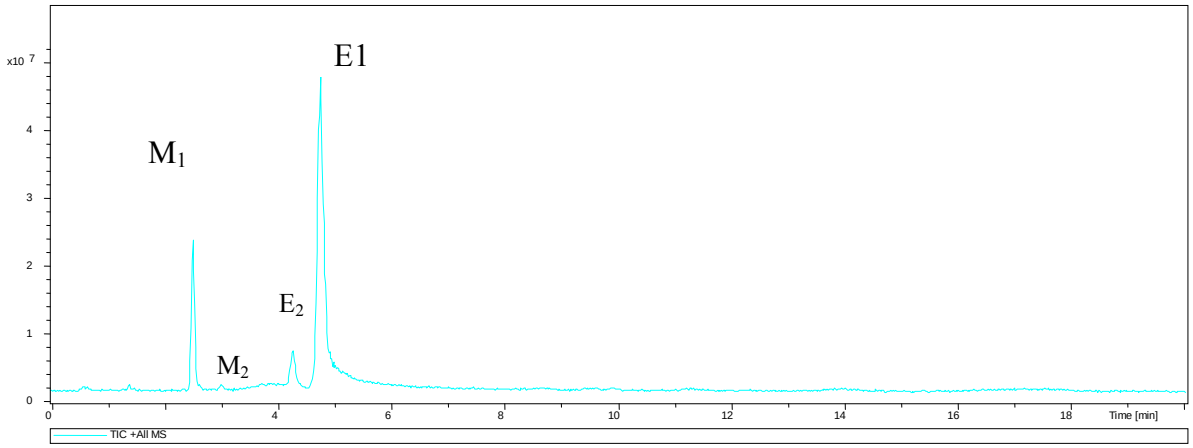

Figure G1 HPLC chromatogram of irradiated AU5 analysed on the Agilent Zorbax Eclipse XDB-C18 column by isocratic elution at a flow rate of 1 mL min^{-1}, injection volume 5 µL with the Agilent 1100 Series HPLC with UV detection at 310 nm. The order of elution was *trans*-MBC, *cis*-MBC, *cis*-2-EHMC and *trans*-2-EHMC.

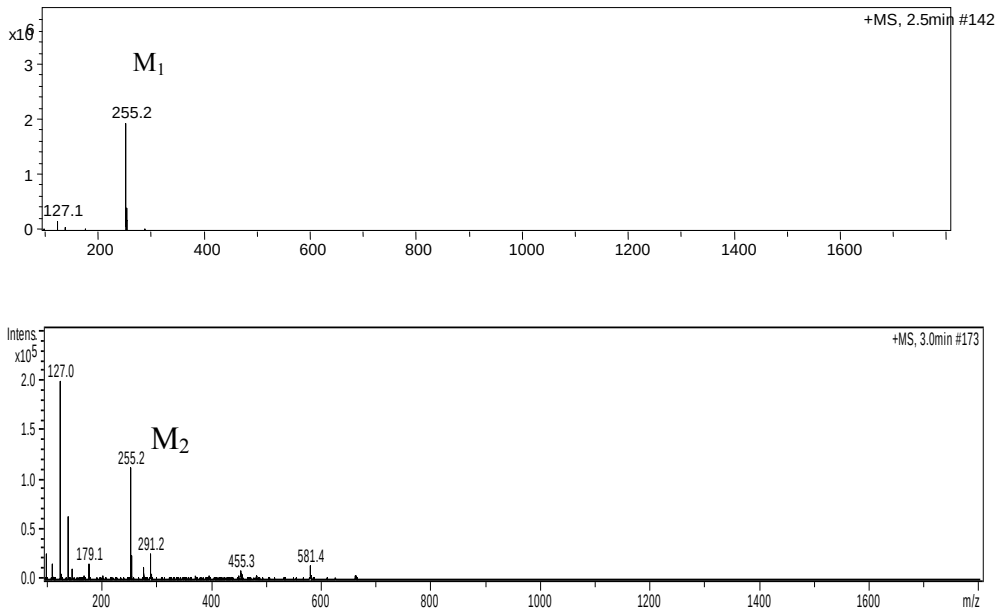

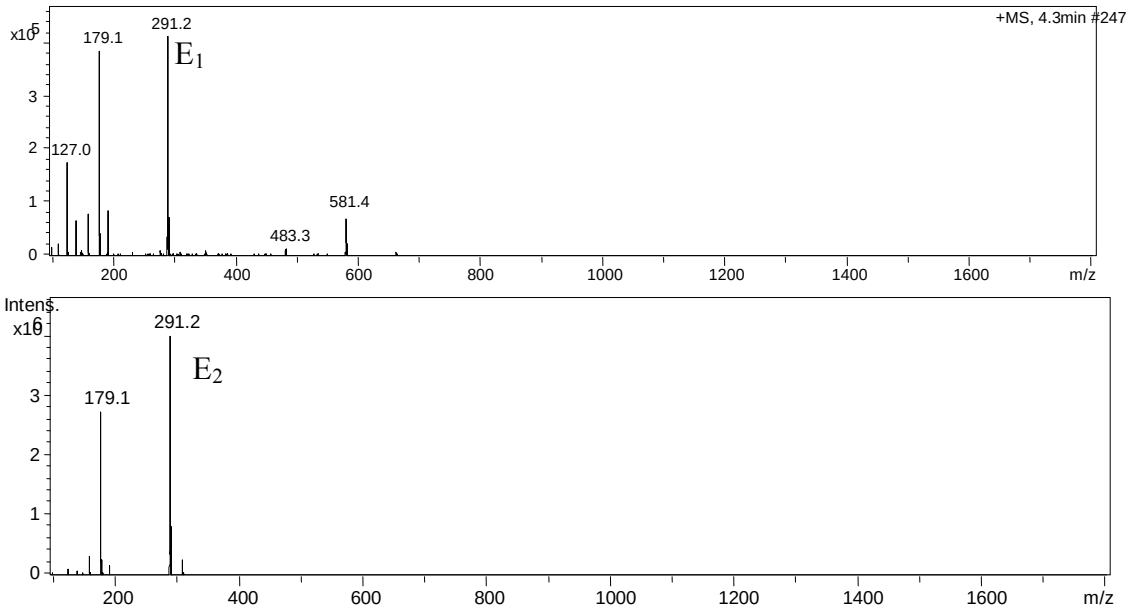

Figure G2 Mass spectra of the peaks labeled M1, M2, E1 and E2 in Figure G1.

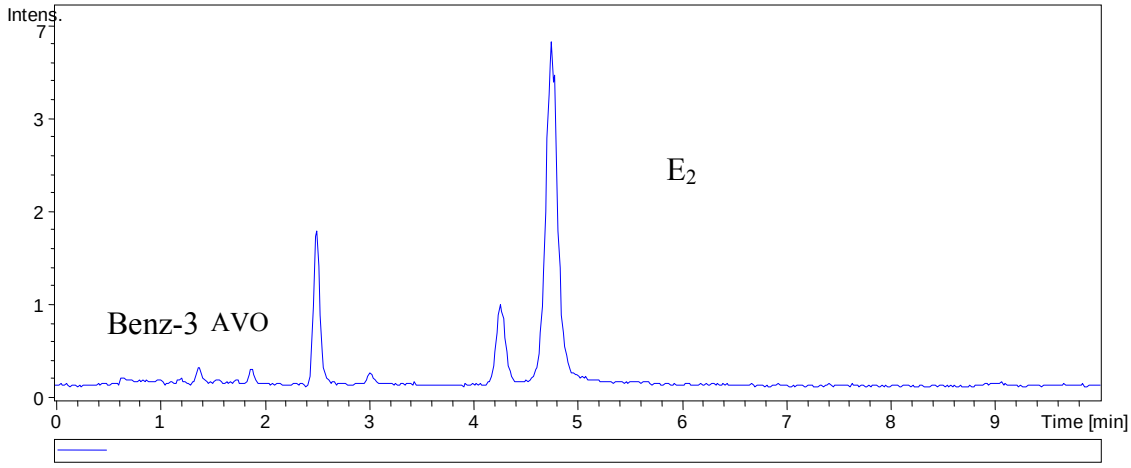

Figure G3 HPLC chromatogram of irradiated AU24 analysed on the Agilent Zorbax Eclipse XDB-C18 column by isocratic elution at a flow rate of 1 mL min^{-1}, injection volume 5 µL with the Agilent 1100 Series HPLC with UV detection at 310 nm. The order of elution was Benz-3, AVO, *cis*-2-EHMC and *trans*-2-EHMC.

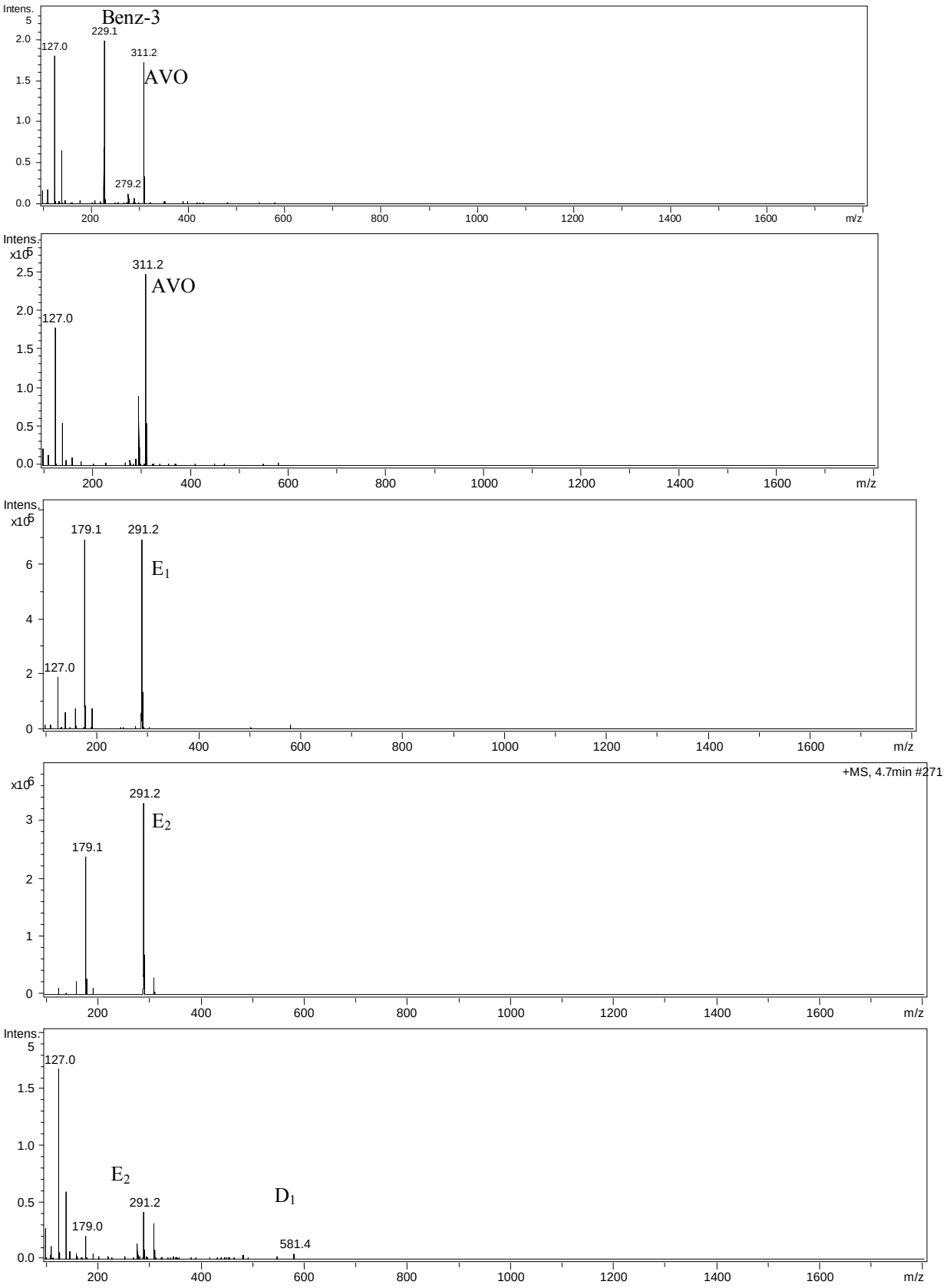

Figure G4 The mass spectra of the peaks labeled for the irradiated sample AU24 in Figure 3.

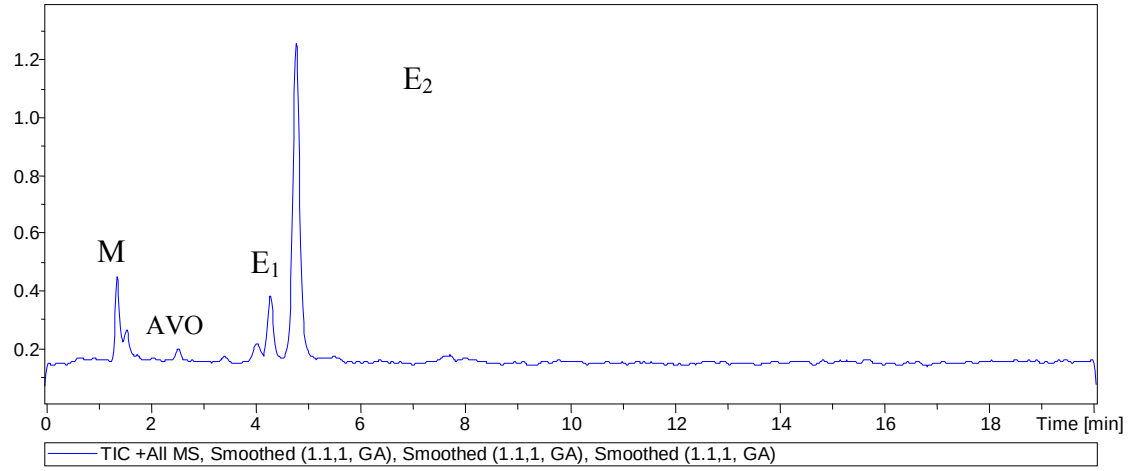

Figure G5 HPLC chromatogram of irradiated AU1 analysed on the Agilent Zorbax Eclipse XDB-C18 column by isocratic elution at a flow rate of 1 mL min^{-1}, injection volume 5 µL with the Agilent 1100 Series HPLC with UV detection at 310 nm. The order of elution was MBC, AVO, *cis*-2-EHMC and *trans*-2-EHMC.

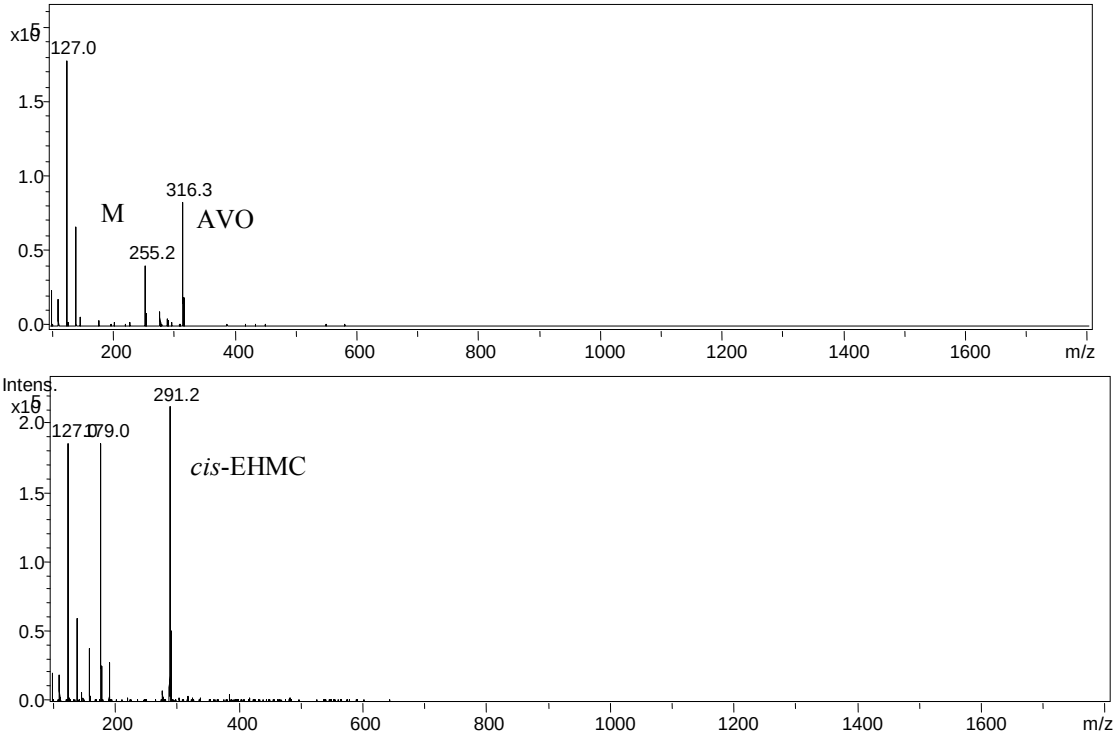

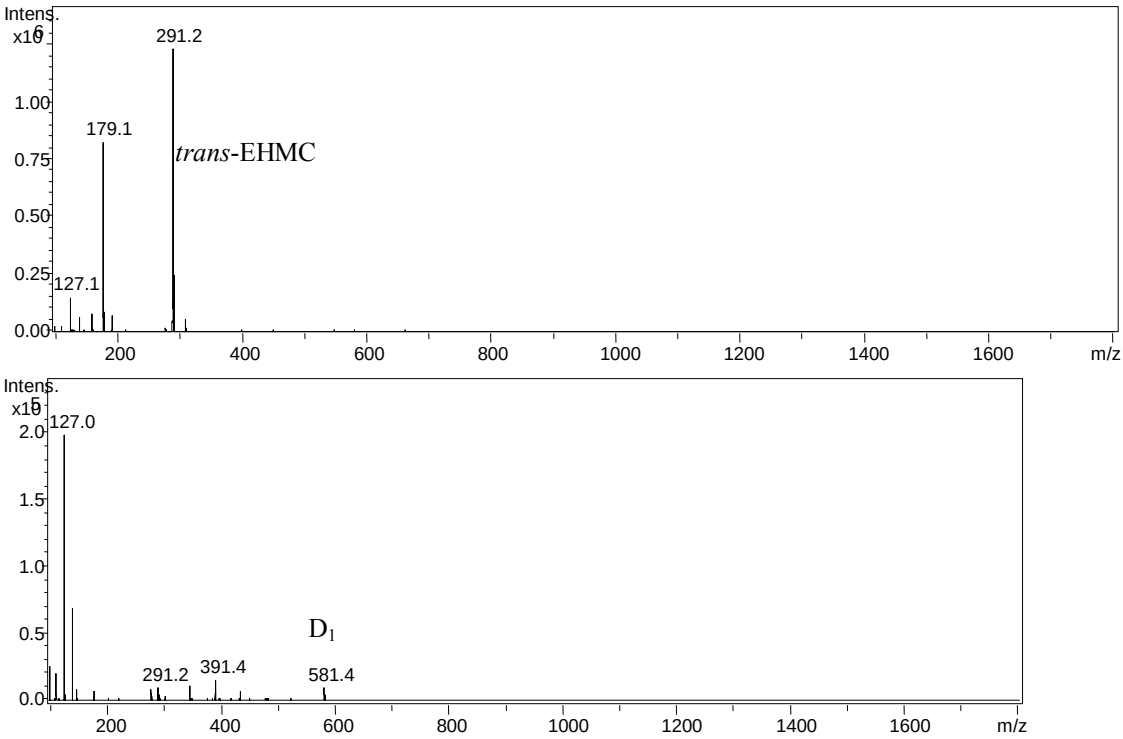

Figure G6 The mass spectra of the peaks labeled for the irradiated sample AU1 in Figure 5

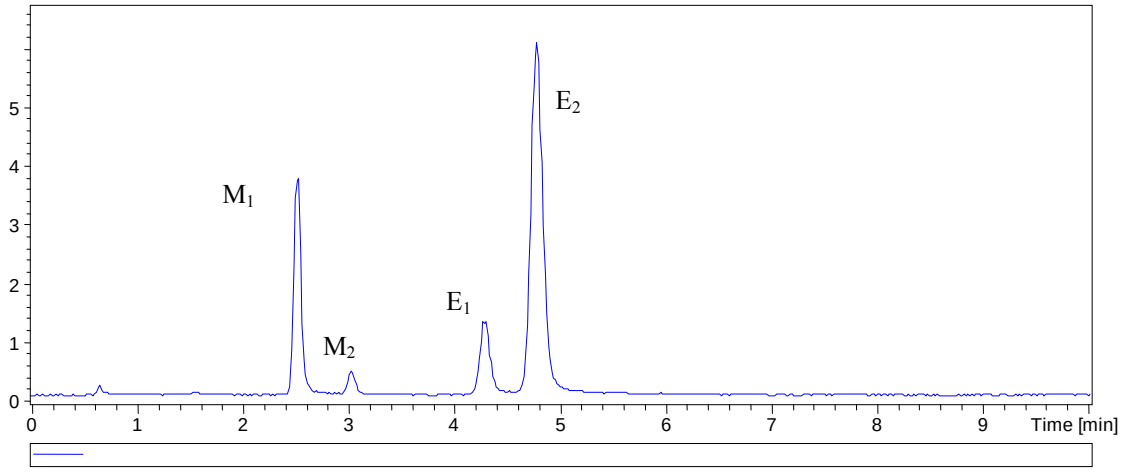

Figure G7 HPLC chromatogram of irradiated AU19 analysed on the Agilent Zorbax Eclipse XDB-C18 column by isocratic elution at a flow rate of 1 mL min^{-1}, injection volume 5 µL with the Agilent 1100 Series HPLC with UV detection at 310 nm. The order of elution was *trans*-MBC, *cis*-MBC, *cis*-2-EHMC and *trans*-2-EHMC.

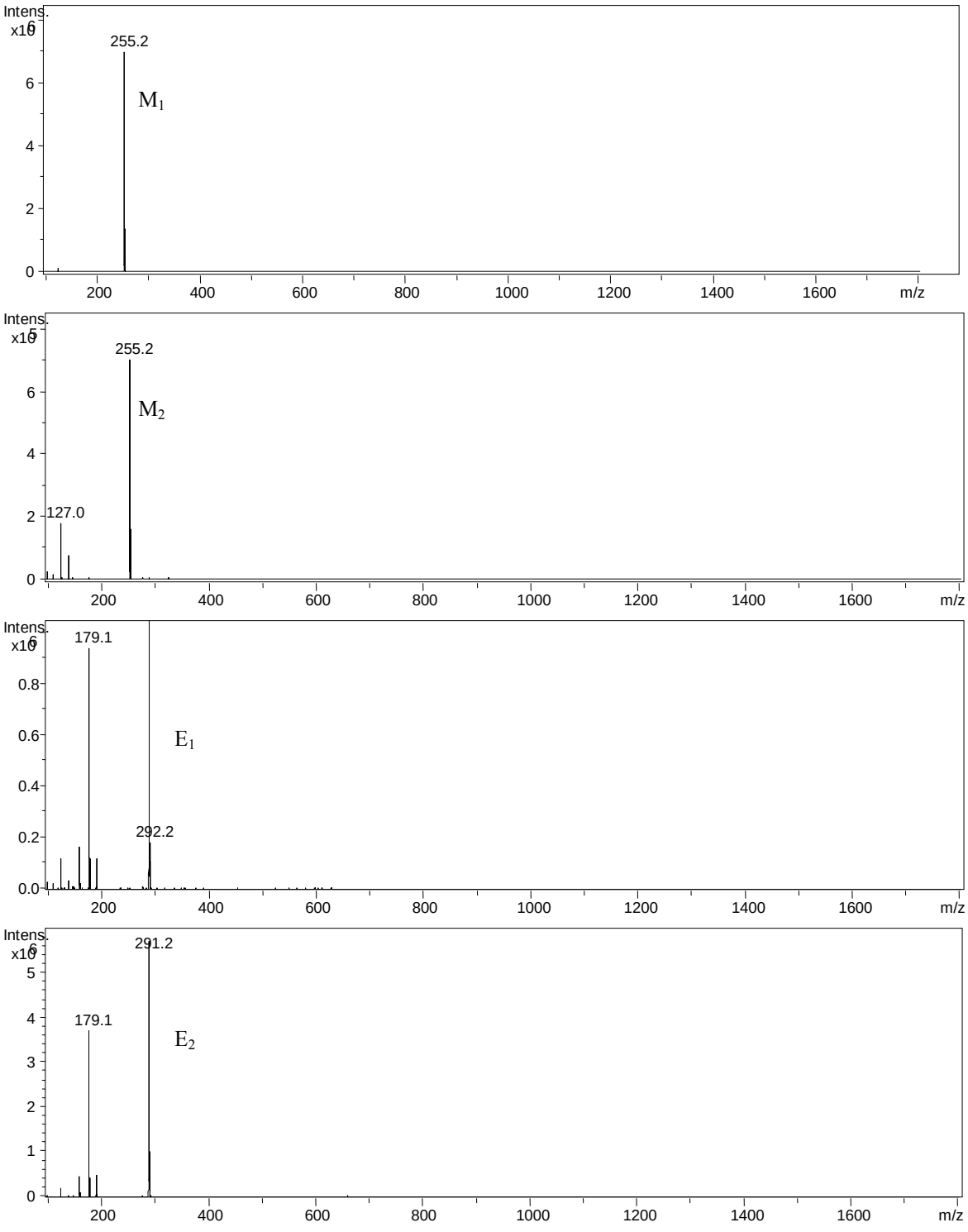

Figure G8 The mass spectra of the peaks labeled M_1, M_2, E_1 and E_2 for the irradiated sample AU19 in Figure G7.

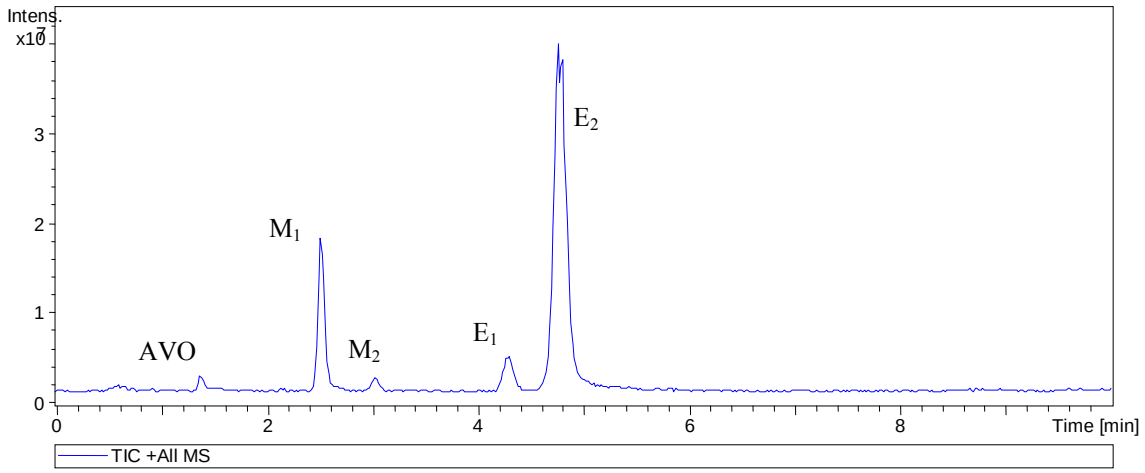

Figure G9 HPLC chromatogram of irradiated AU10 analysed on the Agilent Zorbax Eclipse XDB-C18 column by isocratic elution at a flow rate of 1 mL min^{-1}, injection volume 5 µL with the Agilent 1100 Series HPLC with UV detection at 310 nm. The order of elution was, AVO, *trans*-MBC, *cis*-MBC, *cis*-2-EHMC and *trans*-2-EHMC.

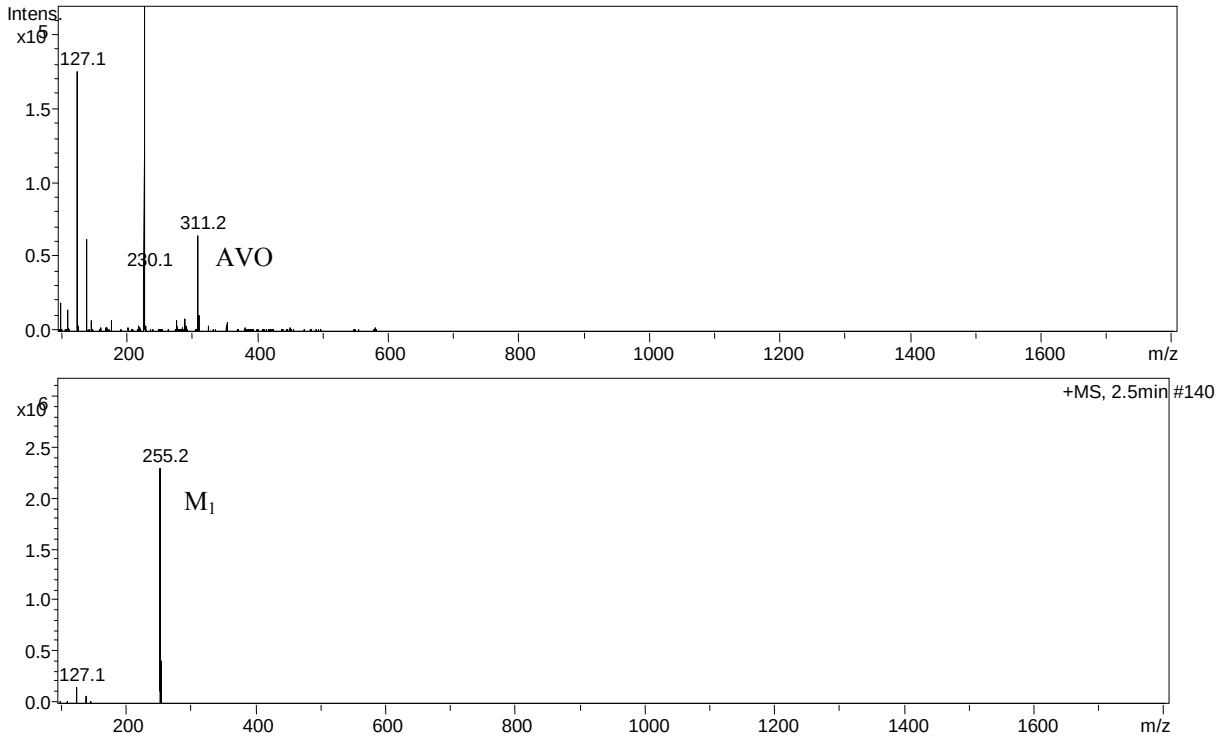

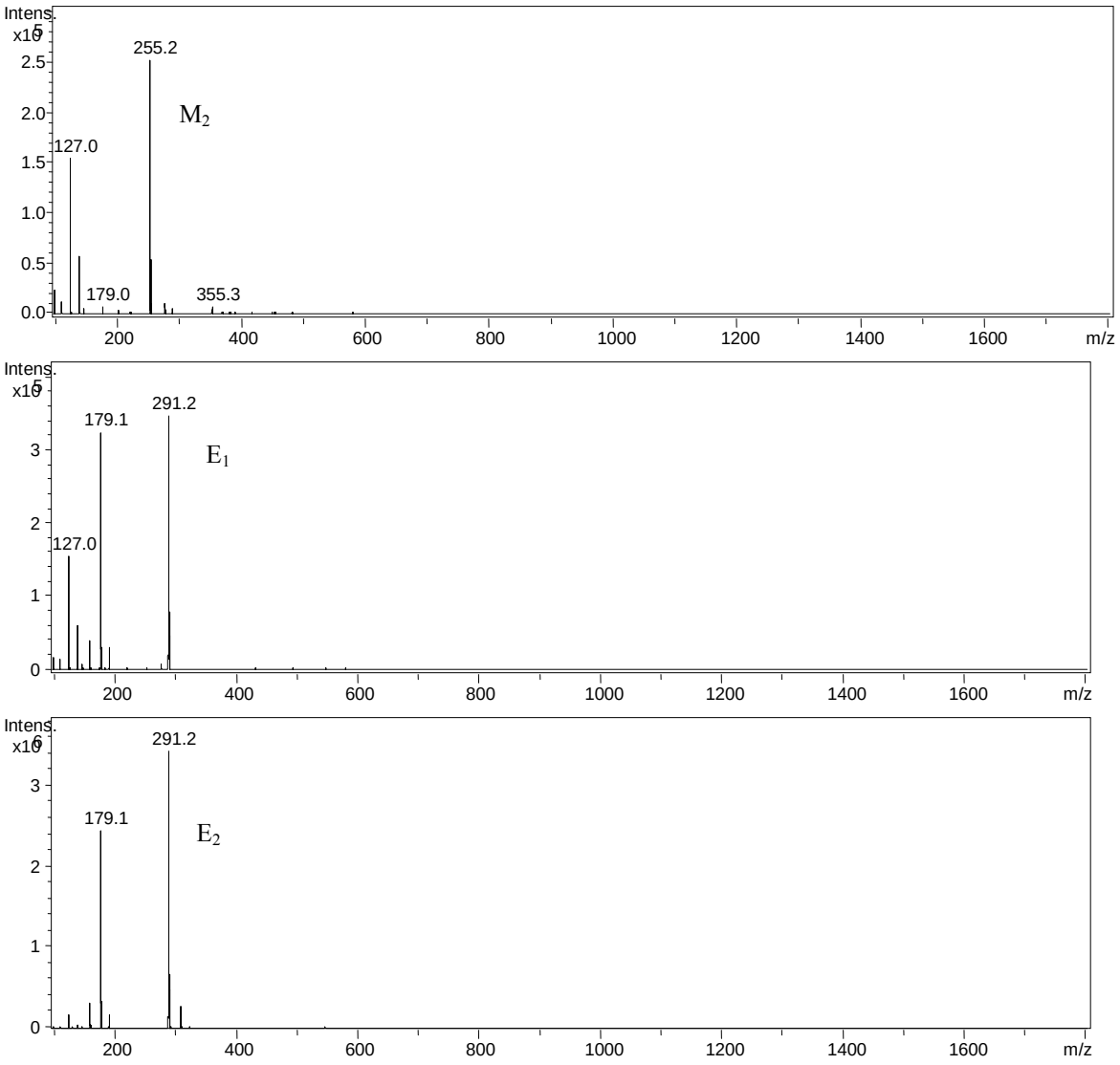

Figure G10 The mass spectra of the peaks labeled AVO, M_1, M2, E1 and E2 for the irradiated sample AU10 in Figure G9.

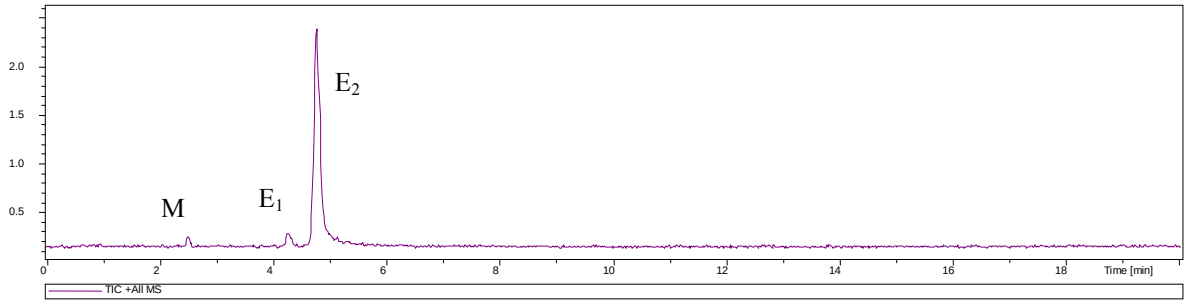

Figure G11 HPLC chromatogram of irradiated AU12 analysed on the Agilent Zorbax Eclipse XDB-C18 column by isocratic elution at a flow rate of 1 mL min^{-1}, injection volume 5 µL with the Agilent 1100 Series HPLC with UV detection at 310 nm. The order of elution was MBC, *cis*-2-EHMC and *trans*-2-EHMC.

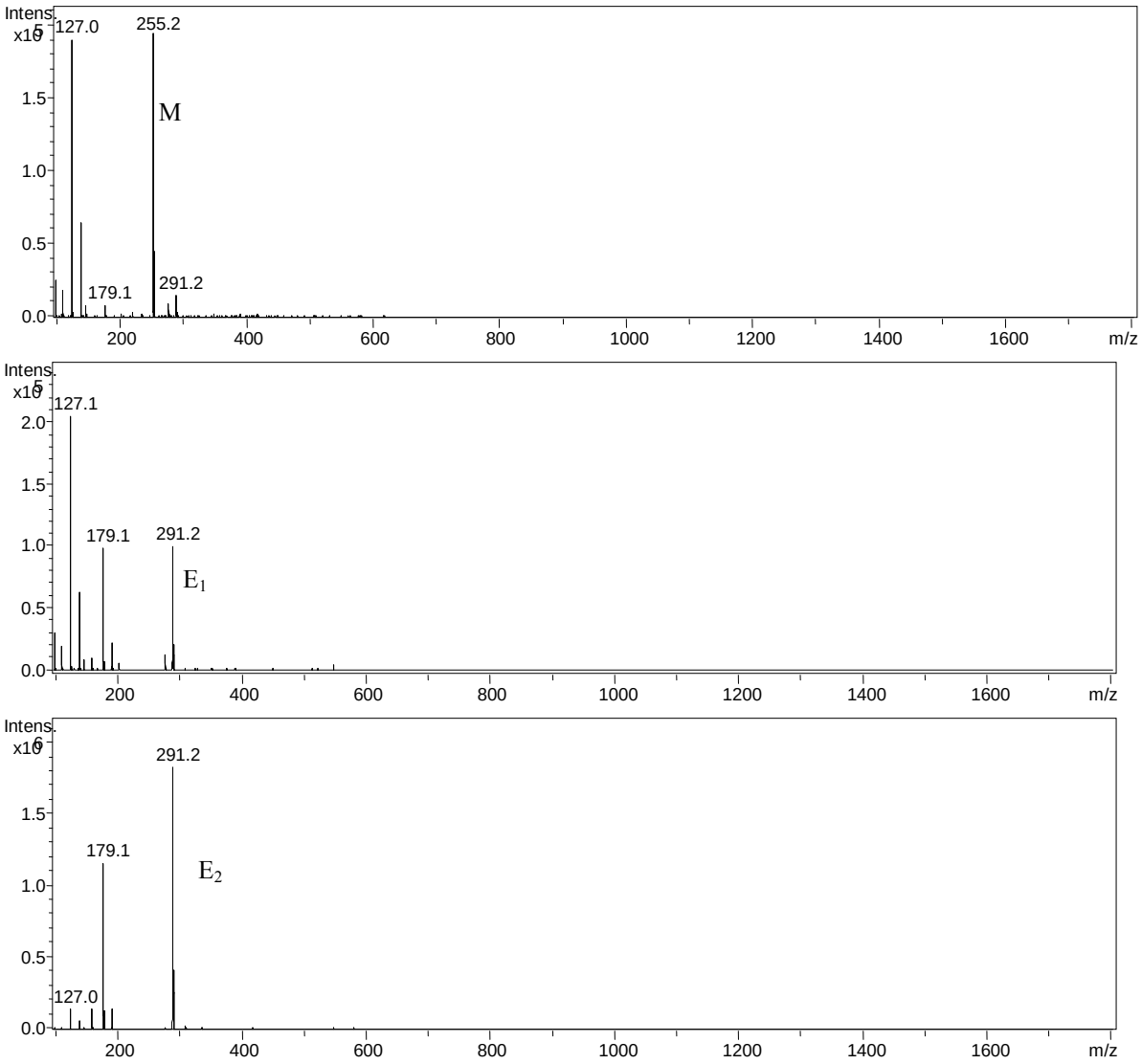

Figure G12 The mass spectra of the peaks labeled M, E_1 and $E_2$for the irradiated sample AU12 in Figure G11.

APPENDIX H

Raw data for suncare products

The following tables list the peak areas for the active chemical ingredients in the different sunscreens analyzed by HPLC

Chromatographic conditions: eluent 85%v/v MeOH/H_2O, flow rate: 1 mL min^{-1}, column: Nucleosil C100 C18, injection volume: 10 µl, mass extracted: 0.5 g.

Raw data for quantification of the active chemical ingredients in the commercial sunscreen products

AU 1			AU2		
EHMC	**AVO**	**MBC**	**EHMC**	**AVO**	**Benz-3**
36567191	10791597	26423365	38657671	6035158	5876326
36685135	11915022	25714567	36534135	5982389	5960516
37271425	10246742	25431991	35125765	6048853	5693422
35068464	11097527	23245864	39687323	5836286	5640954
34906783	10504434	22473775	38875418	5664640	5692586
35902174	11575905	22400580	37167541	5645863	5466178
36473849	12096506	25442114	32647569	5590286	6672682
37195973	11042020	25698617	30871129	5471985	6569067
36251129	12002565	25908061	31259437	5594386	6573192

AU 3		AU 4		AU 5	
EHMC	**PBSA**	**EHMC**	**OCT**	**EHMC**	**MBC**
30653455	460704	29757566	417082	35531569	26200335
29150975	477252	28915653	428067	38569167	26411577
30232372	473525	30453232	418578	36045223	26501312
33968723	431530	31549728	409577	37954728	22734654
32854878	455149	32385878	429463	36432374	21589755

31675491	453582	31766751	420572	37087667	22540012
34275569	442164	30675227	389574	35000667	24600421
34087929	423637	31907429	409067	34190754	23759862
32509437	422093	31096437	398175	35196427	21809584

AU 6		AU 7			
EHMC	**MBC**	**EHMC**	**AVO**	**MBC**	**OT**
30055358	27625645	32730858	6208235	35679905	2037406
29851767	26754207	33068312	6067289	36492907	2142371
31452283	26895782	33908143	6098323	36002242	2036120
32575658	23778874	30255665	6938646	33164354	2256416
36032304	22157655	31464343	6668620	32379550	2056219
36208707	23878712	30320871	6643765	32304743	2346787
31506677	21442021	33366566	6568286	34157421	2092506
32190654	22379871	32988544	6458165	33981045	2021482
33510896	23881884	30951807	6583496	35480014	2178396

AU 8		AU 9		AU 10		
EHMC	**MBC**	**EHMC**	**Benz-3**	**EHMC**	**AVO**	**MBC**
32308958	9385811	42789307	5956009	32789433	10532657	34230985
30658322	9806496	43305412	6076541	34354302	11005422	32438944
29143683	9714356	43990081	5906754	33430011	10468458	32745371
33257865	9767333	40287180	6186087	32472178	11156165	31045643
34603403	9442958	43478973	6252172	34340973	10545803	30973676
33620717	9398236	44035471	6230964	33340315	10250590	30456980
30366436	9794823	39367436	5702980	39368726	12572184	30144324
32189654	9814984	36298874	5798634	36629334	12164520	28972717
30510887	9385412	37092547	5952432	36609877	12386625	31015461

AU 11		AU 12		AU 13	
EHMC	**AVO**	**EHMC**	**MBC**	**EHMC**	**Benz-3**
37686673	12934270	34896914	9335641	37869453	6565465
36556422	12522982	33564252	9509896	35643542	6976431
37534351	12376423	35033403	9429044	35340301	6815676
30247937	10436955	29224708	9886553	29247187	6585560
32049823	10654983	30856923	9976430	30434323	6682152
31476547	11652505	31358042	9954386	33534803	6848354
35096546	11549284	30962326	9564827	30937626	6502451
33668351	10543870	32446514	9680684	32663344	6334590
33006011	11300455	31305790	9476682	33060975	6305042

AU 14		AU 15		
EHMC	**MBC**	**EHMC**	**AVO**	**OT**
39974364	25121545	44986084	11604550	4735901
40655247	24900976	41965222	10992189	4879067
42257683	26607652	42533563	11204653	4710552
34009412	25033468	39402934	10996432	3647865
33906205	24269895	36204346	9965085	3743239
32807947	23912428	38047897	9908906	3833237
29013346	22364901	40346536	12438280	4296092
30857571	22637543	43858371	10158038	3980907
29812538	23098644	41581681	10059674	4248945

AU 16		AU 17		AU 18		
EHMC	**MBC**	**EHMC**	**MBC**	**EHMC**	**AVO**	**MBC**
30093644	9543671	34477744	9678956	30512333	12368970	26635605
33406477	9820268	34040377	9729872	31347054	11285489	26564989
30428363	9815046	33423633	9886536	30536383	11537668	25762842
33441212	9280918	30444324	9598518	38992353	10675430	24233327

35596235	9259028	35596235	9228056	37056359	10395970	23739956
32384797	9481256	33876327	9482536	37670081	10476354	24939073
32901633	10048023	32436214	9948023	35243344	11906434	24655123
29851171	9934084	29008553	9809871	33091553	10457453	24989845
29188388	10127882	31185337	9825462	34138338	11557436	25754014

AU 19		AU 20			
EHMC	**MBC**	**EHMC**	**Benz-3**	**HS**	**ODM-PABA**
29054566	9590546	28706646	10995605	495094	89453566
30754784	9897322	28754484	10886731	485163	92504345
30253883	9856430	27099324	10681576	509209	93990663
35832993	9750098	27899516	10158510	498821	93190401
35056573	9522230	28004565	10201225	509473	94847873
33347672	9876536	27334562	10038582	506690	97854391
29524454	9494843	27098478	10250542	501490	96296755
33109343	9378071	26310993	10435345	489194	94768917
32413438	9482452	26954878	10296518	488627	95598576

AU 21		AU 22		AU 23	
EHMC	**OCT**	**EHMC**	**OCT**	**EHMC**	**Benz-3**
46549071	769701	45774333	786971	35587758	8936405
45641843	764107	43434407	764196	34496781	9083731
44092674	786989	41369783	787689	34929454	9118681
46337651	800975	39900423	788675	30569277	8715010
43676468	825465	38559355	792556	30679915	8601533
43343218	816534	37676381	806594	29334574	8738582
39083447	847676	38242343	857021	30392743	8546342
39094320	856984	39110355	835645	29403890	8509845
40190678	865624	38133738	837005	30405918	8459188

AU 24			AU 25	
EHMC	**AVO**	**Benz-3**	**EHMC**	**AVO**
36555871	8236973	7043160	35873258	10455160
34184967	8189989	6934131	36928771	10925289
34092544	8338862	7115526	36293244	10465413
33056951	8617560	6656050	39992817	9955546
36675418	8307955	6468892	40565615	10039835
33300354	8465454	6384544	41562334	9965098
30028476	8691635	6850215	39298748	10034280
30947990	8457456	6995590	40340310	10183058
31905918	8505036	7056312	40859518	10067495

APPENDIX I

Conference presentations

- W. Waudo, B.S. Martincigh, H. G. Kruger, *Computational studies of the photodimerisation of 2-ethylhexyl-para-methoxycinnamate,* South African Chemical Institute Colloquium, University of Zululand, 18th September 2007.

- W. Waudo, A *study of photoinduced transformations of commercial sunscreens*, 38th Convention of the South African Chemical Institute, University of KwaZulu-Natal, Durban, 3rd- 8th December 2006.

- W. Waudo, A *study of Photoinduced transformations of commercial sunscreens*, Faculty of Science and Agriculture, Postgraduate Research Symposium, University of KwaZulu-Natal, Pietermaritzburg, 7th November 2006

- W**.** Waudo, B.S. Martincigh, H. G. Kruger, *Computational studies of the photodimerisation of 2-ethylhexyl-para-methoxycinnamate,* 11th Congress of the European Society of Photobiology, Aix-les-Bains, France, 3rd -8th September 2005.

- W. Waudo, H.Gert Kruger and B.S. Martincigh, *Separation and Identification of photoproducts of chemical sunscreen absorbers*, XX IUPAC Symposium on Photochemistry, Granada, Spain, 17th - 22nd July 2004.

- W. Waudo, *Computational studies of the photodimerisation of 2-ethylhexyl-para-methoxycinnamate*, Faculty of Science Postgraduate Research Day, University of KwaZulu-Natal, 14th August 2004.

- W. Waudo and B.S. Martincigh, *The characterisation of photoproducts of 2-ethylhexyl-p-methoxycinnamate,* South African Chemical Institute Colloquium, University of KwaZulu-Natal, Pietermaritzburg, 19th September 2003.

- W. Waudo and B.S. Martincigh, *The characterisation of photoproducts of 2-ethylhexyl-p-methoxycinnamate,* Post-graduate Research Day, Faculty of Science, University of KwaZulu-Natal, Howard College Campus, Durban, 9th August 2003.

- W. Waudo, H.Gert Kruger and B.S. Martincigh, *The characterisation of photoproducts of the 2-ethylhexyl-p-methoxycinnamate*, 36th Convention of the South African Chemical Institute , Port Elizabeth, 1-5th July 2002.